UNIVERSITÀ DEGLI STUDI DI PAVIA

DOCTORAL SCHOOL OF CHEMICAL AND PHARMACEUTICAL SCIENCES

DEPARTMENT OF DRUG SCIENCES

"Synthesis of bicyclolactam scaffolds as dipeptide turn mimics for the obtainment of c-RGD based bioconjugates"

Tutor: Prof. Lino COLOMBO

Co-tutor: Dr. Massimo SERRA

Co-ordinator: Prof. Mauro FRECCERO

Dr. Eric Bernardi
441443

XXXI cycle (2015-2018)

Table of contents

1. Introduction

1.1. The biological role of integrins

Integrins are among the most representative and studied receptors involved in cellular adhesion processes and, through the binding with their endogenous ligands, they mediate cell-cell and cell-ECM (extracellular matrix) interactions. The integrinic receptor is a dimer composed of two non-covalently bound glycoproteic transmembrane subunits (α and β). To date, 18 types of α subunits and 8 types of β subunits, which can combine in order to form 24 different combinations characterized by different roles[1] and different tissue distribution[2], have been identified. Integrins may also be classified with respect to the type of endogenous ligand or specific amino acidic sequences recognised, such as collagen, laminin or ligands containing the RGD (Arginine-Glycine-Aspartic acid) recognition motif (*e.g.* fibronectin and vitronectin) [3] (Figure 1).

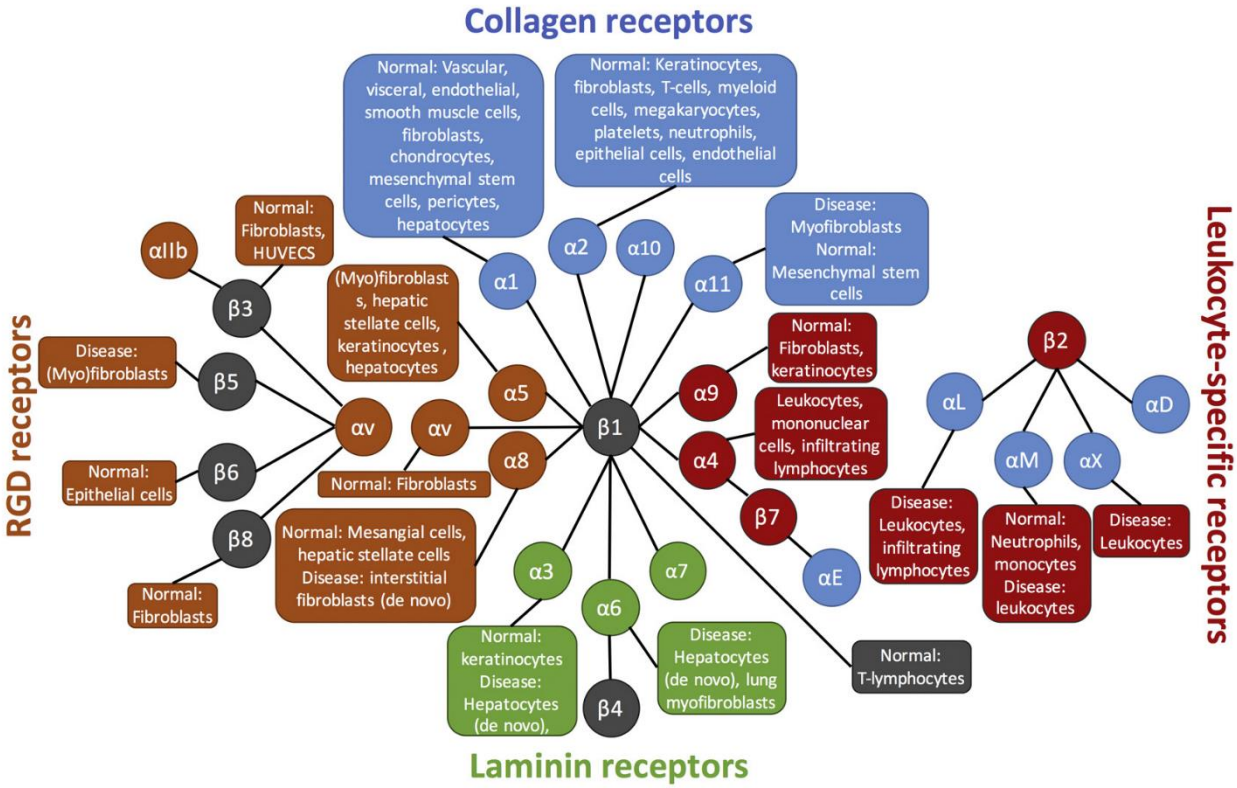

Figure 1 Integrin receptors, their ligand specificity and expression on healthy and pathogenic cells.

The preference for a type of ligand is mainly decided by the type of α subunits, whereas both α and β subunits are involved in the signal transduction cascade after a conformational switch caused by the interaction with the ligand. The complex intracellular signal transduction, started by integrins activation, is involved in many biological functions such as cell adhesion, motility, anchorage dependent survival, proliferation, growth, gene expression, cytoskeletal remodelling, embryogenesis, haemostasis, inflammation and immune response.[4] The α and β subunits are both characterized by a wider globular extracellular domain (N-terminal), involved in the ligand-binding events with ECM components, a single transmembrane portion and a small cytoplasmic domain (C-

terminal), the only exception being the β_4 subtype, which is characterized by an extended intracellular domain.[5] The cytoplasmic tail links the receptor to the actin cytoskeleton and to intracellular proteins that control integrin activation, recruitment to adhesion sites, and trafficking.[6] Furthermore, the cytoplasmic domains associate with numerous cytoskeletal proteins and intracellular signalling molecules including α-actinin, talin, filamin, paxillin, and tensin.[7] Even though the α and β extracellular domains both determine ligand binding specificity, only the β subunit seems crucial to determine intracellular interactions.[2] The main signalling pathway in which integrins are involved is the Src/FAK complex.

1.2. Integrin signal transduction

The integrinic receptor is activated through the interaction with ECM proteins, therefore enabling the cell to sense and respond to the cellular microenvironment. Integrins transmit bidirectional signalling across the plasma membrane: the outside-in signalling enables the transmission of extracellular conformational changes to the transmembrane and cytoplasmic domains[8], resulting in signal transduction (*vide infra*), whereas the inside-out signals regulate integrin affinity for adhesive ligands.[9] three affinity states have been hypothesized[10]: a low-affinity state, an intermediate affinity state with a partially activated extended conformation, and a high-affinity state exhibiting a fully activated open ligand-binding conformation (Figure 2).[11]

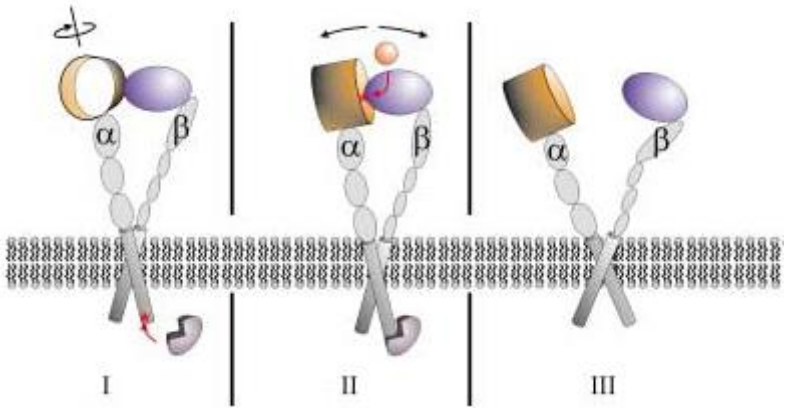

Figure 2 Affinity states model: low affinity (I), intermediate affinity (II), high affinity (III).

Recruitment of talin, an adaptor protein, to the integrin tail induces a conformational switch in the integrin extracellular domain, leading to receptor activation and increased affinity for ECM ligands (inside-out signalling) (Figure 3). After being activated, the conformational change arising from the interaction with the ligand enables the clustering of integrin receptors and the intracellular recruitment of a complex network of proteins (outside-in signalling, Figure 3) forming a supramolecular structure called adhesome.[12] The integrin receptor lacks an intrinsic kinase activity,

therefore the signal is propagated by other proteins bound to the cytoplasmic portion of the β subunit, the most important being FAKs (Focal adhesion kinases) and SFKs (Src family kinases). These macromolecules start the transduction pathway by activating, among others, the MAPK ERK (mitogen activated protein kinase ERK) cascade, which is implicated in signals supporting cell survival and cell proliferation.[13] The signalling pathways is further complicated by the cross-talk with other receptors (Figure 3), for instance, EGFR (Epidermal growth factor receptor), IGFR (insulin-like growth factor receptor), PDGFR (platelet derived growth factor receptor), VEGFR (vascular endotelial growth factor receptor) e GFR (growth factor receptor).[14a-15]

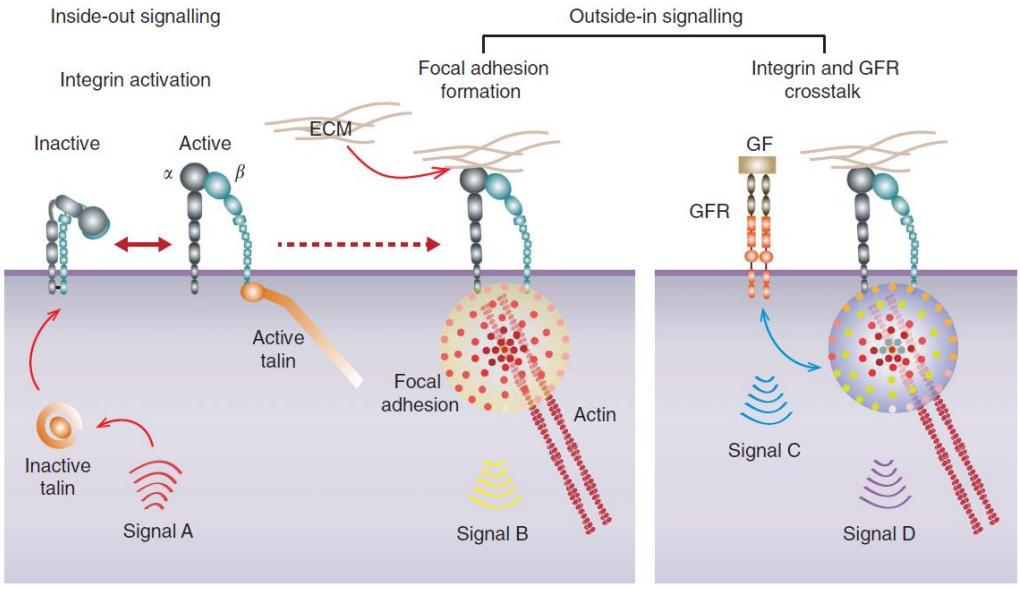

Figure 3 Inside-out signalling, outside-in signalling and GFR crosstalk. After the recruitment of Talin, the receptor undergoes a conformational change with unclasping of the transmembrane domanins of the two subunits (inside-out signalling). After the ligand-binding event, the fully activated integrins start to cluster, via oligomerization of transmembrane domains[16], and the signal transduction cascade begins (outside-in signalling). Signal C derives from the activation of GFR, whereas signal D may arise from the cross-talk with integrins to generate a different transduction cascade.[17]

FAK was recently shown to have many implications in cancer-relevant pathways that lead to cell survival, cell migration, infiltrative behaviour and cell resistance to anoikis, a form of anchorage-dependant programmed cell death that prevents cells from growing and spreading when unconnected to the ECM.[17] Cell survival, metastatic behaviour and anchorage-independent growth were proven to be mediated by FAKs associated with integrins present on the surface of endosomes deriving from the internalization of the activated receptors (Figure 4).[18] This sheds some light on the possible mechanism which enables tumour cells to avoid anoikis during the metastatic spread. FAK, Src and talin, associated with endosomes containing unligated active integrins, are also key players in coordinating cell migration in fibroblasts (Figure 4).[19] In squamous cell carcinoma, FAK was detected in the nucleus where it acts as a scaffold to regulate the transcription of immunomodulatory genes, required to promote tumour tolerance, suggesting a cross-talk between integrins and the immune system (Figure 4).[20]

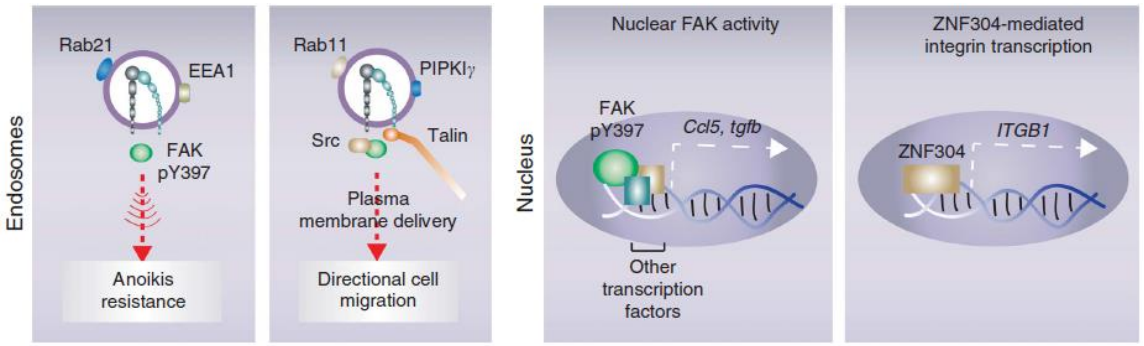

Figure 4 Activated integrin in endosome and FAK nuclear activity.

Activated integrins were also found in tumour intercellular exosomes and they were shown to contribute to cancer horizontal progression[21] and to determine a tissue preference in metastatic spreading. These tumour-secreted exosomes serve to initiate the formation of a premetastatic niche. Furthermore, the biodistribution of these vesicles depends on the type of integrins present on their surfaces. For example, the presence of $\alpha_6\beta_1$ and $\alpha_6\beta_4$ integrins was associated with lung metastasis and the presence of $\alpha_v\beta_5$ integrin is diagnostic of liver metastasis (Figure 5).[22] α_v integrins also regulate the activity of TGF-β1, which was also found in the previously mentioned exosomes, and is implied in the formation of tumour-supportive myofibroblasts from bone marrow mesenchymal cells and in the preparation of the metastatic niche (Figure 5).[22-23] To complicate things even further, the cross-talk between integrins and growth factors (GFs) and GF receptors (GFRs) must be considered in order to fully understand these pathological processes.[24]

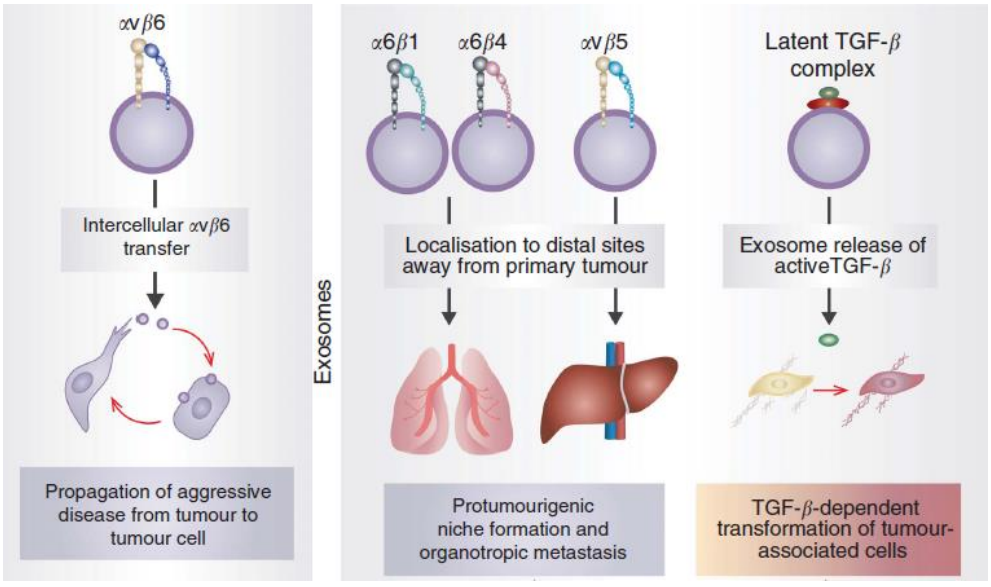

Figure 5 Exosome-mediated horizontal progression, exosomes implication in metastatic spreading and TGF-β role.

These discoveries confirmed the pivotal role of integrins along with novel implications that prompt the study and development of new diagnostic and therapeutic tools targeting the integrinic receptors. Many results have already been achieved (Figure 6), thus confirming the importance of these targets from a medicinal chemistry point of view.

Integrin class	Clinically targeted in?	Main ligands[a]
α4 Family		
α4β1	MS, autoimmune, Crohn's, IBD	VCAM-1, FN
α4β7	MS, autoimmune, arthritis	MAd-CAM-1
α9β1	Cancer	VCAM-1, Opn, VEGF-C,-D
Leukocyte cell adhesion		
αLβ2	Inflammation, psoriasis, stroke, ischemia, fibrosis	ICAM-1,-2,-3
αMβ2	Inflammation, autoimmune	iC3b, Fbg
αXβ2	Inflammation	iC3b, Fbg
αDβ2	Inflammation	ICAM-3, VCAM-1
αEβ7	Inflammation	E-cadherin
RGD-binding		
gpIIbIIIa	Thrombosis, stroke, myocardial ischemia	Fbg, vWf
α5β1	Cancer, AMD	FN
α8β1	None	Npn, FN, VN
αvβ1	Cancer	VN, FN
αvβ3	Cancer, osteoporosis	VN, Opn, vWf, FN, Fbg[b]
αvβ5	Cancer	VN
αvβ6	Fibrosis, transplant rejection, cancer	FN, TGF-β1,-3
αvβ8	Cancer	FN, TGF-β1,-3
I domain: collagen binding		
α1β1	Fibrosis, cancer	Col
α2β1,	Fibrosis, cancer	Col
α10β1, α11β1	None	Col
LN binding		
α3β1	None	LN-5
α6β1,α7β1	None	LN-1, -2
α6β4	None	LN-2, -4, -5

Figure 6 [a]Abbreviations: Col, collagens; Fbg, fibrinogen; FN, Fibronectin; LN, laminin; Npn, nephronectin; Opn, osteopontin; VN, vitronectin; vWF, von Willebrand factor. [b]Among many other ligands.

1.3. $\alpha_v\beta_3$ and $\alpha_v\beta_5$ integrins as therapeutic targets

$\alpha_v\beta_3$ and $\alpha_v\beta_5$ integrins are of interest in the field of drug discovery because of their important role in many biological processes and in many diseases (embryonic development[25-26], cardiovascular disease, cancer[14-27], osteoporosis[28]). These integrins are overexpressed on the surface of different types of tumour cells and on the endothelium of neoangiogenic vessels.[29-30] These receptors were shown to have a primary role in the promotion of metastatic spreading through the binding of MMP-9 (Matrix metalloproteinase-9) and uPAR (urokinase plasminogen receptor)[31], which are enzymes involved in the degradation of the ECM. $\alpha_v\beta_3$ also mediates the binding of tumour cells with platelets and with endothelial cells, thus enhancing cell survival, migration and metastasis.[32] Furthermore, this integrin has a major role in neoangiogenesis, which is the formation of new blood vessels that sustain tumour growth by supplying it with nutrients and oxygen and facilitate metastasis.[33] This process is favoured by metabolic stress, metabolic acidosis, oxidative stress, mechanical stress, inflammatory response, hypoxia and genic mutations. [34] Recently α_v integrins were shown to have a role in the activation of Transforming growth factor β1 (TGF-β1), in endothelial to mesenchymal transition (EMT) and in the maintenance of Cancer stem cells (CSCs). Transforming growth factor β1 (TGF-β1) is a cytokine that can function as both tumour suppressor and tumour promoter. Cancer cells undergo mutations that allow them to withstand the growth-suppressive effects of TGF-β1 and instead the cytokine starts promoting invasiveness and modulating the microenvironment so that it may be suitable for tumour growth (Figure 7).[35]

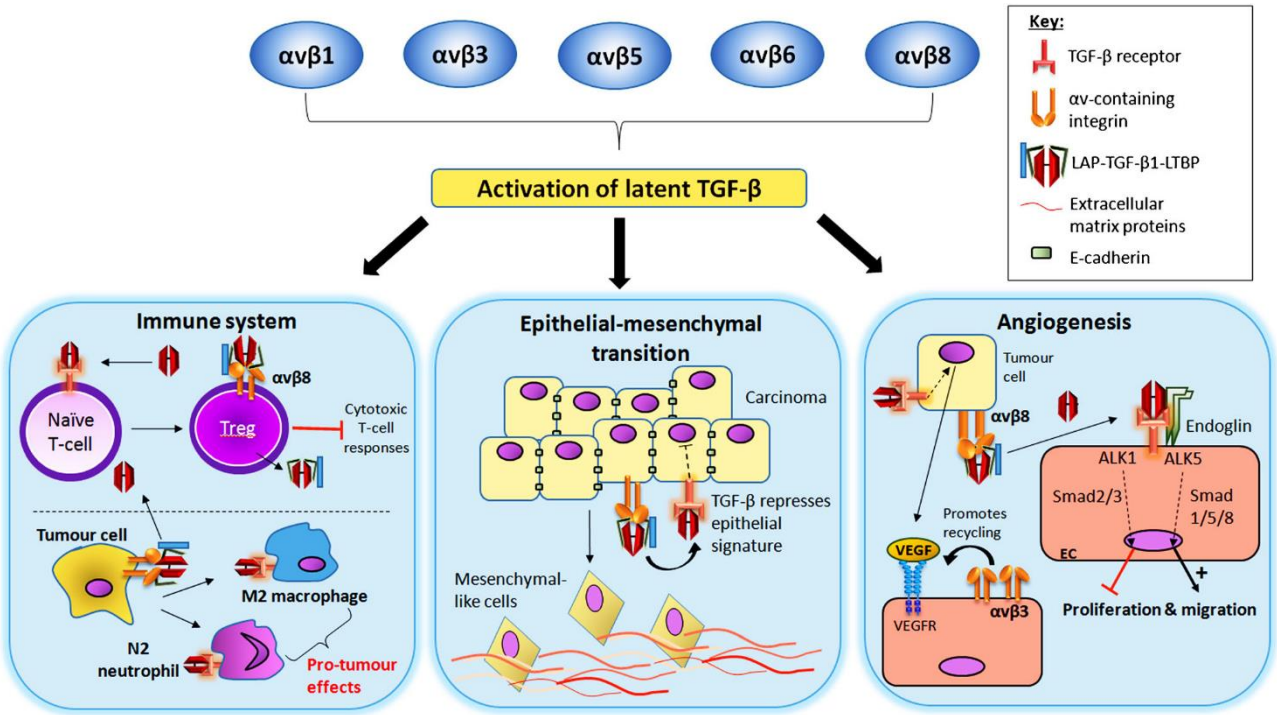

Figure 7 Integrins involved in TGF-β1 activation and role in promoting cancer cells survival

To do so, TGF-β1 promotes the differentiation of fibroblasts into myofibroblasts, responsible for matrix-remodelling, matrix-stiffening and cancer promotion,[36] angiogenesis and epithelial-to-mesenchymal transition (EMT). Endothelial to mesenchymal transition (EMT) is a process during which some cells undergo a transformation that enables them to reduce their adhesion and increase proliferation, motility and invasiveness, thus contributing to the conversion of tumours from low-grade to high-grade malignancy.[37] Integrins are key players in this process because they can activating TGF-β1 (*vide supra*), upregulate chemokine expression and enhance the secretion of tumorigenic soluble factors.[38] Cancer stem cells (CSCs), also known as tumour-initiating cells, are characterized by self-renewing properties and resistance to both chemotherapy and radiotherapy, furthermore, they are thought to be responsible for long-term tumour propagation and metastasis.[39] $\alpha_v\beta_3$ integrin seems to be important for some of the main properties of CSCs, prompting the stemness, the drug resistance, the anchorage-independent survival, self-renewal and tumour initiation properties. For these reasons, the development of novel and more potent integrin antagonists to treat cancer is an area of extensive and continuing research.

In 1984 the RGD sequence (Arginine-Glycine-Aspartic acid) was discovered as recognition motif of $\alpha_v\beta_3$ and $\alpha_v\beta_5$ integrins (and others, *vide supra*) with the components of the ECM.[40] From this starting point, extensive SAR (structure activity relationships) studies were carried out by considering the importance of the different conformations in which the RGD sequence could exist in endogenous ligand, since it was the key point to explain the selectivity showcased by different ECM components for different RGD-binding integrins. Kessler and co-workers were the first to discover an active compound with antagonistic behaviour against $\alpha_v\beta_3$ and $\alpha_v\beta_5$ integrins from a library of cyclopenta- and cyclohexapeptides.[41-42]

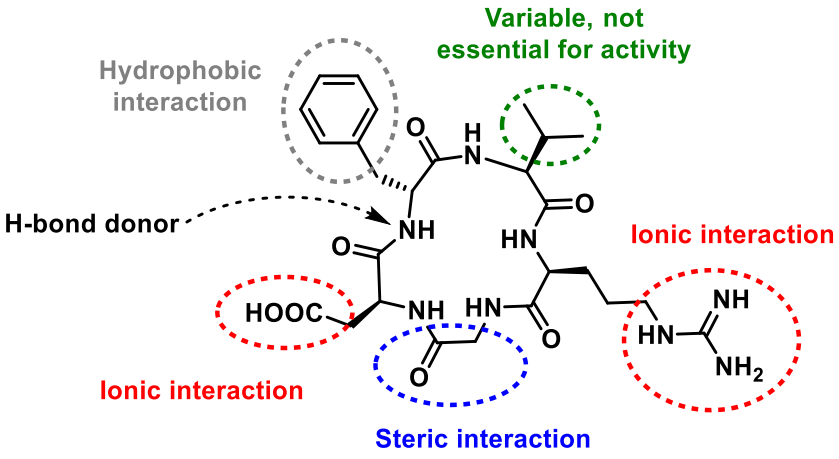

Figure 8 c(RGDfV) and hypothesized pharmacophoric model

In addition to being cyclic compounds, which allowed a drastic reduction of the possible conformations of the peptide backbone and improved the metabolic stability of the compound, the presence of a D amino acid was shown to be mandatory to restrain the cycle in the proper

conformation. The secondary structures required for an optimal interaction with the biological target were shown to be a βII-turn and a γ-turn. This led to the discovery of c(RGDfV) (Arg-Gly-Asp-D-Phe-Val, Figure 8), a cyclopentapeptide which showed good affinity towards the biological targets. SAR studies highlighted the importance of the negatively and positively charged side chains of Arginine and Aspartic acid, the steric interactions of the Glycine residue, the hydrogen bond formed with the D-Phenylalanine's nitrogen and the hydrophobic interactions of the D-Phenylalanine side chain. To further optimize the pharmacokinetic properties, reduce the conformational freedom and improve the affinity towards the biological target, a N-methylation procedure was devised.

Among the different N-methylated peptides, the one showing the best affinity ($\alpha_v\beta_3$ IC_{50}: 0.9-3 nM, $\alpha_v\beta_5$ IC_{50}: 25-37 nM) was *cyclo*(Arg-Gly-Asp-D-Phe-[*N*Me]Val) also called Cilengitide® (Figura 9B).[43] Cilengitide® showed antiangiogenic, anti-metastatic, pro-apoptotic activities, and almost no side effects. It reached phase III clinical trials (CENTRIC), in association with temozolomide and radiotherapy, for the treatment of Glioblastoma (GBM), a frequent and aggressive primary brain tumour with few available therapeutic options.[44] The results of CENTRIC phase III trial showed no improvement of the overall survival and progression-free survival in patients treated with Cilengitide® with respect to patients treated with standard care (radiotherapy in association with temozolomide chemotherapy). Other phase II clinical trials aimed to evaluate the efficacy of Cilengitide® were conducted on patients with other types of cancers, but the results remained substantially unchanged.[45] Furthermore, another study showed that prolonged low plasma concentrations of the drug (0,2-20 nM) favour an increase in cell proliferation and angiogenesis due to an increased recruitment of $\alpha_v\beta_3$ and VEGFR2, responsible for neoangiogenic vessel formation.[46] The agonistic behaviour displayed at low concentrations could be avoided by synthesizing pure antagonists, which, as suggested by a study performed on a mutated form of fibronectin, can be accomplished by introducing an additional aromatic portion to the molecule.[47a] 1a-RGD[47b,c], *cyclo*[DKP-RGD] and *cyclo*[DKP-*iso*DGR][47d] (Figure 9A) are examples of pure $\alpha_v\beta_3$ integrin antagonists, in fact they have shown pure antagonistic behaviour towards the integrinic receptor in *in vitro* biological assays at nanomolar concentrations.

The resolution of integrin $\alpha_v\beta_3$ X-ray structure in free form and bound to Cilengitide®[51], showed the importance of the distance between the carboxylic moiety and the Arginine side chain. In fact, in order to maximize the affinity for this receptor, a smaller distance between these groups is required with respect to other RGD-binding integrins, such as integrin $\alpha_{IIb}\beta_3$. The carboxylic function is required to bind a region of the β subunit called MIDAS (metal ion-dependent adhesion site) through a salt bridge with the divalent cation bound to the integrin (Ca^{2+}, Mg^{2+} or Mn^{2+}), whereas the Arginine binds to the β propeller domain of the α subunit. Although the presence of a carboxylic acid group is mandatory, a genuine guanidine function is not essential. A strict requirement is the proper special arrangement of a basic nitrogen atom mimicking the guanidine function.

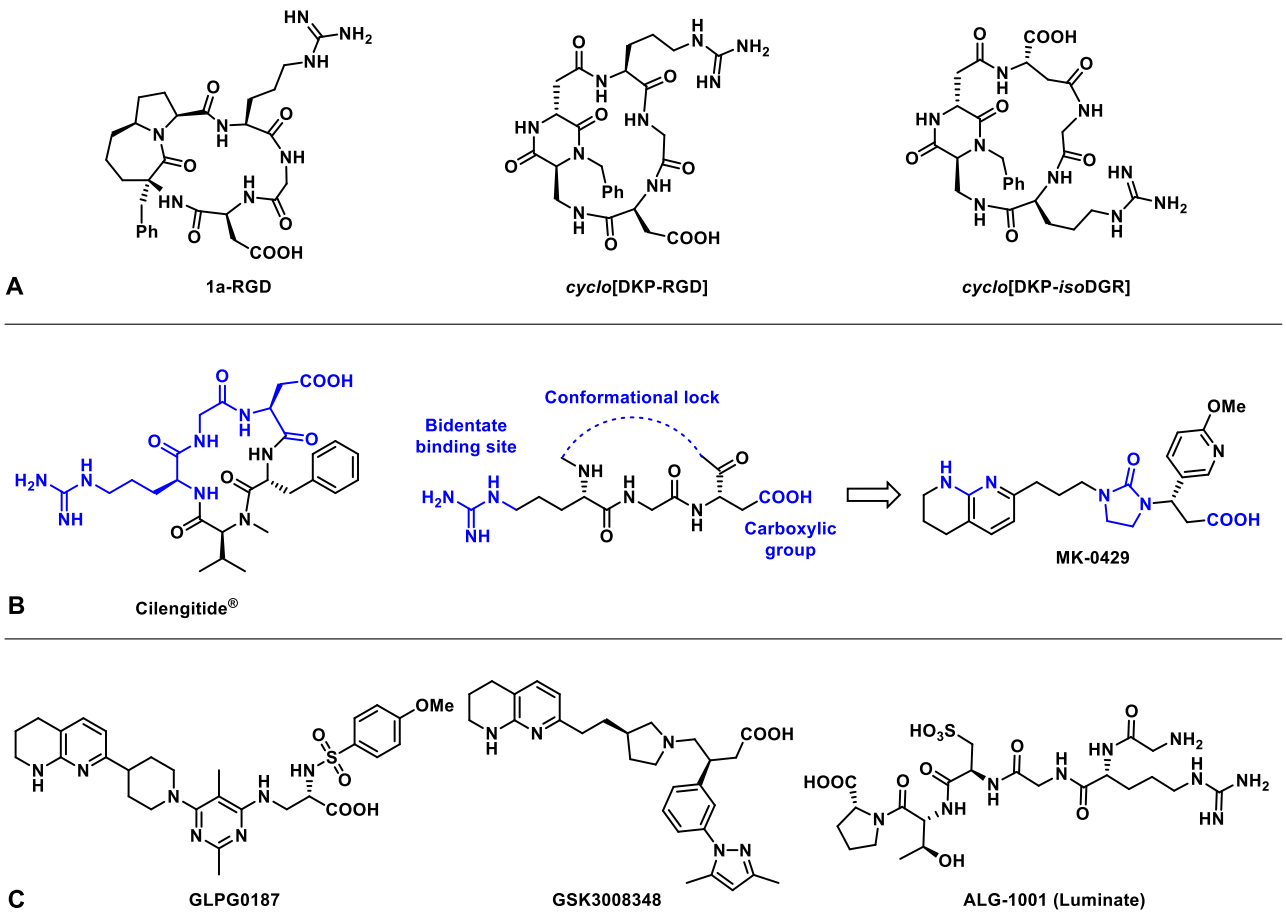

Figure 9 A. 1a-RGD[47b,c], *cyclo*[DKP-RGD] and *cyclo*[DKP-*iso*DGR][47d], integrin $\alpha_v\beta_3$ pure antagonists; **B.** Cilengitide® with RGD Recognition sequence highlighted in blue. Rational drug designed to obtain the non-peptide SMIA (small molecule integrin antagonists) MK-0429 from the RGD recognition motif with highlight on key pharmacophoric elements; **C.** Other $\alpha_v\beta_3$ integrin antagonists that reached clinical trials: GLPG0187[48], a pan-α_v and $\alpha_5\beta_1$ integrins antagonist; GSK3008348[49], multi-α_v, $\alpha_5\beta_1$ and $\alpha_8\beta_1$ integrins antagonist; ALG-1001[50] (Luminate), $\alpha_v\beta_3$, $\alpha_v\beta_5$ and $\alpha5\beta_1$ integrins antagonist.

These considerations led to the development of new orally active non-peptide SMIAs (small molecule integrin antagonists), such as MK-0429 (Figure 9B), a subnanomolar (IC_{50}: 0.08 nM) $\alpha_v\beta_3$ antagonist with additional activity against $\alpha_v\beta_5$ (IC_{50}: 10 nM) and $\alpha_{IIb}\beta_3$ (IC_{50}: 34.7 nM). This compound was originally developed as a drug against osteoporosis[52], but since it showed promising anticancer activity, it reached and completed phase I and II clinical trials for the treatment of solid tumours and showed no safety issues.[53] Other examples of SMIAs targeting integrins $\alpha_v\beta_3$ and $\alpha_v\beta_5$ that reached clinical trials are depicted in Figure 9C and many others are currently in preclinical development.[50b]

Another strategy employed to target integrins relies on the use of antibodies, characterised by several advantages, such as very high potency (typically pM), selectivity and half-life. The main drawbacks consist of low aqueous solubility, limited permeability and high manufacturing cost.

Abciximab is the first integrin-targeting antibody that reached therapeutic market. It is a pan-β_3 inhibitory humanized antibody used in anti-thrombotic therapy. It is used to prevent cloth formation during surgical operations, such as coronary angioplasty, and it was recently registered for the use in unstable angina.[54-55] Another $\alpha_v\beta_3$-targeting monoclonal antibody is Etaracizumab, which

reached phase II clinical trial for the treatment of melanoma and metastatic castration-resistant prostate cancer.[56] Since α_v integrins proved to be interesting targets in cancer treatment because of their role in many tumour associated processes (*vide supra*), this led to the development of antibodies targeting pan- α_v integrins, two examples being Abituzumab and Intertumumab. Intertumumab was tested in phase II clinical trials as monotherapy and as combination with dacarbazine, but it did not display significant efficacy compared to the standard therapy.[57] Another phase II trial was conducted with Intertumumab associated with docetaxel and prednisone and, although tolerability was acceptable, it failed to improve patient conditions.[58] Interestingly, an antibody-drug conjugate (IMGN-388), based on Intetumumab bound to maytansinoid cytotoxic agent DM4, has been investigated in a phase I trial.[59-60] Abituzumab is a humanised antibody that recently underwent a phase I and II clinical trial (POSEIDON trial[61]) in combination with cetuximab and irinotecan for the treatment of K-RAS wild-type metastatic colorectal cancer. It was acceptably tolerated but provided no significant survival benefit. However, the treatment with Abituzumab decreased the chances of death by 59% in patients with high tumour expression of $\alpha_v\beta_6$.[36]

Despite the amount of funds and energies invested in this fields during the last 30 years, very few integrin-targeting drugs have proven to be successful, especially in cancer therapy. These results may be explained by considering the complex biological implications of integrins and the lack of knowledge of all the mechanisms involving these targets. For example, the importance of their expression on the surface of tumour-derived exosomes, their involvement in EMT, and their role in the activation of TGF-β1, were discovered only after the clinical investigation of many of these therapeutic tools.[54] In future, novel approaches to target integrins and to develop more sophisticated therapeutics, along with a deeper understanding of their biological and pharmacological implications, might enable the discovery of therapeutically successful drugs. One of the main focus in this field of research is the design of target delivery systems. In fact, by taking advantage of the overexpression of integrins on tumour cells and on neoangiogenic vessels as well as the relatively low toxicity of integrins antagonists, it may be possible to deliver highly cytotoxic drugs selectively to the site of action, in order to reduce dosage, side effects and to improve therapeutic efficacy.

1.4. Integrin-targeting delivery systems

Cancer therapy currently relies on many therapeutic strategies, such as surgery, chemotherapy, radiation and immunotherapy, either singularly or in combination. Despite the huge improvement witnessed during the past decades, anticancer therapy fails to properly address many issues and complications associated with these diseases, from metastasis to the severe side effects associated with chemotherapy and radiotherapy. Regarding chemotherapy, the efficacy of anticancer drugs is limited due to the lack of selectivity with respect to healthy cells, especially those composing constantly renewing tissues, such as blood, bone marrow, and mucous membranes. Furthermore, because of their genetic instability and heterogenicity, cancer cells often acquire multidrug resistance (MDR), which further reduces therapeutic efficacy.[62] The development of targeted delivery systems seems to be a promising approach to reduce these drawbacks and to improve anti-tumour effects.[63] The idea of therapeutic tools able to selectively carry a toxic agents to the site of action was originally proposed in 1913 by Paul Ehrlich.[64] These systems should be able to selectively deliver the active principle, for example a cytotoxic drug or an imaging agent, to the site of action, allowing the reduction of systemic side effects and an increase of local drug concentration, thus reducing the required dosage.[65] A targeted delivery system is composed of a targeting moiety, typically a small molecule or an antibody with high selectivity towards the target (IC_{50} at least in nM range), a linker and the bioactive compound, or a more complex nanostructure carrying the drug (Figure 10). The biological targets of these systems must be highly expressed on tumour cells or on neoangiogenic vessels. Their expression must be low or close to zero on healthy cells and it should also undergo internalization following ligand-binding event through receptor-mediated endocytosis, so that the cytotoxic payload can be released into the intracellular environment.[66-67] $\alpha_v\beta_3$ and $\alpha_v\beta_5$ integrins are ideal targets for this type of strategy because of their overexpression on the surface of many tumour cell types and on neoangiogenic vessels.[29-30] Furthermore integrin receptors can undergo internalization following the interaction with a ligand.[68]

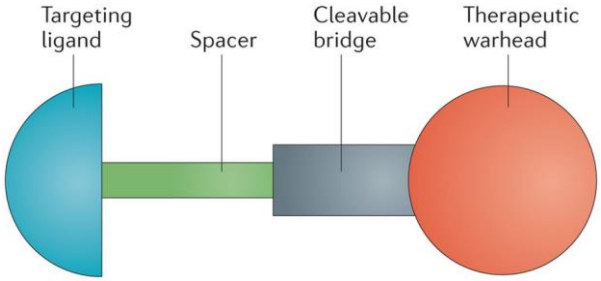

Figure 10 Schematic representation of a targeted delivery system.

1.4.1. Antibody-drug conjugates

Antibody-drug conjugates (ADCs) are targeted delivery systems that exploit antibodies as homing device because of their high affinity (typically pM) and selectivity for their biological targets. Humanized and human monoclonal antibodies (hmAbs) are usually preferred to secure longer half-life and reduced immunogenicity.[69] The FDA approved three ADCs in the past decades: gemtuzumab ozogamicin (Mylotarg®)[70] in 2000 for CD33-positive acute myelogenous leukemia, brentuximab vedotin (Adcetris®)[71] in 2011 for CD30-positive relapsed or refractory Hodgkin's lymphoma and systemic anaplastic large cell lymphoma and trastuzumab emtansine (Kadcyla®) in 2013 for HER2-positive breast cancer (Figure 11).[72] Mylotarg® was withdrawn from the market in 2010 due to a lack of clinical benefit and higher toxicity with respect to standard chemotherapy.[73] There are currently more than 50 ADCs in 125 clinical trials in at least 50 phase I/II studies in patients with solid tumors.[66] This confirms the importance and the growing interest in the development of these therapeutic systems.

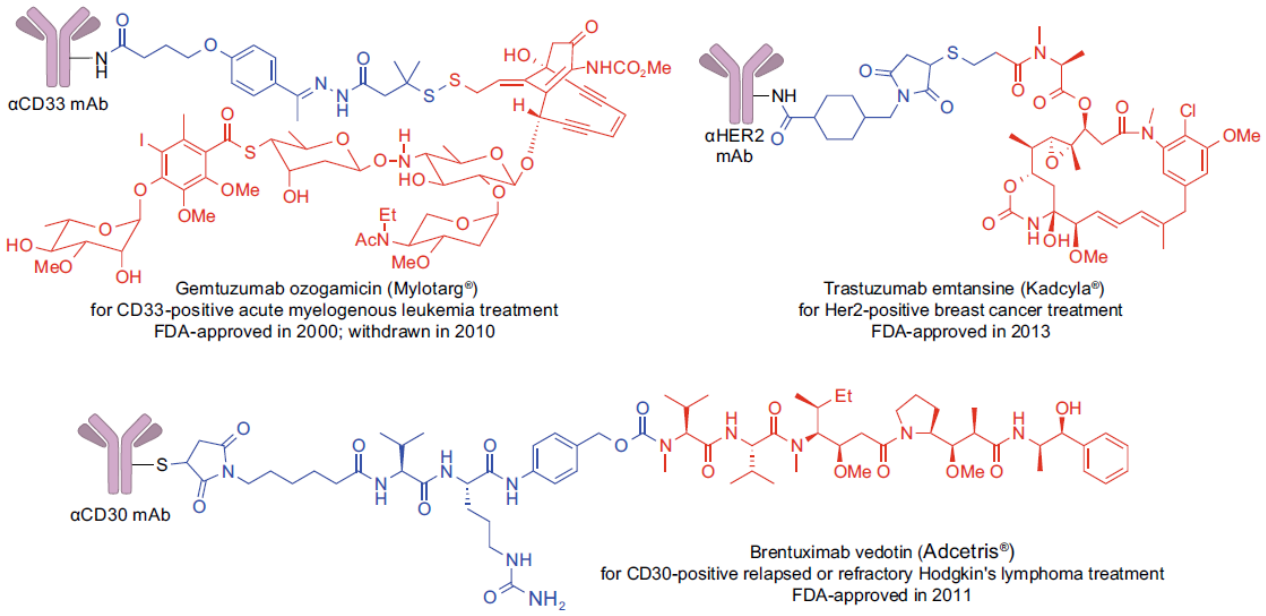

Figure 11 FDA approved ADCs. Linkers and spacers are highlighted in blue and payloads in red.

Because of the high targeting index of antibodies, this approach might currently be the best one to avoid systemic side effects caused by standard chemotherapy.[74] The mechanism of action exploits the highly selective binding of the antibody with its antigen, which should be abundantly and uniquely expressed on the surface of target cells, afterwards the ADC must be internalised to ensure the intracellular release of the cytotoxic component.[75] It is important to assess the ability of the ADCs to be internalised, since the absorption and release of the payload depend on this process.[76] It's important for the cytotoxic agent to be potent at low concentrations, intrinsically more selective for tumour cells and stable in aqueous environment, as well as at low pH, to increase its availability

at the tumour site and to prevent damages to healthy cells.[69-77] The only integrin ADC tested in a phase I clinical trial is IMGN-388, composed of the pan-α_v integrin-targeting antibody intetumumab bound to maytansinoid through a disulphide linker.[59-78]

Despite all the promising premises, ADCs suffer from different drawbacks:

- Their oral availability is very limited, therefore these therapeutics must be administered through parenteral injections.
- Because of their polarity and molecular weight, their penetration in the tumour tissue is highly unlikely, even though neoangiogenic vessels are highly porous[79], and the effect called "binding site barrier" further impedes extravasation.[80] This effect is mainly caused by the high affinity of antibodies for their targets, which restrict the possibility of reaching internal sites of the tumour. For these reasons ADCs demonstrated poor efficacy towards hypoxic regions or tissues with lower vasculature.[81] A possible way to reduce this limitation is to conjugate drugs with good permeability and highly potent cytotoxicity (in pM range).
- The conjugation chemistry is problematic for ADCs, since there may be different reactive sites on the antibody and the drug-antibody ratio (DAR) is a crucial parameter for the overall system's efficacy. High DAR can increase aggregation, clearance rate and may induce unselective release of the payload. A viable solution would be to incorporate a hydrophilic linker, which would prevent aggregation.[69] Furthermore, Lysine coupling, the most common and simple method to achieve conjugation, cannot be a first-choice procedure because some of the potentially available Lysine residues present in an antibody, may be essential for antigen recognition. For these reasons Cysteine are usually employed for the synthesis of ADCs. Another interesting approach that would allow better control of the DAR is the introduction of unnatural amino acids in the antibody sequence. For example, amino acids modified with the addition of a carbonyl functionality may be used to form oxime, whereas the presence of a side chain containing an azide or a double bond may be suitable for further conjugation through copper-catalysed "click chemistry" reactions or Pd-catalysed couplings and Ru-catalysed metathesis. In the case of "click chemistry" reactions, constrained cyclooctynes can be exploited to avoid the presence of copper.[69] Enzymatic conjugation is also a possibility to functionalise the antibody in a site-selective manner and to achieve a highly predictable and reproducible DAR.
- Some studies showed that only a residual part of the administered ADC (from 1.56% to less than 0.01%) can effectively enter the target cells.[82]
- Antibodies are expensive drugs and the manipulations required to obtain the final bioconjugates further increase production costs.

Despite these limitations, ADCs are a viable solution to improve anticancer therapy, as demonstrated by the amount of clinical trials currently ongoing.

1.4.2. Small molecules-drug conjugates targeting $\alpha_v\beta_3$ and $\alpha_v\beta_5$ integrins

Small molecule-drug conjugates (SMDC) are targeted delivery systems in which the targeting moiety is a small molecule. Because of their favourable pharmacokinetic properties, these therapeutic devices represent a possible alternative to ADCs.[83] Unlike the latter, the overall hydrophilicity of a SMDC is easier to assess and optimize, furthermore its lower molecular weight would allow higher tumour penetration and increased extravasation. Moreover, conjugation chemistry is easier to perform and control on small molecules and the overall production costs would be lowered. The biggest shortcoming of these bioconjugates is the lower targeting index (T.I.) with respect to that of ADCs (T.I. = 1000-2000)[84]. The targeting index considers the SMDC's selectivity (S_{SMDC}) towards cells with different target's expression (cell line A and cell line B) and the intrinsic selectivity ($S_{free\ drug}$) of the unconjugated cytotoxic drug.[83]

$$T.I. = \frac{S_{SMDC}}{S_{free\ drug}} \qquad S = \frac{IC_{50}(Cell\ line\ A)}{IC_{50}(Cell\ line\ B)}$$

To improve the TI, an accurate design of the linker is mandatory and may be the key to overcome this issue. The linker is an important component of a bioconjugate, either in SMDC or in ADC, ideally it should be stable enough for the drug-conjugate to reach the site of action intact and it should be readily cleaved within the tumour environment or after internalization to selectively release the drug. Linkers can be divided in two main categories: cleavable and non-cleavable. Cleavable linkers are designed to allow further control on the release of the cytotoxic component, they usually respond to specific stimuli and can be categorized accordingly.

Since tumour cells intracellular environment is acidic because of the higher metabolic activities[85], pH responsive linkers have been developed to exploit the pH shift. The most common acid-labile linkers are based on the presence of an hydrazone moiety, which is stable at physiological pH, but is readily hydrolysed following the cellular uptake of the bioconjugate. The reactivity of these functional groups must be properly tuned and tested, since they may undergo unselective cleavage in the blood stream, as in the case of Mylotarg®[86], leading to the onset of systemic side effects. Other viable options are cis-aconityl, imine, trityl, β-thiopropionate, N-Mannich base, ester and acetal.[87] An example of RGD-based bioconjugate incorporating a pH sensitive linker, is RGD4C-DOX, in which RGD4C is the $\alpha_v\beta_3$ integrin-targeting ligand and doxorubicin is linked to the rest of the molecule through a N-Mannich base (Figure 12).[88]

Another class of linkers exploits the difference in redox potentials between the intracellular environment and the serum; this is caused by the presence of cytoplasmic redox enzymes and higher concentrations of glutathione.[89]

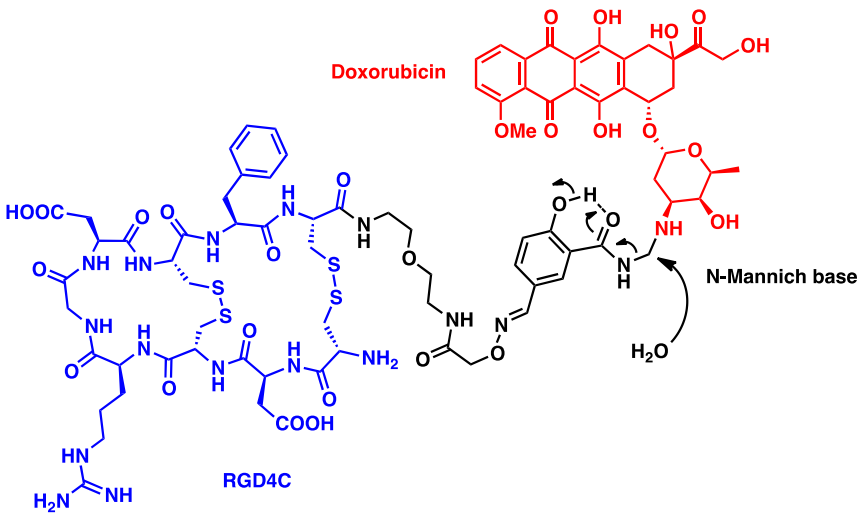

Figure 12 Hydrolysis mechanism of RGD4C-DOX bioconjugate. The targeting moiety (RGD4C, in blue) is linked to the linker through an amide bond and doxorubicin (in red) is attached to the linker via a N-Mannich base.

By introducing reducible moieties into the linker, it is possible to promote a selective reductive cleavage inside target cells. Disulphide bonds are the most used functionalities for this purpose and are especially useful for the synthesis of ADCs (*vide supra*). An example of theranostic SMDC incorporating a red-ox sensitive linker is cyclo[RGDyK]-camptothecin bioconjugate (Figure 13). This $\alpha_v\beta_3$ integrin-targeting bioconjugate was designed to simultaneously release a cytotoxic compound (camptothecin) and an imaging agent (naphthalenimide) that undergoes a red-shift in fluorescence caused by the linker's cleavage, allowing to monitor the internalization and reduction of the disulphide function.[90]

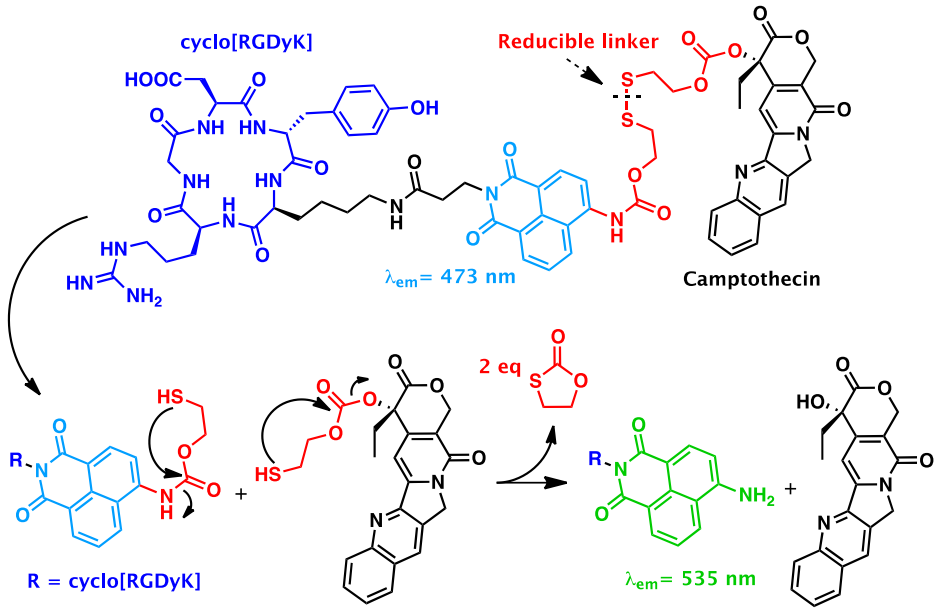

Figure 13 Cleavage mechanism of *cyclo*[RGDyK]-camptothecin. After *cyclo*[RGDyK] (in blue) binds the target, the conjugate is internalized and the sulphide bridge of the linker (in red) is cleaved. The thiol groups can perform intramolecular nucleophilic attacks on the carbamate function and the carbonate group to release the free drug (in black) and naphtalimide (light blue to green). The latter changes emission wavelength following the liberation of the free amine.

One of the most used and promising strategies involves the incorporation of functional groups or amino acidic sequences specifically recognised by enzymes, such as proteases. Usually proteolityc enzymes are not very active in the blood stream[91]; therefore endosomal and lysosomal proteases can selectively cleave the linker following internalization. Many sequences recognised by these enzymes and by matrix metalloproteinases (MMP) have been reported.[92] MMP, particularly MMP-2 and MMP-9, are expressed on tumour cells and their activation is mediated by integrin $\alpha_v\beta_3$. These proteases are known to have a role in cell migration and metastatic spreading.[31-93] This strategy was adopted for the linker portion of different *cyclo*[DKP-RGD]-PXT conjugates (Figure 14). The amino acidic sequences were recognised by many lysosomal enzymes, especially cathepsin B. The SMDC with the Phe-Lys sequence did not exhibit high selectivity (T.I.= 2.1), whereas the bioconjugate containing the Val-Ala sequence showed a very promising targeting index (T.I.= 9.0).[94] Along with Phe-Lys and Val-Ala, another commonly used sequence is the Val-Cit (valine-citrulline). These linkers are also among the most successful for ADCs.[95]

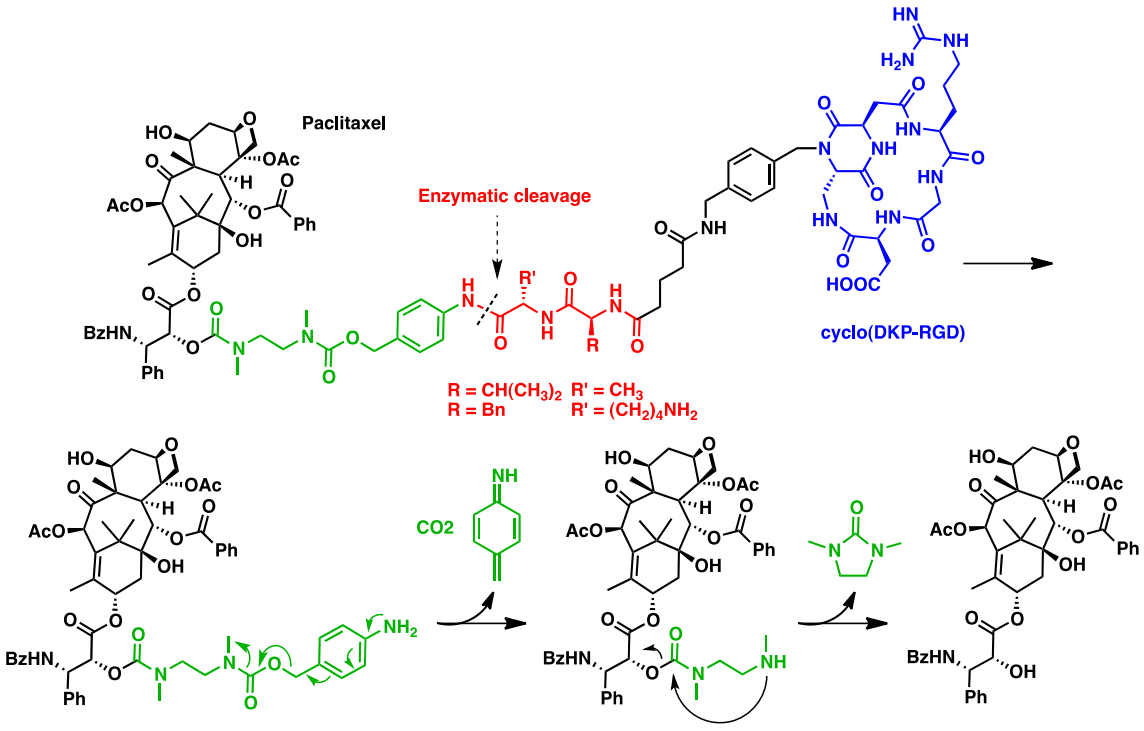

Figure 14 Cleavage mechanism of *cyclo*[DKP-RGD]-PTX. After *cyclo*[DKP-RGD] (in blue) binds the target, the conjugate is internalized and the recognition sequence (in red) is cleaved by lysosomal enzymes. The spacer-PABC moiety (in green) undergoes self-immolative degradation to free the PTX-spacer prodrug. The terminal amino group of the spacer performs an intramolecular nucleophilic substitution to release free PTX.

As seen in the previous examples, spacers can have an active role in the drug releasing process. These portions serve the purpose of reducing the steric hindrance that would result from a direct attachment of the active principle to the targeting moiety through the cleavable function alone. The spacer could alter the properties of the conjugated drugs; therefore, it is preferable for it to undergo self-immolative degradation following the cleavage of the stimuli responsive portion. The previously reported PABC (*p*-aminobenzyl alcohol, Figure 14) is one of the most common self-immolative spacers.[87] Most of the self-immolation mechanisms are based on the release of a nucleophile after

the cleavage. Afterwards, the reactive functional group may attack an electron-deficient carbon and release the drugs, which acts as leaving group. Spacers can also serve the purpose to improve pharmacokinetic properties or to reduce the hydrophobicity of the bioconjugate, for instance hydrophilic PEG (polyethylene glycol) chains are commonly used as spacer, especially in ADCs, to improve solubility and reduce aggregation phenomena.[67-96]

Non-cleavable linkers offer greater chemical stability during the manufacturing processes and improved metabolic stability, but often fail to efficiently release the drug following internalization. Non-cleavable linkers are effective when the drug does not require to be freed to exhibit its biological effects.[97] ^{99m}Tc-Maraciclatide (also known as ^{99m}Tc-NC100692, Figure 15) is a SPECT (single positron emission tomography) imaging agent in which the Tc-chelating moiety is bound through a non-cleavable linker to the RGD antagonist, since the degradation of the linker is not required to trigger the desired effect.[98] This bioconjugate is currently in phase II clinical trial to determine $\alpha_v\beta_3$ integrin expression in skeletal metastases from breast cancer, prostate cancer, and myeloma.[99] Antiangiogenic therapy is difficult to monitor, because it does not cause a sensible reduction of the tumour mass in a short time span. By evaluating the expression of neoangiogenic markers, such as $\alpha_v\beta_3$ integrin, through targeted delivery of imaging agents, it may be possible to assess the efficacy of anti-angiogenic therapies.

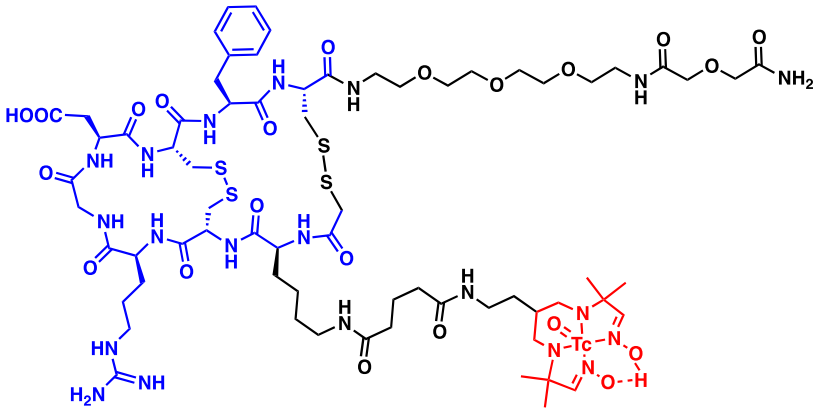

Figure 15 Integrin-targeting moiety highlighted in blue, imaging portion in red.

Another advantage of non-cleavable linkers, when the conjugated drug does not require to be released in order to exhibit its desired effects, is to reduce MDR (multi drug resistance). In fact, it is possible to modulate the hydrophobicity of drug-linker to prevent it from becoming substrate of multidrug transporters, which cause an efflux of the drug from the target cell.[76]

Extensive research is still needed to develop new and more efficient linkers as well as new SMDCs to improve overall efficacy and targeting index of these tools. It is important to design the linkers while evaluating the expected efficacy of the cleavage method with respect to the biological target of choice as well as the compatibility with the drug that is going to be conjugated, since, as previously mentioned, the linker highly affects pharmacokinetic and pharmacodynamic properties of SMDCs or ADCs.

1.4.3. $\alpha_v\beta_3$ and $\alpha_v\beta_5$ integrin-targeting in nano-delivery systems

Integrin antagonists were exploited in the development of functionalised nanocarriers for the target delivery of nanostructured materials carrying a bioactive compound. The use of nano-delivery systems allows the presence of multiple targeting molecules on its surface, thus improving targeting through the increase of ligand-target interactions. The drug is usually adsorbed, absorbed or encapsulated in the nanostructure, thereby improving its pharmacokinetic properties by reducing its metabolism, minimizing its contact with physiological medium, improving its solubility, and preventing non-specific interactions. The dimensions of the carrier system favour internalization through endocytosis and prevent fast renal excretion, thus increasing the overall half-life. These systems accumulate in tumour sites through passive targeting because of the higher extravasation thanks to the abnormal permeability of neoangiogenic vasculature; this phenomenon is called EPR (enhanced permeability and retention).[65]

Furthermore, since solid tumours usually lack lymphatic vessels, elimination of the nanocarriers from the microenvironment is prevented, thus increasing the accumulation in the site of action.[100] Integrin-targeting nano-delivery systems may also find applications in gene therapy to deliver DNA or RNA fragments to avoid safety issues caused by using viral vectors.

Nanocarriers can have different chemical nature, such as polymeric, proteins-based and inorganic. Polymer based vehicles are the most commonly used nanomaterials, especially polypeptide-based and phospholipids-based, due to their relatively low toxicity and biodegradability. They are well known and can be structured in different manners, such as liposomes, micelles, nanoparticles or nanocapules, through well-known procedures. Drugs can be easily encapsulated or reversibly chemically bound to the structure and they can be easily modified to modulate their properties, for example, nanoparticles can be PEGylated to improve their water solubility and reduce detrimental protein interaction in plasma.[65-101-102]

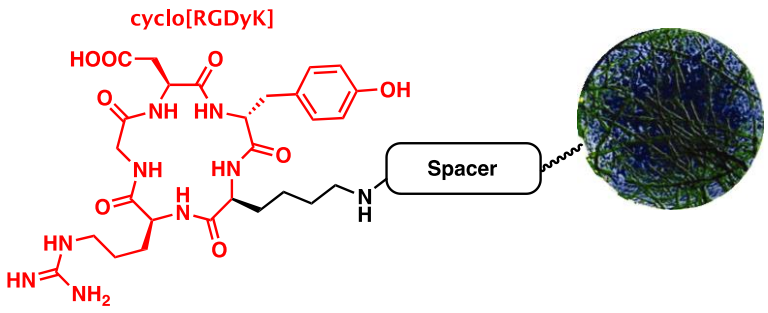

Figure 16 Integrin antagonist *cyclo*[RGDyK] (in red) linked to an albumin nanoparticle through a non-cleavable linker.

Protein-based nanoparticles are a viable alternative to polymeric structures, because of the lower toxicity, better biocompatibility and higher water solubility. For example, albumin is one of the most used proteins for this purpose and it was used to develop an RGD-based nano-delivery system exploiting *cyclo*[RGDyK] as targeting moiety and Gemcitabile as payload (Figure 16).[103] The

conjugation led to successful targeting as well as improved intracellular uptake, as demonstrated by fluorescence studies.

There are several examples of integrin-targeting inorganic nanoparticles in literature.[65-101-102] Although the toxicity profile of inorganic nanostructures is more concerning with respect to other materials, the easier production and their unique properties make them an interesting option as nano-carriers. For example, gold nanorods conjugated to *cyclo*[RGDyK] through thiol chemistry have been tested *in vitro* for plasmonic photothermal therapy (PPTT).[104] Integrin-targeted Graphene oxide nanoparticles were also tested for photoablation *in vitro* and displayed no cytotoxicity in absence of irradiation.[105] Unfortunately there are still major drawbacks to overcome in this field of research:

- The above-mentioned EPR effect is often overestimated, due to high variability of the vasculature's and tumour's properties.[106]
- Animal models are misleading, since neovasculature permeability is further increased because of the faster tumour growth.[107] Penetration of a nanocarrier deep into tumour tissues is prevented by high cellular density and interstitial fluid pressure.[108] A possible solution involves the use of stimuli responsive nanocarriers that release the drug upon extravasation.
- Active targeting does not seem to improve tumour concentrations of nano-system significantly, probably because of the binding-site barrier effect.[107-109]
- The targeting moiety can cause enhancement of immunogenicity, which reduces half-life and concentrations at the desired site.
- Another major problem involves metastasis, due to the fact that these tools are extensively experimented and developed for solid tumours. To improve efficacy of nanomedicine against metastatic tumours it is possible to deliver chemotherapeutics to sentinel lymph nodes or to activate the immune systems. For this reasons polymeric nanoparticles made of HPMA (N-(2-hydroxypropyl)methacrylamide) and containing doxorubicin and a human immunoglobulin (Dox-HPMA-HuIg) have been developed and tested.[110] This nano-delivery system showed increased activation of NK (natural killer) cells and LAK (lymphocyte activated killer) as well as improvement in patients' clinical conditions.

Despite these drawbacks, nano-delivery systems are still key players in the field of drug delivery because of the enhanced cellular uptake, the lower toxicity displayed *in vivo* and the improved efficacy of radiochemotherapy and chemotherapy combinations.[107]

2. Results and discussion

2.1. Introduction to the work

2.1.1. Azabicyloalkane scaffolds and 1a-RGD

The conformational properties of peptidomimetics and peptide drug candidates are pivotal features to ensure successful drug design. An important class of secondary structures, especially for an optimal recognition with the integrinic receptors, are reverse turns, structural motifs that cause directional changes in the polypeptide backbone. Reverse turns are stabilized by intramolecular hydrogen bonds and can be divided into two categories (Figure 17):

- γ-turn, which are characterised by a hydrogen bond between the carbonyl oxygen of a residue (*i*) and the amide hydrogen of an amino acid 2 residue apart (*i*+2), forming a 7-membered cycle;
- β-turn, which are characterised by a hydrogen bond between the carbonyl oxygen of a residue (*i*) and the amide hydrogen of an amino acid 3 residue apart (*i*+3), forming a 10-membered cycle;

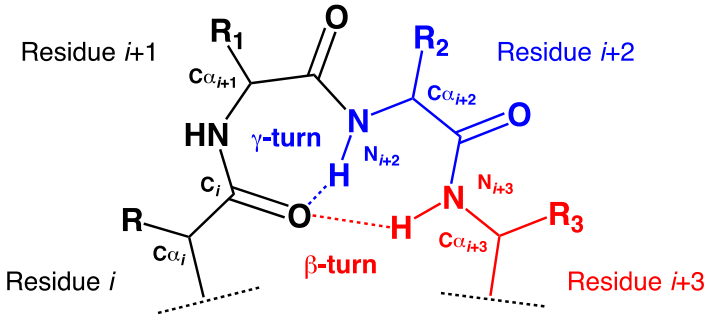

Figure 17 β-turn stabilized by a hydrogen bond between the carbonyl group of residue *i* and the amide group of residue *i*+3 (in red). γ-turn stabilized by a hydrogen bond between the carbonyl group of residue *i* and the amide group of residue *i*+2 (in blue).

Azabicycloalkane scaffolds have shown to be efficient reverse turn inducers in many biologically active small molecules and, among them, 7,5- and 6,5-fused systems are useful intermediates for the synthesis of many biologically active compounds requiring conformational constrains in order to exhibit their activity.[111] Furthermore, the presence of a rigid and stable scaffold can improve the pharmacokinetic properties of the peptidomimetic with respect to an unmodified peptide chain. For example, these classes of compounds include integrins $\alpha_v\beta_3$ and $\alpha_v\beta_5$ antagonists[112], Smac mimics/XIAP inhibitors[113], Bradykinin B2 receptor antagonists[114], Thrombin and factor VIIa inhibitors[115], prostaglandin $F_{2\alpha}$ receptor modulators and Tachykinin NK-2 receptor antagonists. Furthermore, Indolizin-5(1H)-one is a structural motif frequently found in many biologically active natural alkaloids.[116] Professor Colombo and co-workers developed a $\alpha_v\beta_3$ and $\alpha_v\beta_5$ integrins antagonist selected from a small library of constrained cyclic pentapeptides incorporating different azabicycloalkane scaffolds as reverse turn inducers and the RGD recognition sequence.[112] **1a-RGD** (Figure 18), characterised by the presence of the 7,5-fused bicyclolactam **1a**, turned out to be the

most promising RGD antagonist of the library. The absolute configuration of the quaternary stereocenter at the C3 carbon of the lactam ring is pivotal for an optimal interaction with the biological target.

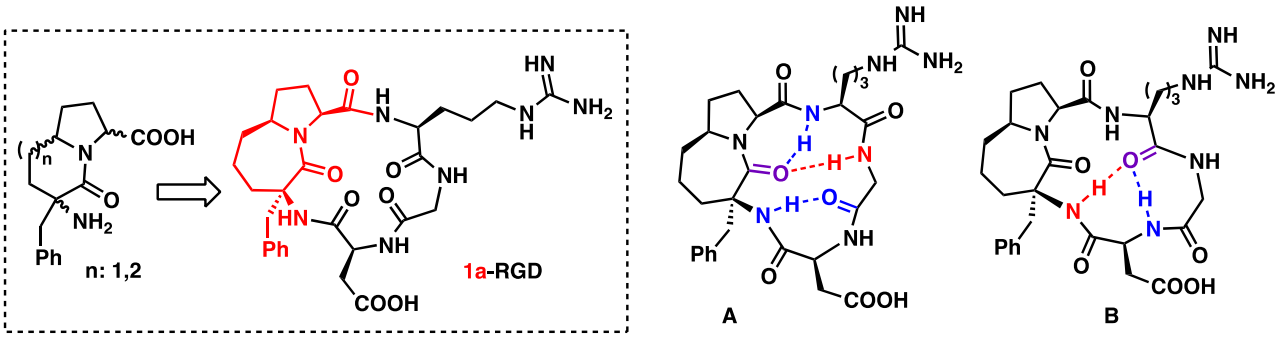

Figure 18 Bicyclic lactams scaffolds general structure, **1a-RGD** (scaffold **1a** highlighted in red) and hydrogen bonds network in the two main conformations (A and B) of **1a-RGD** in solution (determined by NMR spectroscopy). β-turns and γ-turns are highlighted in red and blue. The carbonyl moiety is coloured in purple if involved in both.

NMR studies showed that the RGD moiety can exists in two main conformations, stabilized by different hydrogen bond patterns. In one of the two conformers a hydrogen bond is formed between the carbonyl group of the Gly residue and the nitrogen bound to the quaternary stereocenter of the scaffold, which means that a γ-turn could be formed. Alternatively, the peptide chain may form a β-turn stabilized by the hydrogen bond between the amide group of the Gly residue and the carbonyl of the lactam ring. A second γ-turn is established through the formation of a hydrogen bond involving the amide nitrogen of the Arg residue and the carbonyl of the 7-membered ring ("A" in Figure 18). In the second conformation the peptide backbone forms a β-turn stabilised by the hydrogen bond of the amide NH adjacent to the quaternary stereocenter and the carbonyl group of the Arg residue. A γ-turn is also formed between the carbonyl function of the Arg residue and the amide group of the Asp residue ("B" in Figure 18). Docking studies were performed to evaluate binding with integrin $\alpha_v\beta_3$ and, by comparison with Cilengitide®**.** The calculations were performed starting from the three representative cyclopeptide backbone conformations of **1a-RGD** (γ-(Gly)/β(Gly-Asp), Invγ(Asp)/β(Gly-Asp), Invγ(Asp)/β(Pro-Arg)) obtained from computational studies (free-state molecular mechanics conformational searches and molecular dynamics simulations). The results showed retention of all the main interactions inside the binding pocket. **1a-RGD** proved to be a nanomolar inhibitor of $\alpha_v\beta_3$ and $\alpha_v\beta_5$ integrins in [^{125}I]Echistatine displacement assays. The measured IC_{50} were 6.4±0.1 nM and 7.7±0.04 nM respectively.[112] Further pharmacological studies showed that **1a-RGD** can reduce cell viability, proliferation, adhesion and migration in glioblastoma cell lines. **1a-RGD** was also capable of inducing cytoskeleton disassembly, FAK inhibition and anoikis.[47b] On the basis of these encouraging results, **1a-RGD** would be a good candidate for the development of novel RGD-based bioconjugates incorporating **1a-RGD** as targeting moiety. To do so, the synthetic scheme had to be revised to introduce a functional group exploitable for conjugation in an appropriate position.

2.1.2. *Functionalised bicyclic lactams, previous results*

In order to preserve the conformational features of **1a-RGD** and, consequently, to retain its binding properties, the functionalisation of the scaffold had to be performed in a position that wouldn't affect the spatial arrangement of the RGD sequence. An alkenylarylamide side chain at the C5 position of the lactam ring was chosen as spacer between the integrin antagonist and the conjugation site, leading to the development of **2a-RGD** and **2b-RGD** as study compounds (Figure 19).

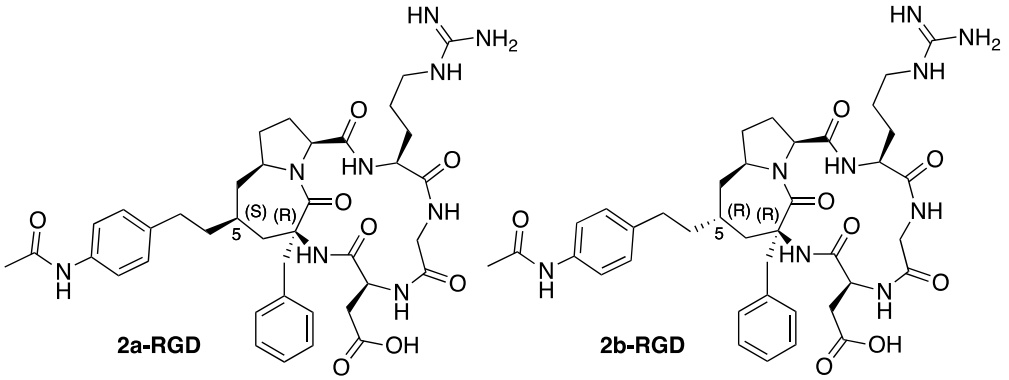

Figure 19 2a-RGD and **2b-RGD** with absolute configuration of stereocenters at C3 and C5.

Computational calculations on the two modified cyclopentapeptides demonstrated the suitability of that anchoring point, since the conformation of the recognition sequence wasn't influenced by the presence of the side chain in that position. The first approach developed allowed the modification of scaffold **1a** with a vinyl moiety, characterised by synthetic versatility, stability and the limited steric requirements (Scheme 1).[117]

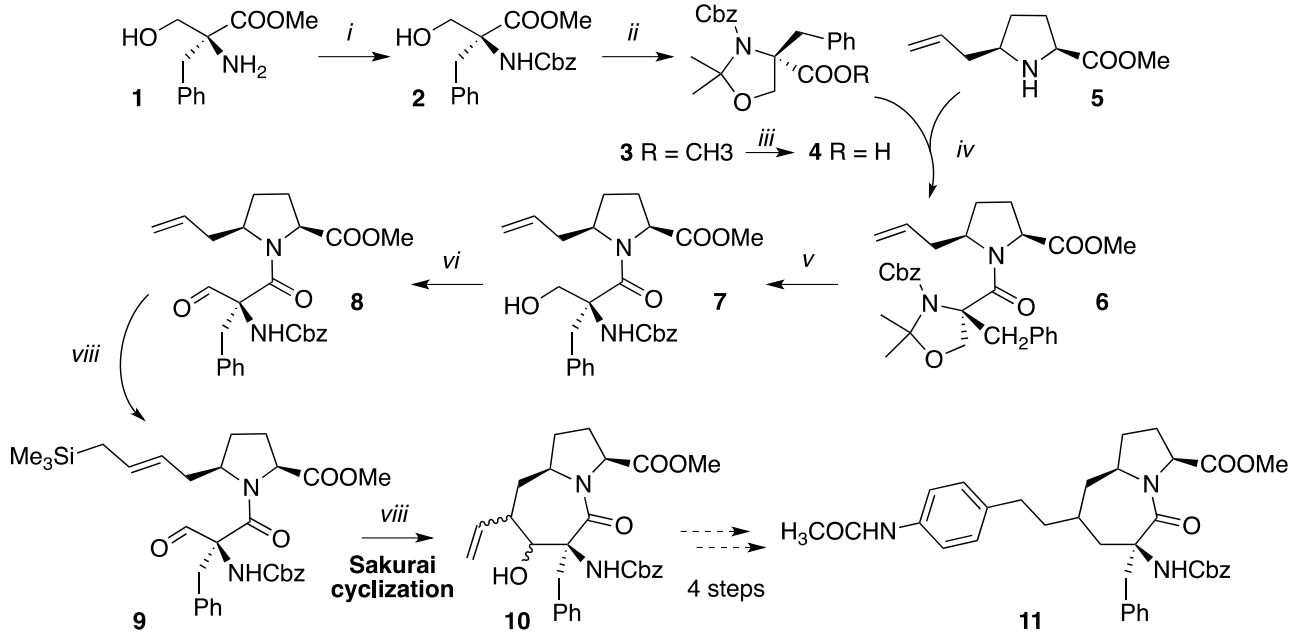

Scheme 1 Reagents and conditions: *i*) $(Cbz)_2O$, THF, 0°C, 15 min, y: 95%; *ii*) DMP, TsOH, benzene, reflux, 4 h, y: 94%; *iii*) LiOH, THF–H_2O–MeOH, rt, 24 h, y: 92%; *iv*) PyBroP, DIPEA, DMAP, CH_2Cl_2, rt, 24 h, y: 85%; *v*) $Bi(OTf)_3$, CH_3CN, rt, 10 min, y: 86%; *vi*) $(COCl)_2$, DMSO, TEA, CH_2Cl_2, –60 °C → 0 °C, 2 h, y: 88%; *vii*) allyltrimethylsilane, HG2, DBBQ, CH_2Cl_2, reflux, 8 h, y: 84%; *viii*) $Sc(OTf)_3$, CH_2Cl_2, -10 °C then *rt*, 5 h, y: 86%.

The key reaction of the synthetic scheme is an intramolecular Sakurai reaction that allowed the attainment of scaffold **10** functionalised with a double bond moiety. Compound **11** was readily obtained after 4 more steps and underwent the RGD binding procedure to afford **2a-RGD** and **2b-RGD**. Biotinylated vitronectin displacement assays showed retention of affinity toward $\alpha_v\beta_3$ integrin, with an IC_{50} of 16,3 ± 2,7 nM for **2a-RGD** and 9,3 ± 5,6 nM for **2b-RGD** (Table 1).

Molecule	$\alpha_v\beta_3$ IC_{50} (nM)
2a-RGD	16,3 ± 2,7
2b-RGD	9,3 ± 5,6
1a-RGD	3,3 ± 0,1
c(RGDfV)	3,2 ± 1,3

Table 1

Another approach to install an exocyclic olefin on the 7-membered ring was developed in order to reduce the number of steps required for the previously mentioned synthetic sequence. Furthermore, the feasibility of the functionalisation in a different position, *i.e.* the C6 of the lactam ring, was explored (Scheme 2).

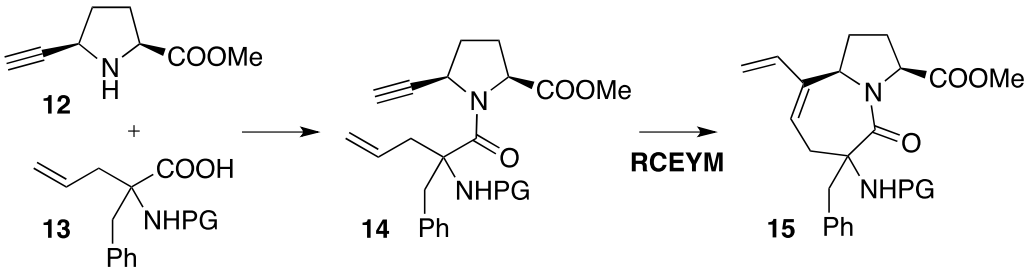

Scheme 2 Synthetic approach for the synthesis of C6-functionalised bicyclic lactam scaffolds

Through a ring-closing enyne metathesis (RCEYM) it would be possible to convert in one step the dipeptide **14** into the cyclic diene **15** substituted with an exocyclic double bond at the C6 carbon. At first the synthesis of the two precursors, 5-ethinylproline **12** and α-allyl quaternary α-amino acid **13**, was developed.[118]

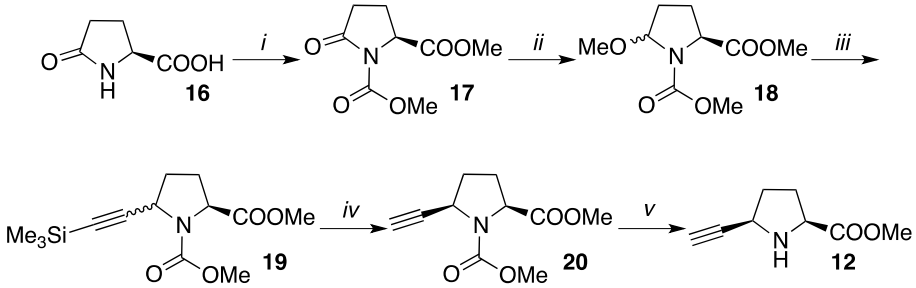

Scheme 3 Reagents and conditions: *i*) a. $SOCl_2$, MeOH, 0 °C → rt; b. NaHMDS, $ClCO_2CH_3$, THF, −78 °C → 0 °C, y: 83%; *ii*) a. $LiEt_3BH$, THF, −78 °C; b. $CH(OCH_3)_3$, PPTS, MeOH, y: 90%; *iii*) bistrimethylsilylacetylene, $SnCl_4$, $AlCl_3$, CH_2Cl_2, −45 °C → rt, **19a** (2S,5R) y: 41%, **19b** (2S,5S) y: 34%; *iv*) TBAF, THF, −20 °C → 0° C, y: 90%; *v*) TMSI, CH_2Cl_2, 65 °C, y: 78%.

Compound **12** was synthesized from L-pyroglutammic acid **16** (Scheme 3) in 5 steps. Protection of the amino and carboxylic groups of compound **16** as methyl carbamate and methyl ester respectively, afforded compound **17**, that was converted into the aminal **18** through reduction with $LiEt_3BH$ and subsequent treatment with $CH(OCH_3)_3$ (trimethyl orthoformate) in the presence of an acid catalyst. Compound **19** was attained through addition of bis(trimethylsilyl)acetylene in presence of two Lewis acids. After chromatographic purification, compound **19a** was converted to 5-ethinylproline methyl ester following deprotection of the trimethylsilyl group and the methyl carbamate.

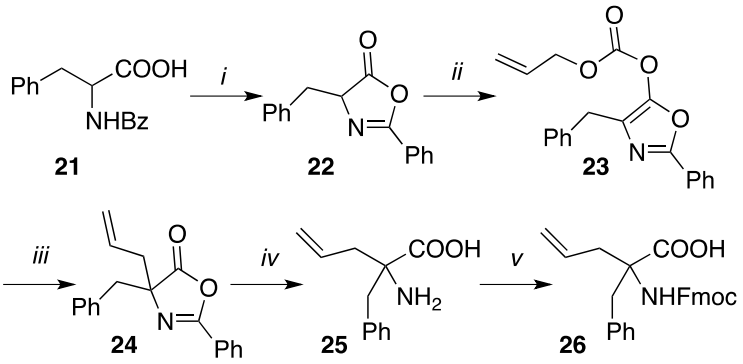

Scheme 4 Reagents and conditions: *i*) DCC, CH_2Cl_2, 0 °C y: 80%; *ii*) Allyl chloroformate, Et_3N, THF, 0 °C y: 96%; *iii*) $Pd_2(dba)_3$*$CHCl_3$, 1,2-bis(diphenylphosphino)ethane (dppe), THF, y: quantitative; *iv*) TFA, 100 °C, y: quantitative; *v*) Fmoc-Cl, $NaHCO_3$, THF/H_2O, y: 45%.

Racemic compound **26** was synthesized from N-benzoyl phenylalanine as depicted in Scheme 4. Compound **21** was converted to the corresponding azlactone **22** by DCC-mediated (N,N'-dicyclohexylcarbodiimide) cyclodehydration and subsequently enolized and allylated with allyl chloroformate to afford allyl enol carbonate **23**. The key Tsuji decarboxylative allylation was performed in presence of $Pd_2(dba)_3$ (Tris(dibenzylideneacetone)dipalladium(0) chloroform adduct) and bis(diphenylphosphino)ethane (dppe) to obtain compound **24**. The final N-Fmoc α-allyl quaternary α-amino acid was obtained through TFA-mediated (trifluoroacetic acid) ring opening of the azlactone **24** and subsequent protection with Fmoc-Cl (9-Fluorenylmethyl chloroformate). The two building blocks **12** and **26** were condensed in presence of BOP-Cl (bis(2-oxo-3-oxazolidinyl)phosphinic chloride) to afford compound **27** in 45% yields on a gram scale. Although compound **27** proved to be unreactive towards ring-closing enyne metathesis (RCEYM), in presence of a styrene derivative underwent a Ru-catalysed *domino* cross-enyne metathesis/ring-closing metathesis (CEYM/RCM) (Scheme 5). The proposed mechanism is an exo yne-then-ene process. Different styrene derivatives were tested in the optimisation steps and it was possible to directly attach in a one-pot the alkenylarylamide spacer bearing a suitable functional group for the conjugation step, thus reducing time and costs of the process. The best results were obtained by slowly adding a solution of HG2 (Hoveyda Grubbs 2nd generation catalyst) to the reaction mixture in 7 hours with the aid of a syringe pump.[118] The reaction was highly stereoselective for the formation of the exocyclic double bond, as only the E isomer of both diastereoisomeric compounds with

opposite configuration on the quaternary C3 position were obtained after chromatographic separation. The following reaction sequence, aiming at preparing the scaffold for the RGD binding procedure, was carried out on compound **32a**, characterized by "R" absolute configuration at C3 position.

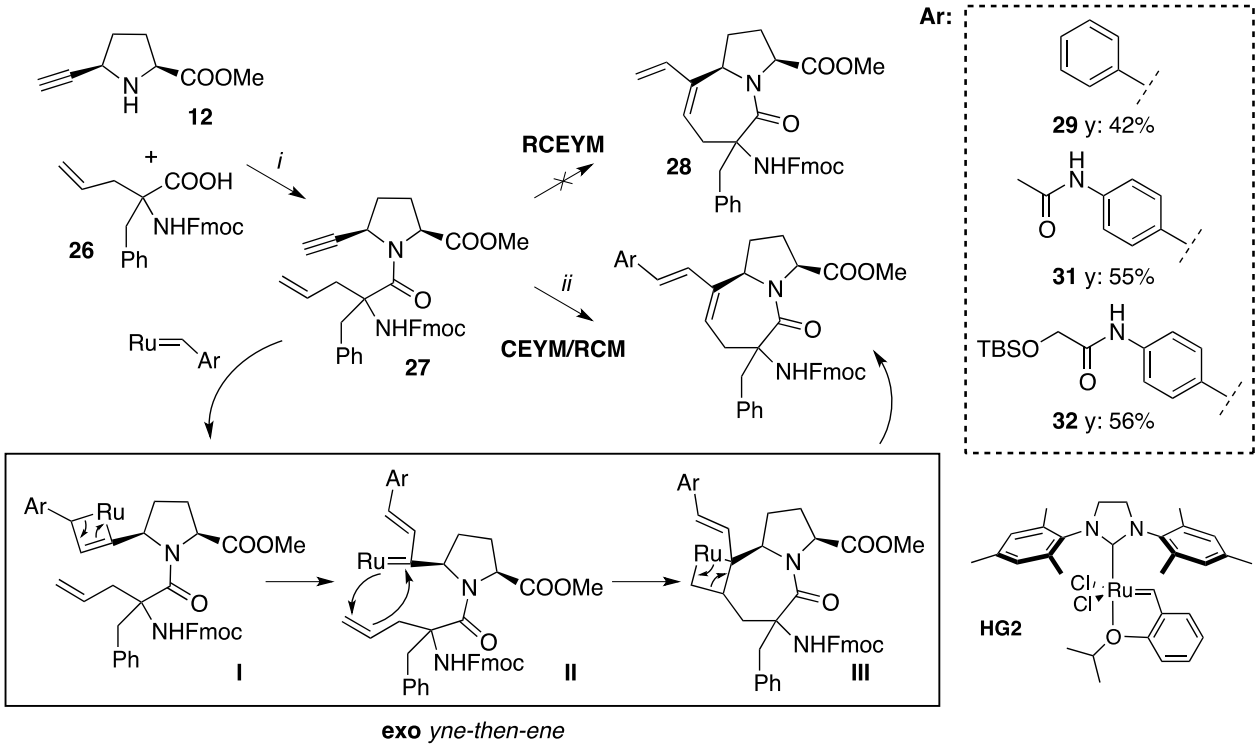

Scheme 5 Reagents and conditions: *i*) BOP-Cl, THF, 70 °C, y: 45%; *ii*) Styrene derivative, HG2 (10% mol, slow addition in 7 h), Toluene, 80 °C.

Compound **32a** was treated with H_2 in presence of Pd/C (en) (Pd/C ethylenediamine complex) to selectively reduce the diene moiety, thus preventing OTBS cleavage. Interestingly, compound **33** was obtained as a single diastereoisomer. Afterwards, the newly obtained compound **33** was converted to the Cbz (benzyloxycarbonyl) protected scaffold **34**, which is suitable to undergo the RGD-binding procedure (Scheme 6).

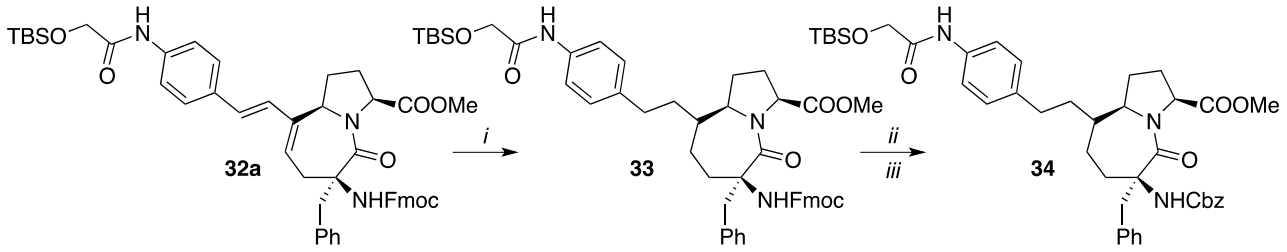

Scheme 6 Reagents and conditions: *i*) H_2, Pd/C (en) (10% mol), MeOH, y: 77%; *ii*) piperidine, THF; *iii*) Cbz-Cl, DMAP, THF, y: 66% (over two steps).

2.2. Synthesis of first generation 1a-RGD-based bioconjugates

Part of the work described in this Chapter was published in the following article:

- Massimo Serra, Elena Giulia Peviani, Eric Bernardi, Lino Colombo *Journal of Organic Chemistry,* **2017**, *82*, 11091–11101.

2.2.1. Aim of the work

The final aim of this project is the development of an efficient synthetic scheme that could allow the attainment of RGD-based bioconjugates incorporating scaffold **1a**. Preliminary computational studies have been performed to confirm the retention of the conformational requirement of the newly obtained bicyclic system. N-acetyl-N-methylamide dipeptide analogues **36a** and **36b**, differing for the absolute configuration at C6, were used to assess reverse-turn inducing capabilities. The presence of the capping groups on the N and C-termini mimics the presence of the amide bond of the peptide chains linked to the scaffold. The preferred conformations of each stereoisomeric scaffold were compared to the structures of compound **35**, a derivative of scaffold 1a. **36a** and **36b** showed retention of all the conformational properties of scaffold **35** (Figure 20).

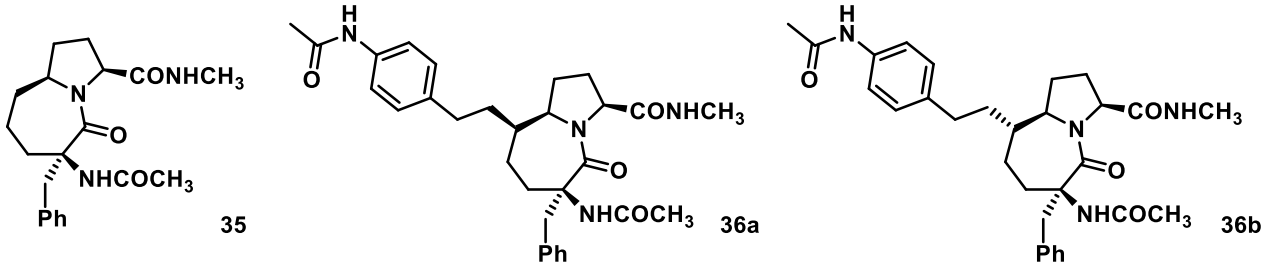

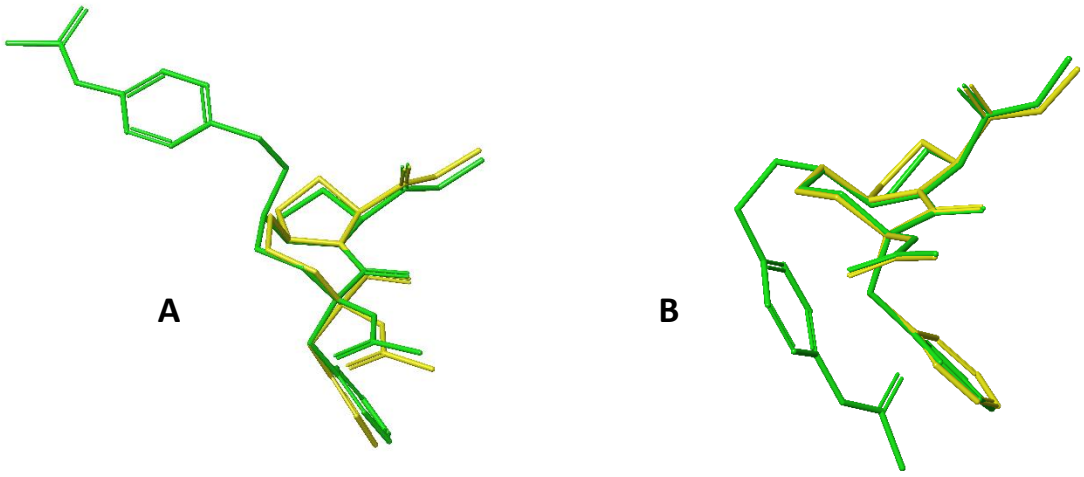

Figure 20 A: superposition of minimum energy conformer of **35** (yellow) with **36a** (green). **B**: superposition of minimum energy conformer of **35** (yellow) with **36b** (green).

The first part of the project was the optimisation of poorly yielding reactions, such as the protection of the amino group of the α-allyl quaternary α-amino acid (Scheme 4, step *v*) and the condensation between building blocks **12** and **26** (Scheme 5, step *i*). Afterwards, the RGD binding protocol has to be performed and optimised on the newly obtained scaffold **34**, starting from a known procedure.[112] Once obtained, the new cyclopentapeptide should be tested in conjugation reactions with non-cleavable linkers to assess the reactivity of the side chain and the most suitable conjugation method. For instance, after complete deprotection of the RGD antagonist, the hydroxyl group of the side chain can be converted to an azide, exploitable for a "click chemistry" reaction (Huisgen (2+3) Cycloaddition) to bind a linker or a bioactive compound. Non-cleavable linkers are characterised by high chemical stability; therefore they are relatively simple substrates to handle. The final goal of this work is to synthesise first generation bioconjugates characterised, for example, by the presence of a fluorescent probe to better evaluate the behaviour of **1a-RGD** in biological assays. (Scheme 7)

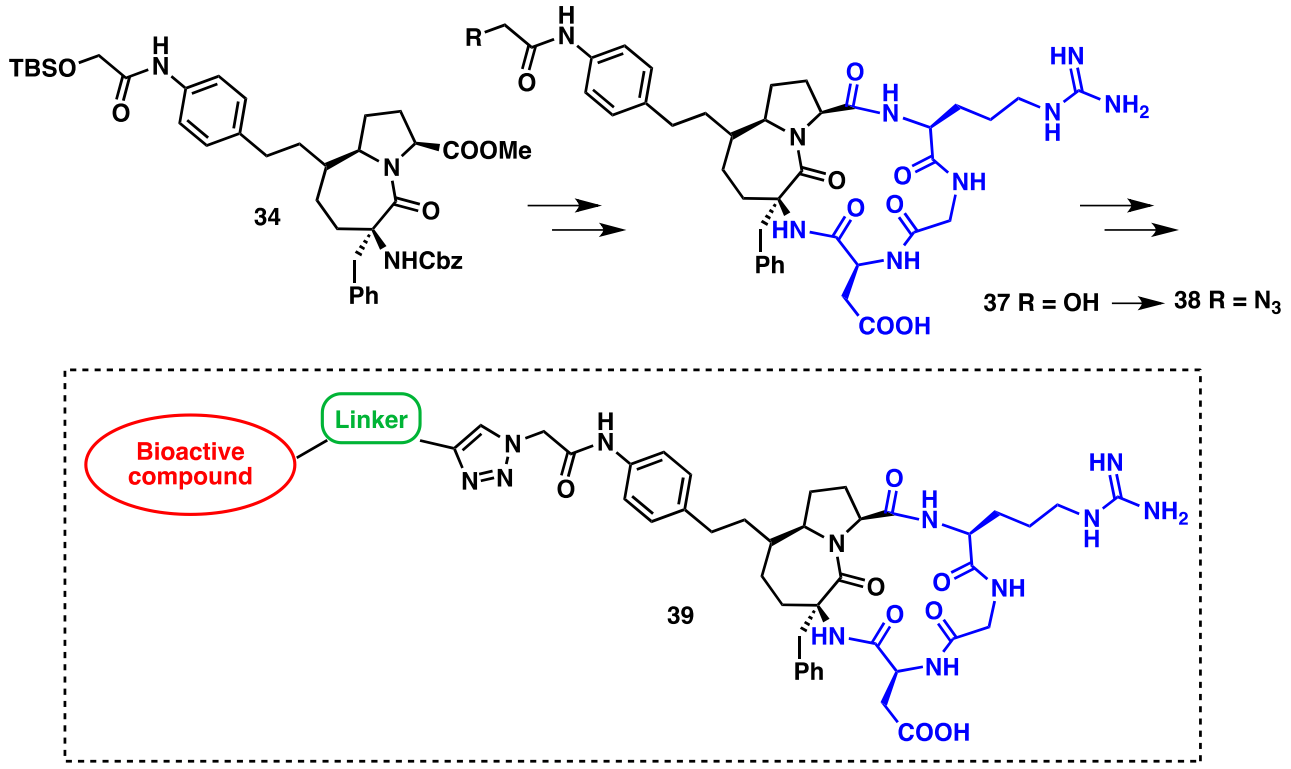

Scheme 7

2.2.2. *Precursor's synthesis optimisation*

The first reaction examined was the N-protection of quaternary amino acid **25**. The low conversion to the protected product was probably caused by the poor reactivity of the unnatural amino acid, allowing a faster reaction of the reagent Fmoc-Cl with water, thus reducing the efficiency of the process. A way to solve the problem would be avoiding water in the reaction mixture. Following a literature procedure[119], the carboxylic group of the amino acid was silylated by treatment with TBSCl (*tert*-Butyldimethylsilyl chloride) for 8 hours in CH_2Cl_2 under reflux. Afterwards, the reaction mixture was cooled at 0°C and added with Fmoc-Cl and DIPEA (N,N-Diisopropylethylamine). Chromatographic purification afforded the product in quantitative yields (Scheme 8).

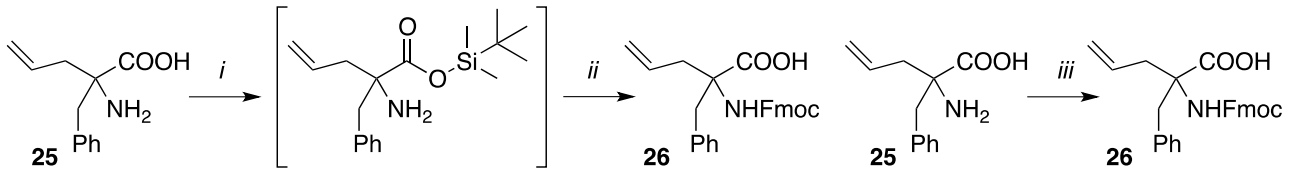

Scheme 8 Reagents and conditions: *i*) TBSCl, CH_2Cl_2; *ii*) Fmoc-Cl, DIPEA, CH_2Cl_2, y: quantitative; *iii*) Fmoc-OSu, Na_2CO_3, THF/H_2O, y: quantitative.

Since the method tested was time consuming and expensive, another approach was experimented to further improve the efficiency of the process. By reacting amino acid **25** with Fmoc-OSu in presence of Na_2CO_3 in H_2O/THF, the product was obtained in quantitative yields. This could be explained by the higher water-stability of Fmoc-OSu (N-(9-Fluorenylmethoxycarbonyloxy)-succinimide) with respect to Fmoc-Cl (Scheme 8). The condensation between N-Fmoc protected amino acid **26** and ethinylproline **12** have been tested during a previous project (Scheme 9).

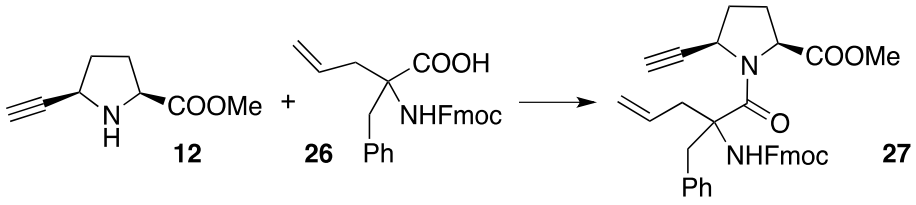

Scheme 9

After an extensive screen of condensing agents and solvents, BOP-Cl showed the best results using THF as solvent, but the yield resulted quite low. Therefore, a study of the other reaction parameter was performed (Table 2). The presence of a sterically hindered tertiary amine as base turned out to be detrimental, leading to the partial cleavage of the Fmoc protecting group as evidenced by the small amount of isolated product and the concurrent formation of the deprotonated amino acid (Table 2, entry 1). 1-[Bis(dimethylamino)methylene]-1H-1,2,3-triazolo[4,5-b]pyridinium 3-oxid hexafluorophosphate (HATU) and 3-(diethoxyphosphoryloxy)-1,2,3-benzotriazin-4(3H)-one (DEPBT) were also tested under these conditions, but similar problems aroused, suggesting that a weaker base was needed to improve the conversion. A proton scavenger resin (Tetraalkylammonium carbonate, polymer-bound) was added to the reaction mixture in order to neutralise the acidity

developing during the reaction but, at the same time, decrease the rate of deprotonation of the acid fluorenyl hydrogen, responsible of the Fmoc deprotection (Table 2, entry 4 and 5). The yield improved, but not quantitative although TLC analysis suggested complete conversion of the amino acid. By heating through microwave irradiation (Table 2, entry 6) the yields dropped dramatically. To investigate the reasons behind these results, the resin was washed with an acidic solution and it was noted that the amino acid was partially adsorbed on the polymer, probably through an ion-exchange mechanism. To avoid this issue, instead of the carbonate-based resin, solid sodium bicarbonate was added to the reaction mixture (Table 2, entry 7) to increase pH without inducing Fmoc cleavage. When sodium bicarbonate was added portion-wise to correct pH variations, the product was isolated in 70% yields (Table 2, entry 8). This result was confirmed to be reproducible on a gram-scale.

Entry	Condensing agent	Temperature (°C)	Solvent (0.05M)	Base	Time	Yield
1	BOP-Cl	50	THF	DIPEA	24 h	20%
2	DEPBT	35	THF	DIPEA	48 h	N.R.
3	HATU	50	DCE	DIPEA	48 h	20%
4	BOP-Cl	50	THF	Proton scavenger	24 h	54%
5	BOP-Cl	50	THF	Proton scavenger	36 h	55%
6	BOP-Cl	80 (MW)	THF	Proton scavenger	4.5 h	20%
7	BOP-Cl	50	THF	$NaHCO_3$	24 h	53%
8	BOP-Cl	50	THF	$NaHCO_3$	48 h	70%

Table 2

Before implementing the RGD binding procedure, the configuration of the stereocenter at position C6 of the lactam ring in compound **33** had to be evaluated. The NMR spectrum of compound **33** was complicated by the presence of conformers, therefore the configurational assignment was performed on compound **34**, where the N-Fmoc protecting group was replaced by a N-Cbz group. An HSQC-DEPT experiment allowed the assignment of the proton bound to C6 among the complex signals of the alkylic protons, since it is the only one bound to a tertiary carbon (Figure 21). Afterwards, a COSY and a NOESY experiment were performed (Figure 22). There is a NOE between H_6 and H_7 diagnostic for the absolute configuration at C6, in fact when protons face opposite directions in these systems, no magnetization transfer occurs, as Lubell and co-workers reported for similar compounds.[120] Furthermore it is interesting to note that there is no COSY coupling between H_6 and H_7, which could be explained by assuming that the coupling constant between the two protons is low due to a dihedral angle close to 90° between them, which is more plausible for two protons with similar orientation (Figure 22). This led to believe that the configuration of the stereocenter should be *R*.

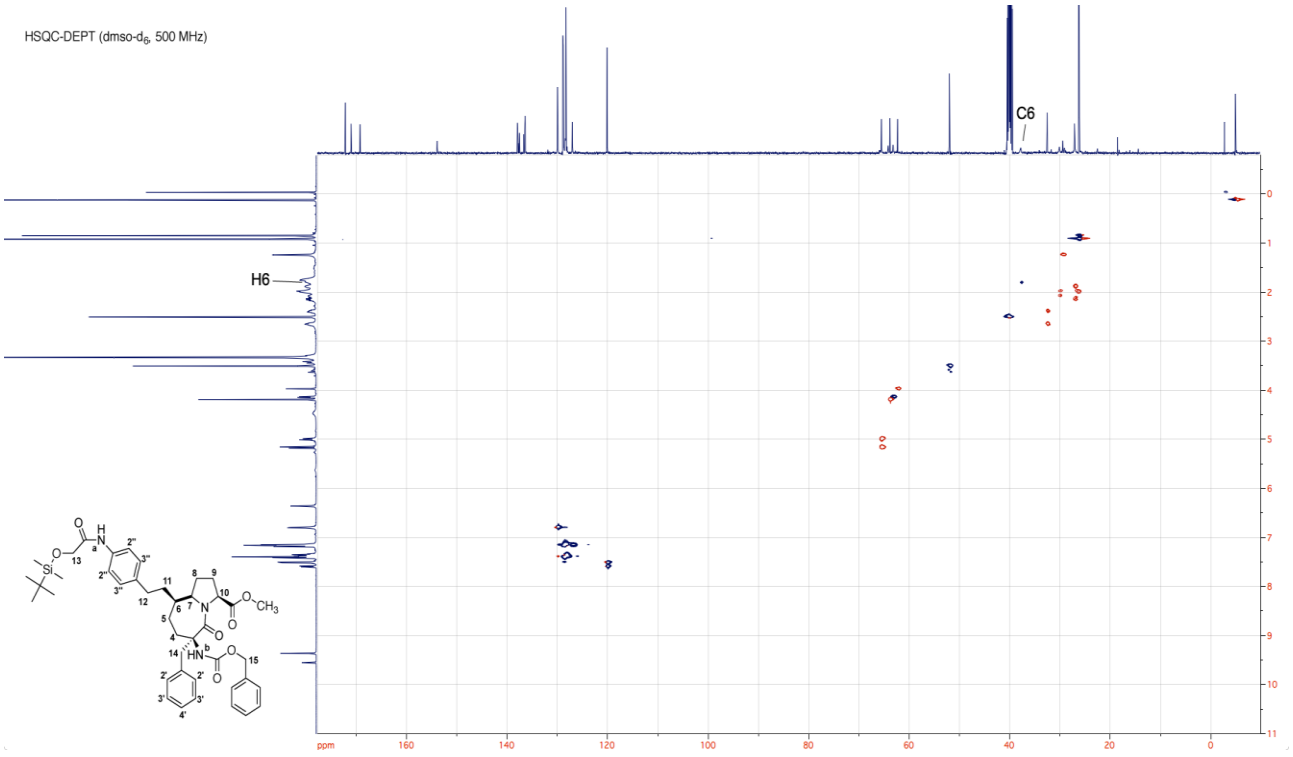

Figure 21 HSQC-DEPT (dmso-d_6 500 MHz).

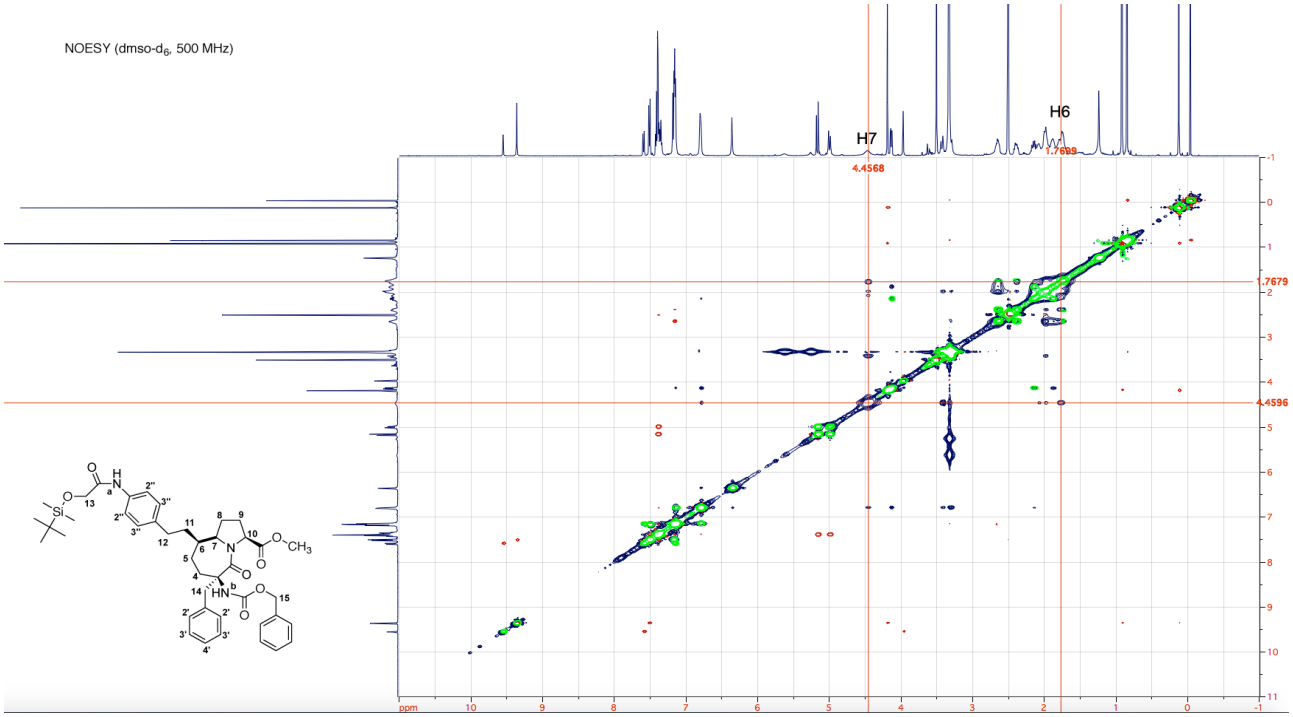

Figure 22 NOESY (dmso-d_6 500 MHz) in blue, COSY (dmso-d_6 500 MHz) in green.

To further confirm this hypothesis, molecular mechanics calculations were performed on compound **34**(*6R*) and **34**(*6S*) using the software Maestro (Schrödinger suite) and OPLS 2005 force field. Each diastereoisomer was subjected to a Monte Carlo/Energy Minimization (MC/EM) conformational search, using the implicit $CHCl_3$ GB/SA solvation model, to identify minimum energy conformations. In order to better evaluate the magnitude of the coupling constants (*J*) between H_7 and its adjacent

protons H_6 and H_8, a ^{1}H-NMR spectrum of **34** was acquired at 80°C (353.15 K) and the same temperature was applied for the calculation of the Boltzmann population. The Coupling constants of interest were derived from the sum of the weighted constants of every conformation with respect to the Boltzmann population. The calculated coupling constant between H_6 and H_7 resulted very small in compound **34**(*6R*), probably not detectable by the 2D-COSY experiments, thus confirming the hypothesis. In contrast, compound **34**(*6S*) was characterized by a large $J_{6\text{-}7}$ coupling constant (10 Hz), which should have been well visible in the 2D-COSY spectrum (Figure 23).

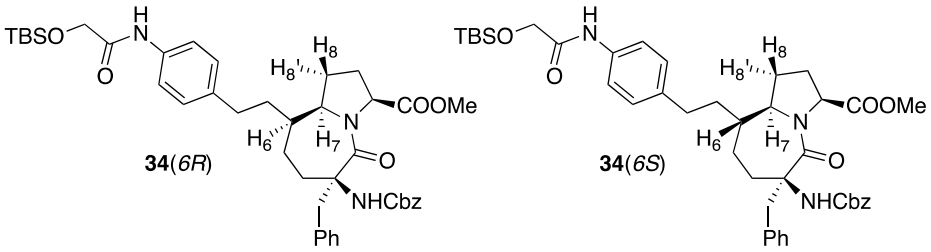

Compound	Force Field	n. of conf.	$J_{7\text{-}6}$	$J_{7\text{-}8}$	$J_{7\text{-}8'}$
34(*6R*)	OPLS_2005	877	1.4	9.3	7.2
34(*6S*)	OPLS_2005	1465	10.0	9.9	6.9

Figure 23 Calculated coupling constants between H_7 and the neighbouring protons (H_6 and H_8) for both diastereoisomers of compound **34**.

Moreover, after acquiring the ^{1}H-NMR spectra of **34** at 90 °C, the broad signal of H_7 turned out to be a broad triplet with coupling constants comparable with those calculated for **34**(6*R*) (Figure 24).

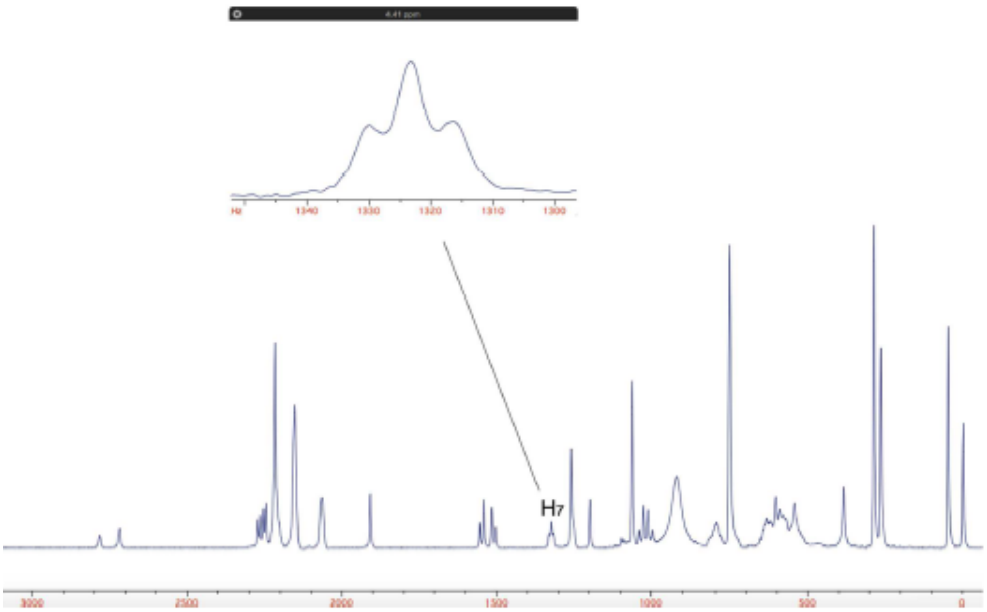

Figure 24 Experimental ^{1}H-NMR spectrum of compound **34** with H_7 multiplicity highlighted.

2.2.3. *Scaffold elaboration*

Once optimised the previously developed synthetic protocol and assessed the configuration of compound **34**, the attention was focused on the next synthetic steps. The first reaction of the RGD binding procedure is the hydrolysis of the methyl ester group, which is performed by addition of LiOH (1.6 M in H_2O) to a solution of **34** in THF/MeOH (Scheme 10). The reaction proved to be challenging, as compound **34** underwent cleavage of the TBS protecting group to afford compound **41** in 55% yields.

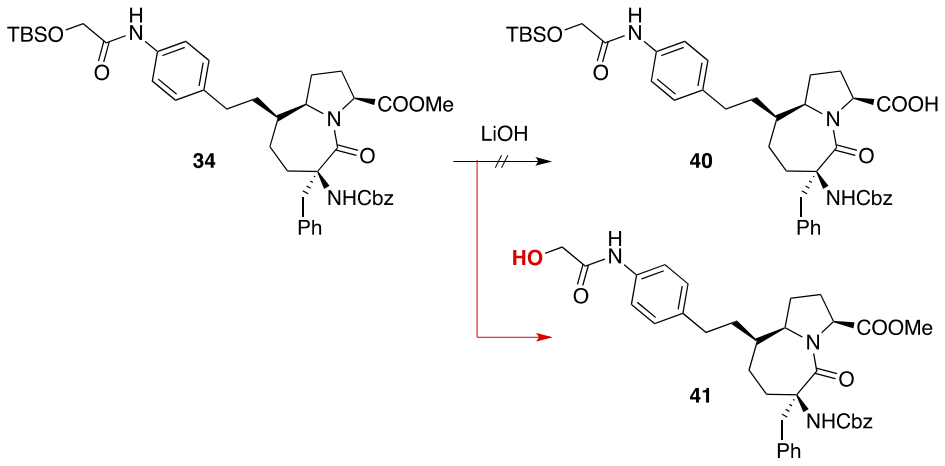

Scheme 10

To overcome this issue, compound **34** was treated with trimethyltin hydroxide ($(CH_3)_3SnOH$), which was used in literature to hydrolyse esters under mild conditions.[121] The metal coordinates the carbonyl oxygen and the hydroxyl group can hydrolyse the ester selectively. Even after heating (60°C), and further additions of trimethyltin hydroxide, no product was isolated. Instead Cbz-deprotected compound **42** was isolated in 35% yield (Scheme 11).

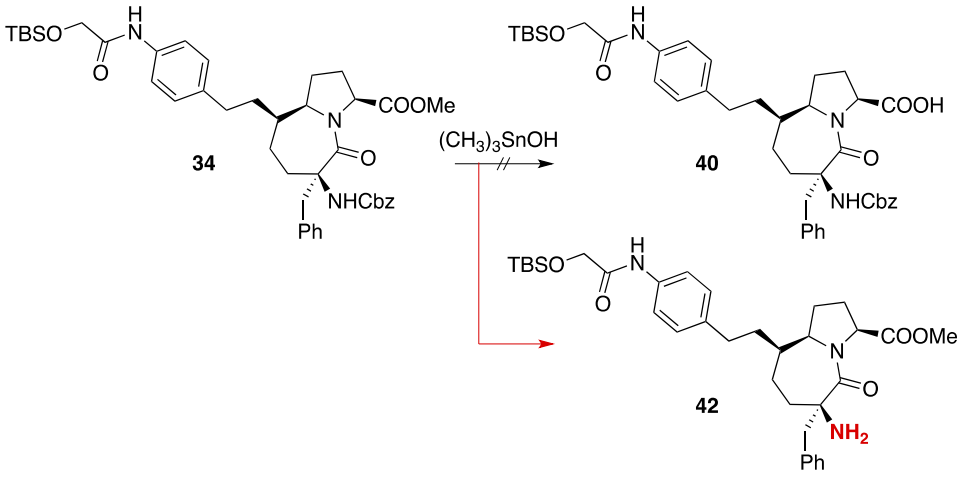

Scheme 11

To avoid side reactions involving the TBS protecting group, the synthetic scheme was revisited to incorporate a side chain bearing an aryl bromide, which could be exploited for conjugation through Pd-catalysed coupling reactions. Compound **43**, which can be readily synthesised from 4-

bromobenzaldehyde, was reacted in the *domino* CEYM/RCM with compound **27** to afford the two diastereoisomers **44**, readily separated by flash chromatography, in 71% yields, over two steps (Scheme 12).

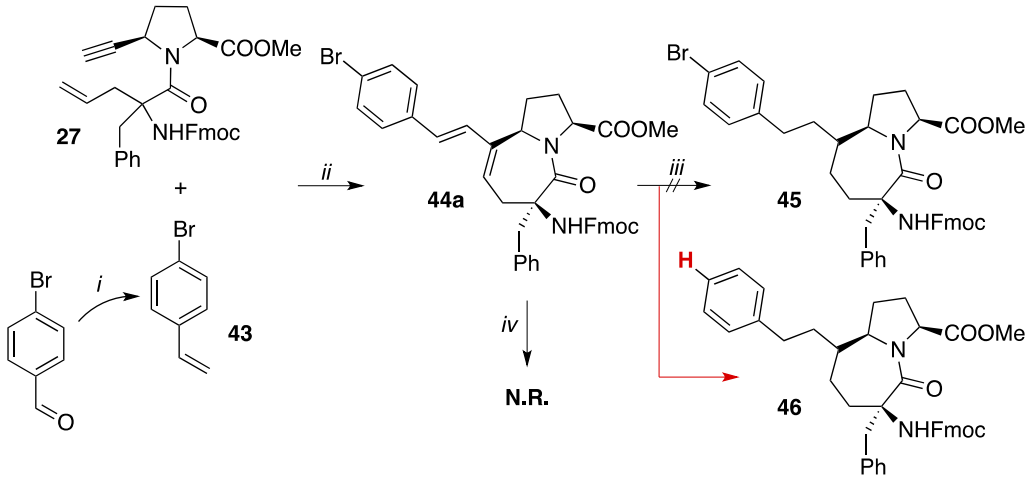

Scheme 12 Reagents and conditions: *i*) Methyltriphenylphosphonium bromide, 4-Bromobenzaldehyde, NaH, THF, 0 °C → rt, y: 62%; *ii*) HG2 (10% mol), Toluene, 80 °C, y: 71%; *iii*) H_2, Pd/C (10% mol), MeOH, y: 53%; *iv*) H_2, Pd/Fibroin (10% mol), THF.

Attempted reduction of the diene moiety of **44a** did not afford the desired product; instead de-brominated compound **46** was isolated in 53% yields. Dehalogenation of arylic halides is a known phenomenon that occurs in presence of a hydrogen donor. The proposed mechanism usually involves an oxidative addition of the metal to the carbon-halogen bond followed by a reductive elimination to form the hydrogenated product.[122] To achieve chemoselective reduction of the double bonds, a procedure exploiting Pd supported on Silk Fibroin was tested[123], but no reaction occurred (Scheme 12). Following these results, the *p*-bromo substituent was replaced by a protected amino group. Boc-protected 4-vinylaniline was chosen as substrate for the CEYM/RCM because the amino group installed on the side chain could be exploited for the conjugation either through formation of an amide bond or by conversion to an azide followed by a "click chemistry reaction" (Scheme 13).

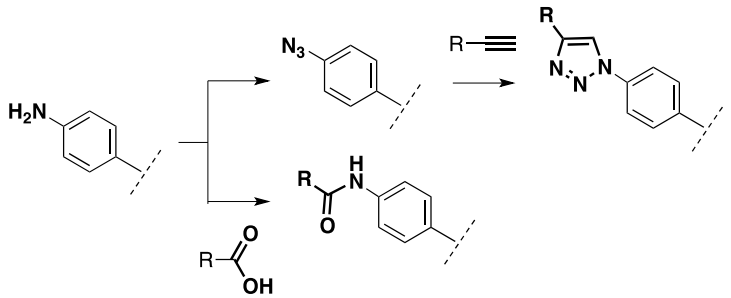

Scheme 13

4-vinylaniline was protected with $(Boc)_2O$ (di-*tert*-butyl dicarbonate) and reacted with dipeptide **27** in a *domino* CEYM/RCM to afford the two diastereoisomers **48** in 55% yield over two steps (Scheme 14). The reduction step was performed on diastereoisomer **48a**, but the hydrogenation in presence of Pd/C afforded only traces of the desired product **49**.

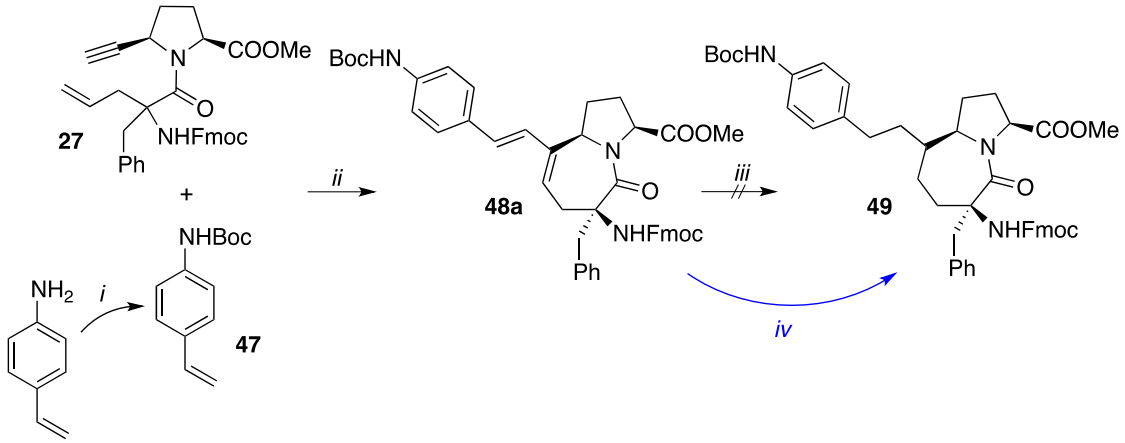

Scheme 14 Reagents and conditions: *i*) $(Boc)_2O$, CH_2Cl_2, y: 95%; *ii*) HG2 (10% mol), Toluene, 80 °C, y: 54%; *iii*) H_2, Pd/C (10% mol), MeOH; *iv*) H_2, PtO_2 (cat), MeOH, y: 91%.

By changing catalytic system with the more active PtO_2 (Platinum(IV) dioxide), the reaction proceeded smoothly and compound **49** was obtained in 91% yield as a single diastereoisomer (Scheme 14). The absolute configuration at C6 of the lactam ring is yet to be determined. Afterwards, the synthetic procedure developed for scaffold **32a** (*vide supra*) was implemented. Compound **49** was reacted in presence of piperidine to attain scaffold **50** in 85% yields (scheme 15). Despite encouraging results on milligram scale, the protection of the amino group of compound **50** with Cbz-Cl (benzyl chloroformate) resulted in variable yields and in-column degradation during chromatographic purification, which further lowered the efficiency of the reaction.

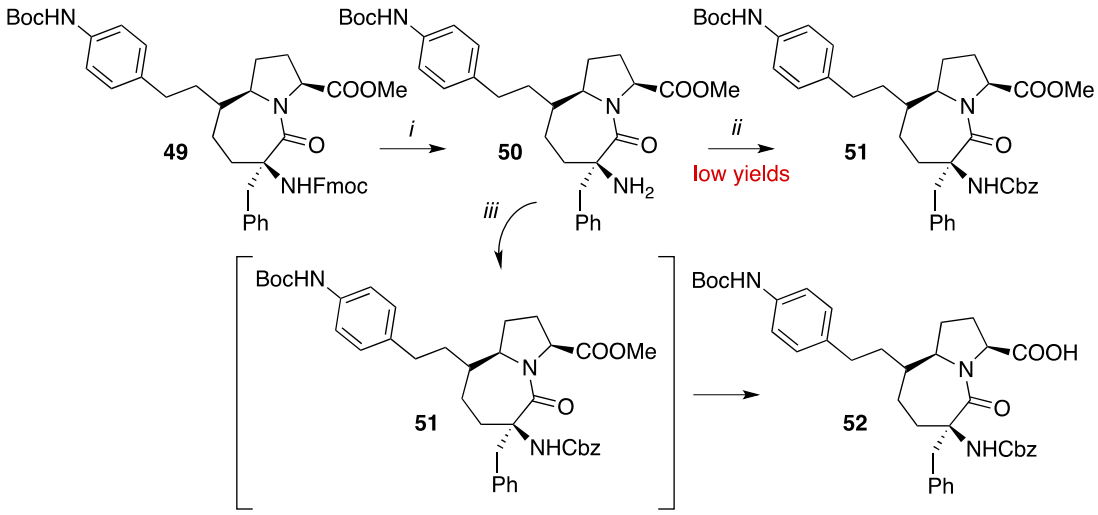

Scheme 15 Reagents and conditions: *i*) Piperidine, THF, y: 85%; *ii*) Cbz-Cl, DMAP, THF, y: variable. *iii*) $(Cbz)_2O$, THF, 0 °C → rt. Then, LiOH (1.6 M in H_2O), 60 °C, y: 96% (over two steps).

A one-pot procedure was developed to avoid intermediate purification. Compound **50** was treated with $(Cbz)_2O$ (dibenzyl dicarbonate) instead of Cbz-Cl and the conversion into compound **51** was monitored through TLC analysis. After reaction completion, a solution of LiOH was added and the mixture was heated to 60 °C overnight. Compound **52** was isolated in excellent yields after chromatographic purification.

2.2.4. RGD binding protocol

Before starting the RGD binding sequence, dipeptide **56** (Scheme 16) had to be synthesised. Starting from N-Cbz Arginine, with the guanidine group of the side chain protected as Pbf (2,2,4,6,7-Pentamethyldihydrobenzofuran-5-sulfonyl), a condensation with Glycine methyl ester was performed in presence of isobutyl chloroformate and NMM (N-methylmorpholine). After chromatographic purification, dipeptide **55** was obtained in 80% yields. Compound **56** was easily prepared in quantitative yields through hydrogenolysis of the Cbz protecting group.

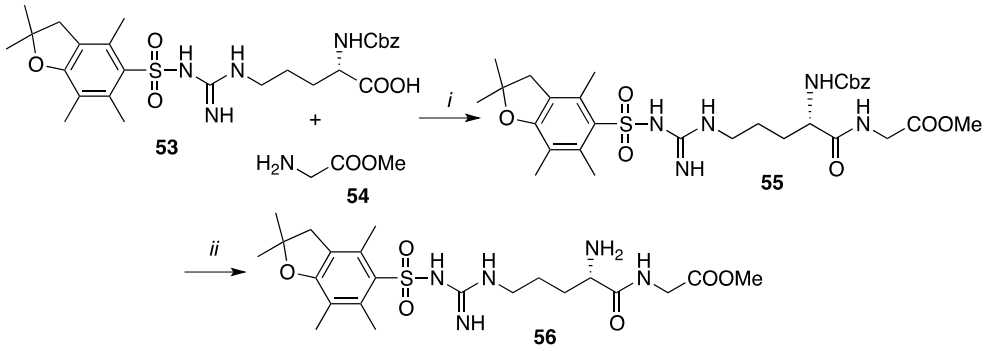

Scheme 16 Reagents and conditions: *i)* NH_2-Gly-OMe, NMM, *i*BuOCOCl, THF, -30°→ rt, y: 80%; *ii)* H_2, $Pd(OH)_2$/C, MeOH, y: quantitative.

The optimised synthesis of the cyclopentapeptide is achieved through a first condensation between the Arg-Gly dipeptide and the scaffold. Afterward, the Asp residue is attached and, following a transesterification step, the pentapeptide undergoes cyclization through coupling of the Gly and Asp (Scheme 17). The first condensation was performed following the known procedure. Treating dipeptide **56** and scaffold **52** with isobutyl chloroformate and NMM, compound **57** was attained in 78% yield after 12 hours. Because of the complexity and the cost of these advanced intermediates, another procedure was tested in order to improve the efficiency of the synthetic scheme. By using HATU as condensing agent, the reaction lasted only three hours, no cooling was needed, and chromatographic purification afforded compound **57** in 95% yield. The Cbz protecting group of compound **57** was removed through $Pd(OH)_2$ catalysed hydrogenolysis (y: 87%) and the Asp residue was coupled. The known procedure with isobutyl chloroformate afforded the product in 84% yields, whereas by using HATU as condensing agent, the reaction went to completion in three hours at room temperature and compound **58** was obtained in 96% yields. The Cbz cleavage and the condensation with the Asp residue were also performed without intermediate purification to afford directly compound **58** in 83% yield (over two steps). The ester group of the Gly residue was transesterified to a benzyl ester in presence of Titanium(IV) isopropoxide (Ti(*i*PrO)$_4$) and benzyl alcohol. Cromatographic purification afforded the product in 77% yields. Cleavage of the Cbz and benzyl ester of compound **59** was performed in presence of $Pd(OH)_2$ and the crude mixture was treated with HATU to attain the protected cyclopentapeptide **60** in 73% yields over two steps. At last, compound **60** was treated with TFA in presence of scavengers (thioanisole, anisole, 1,2-

ethanedithiol) to remove all the protecting groups from the amino acids residues and from the amino group of the scaffold's side chain. The crude mixture was purified by semipreparative HPLC (stationary phase: C18, mobile phase: 75:25:0.1 H_2O:CH_3CN:TFA) and **3a-RGD** was isolated in 68% yields.

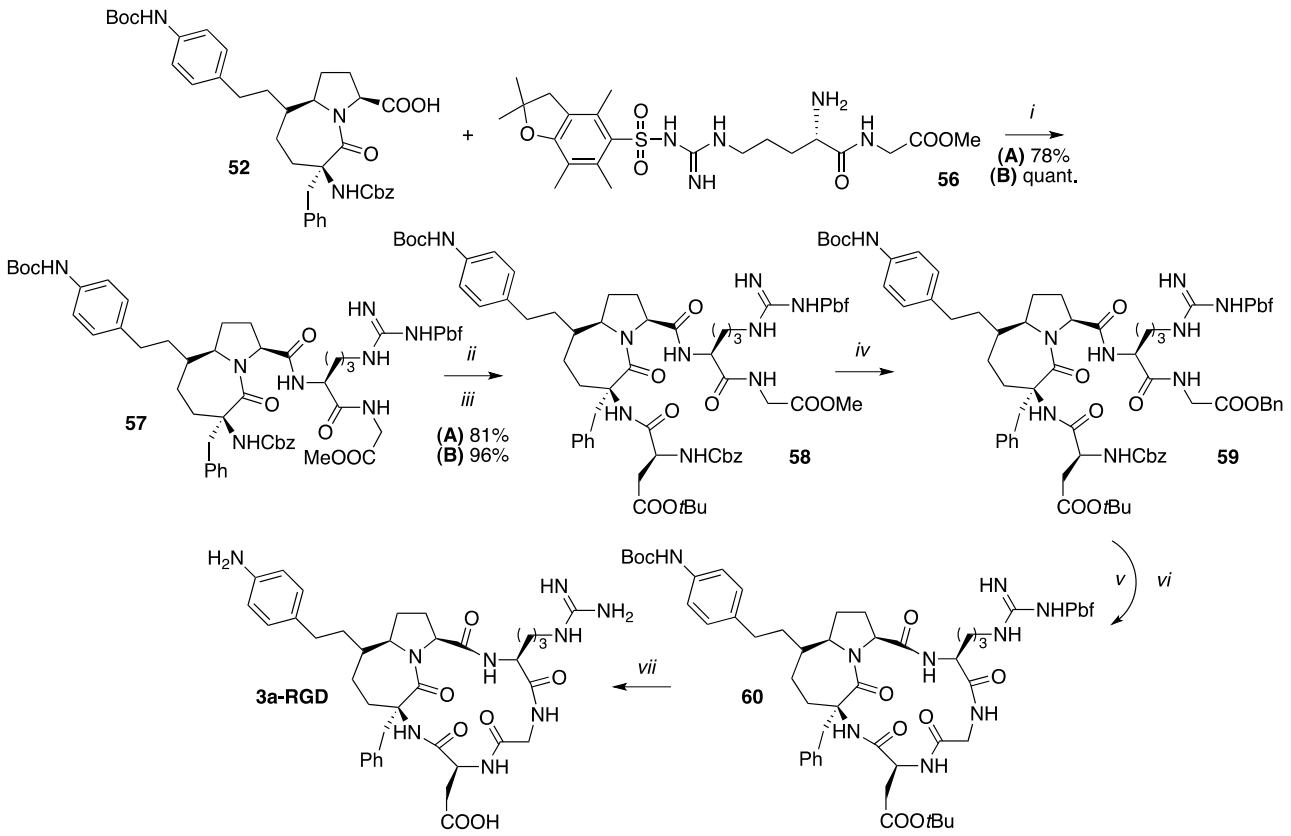

Scheme 17 Reagents and conditions (literature procedure) (A) *i)* NMM, *i*BuOCOCl, THF, -30°→ rt; *ii)* H_2, $Pd(OH)_2$/C, MeOH, y: 81%; *iii)* Z-Asp(O*t*Bu)-OH, NMM, *i*BuOCOCl, THF, -30°→ rt; *iv)* BnOH, Ti(*i*PrO)$_4$, THF, 90°C; *v)* H_2, $Pd(OH)_2$/C, MeOH; *vi)* HATU, DIPEA, THF; *vii)* TFA, Scavengers. **Reagents and conditions (optimised procedure) (B)** *i)* HATU, THF, rt; *ii)* H_2, $Pd(OH)_2$/C, MeOH; *iii)* Z-Asp(O*t*Bu)-OH, HATU, THF, rt; *iv)* BnOH, Ti(*i*PrO)$_4$, THF, 90°C; *v)* H_2, $Pd(OH)_2$/C, MeOH; *vi)* HATU, DIPEA, THF; *vii)* TFA, Scavengers.

Prof. Schinelli's research group will perform biological assays on **3a-RGD** to assess the retention of biological activity of the new cyclopentapeptide. The reactivity of the side chain was tested in the first conjugation reaction to evaluate the best method to attain first generation bioconjugates.

2.2.5. *First generation bioconjugates*

The first methodology that was devised involved the conjugation of **3a-RGD** to a bioactive compound through a non-cleavable linker. Because of the simplicity and chemical stability of these types of linkers, this strategy was thought to be a suitable starting point for the evaluation of the reactivity of the aromatic amine in **3a-RGD** (Figure 25).

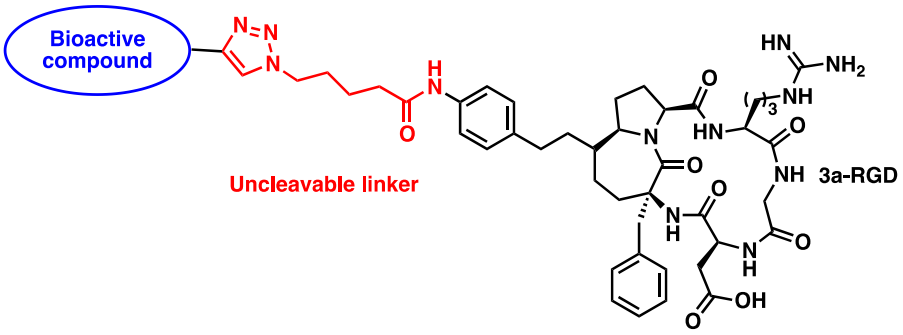

Figure 25 General structure of a **3a-RGD** based bioconjugate.

The linker is attached to **3a-RGD** through an amide group formed by the aromatic amine of the scaffold's side chain and a carboxylic group on the linker. The linker developed for this purpose was a simple acid bearing an azide on the opposite side of the carbon chain. This group can take part in a "click chemistry" reaction, for instance a Huisgen (2+3) cycloaddition as these types of reactions usually allow the attainment of the desired products rapidly, with few side-products and the advantage of being performed in aqueous solutions. 5-azidopentanoic acid was chosen as linker (Scheme 18).

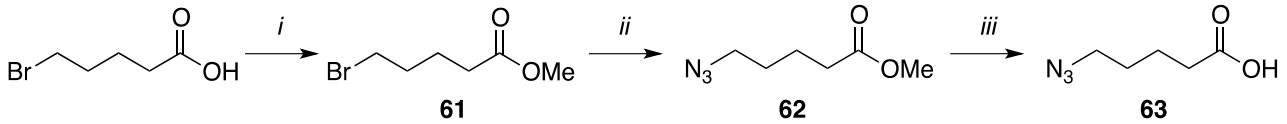

Scheme 18 Reagents and conditions: *i)* $SOCl_2$, MeOH, 0°C → rt. *ii)* NaN_3, DMF, 80 °C (MW heating), 20 min, y: 87% over two steps. *iii)* LiOH, MeOH, y: quantitative.

5-bromopentanoic acid was treated with thionyl chloride ($SOCl_2$) in MeOH to protect the carboxylic moiety as methyl ester. Compound **61** was treated with NaN_3 (sodium azide) in DMF (N,N-dimethylformamide) and reacted at 80 °C, through microwave-assisted heating, for 20 minutes to afford the corresponding azide **62** in 87% yields over two steps. Compound **62** was easily converted to the free acid **63** by basic hydrolysis in quantitative yields. In collaboration with Prof. Torre's research group, a synthetic procedure aimed at functionalising silk fibroin nanoparticles with **3a-RGD** was developed. Silk fibroin is a natural polymer widely studied for tissue engineering and drug delivery because of its biocompatibility, controllable biodegradability, low toxicity and immunogenicity. Furthermore, being a protein-based nanoparticle, it may be chemically modified exploiting the side chains of the peptide backbone.[124] Curcumin was selected as drug model to be loaded into fibroin nanoparticles because of its efficacy in treatment and prevention of many

diseases, due to its proved antioxidant, anti-inflammatory, apoptosis-inducing and anti-angiogenic activities.[125] Another advantage of curcumin is its intrinsic fluorescence, which could be exploited to monitor the active nanocarrier's behaviour in biological assays. At first the nanoparticles had to be functionalised with a suitable linker for the Huisgen cycloaddition. Lys residue on the surface of fibroin, 80 nmol/mg of protein on average[126], were chosen as anchoring point for the linker through a condensation reaction. Compound **65**, characterised by the presence of an alkyne moiety exploitable for the conjugation step, was synthesised following a literature procedure (Scheme 19).[127]

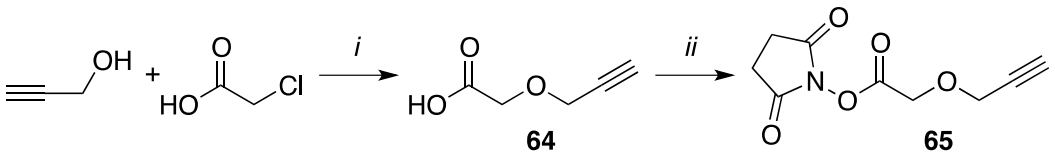

Scheme 19 Reagents and conditions: *i)* NaH, THF, 0°C → rt, y: 49%; *ii)* NHS, EDC*HCl, CH_2Cl_2, y: 96%.

Propargily alcohol was added to a solution of NaH at 0 °C followed by addition of chloroacetic acid. Chromatographic purification afforded compound **64**, which was reacted with EDC*HCl (N-(3-Dimethylaminopropyl)-N'-ethylcarbodiimide hydrochloride and NHS (N-hydroxysuccinimide) to obtain compound **65** in 96% yields. Compound **65** was reacted with fibroin nanoparticles in phosphate buffer (Scheme 20). The functionalised nanoparticles were submitted to dialysation to remove all non-covalently linked small molecules (cut-off: 10 KDa). To evaluate the effective binding of the linker and the feasibility of the subsequent step, the functionalised nanoparticles were reacted with Azide-fluor 545 in the typical condition of the Huisgen cycloaddition ($CuSO_4$ and sodium L-ascorbate in phosphate buffer) (Scheme 20).

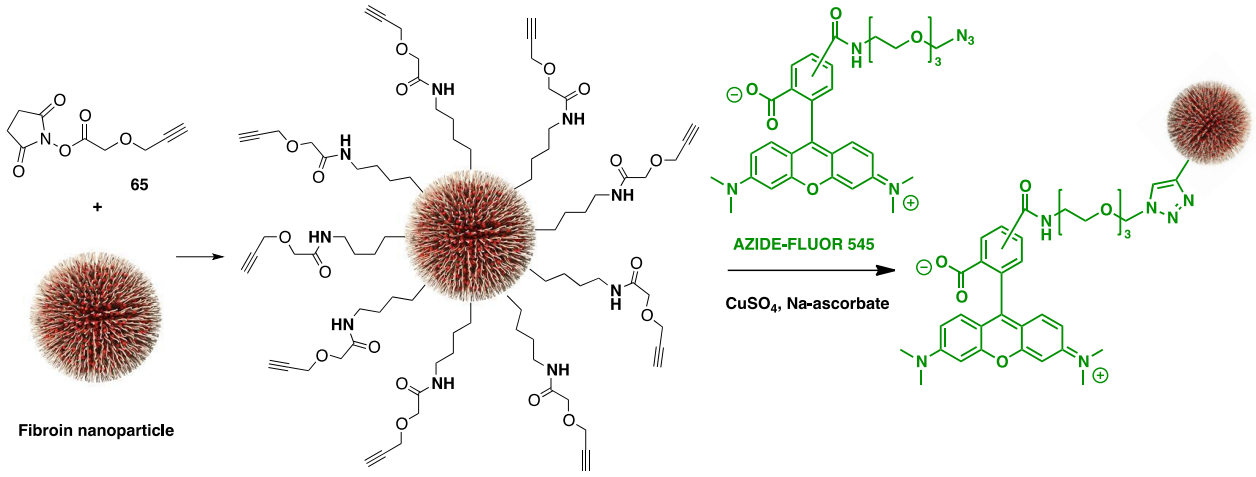

Scheme 20

The Azide-fluor derived nanoparticles were dialysed to ensure desorption of any small molecule not covalently linked to the nanosystem. Preliminary spectrophotometric analysis confirmed the presence of Azide-fluor 545 absorption band, thus giving support to the feasibility of the methodology developed. After conversion of compound **63** to the corresponding NHS activated ester **66** in presence of NHS and EDC*HCl, it was reacted with **3a-RGD** in phosphate buffer (Scheme

21). Despite the complexity of the ^{1}H-NMR spectrum, the formation of the desired product was confirmed by MALDI-TOF mass spectrometry. Compound **67** was reacted in the same condition as Azide-fluor 545 with fibroin nanoparticles functionalised with alkyne groups to afford the first **3a-RGD**-based bioconjugate (Scheme 21).

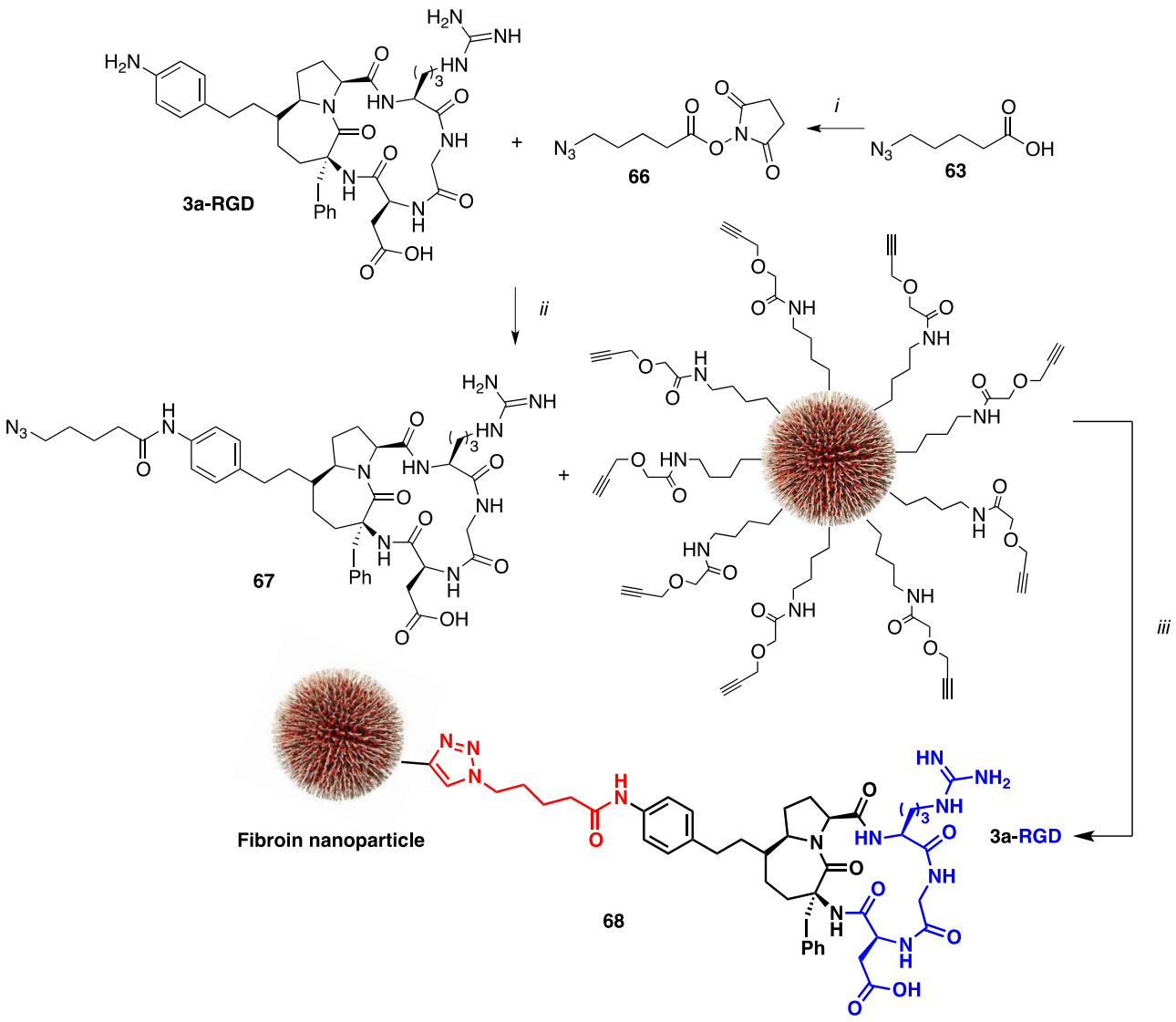

Scheme 21 Reagents and conditions: *i)* NHS, EDC*HCl, CH_2Cl_2, y: 97%; *ii)* **66**, phosphate buffer/CH_3CN, 24 h. *iii*) $CuSO_4$, Na-ascorbate, phosphate buffer, 72 h.

Prof. Torre's research group is currently performing preliminary biological assays to evaluate active targeting and to assess internalization. The loading of compound **68** on the surface of the nanoparticles is yet to be determined. A procedure based on the attachment of a suitable fluorinated probe to evaluate the amount of **3a-RGD** bound is currently under study. By doing so, it would be possible to quantify the amount of compound effectively bound to the fibroin's side chains by comparison with an internal standard through a ^{19}F-NMR technique.

The possibility of developing a bioconjugate for the delivery of photosensitizing agents for photodynamic therapy (PDT) was also explored. The PDT approach is based on the release of ROS (reactive oxygen species) following the activation of a photosensitizer through irradiation of light of

appropriate wavelength. The oxidative stress caused by the radical cascade started by ROS ultimately leads to cell death.[128] Some photosensitizer may also be exploited to enhance penetration of other chemotherapeutics, to reduce multi-drug resistance developed by tumour cells or to develop imaging agents and theranostics.[129] Prof. Fagnoni's research group developed a photoactive compound that can produce aryl radicals through UV light-promoted (450 nm) degradation of an azosulfone group (Scheme 22).[130]

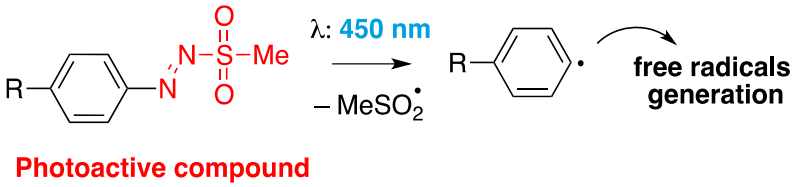

Scheme 22

To test the possibility of using such device in chemotherapy, it was decided to conjugate the photoactive moiety to **3a-RGD** to achieve active targeting and selectively accumulate the molecule at the site of action. Afterwards, it would be possible to trigger a radical cascade through *in situ* irradiation in order to damage tumour cells. Since the photolabile group does not require to be released from the bioconjugate to exhibit its effect, it is an interesting compound for an uncleavable linker strategy. To conjugate the azosulfone to **3a-RGD** through the Huisgen cycloaddition, an alkyne moiety had to be installed on the photoactive compound. To this purpose compound **69** was designed and synthesised by Prof. Fagnoni's research group. To test the reactivity of the modified azosulfone and to simulate bioconjugation conditions, compound **69** was reacted with the linker **63** in presence of $CuSO_4$ and sodium L-ascorbate in H_2O/CH_3CN (Scheme 23). No product was isolated, probably due to degradation of the azosulfone caused by the presence of a reducing agent. Change of the catalytic system did not show any benefit. No product was isolated in presence of chlorocyclopentadienylbis(triphenylphosphine)ruthenium(II) ($CpRu(PPh_3)_2Cl$).[131a] The solvent did not show any effect on the course of the reaction and heating, either conventional or microwave-assisted, only increased the rate of degradation.

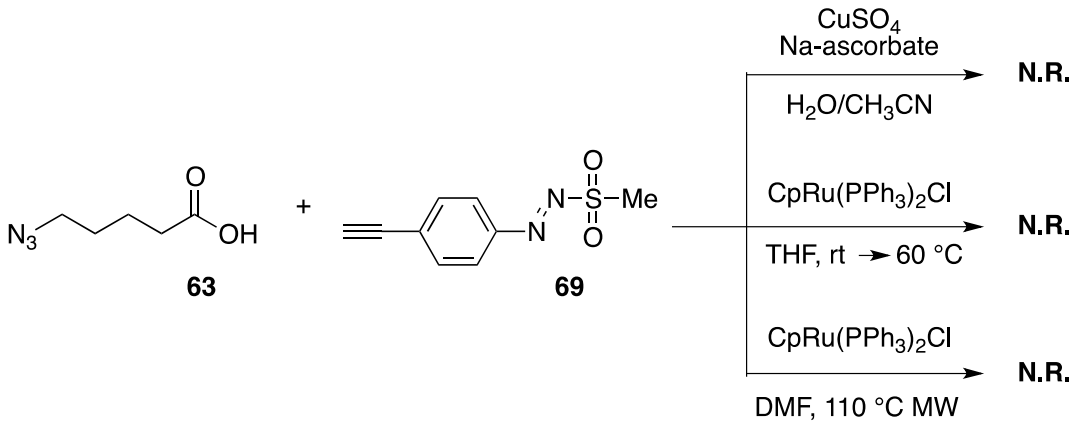

Scheme 23

Inspired by a paper by Hu and co-workers where the contemporary presence of an acid and a base was found beneficial to the outcome of alkyne-azide cycloadditions[131b], a similar procedure was tested on compounds **63** and **69** (Scheme 24).

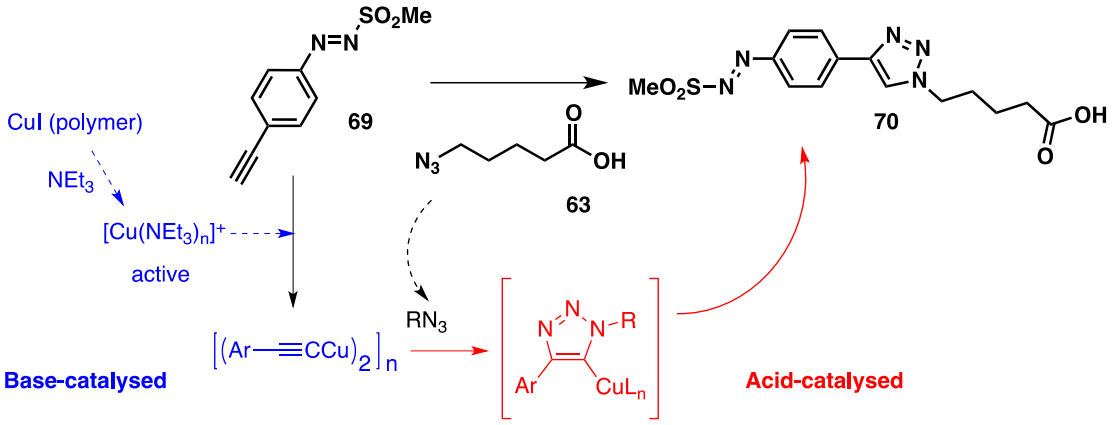

Scheme 24 Reagents and conditions: CuI, NEt_3, THF, rt.

Since an acidic moiety was already present in one of the reagents, triethylamine was added to a solution of compounds **63** and **69** in THF in presence of catalytic amounts of CuI. After 1 hour the reaction was over and the crude mixture was reacted with NHS and EDC*HCl to afford compound **71** in quantitative yields over two steps (Scheme 25).

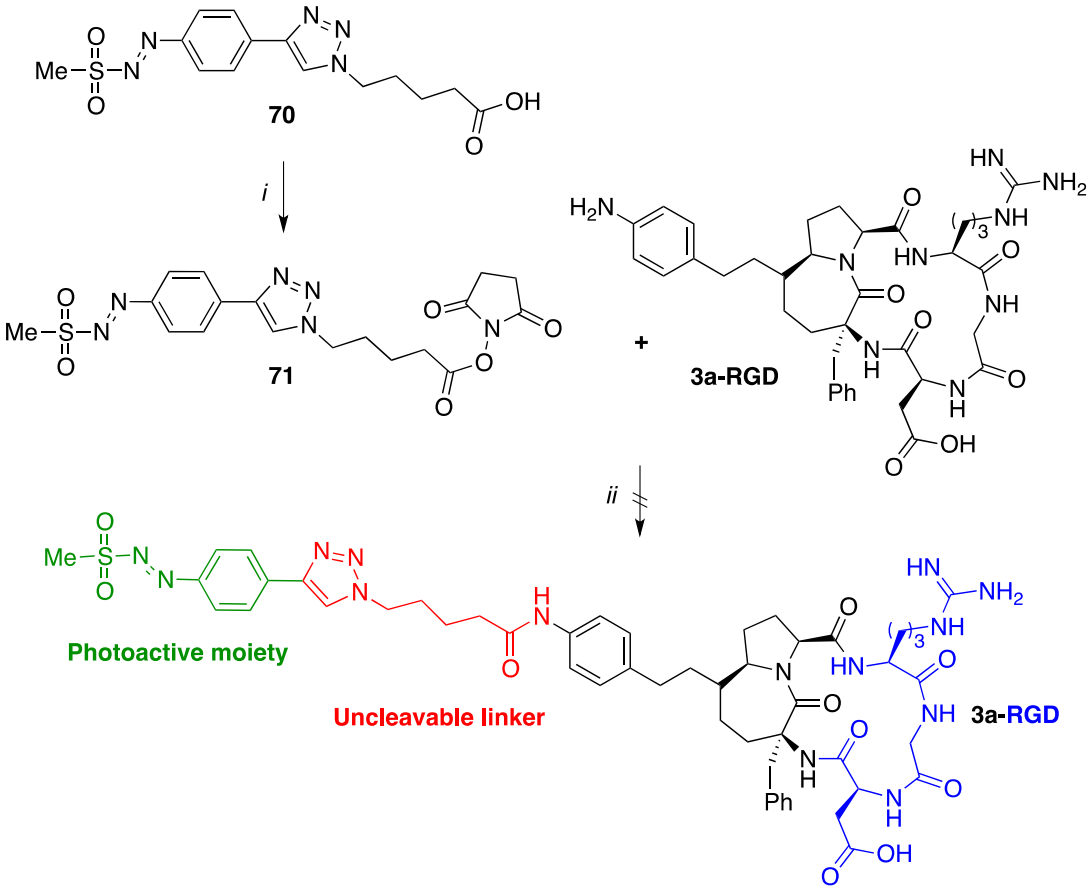

Scheme 25 Reagents and conditions: *i)* NHS, EDC*HCl, CH_2Cl_2, y: quantitative. *ii)* Phosphate buffer/CH_3CN, 48 h.

Unfortunately, no reaction occurred between compound **71** and **3a-RGD**, probably because of the intrinsic instability of the azosulfone group and the low nucleophilicity of the aromatic amine of the side chain of **3a-RGD**. Further studies must be performed to optimise this reaction. Compound **71** low solubility in aqueous medium may also be an issue, in fact it had to be dissolved in an organic solvent (acetonitrile) prior to being added to the reaction mixture. Therefore, a solvent that has affinity for both the hydrophobic compound **71** and the hydrophilic **3a-RGD**, is required. For these reasons, the use of a different solvent and/or the carboxylic acid **70** in the presence of condensing agents may be a viable alternative to NHS-activation to increase reaction rate.

2.2.6. Novel synthesis of 5,6- and 5,7-fused bicyclic lactams

To further extend the substrate scope of the CEYM/RCM reaction, dipeptide **73** was synthesised to evaluate the possibility to extend this methodology for the attainment of 5,6-fused functionalised lactam rings, such as compound **74**. Dipeptide **73** can be obtained from 5-ethynylproline, which was synthesised as previously reported (Scheme 3), and amino acid **72** (Scheme 26).

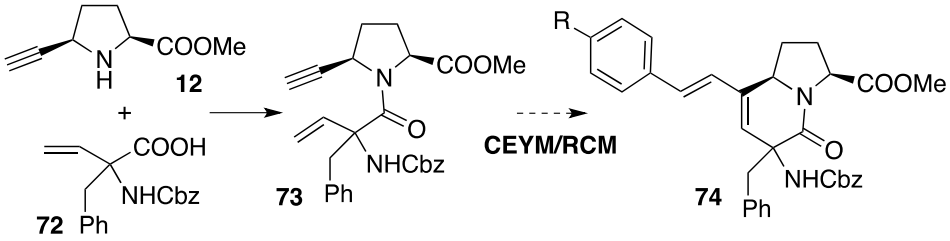

Scheme 26

The latter was synthesised following a one-pot vinylation method previously developed in Prof. Colombo's laboratory.[132]

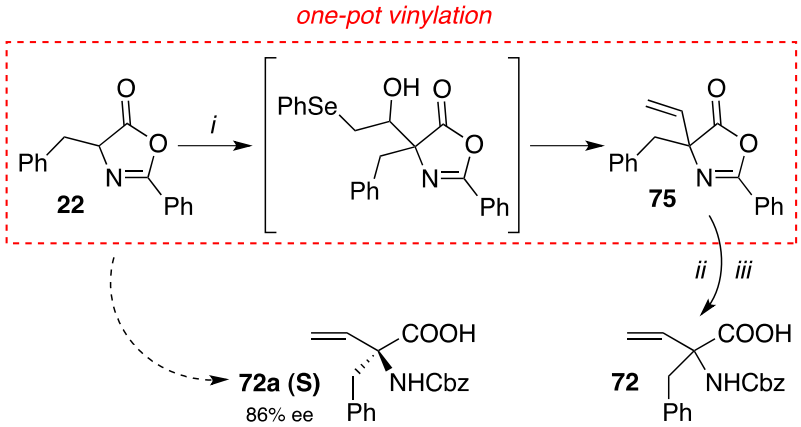

Scheme 27 *i)* a. (Phenylseleno)acetaldehyde, NEt_3, -10 °C, THF; b. MsCl, NEt_3, rt; c) TBAI, 110 °C (MW), 10 min, y: 82% (over 3 steps); *ii)* TFA, 100 °C, y: 98%; iii) $(Cbz)_2O$, TBAH, CH_3CN, y: 96%.

Oxazolone **22** was reacted in an aldol addition with (phenylseleno)acetaldehyde in presence of NEt_3. Afterwards, MsCl (methanesulfonyl chloride) is added to the reaction and the mesylated

intermediate undergoes tetrabutylammonium iodide-mediated (TBAI) elimination to afford the vinylated oxazolone **75**. After treatment with TFA and subsequent protection with $(Cbz)_2O$, amino acid **72** was obtained (Scheme 27). An enantioenriched variant of the vinylation was also experimented (*vide infra*) to attain predominantly the S enantiomer.

The coupling reaction between compound **12** and amino acid **72** (Scheme 26) required long reaction time and heating, probably due to the stereoelectronic properties of the two unnatural amino acids to be coupled (Table 3). A preliminary experiment, following a known procedure[117], was performed. Compound **12** and **72** were reacted in CH_2Cl_2 in presence of PyBroP (Bromotripyrrolidinophosphonium hexafluorophosphate) as condensing agent, catalytic amounts of DMAP (4-dimethylaminopyridine) and DIPEA (Table 3 entry 1).

Entry	Condensing agent	Temperature (°C)	Solvent	Base	Time	Yield 73a (S) + 73b (R)
1	PyBroP/DMAP	Rt	CH_2Cl_2	DIPEA	26 h	50%
2	PyBroP/DMAP	rt → 50	THF	DIPEA	36 h	61%
3	PyBroP/DMAP	60	DCE	DIPEA	30 h	60%
4	HATU	60	DMF	DIPEA	24 h	N.R.
5	HATU	100 °C (MW)	DMF	DIPEA	30 min	N.R.
6	HATU	rt → 50	THF	DIPEA	20 h	69%
7	HATU	60	THF	DIPEA	26 h	77%

Table 3

By using THF as solvent and heating the reaction mixture, the yields of the product increased to 61% (entry 2), but the use of DCE (1,2-dichloroethane) and heating to 60 °C did not improve it further (entry 3). Interestingly, when HATU was used with DMF as a solvent (entry 4 and 5), only side-product **76** was isolated. The by-product derived from the condensation of the amino acid and N,N-dimethylamine, probably formed from the thermal degradation of DMF (Scheme 28).

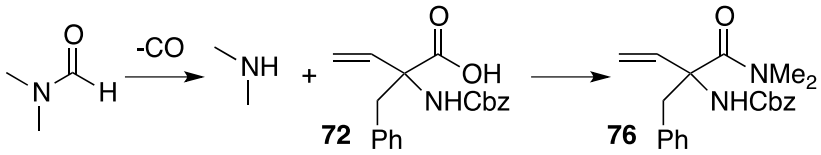

Scheme 28

By substituting DMF with THF, the yield increased to 69% and further improved to 77% when heating at 60 °C from the start (Table 3, entry 6 and 7). The two diastereoisomers were separated by flash chromatography and only the dipeptide with S configuration at the quaternary stereocenter was submitted to the next reaction (Scheme 29). Compound **73a** was reacted under *domino* CEYM/RCM optimised conditions, but the desired product **74a** did not form, instead the reaction allowed the attainment of compound **77a** in 38% yields, which is probably formed *via* a RCEYM reaction. To

increase conversion of dipeptide **73a**, Mori's conditions, which required the reaction to be performed in ethylene atmosphere, were applied[133].

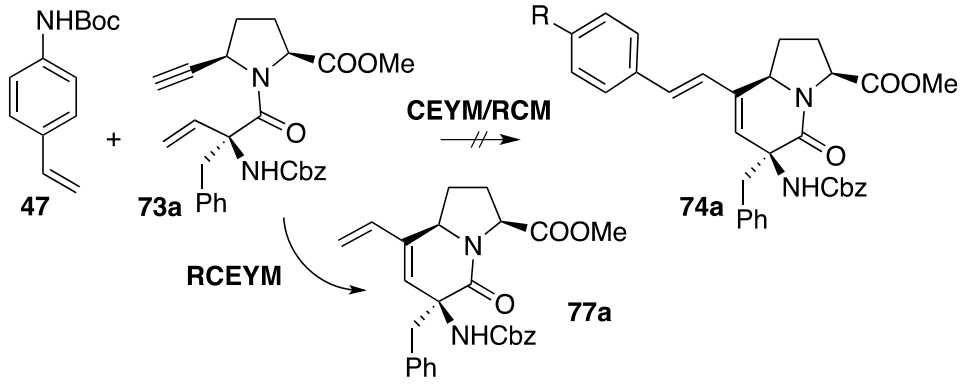

Scheme 29 Reagents and conditions: *i*) HG2 (10% mol, slow addition in 7 h), Toluene, 80 °C.

Mori and co-workers noted that the presence of ethylene increases catalyst's regeneration and turnover, thus improving the rate and efficiency of metathesis reactions. Surprisingly, only small amounts of compound **77a** was isolated (y: 15%), whereas the major product turned out to be triene **78a** (y: 41%), deriving from a CEYM mechanism with ethylene (Scheme 30). Following this result, the reactivity of the triene intermediate was assessed by reacting **78a** in presence of HG2 at 80 °C. Instead of compound **77a**, the 5,7-fused bicyclic lactam **79a** was the only product isolated. The overall good yield (70%) and the possibility to recover unreacted triene (89% conversion), prompted the development of a novel synthetic sequence aiming at obtaining 5,7-fused systems and 5,6-fused systems starting from the same key intermediate **73a**.

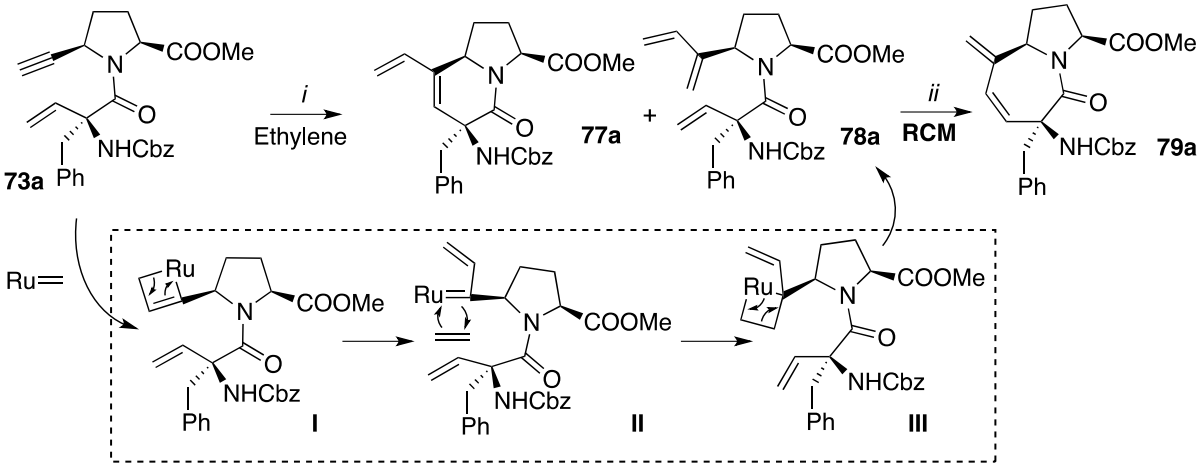

Scheme 30 Reagents and conditions: *i*) Ethylene atmosphere, HG2 (10% mol), toluene, rt, 6 h (Table 4, entry 1); *ii*) HG2 (10% mol), toluene, 80 °C.

The work was focused on the optimisation of the reaction's parameters (Table 4). At first G1 (Grubbs first generation catalyst) and G2 (Grubbs second generation catalyst) were screened to evaluate their catalytic activity. The G1-catalysed reaction did not afford any product, whereas in the presence of G2 the product was isolated in 44% yields after 10 hours at 40 °C (Table 4, entry 2 and 3). With HG2 in the same conditions the reaction yields remained stable at 45% (entry 4). Since slow

addition of catalyst proved to be beneficial in the previously reported CEYM/RCM (Scheme 5), HG2 was added in 4 hours with a syringe pump. This approach proved to be detrimental and the yields dropped to 11% and 18% (entry 5 and 6). Because of the slight improvement observed under gentle heating, the reaction was also performed at 80 °C, but the yield of compound **78a** decreased to 23% (entry 7). It is worth noting that by heating the reaction mixture to higher temperatures, the yield of **77a**, deriving from a RCEYM mechanism, increased to 29 % (data not shown in the table). The most successful result was attained when ethylene gas was bubbled portionwise every hour into the reaction mixture (entry 8). After 8 hours the reaction went to completion and the product **78a** was isolated through flash chromatography in 65% yields, whereas compound **77a** was isolated in 21% yields.

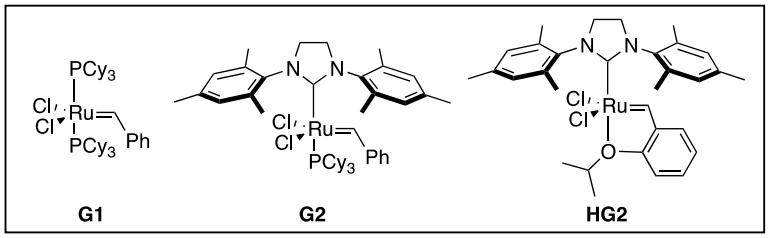

Entry	Catalyst	Temperature (°C)	Solvent (0.1 M)	Time	Yield 78a
1	HG2	rt	Toluene	6 h	41%
2	G1	rt → 40	Toluene	6 h	N.R.
3	G2	rt → 40	Toluene	10 h	44%
4	HG2	rt → 40	Toluene	6 h	45%
5 [a]	HG2	rt	Toluene	18 h	11%
6[a]	HG2	40	Toluene	18 h	18%
7	HG2	80	Toluene	6 h	23%
8[b]	HG2	40	Toluene	8 h	65%

Table 4 a) HG2 was slowly added in 4 h with a syringe pump. b) Ethylene was bubbled for 15 minutes at 1-hour intervals.

The optimised conditions were also applied to convert dipeptide **73b** into the corresponding triene **78b** to demonstrate the synthetic versatility of the methodology (Scheme 31).

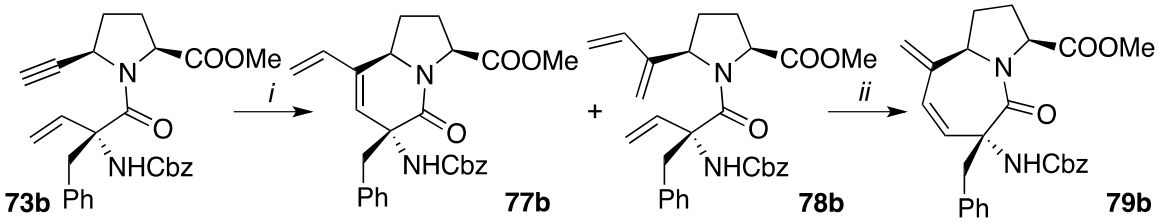

Scheme 31 Reagents and conditions: *i*) Ethylene atmosphere, HG2 (10% mol), toluene, 40 °C, 8 h; *ii*) HG2 (10% mol), toluene, 80 °C.

Compound **78b** was isolated in 33% yields, whereas compound **77b** was attained in 35% yields. Although the triene's yield was not optimal, further optimisation could improve this result.

Compound **78b** was reacted in a RCM to afford compound **79b** in 61% yields. Even in this case unreacted starting material was recovered and the conversion was still very high (89% conversion). Both compounds **73a** and **73b** were also reacted in RCEYM conditions to further demonstrate the synthetic value of these compounds (Scheme 32).

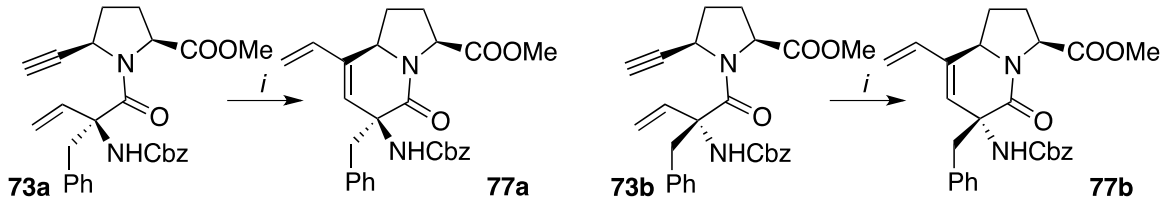

Scheme 32 Reagents and conditions: *i*) HG2 (20% mol), toluene, 65 °C.

Part of the catalyst (12,5% mol) was slowly added with a syringe pump in 16 hours. Chromatographic purification of the crude mixture afforded compound **77a** in 46% yield and compound **77b** in 37% yields. Functionalised 5,6- and 5,7-fused systems could be useful intermediates for the synthesis of bioconjugates or building blocks for the synthesis of more complex structures. For this reason, as a final proof of concept, the reactivity of the diene moiety of compounds **77a** and **79a** was assessed (Scheme 33 and 34).

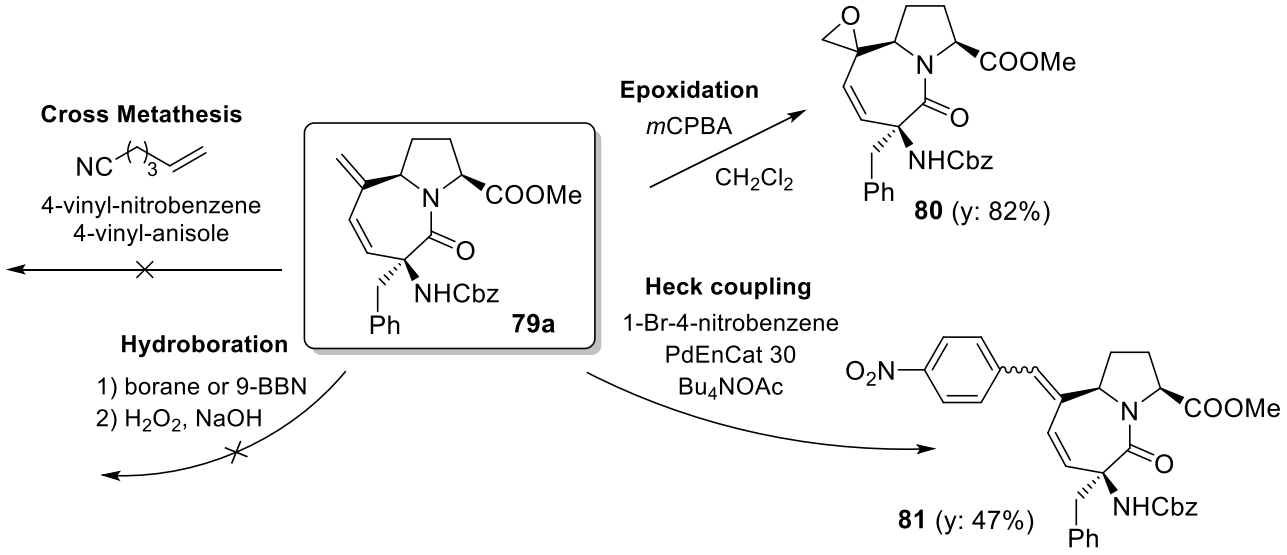

Scheme 33

In order to evaluate the reactivity of the exocyclic double bond as potential handle for further functionalisation, compound **79a** was tested in a Heck reaction. Very few examples of regioselective Pd catalysed coupling involving conjugated dienes similar to that in compound **79** were found in the literature[134]; therefore the reaction was performed with the same procedure exploited in a previous project.[117] By using PdEnCat 30 as palladium source in presence of tetrabutylammonium acetate (Bu_4NOAc) and 1-bromo-4-nitrobenzene, compound **79a** was converted to the functionalised scaffold **81** in 47% yield, thus proving the reactivity, albeit modest, of the double bond towards Heck-type couplings. Diene **79a** proved to be inert with respect to hydroboration reactions. When reacted with either 9-BBN (9-Borabicyclo(3.3.1)nonane) or BH_3 (borane), no

reaction occurred. Incorporation of a nitrile side chain and a *para*-substituted aromatic ring through a cross metathesis reaction was also attempted. In both cases the diene moiety proved to be unreactive. On the contrary, the conversion of the exocyclic double bond to an epoxide gave very good results, after treating compound **79a** with *m*CPBA (*meta*-chloroperbenzoic acid), the two diastereoisomers of compound **80** were isolated in 82% yield (Scheme 33). Compound **77a** proved to be more reactive towards cross metathesis. After treatment with 5-hexenenitrile in presence of HG2 catalyst, compound **83** was isolated in 43% yields. The exocyclic vinyl moiety of **77a** was proven to be reactive towards Heck reactions by replicating the reaction conditions adopted with compound **79a**, but, instead of microwave irradiation, the reaction was heated to 80 °C through conventional heating. The *para*-nitroaryl derivative **82** was isolated in 55% yields. Since the exocyclic double bond of compound **77a** proved to be more reactive, it was reacted with 9-BBN and BH_3 to assess the feasibility of a hydroxylation, but, even with compound **77a**, no reaction occurred.

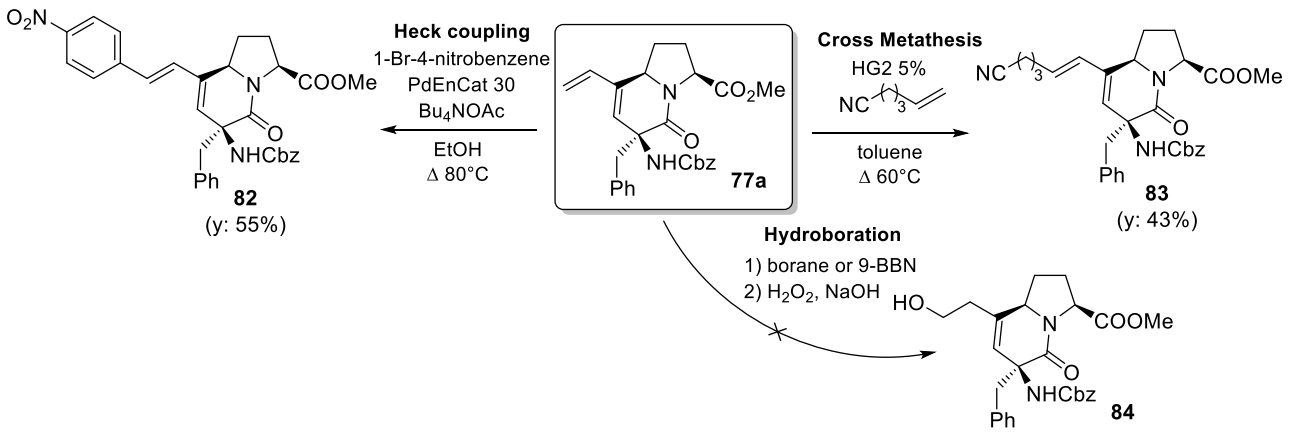

Scheme 34

2.2.7. *Conclusions and future perspectives*

Azabicycloalkane scaffolds are interesting building blocks for the synthesis of biologically active molecules and peptidomimetics because of their conformational features. The protocols reported in this work enabled the attainment of functionalised bicyclic lactam systems in few synthetic steps allowing the reduction of steps usually required to produce these molecules. Furthermore, the *domino* CEYM/RCM reaction proved to be a robust method to modify the scaffold's side chain through the incorporation of different functionality exploitable for further synthetic elaborations. The possibility of tuning the reactivity of the common precursor **73** (Scheme 35) was also experimented leading to the attainment of either 5,6- or 5,7-fused systems depending on the reaction conditions adopted while performing the ruthenium-mediated cyclisation (RCEYM or CEYM followed by RCM).

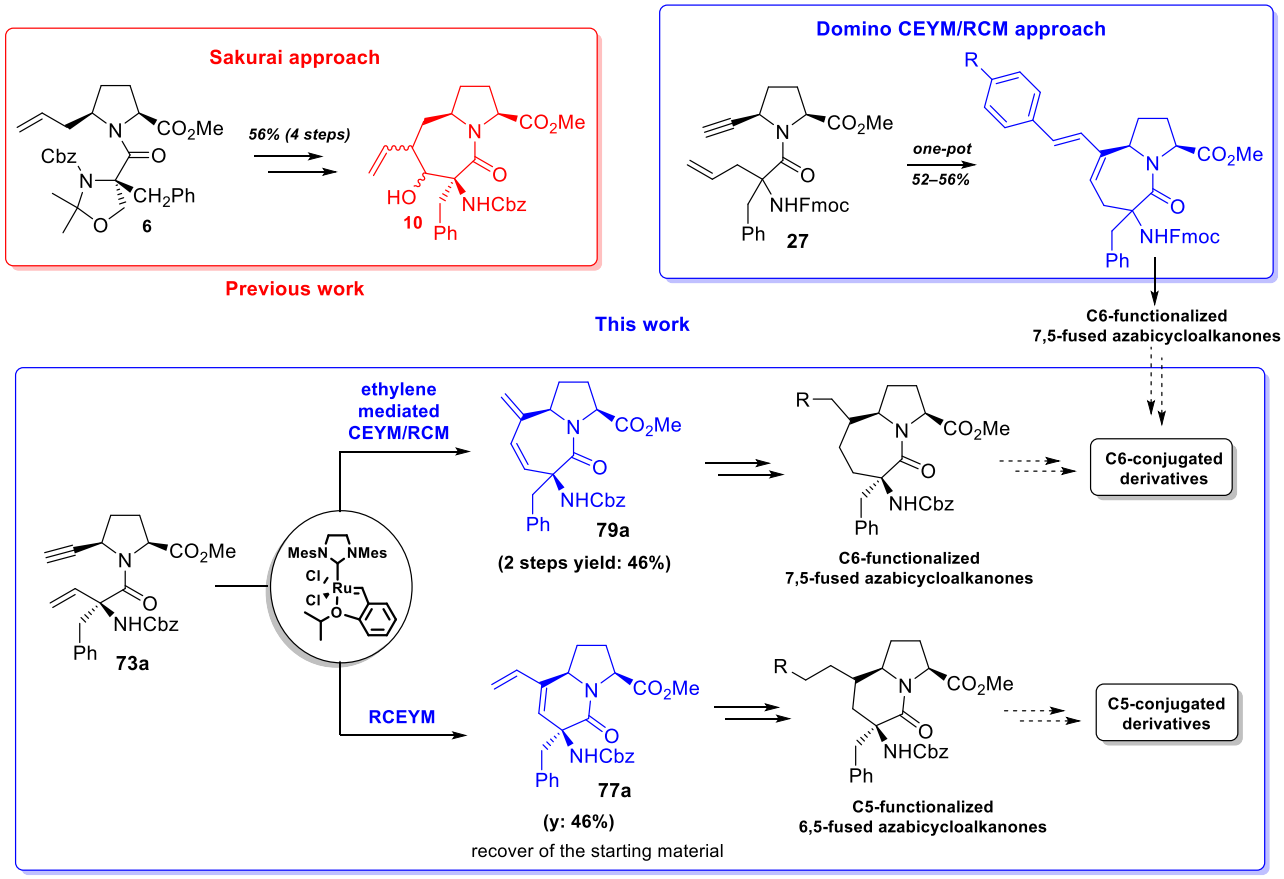

Scheme 35

Cyclopentapeptides incorporating bicyclic lactam scaffolds, such as **3a-RGD**, are also useful intermediates for the development of RGD-based bioconjugate as drug delivery systems. First generation bioconjugates have been synthesised while evaluating the most suitable synthetic strategy for the conjugation. **3a-RGD** proved to be reactive towards amide bond formation and "click chemistry" reactions. Further optimisation is needed to attain the bioconjugate bearing the photolabile azosulfone and to attach a fluorescent probe to **3a-RGD**. The latter would allow, through

biological assays, the evaluation of the targeting properties and the possibility of cell internalisation of the novel **3a-RGD**-based bioconjugates (Scheme 36).

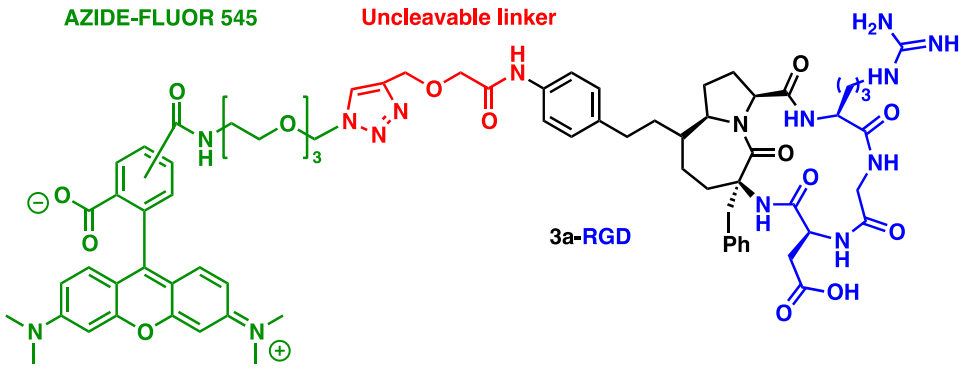

Scheme 36

Afterwards, more sophisticated target delivery systems may be developed by incorporating a cleavable linker into the structure or by synthesising theranostic bioconjugates. Two different strategies will be experimented (Scheme 37). The first one aims at conjugating **3a-RGD** with canertinib, a potent and selective inhibitor of tyrosine kinase associated to EGFR and HER-2. The development of this cytotoxic compound was discontinued due to its severe side effects, but it may be possible to reduce them by selectively deliver the drug to the site of action. It is important to note that this strategy could also affect EGFR mutated forms lacking the extracellular domain, which cannot be targeted by antibodies and confer high malignancy grade to tumours. After integrin-mediated internalization of the bioconjugate, the linker may be cleaved by lysosomal proteases, and a subsequent retro Michael reaction will free canertinib, thus allowing its targeting action towards EGFR and HER-2 tyrosin kinases.

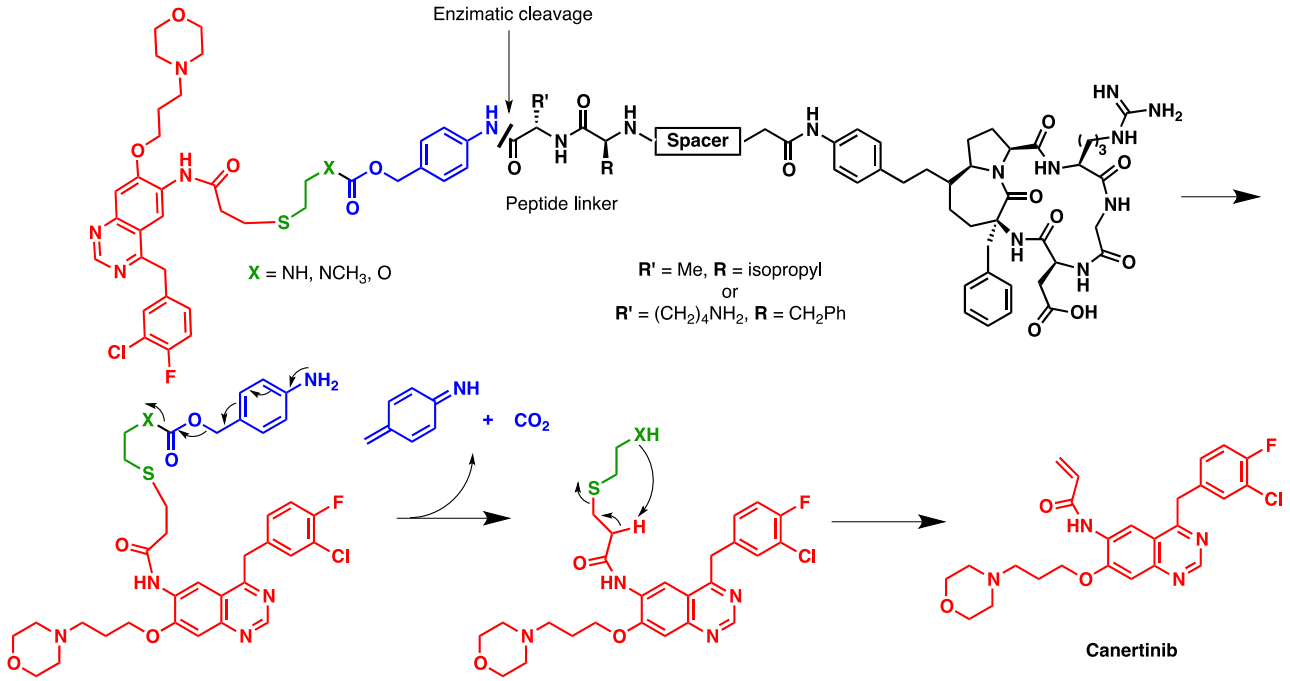

Scheme 37

The second strategy aims at conjugating Dasatinib to **3a-RGD** through a linker containing a consensus sequence for MMP2. Dasatinib is an inhibitor of the Bcr-Abl tyrosin kinase and is also active on the Src kinase family. Once the linker is cleaved by overexpressed MMPs on cells membranes, the cytotoxic compound will be internalized. The low pH and high glutathione concentration in cancer cells will promote an intermolecular reaction that will result in the release of free dasatinib. This approach is aimed to arrest Src mediated cellular proliferation and survival (Scheme 38).

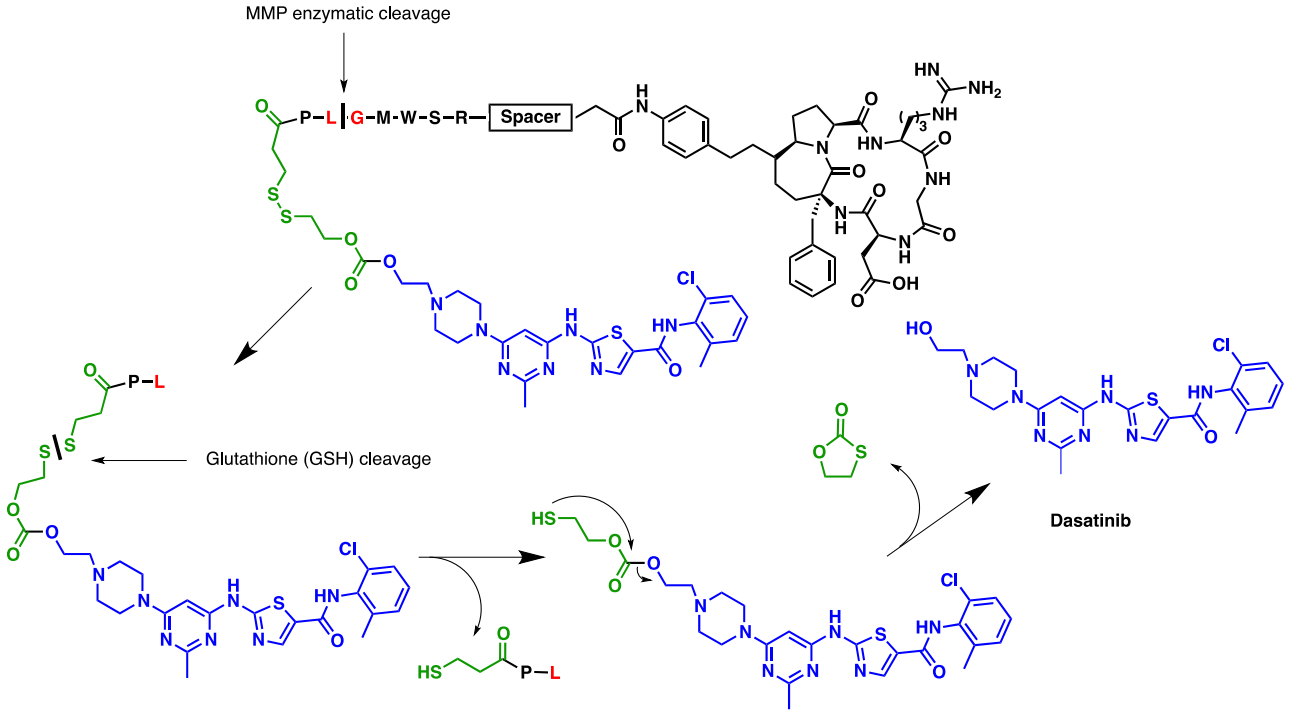

Scheme 38

In collaboration with Prof. Schinelli's research group, biological assays will be performed. Human glioma stem cells (GSC), breast cancer cells (MCF-7), lung adenocarcinoma cells (A549) and vascular endothelial cells (HUVEC) will be used as experimental models. The effects of the **3a-RGD**-conjugates on cell proliferation, apoptosis and anoikis will be studied and modification of the expression levels of target genes will be evaluated by quantitative real time RT-PCR. Further experiments will be performed to evaluate the effect of RGD conjugates on exosomes formation and composition in cancer cells; also, exosomes uptake by HUVEC cells will be measured to evaluate the metastatic potential of cancer cells in the presence and the absence of the compounds.

2.3. α-Vinyl and α-allyl Quaternary Amino Acids

Part of the work described in this Chapter was published in the following article:

- Massimo Serra, Eric Bernardi, Giorgio Marrubini, Lino Colombo *European Journal of Organic Chemistry,* **2017**, *20*, 2964–2970.
- Massimo Serra, Eric Bernardi, Giorgio Marrubini, Ersilia De Lorenzi and Lino Colombo *European Journal of Organic Chemistry,* **2019**, *4*, 732–741.

2.3.1. Introduction

The synthesis of non-proteinogenic amino acids, their incorporation in peptides or proteins, and their use as templates for the obtainment of chemically- and enzymatically-stable derivatives is an area of growing interest in medicinal chemistry and biology.[135] In particular, α,α-disubstituted (quaternary) α-amino acids are characterized by restricted flexibility, increased lipophilicity and stability towards racemization.[136] The presence of a double bond moiety may find interesting application for the rational design of peptidomimetics, in fact, the modified steric features can influence the overall spatial conformation of the structure in which these building blocks are incorporated, thus influencing the biological effects of the final compounds.[137] Furthermore, quaternary amino acids bearing an insaturation on one of their residues may find interesting applications as intermediates for the synthesis of biologically active cyclic[138] and stapled peptides.[139] The presence of a double bond moiety would also allow site-selective peptide modifications[140] and peptide-drug/polymer conjugation.[141] In the field of ADCs, for instance, the incorporation of such unnatural amino acids may be useful to achieve selective conjugation, thus strictly controlling the resulting DAR (drug-antibody ratio) (*vide supra*). This has aroused new attention in the synthesis of α-vinyl and α-allyl amino acids.

2.3.2. One-pot vinylation of azlactones

A synthetic strategy to convert azlactone into the corresponding α-vinyl analogs was developed in professor Colombo's laboratory (*vide supra*, Scheme 27).[132] An asymmetric variant was also developed in order to attain the desired products in an enantioselective fashion. Reaction parameters were screened in a previous project and optimised on compound **22**. The best results were achieved by using Sharpless ligand $(DHQD)_2PHAL$ as chiral base (y: 78% over three steps, *ee*: 86%). To further extend the substrate scope of the reaction, the experimentation was extended to alanine- and valine-derived azlactones **85** and **86** (Scheme 39).

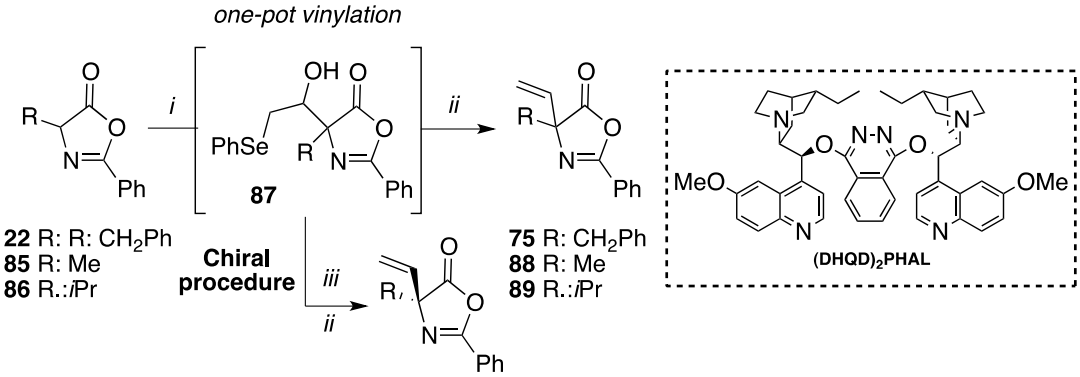

Scheme 39 Reagents and conditions: *i)* (Phenylseleno)acetaldehyde, NEt_3, -10 °C, THF; *ii*) a. MsCl, NEt_3, rt; b. TBAI, 110 °C (MW), 10 min; *iii*) (Phenylseleno)acetaldehyde, **(DHQD)$_2$PHAL**, -10 °C, THF.

$(DHQD)_2PHAL$ proved to be capable of inducing an acceptable level of enantioselectivity, and vinyl azlactones **88** and **89** were formed with 55% *ee* (y: 69) and 45% *ee* (y: 62%), respectively. During this PhD project the work was completed as follows. The reactions were scaled up to evaluate the robustness of the chiral variant. The vinylation was carried out on 1 g of compound **22** and the vinylated oxazolone **75** was isolated in similar yields and with comparable *ee* values. To further prove the applicability of this methodology to peptide synthesis, the azlactones rings of compounds **75**, **88** and **89** were opened by treatment with TFA and the resulting amino acids were protected at the amino group as benzyl carbamates (Scheme 40).

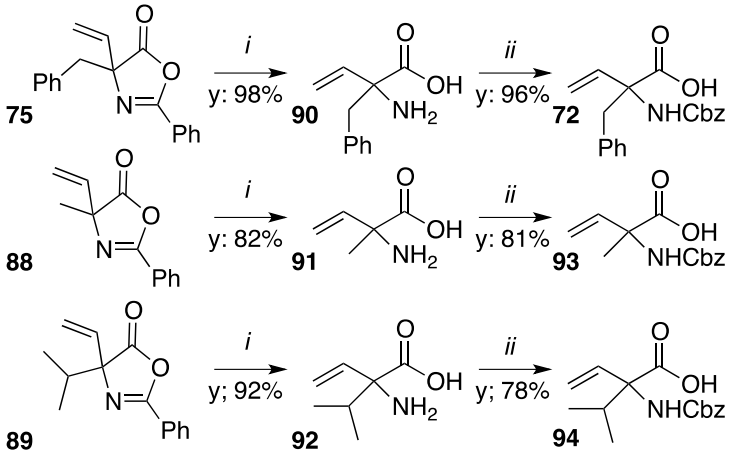

Scheme 40 Reagents and conditions: *i)* TFA, 100 °C; *ii)* $(Cbz)_2O$, TBAH, CH_3CN.

As a final proof of concept, the reactivity of the double bond was assessed by performing an Heck reaction in presence of 1-bromo-4-nitrobenzene and PdEnCat 30. Under these reaction conditions, the double bond of compound **75** was functionalised and the azlactone ring was opened in a one-pot fashion. Chromatographic purification afforded the N- and C-protected quaternary amino acid **95** in 81% overall yields (Scheme 41).

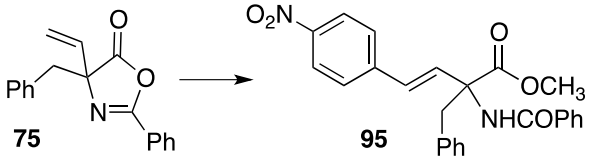

Scheme 41 Reagents and conditions: *p*-Br-nitrobenzene, PdEnCat 30 (10% mol), Bu_4NOAc, MeOH, 120 (MW).

2.3.3. *Decarboxylative Allylation of Azlactone Enol Carbonates*

In a previous work a gram scale Pd-catalyzed synthesis of α-allylphenylalanine **25** was developed Scheme 42. [118] Starting from phenylalanine, allyl enol carbonate **23** was obtained and submitted to an intramolecular Tsuji decarboxylative allylation in the presence of a Pd/diphosphine 1:4 complex composed by $Pd_2(dba)_3$ and 1,2- bis(diphenylphosphino)ethane (dppe) to give the 4-allyl azlactone **24**. The synthetic scheme proved to be a fast, efficient and robust method for the obtainment of the free quaternary α-amino acid **25**. These results prompted the development of a synthetic methodology based on an asymmetric Tsuji decarboxylative allylation that would allow the attainment of enantioenriched quaternary amino acids endowed with an allyl moiety (Scheme 42).

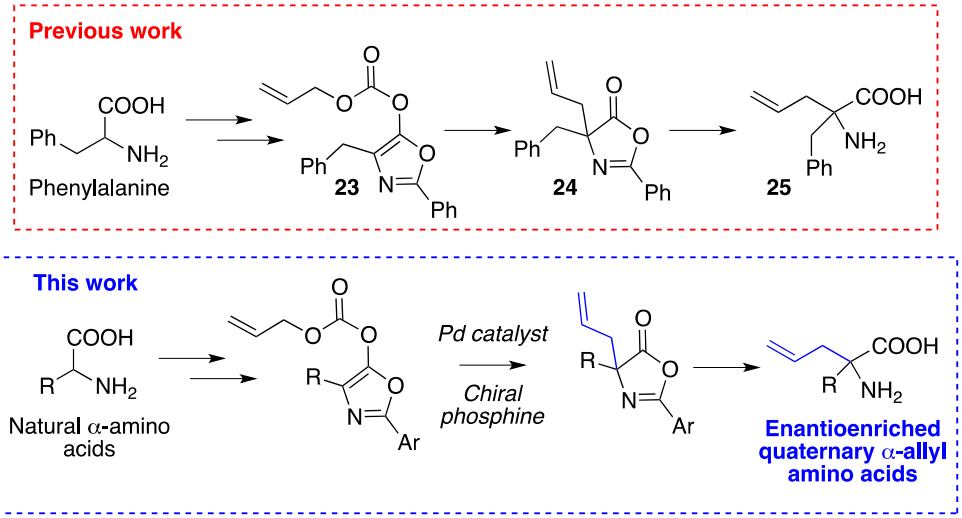

Scheme 42

Since the absolute configuration of the quaternary stereocenter at the C3 of bicyclic lactam scaffolds is mandatory for the biological activity of the RGD antagonist, the attainment of a single diastereoisomer of dipeptide **27** (Scheme 5, *vide supra*) would increase the overall efficiency of the protocol. For this reason, the enantioselective synthesis of amino acid **24** is of great interest. Only one example of enantioselective intramolecular Tsuji allylation was found in literature on 4-allyl-4-methyl-oxazol-5-one, but the product was attained in 2% *ee*.[142] From this starting point, the reaction parameters were carefully studied to achieve higher enantioselectivity. Natural amino acids are converted to the corresponding allyl enol carbonate through Schotten-Baumann benzoylation, DCC-promoted cyclodehydration and the final conversion of the obtained oxazolone into the corresponding allyl enol carbonate by formation of the enolate and subsequent treatment with allyl chloroformate. The yields reported in Scheme 43 are calculated over three steps, since no intermediate purifications were required during these steps. An advantage of allyl enol carbonates is the higher chemical stability with respect to the corresponding oxazolones, which undergo in-column degradation by reacting with the silanol groups of silica gel. Moreover, they can be stored for months at –4 °C without any apparent loss in titer and purity.

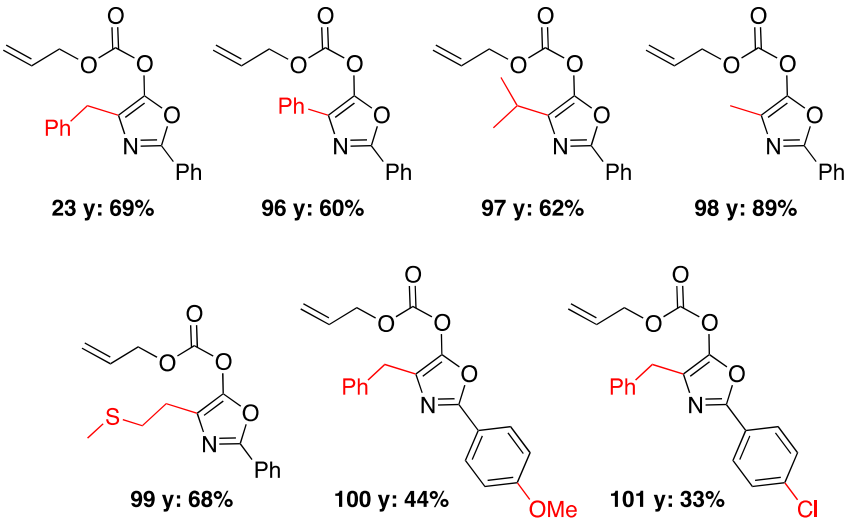

Scheme 43

The screening of the best chiral ligand for the transformation was performed on compound **98**, to better reproduce and improve the literature procedure (Scheme 44).

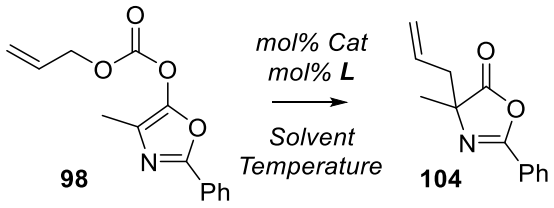

Scheme 44

The enol carbonate was reacted in presence of $Pd_2(dba)_3$/phosphine in 1:2.5 ratio in THF, according to the literature procedure[143], and the Pd catalyst was used in 2.5 mol%. Among all the ligands tested (Figure 26), (*R*,*R*)-DACH-phenyl Trost (**L6**) gave the best results, affording the product in 24% *ee*.

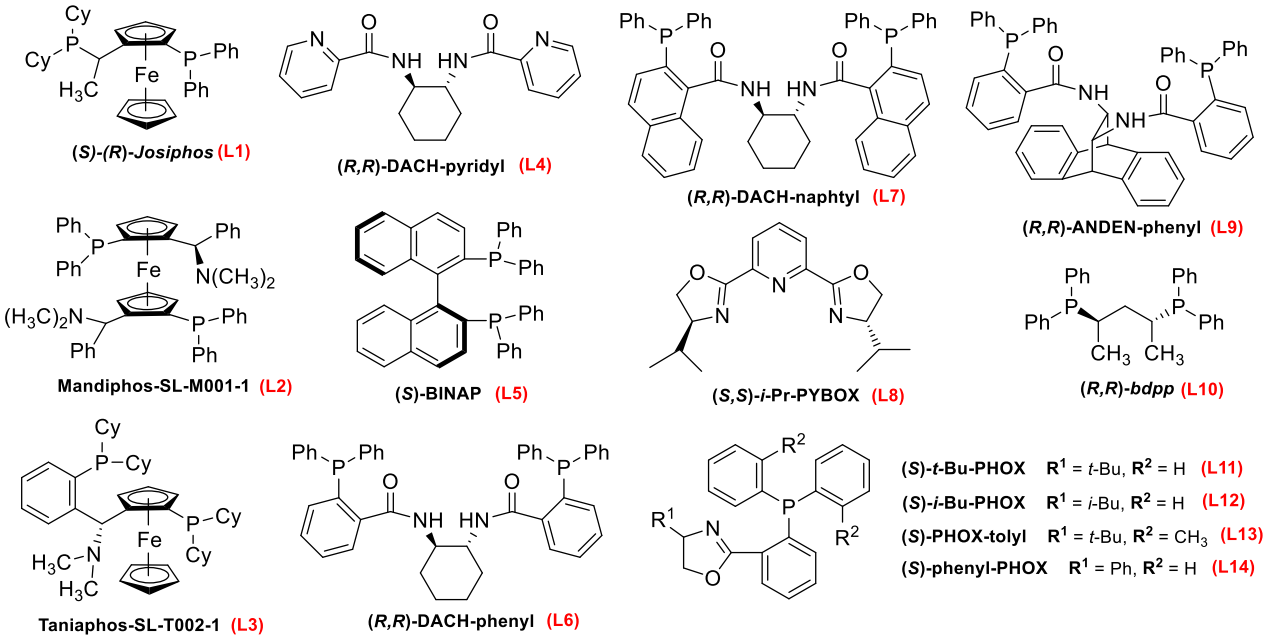

Figure 26

After the screening of different solvents (Table 5), acetonitrile was selected as the best performing, allowing the attainment of the product in 40% *ee* and very high yields (y: 92%).

Entry	Solvent	Yield	*ee*[a]
1	THF	98%	24%
2	Et_2O	86%	25%
3	CH_2Cl_2	49%	28%
4	Toluene	68%	10%
5	DMSO	63%	30%
6	CH_3CN	92%	40%
7	MeOH	N.R.	-
8	DME	45%	2%
9	1,4-Dioxane	37%	2%

Table 5 [a] The *ee* values were determined by chiral HPLC with a constant flow rate of 1 mL/min using Hexane/isopropanol 99,75:0,25 as the mobile phase.

Since allyl oxazolone **24** was the intermediate needed for the synthesis of bicyclic lactam scaffolds (*vide supra*), the following optimization process was performed on allyl enol carbonate 23 (Scheme 45).

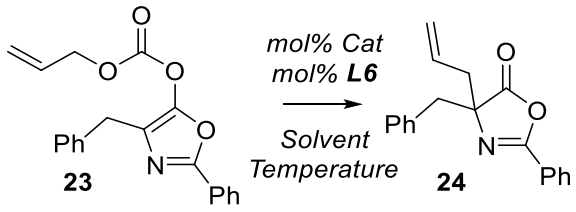

Scheme 45

By performing the reaction in the same conditions experimented for compound **98**, the results remained unchanged (Table 6, entry 1). The *ee* and yield did not seem to be substantially influenced by the increase in reaction time or by lowering the temperature to 0 °C (entry 3 and 4). The effect of $Pd_2(dba)_3$/phosphine ratio was assessed, since different catalytic species may form in the reaction mixture depending on the relative amount of ligand with respect to the catalyst. By increasing the ratio to 1:4 a slight increase in ee was observed (entry 5). By lowering the concentration to 0.01 M., an increase in the *ee* was observed (entry 6), which reached 59% when azlactone **24** was slowly added to the reaction mixture with a syringe pump (entry 9). The ee was not influenced by temperature increase (entry 10) of by increase in $Pd_2(dba)_3$/phosphine ratio (entry 11). The slow addition of the catalyst to a solution of compound **23** resulted in almost complete loss of enantioselectivity (entry 12). Since it was reported in literature that relatively high concentration of catalyst may be detrimental to the *ee* due to the formation of Pd clusters[143], the mol % of palladium catalyst were reduced to 1 (entry 14), 0.5 (entry 15) and 0.1 (entry 16). No benefit was observed

when reducing the equivalents of palladium to 1 mol% and the *ee* was completely lost when adding 0.1 mol% of $Pd_2(dba)_3$, although it is interesting to note that reaction yields remained excellent (y: 98%). The best results were achieved when adding 0.5 mol% of palladium (entry 15); allyl oxazolone **24** was isolated in 98% yields and 64% *ee*.

Entry	Time	Temperature	Conc [M]	$Pd_2(dba)_3$ (mol%)	L6 (mol%)	Yield [%]	*ee*[a] [%]
1	1 h	rt	0.1	2.5	6.25	94	41
2	1 h	rt	0.1	2.5	7.5	98	43
3	6 h	rt	0.1	2.5	7.5	98	40
4	1 h	0 °C	0.1	2.5	7.5	95	38
5	1 h	rt	0.1	2.5	10	98	47
6	1 h	rt	0.01	2.5	10	97	52
7	30 min	rt	0.01	2.5	10	96	52
8	5 min	rt	0.01	2.5	10	92	50
9[b]	30 min	rt	0.01	2.5	10	98	59
10[b]	30 min	50 °C	0.01	2.5	10	96	58
11[b]	30 min	rt	0.01	2.5	15	96	59
12[c]	30 min	rt	0.01	2.5	10	91	4
13[b]	30 min	rt	0.01	5	20	98	40
14[b]	30 min	rt	0.01	1	4.0	98	58
15[b]	**30 min**	**rt**	**0.01**	**0.5**	**2.0**	**98**	**64**
16[b]	30 min	rt	0.01	0.1	0.4	98	1

Table 6 Screening of the optimal reaction conditions. [a] The *ee* values were determined by chiral HPLC with a constant flow rate of 1 mL/min using hexane/isopropanol 99,75:0,25 as the mobile phase. [b] The allyl enol carbonate **23** was slowly added to the reaction mixture using a syringe pump. [c] The chiral catalyst was slowly added to a solution of the allyl enol carbonate **23** through a syringe pump.

Different palladium sources were also screened while maintaining the other parameters unchanged (Table 7). In presence of $PdCl_2$ (entry 2) and $Pd(OAc)_2$ (entry 4) the *ee* dropped to 18 and 0 respectively. $[(Cinnamyl)PdCl]_2$ did not improve the previous results (entry 3), whereas a slight increase in *ee* was observed with $[PdCl(allyl)]_2$ (entry 5). Increase in mol% of palladium led to a slight decrease of the *ee* (entry 7 and entry 8), whereas the use of 1.0 mol% enabled the attainment of the product in 70% *ee*. When 0.1 mol% of $[PdCl(allyl)]_2$ were used (entry 9), *ee* dropped to 30%, consistently with the previous results (Table 6, entry 16). At last, changes in the catalyst/phosphine ratio did not prove to be beneficial (Table 7, entry 10). Interestingly, in all these experiments the yields remained higher than 90%.

Entry	Pd Catalyst	Pd (mol%)	L6 (mol%)	Yield %	ee %
1	$Pd_2(dba)_3{\cdot}CHCl_3$	0.5	2.0	98	64
2	$PdCl_2$	1.0	2.0	92	18
3	$[(Cinnamyl)PdCl]_2$	0.5	2.0	93	62
4	$Pd(OAc)_2$	1.0	2.0	97	0
5	$[PdCl(allyl)]_2$	0.5	2.0	98	66
6	**$[PdCl(allyl)]_2$**	**1.0**	**4.0**	**98**	**70**
7	$[PdCl(allyl)]_2$	2.5	10	98	62
8	$[PdCl(allyl)]_2$	5.0	20	98	53
9	$[PdCl(allyl)]_2$	0.1	0.4	98	30
10	$[PdCl(allyl)]_2$	1.0	2.5	98	64

Table 7 Screening of the palladium source. [a] The *ee* values were determined by chiral HPLC with a constant flow rate of 1 mL/min using hexane/isopropanol 99,75:0,25 as the mobile phase.

The optimized conditions, *i.e.* acetonitrile as a solvent, $[PdCl(allyl)]_2$/chiral ligand **L6** in 1:4 ratio, and 0.01M as final concentration, were extended to all the other substrates (Figure 27).

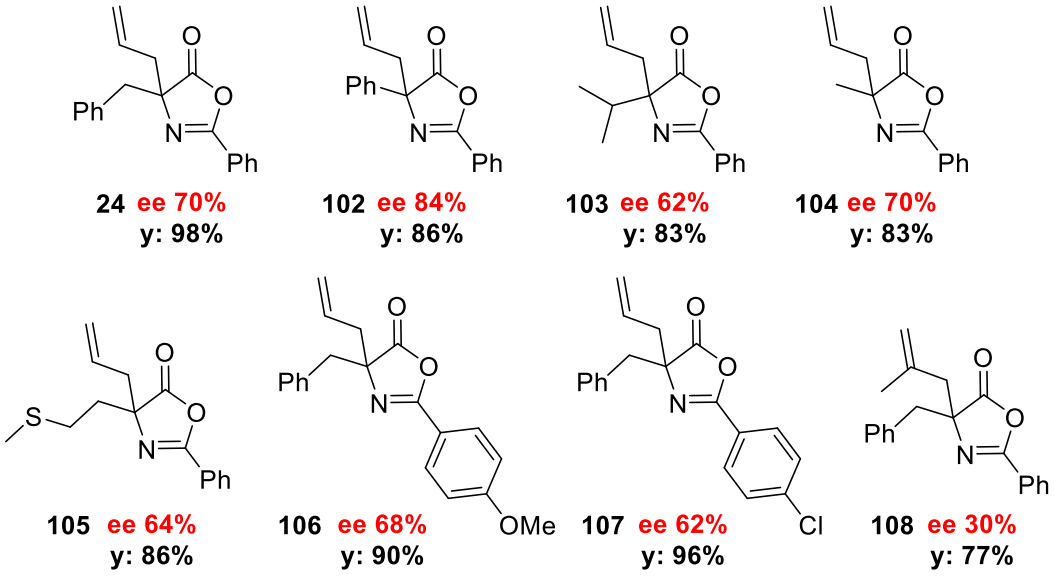

Figure 27 The ee value of compound **105** was determined on the corresponding N-Bz quaternary amino ester (Scheme 48). The ee value of compound **102** were also determined on the corresponding N-Bz quaternary amino ester to ascertain that the opening of the oxazolone ring occurs without racemization (Scheme 48).

The method developed proved to be robust and efficient, allowing the attainment of a wide range of allylated derivatives in very high or excellent yields. The lower enantiodiscrimination was observed in compound **103**, characterized by a sterically hindered isopropyl side chain, with an *ee* of 62%. The presence of a side chain incorporating a heteroatom such as sulfur was well tolerated, allowing the attainment of compound **105** in 64% *ee*. Substitution at the phenyl ring in position 2 of phenylalanine-derived oxazolones was not beneficial, with *ee* ranging from 68%, in the case of *para*-methoxy-substituted compound **106**, to 62%, for *para*-chloro-substituted compound **107**.

Phenylglycine-derived oxazolone showed the best results in terms of enantioselectiviy, in fact compound **102** was attained in 84% *ee*. Compound **108** was synthesized mainly as reference to perform a cross-over experiment to get some insight into the mechanism of the reaction (Scheme 46). Compound **109** was prepared by treating oxazolone **22** with compound **110**, which was prepared in situ from 2-methylprop-2-en-1-ol. The introduction of a methyl group at position 2 of the allyl moiety caused a significant drop of the enantioselectivity (*ee*: 30%).

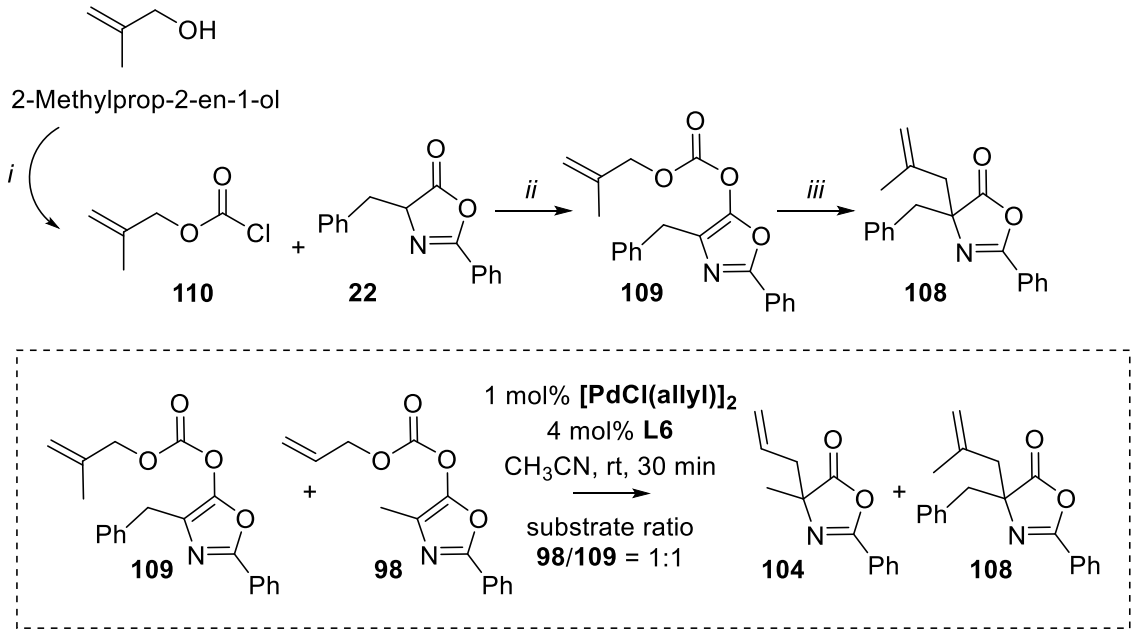

Scheme 46 Reagents and conditions: *i*) triphosgene, K_2CO_3, toluene; *ii*) Net_3, THF, 0 °C → rt; *iii*) $[PdCl(allyl)]_2$ (1 % mol), L6 (4% mol), CH_3CN, rt.

By reacting an equimolar mixture of enol carbonates **109** and **98** under optimized conditions, only compounds **104** and **108** were isolated. This result suggests that the allylation proceeds via a tight ion pair intramolecular process.[144] The reactivity of the double bond was also assessed by reacting allyl oxazolone **24** in a Heck coupling and a cross metathesis reaction (Scheme 47).

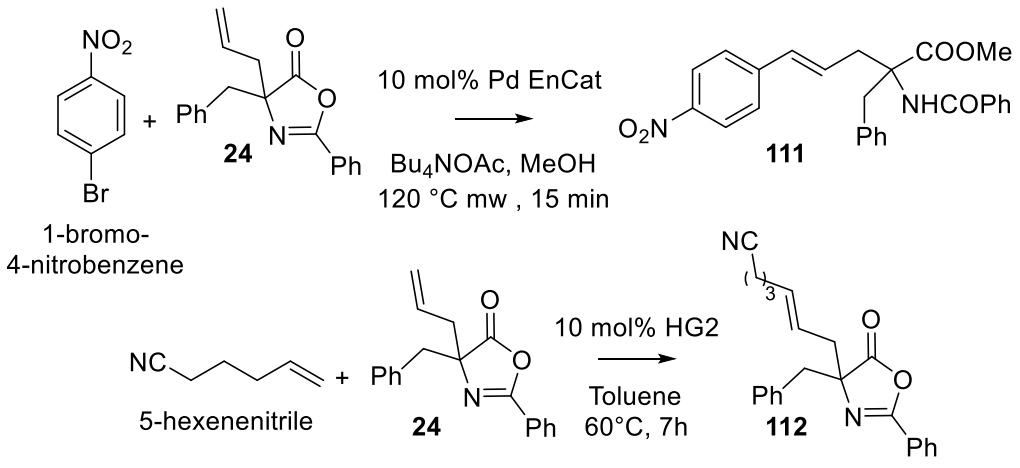

Scheme 47

The reaction between 1-bromo-4-nitrobenzene and compound **24** in presence of Bu_4NOAc and Pd EnCat 30 afforded N- and C-protected quaternary amino acid **111** in 75% yields in one-pot operation,

whereas the metathesis reaction in presence of HG2 catalyst and 5-hexenenitrile afforded compound **112** in 81% yield. To further extend the application of these substrates and to compare optical properties with known literature data, derivatives **25** ,**113**, **114**, **115**, **116**, **117** were synthesized (Scheme 48).

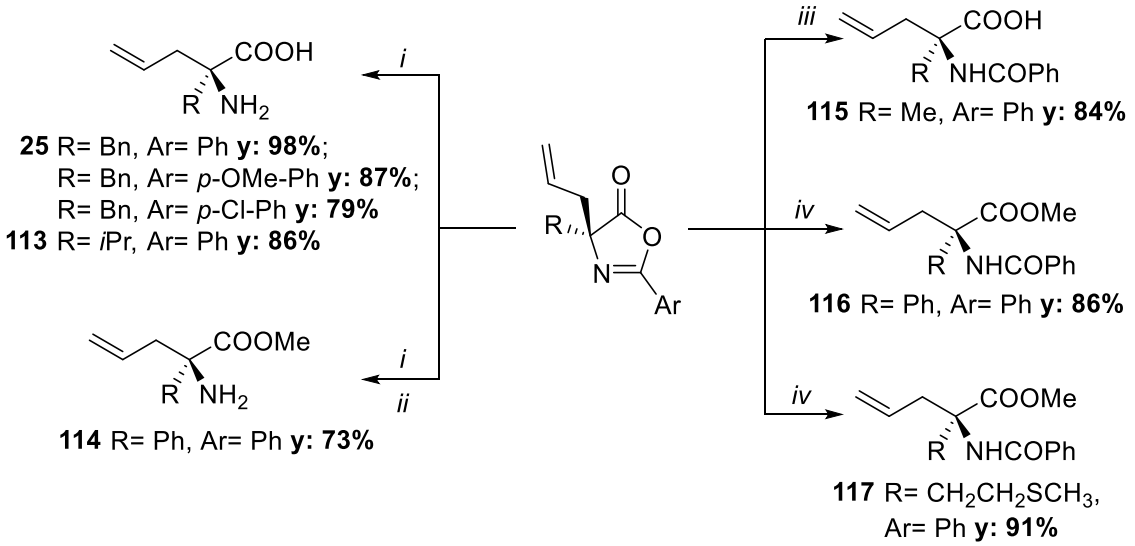

Scheme 48 Reagents and conditions: *i*) TFA, 100 °C; *ii*) CH_2N_2, MeOH; *iii*) LiOH, MeOH, rt; *iv*) MeOH, HCl, 120 °C (MW).

The successful conversion of the allyl oxazolones in variously protected amino acids confirms the versatility of the developed synthetic scheme for the attainment of quaternary amino acids, which may find interesting applications in peptide synthesis. The optical rotation of these derivatives was measured and compared with the literature values to assess the absolute configuration of the quaternary stereocenter.[145] The absolute configuration of compound **117** was determined by the order of elution of the enantiomers in chiral HPLC in relation to compound **116**.

2.3.4. *Conclusions and future perspectives*

During this PhD project a fast and efficient protocol for the synthesis of α-allyl quaternary amino acids was developed. This methodology allows the attainment of a wide range of unnatural amino acids starting from commercially available and cheap starting materials in few steps with minimal purifications required. The reactivity of the double bond installed may be exploited to further modify the allyl oxazolone intermediates, thus expanding the possible range of final products. Another advantage of the reported protocol is the use of allyl enol carbonates as key intermediates, because of their high stability and facile purification. Furthermore, the reactions involved proceed with very high yields and the achiral Tsuji allylation can also be performed with minimal amount of catalyst, thus resulting in a more atom-economic process which could be easily scalable. Although the *ee* were highly increased with respect to the known literature procedure[142], further studies are required in order to achieve higher levels of enantioselectivity. A strategy that may be experimented revolves around the use of a different metal for the allylation process. Hartwig and co-workers developed a method for stereodivergent allylic alkylation of aryl acetic acid esters through the use of an appropriate iridium catalyst in presence of a chiral base.[146] This protocol may be experimented on oxazolones or oxazolones derivative to achieve higher enantiomeric excess, thus further improving the methodology previously described (Scheme 49).

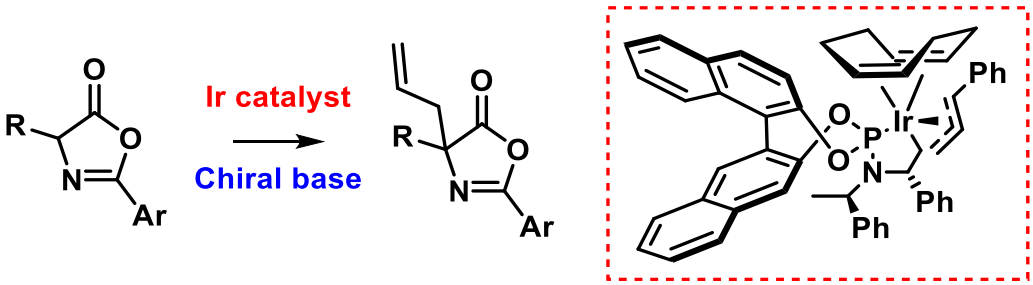

Scheme 49

3. Experimental section

General remarks

All chemicals were of reagent grade and were used without further purification. Solvents were purified according to the guidelines in Purification of Laboratory Chemicals[147]. All solvents were freshly distilled from the appropriate drying agent. THF, and toluene were distilled from sodium/benzophenone ketyl; Net_3, DIPEA, DCE and CH_2Cl_2 from CaH_2. Reactions requiring anhydrous conditions were performed under N_2. Yields were calculated for compounds purified by flash chromatography and judged homogeneous by thin-layer chromatography, NMR, and mass spectrometry. Thin layer chromatography was performed on Kieselgel 60 F_{254} (Merck) glass Plate eluting with solvents indicated, visualized by a 254 nm UV lamp, and stained with aqueous ceric molybdate solution or iodine and a solution of 4,4'-methylenebis-*N,N*-dimethylaniline, ninhydrin, and KI in an aqueous ethanolic solution of AcOH. Flash chromatography was performed on Merck Kieselgel 60 (230–400 mesh). Optical rotations $[\alpha]_D$ were measured in a cell of 5 cm path length and 1 mL capacity with a Jasco DIP-1000 polarimeter. Infrared spectra were recorded on a Perkin–Elmer ATR-FTIR 1600 series spectrometer using neat samples. Mass spectra were acquired with a Thermo Finnigan Q Exactive (API- HESI) FT Orbitrap mass spectrometer. Glassware for all reactions was oven-dried at 110 °C and cooled in a desiccator, or flame-dried and cooled under inert atmosphere prior to use. Liquid reagents and solvents were introduced by oven-dried syringes through septa-sealed flasks under an inert atmosphere.

NMR spectroscopic methods

Nuclear magnetic resonance spectra were acquired using a Bruker Avance 400 MHz spectrometer equipped with Bruker's TopSpin 1.3 software package and a Bruker Avance III HD 500 MHz spectrometer equipped with Bruker's TopSpin 3.5 (patch level 7) and provided with a high-sensitivity 5mm TCI cryoprobe. The abbreviations s, d, t, q, br s, and m stand for the resonance multiplicities singlet, doublet, triplet, quartet, broad singlet, and multiplet, respectively. In the peak listing of 13C spectra abbreviations s and t refer to zero and two protons attached to the carbons, as determined by DEPT-135 experiments. Phase-sensitive 2D-NOESY experiments were performed at 298K by using noesygpph pulse program from the Bruker library (mixing time of 0.5s or 0.8s). Sample temperatures were controlled with the variable-temperature unit of the instrument.

Abbreviations

$(Boc)_2O$	Di-*tert*-butyl dicarbonate
$(Cbz)_2O$	Dibenzyl dicarbonate
9-BBN	9-Borabicyclo[3.3.1]nonane
Boc	*tert*-butyloxycarbonyl
BOP-Cl	Bis(2-oxo-3-oxazolidinyl) phosphinic chloride
Cbz	Benzyloxycarbonyl
Cbz-Cl	Benzyl chloroformate
DBBQ	2,5-Di-*tert*-butyl-1,4-benzoquinone
DCC	*N*,*N*'-Dicyclohexyl carbodiimide
DCE	Dichloroethane
DEPBT	3-(Diethoxy-phosphoryloxy)-1,2,3-benzo[*d*]triazin-4(3H)-one
DIPEA	*N*,*N*-Diisopropylethylamine
DMAP	4-(Dimethylamino)pyridine
DME	1,2-Dimethoxyethane
DMF	*N*,*N*-Dimethylformamide
DMSO	Dimethyl sulfoxide
EDC	*N*-(3-Dimethylaminopropyl)-*N*'-ethylcarbodiimide
Fmoc	9-Fluorenylmethoxycarbonyl
Fmoc-Cl	9-Fluorenylmethoxycarbonyl chloride
Fmoc-Osu	9-Fluorenylmethyl *N*-succinimidyl carbonate
HATU	1-[Bis(dimethylamino) methylene]-1H-1,2,3-triazolo[4,5-*b*]pyridinium 3-oxid hexafluorophosphate
*i*BuOCOCl	Isobutyl chloroformate
*m*CPBA	3-Chloroperbenzoic acid
MsCl	Methanesulfonyl chloride
NaHMDS	Sodium bis(trimethylsilyl)amide
NMM	4-Methylmorpholine
NHS	N-Hydroxysuccinimide
Pbf	2,2,4,6,7-Pentamethyldihydrobenzofuran-5-sulfonyl
$Pd_2(dba)_3$	Tris(dibenzylideneacetone)dipalladium(0)
PPTS	Pyridinium *p*-toluenesulfonate
PyBroP	Bromotripyrrolidinophosphonium hexafluorophosphate
TBAF	Tetrabutylammonium fluoride
TBAH	Tetrabutylammonium hydroxide
TBAI	Tetrabutylammonium iodide
TBSCl	*tert*-Butyldimethylsilyl chloride
TFA	Trifluoroacetic acid
THF	Tetrahydrofuran
TMSI	Iodotrimethylsilane
TsOH	*p*-Toluenesulfonic acid

Synthesis of 2-((((9*H*-fluoren-9-yl)methoxy)carbonyl)amino)-2-benzylpent-4-enoic acid (26)

Compound **25** (1.50 g, 7.31 mmol) was suspended in 1:1 THF/H_2O (43.0 mL, 0.17 M) at 0 °C and was added with *N*-(9-Fluorenylmethoxycarbonyloxy)succinimide (2.74 g, 8.04 mmol) and Na_2CO_3 (1.55 g, 14.6 mmol). After 30 minutes the reaction mixture was warmed to room temperature.
Formation of the *N*-protected derivative was monitored by TLC analysis, R_f = 0.35 (AcOEt/MeOH 95:05). After 24 hours the pH was adjusted to 2 with a HCl 1N solution and extracted three times with AcOEt. The organic layer was dried with anhydrous Na_2SO_4, filtered, and evaporated under reduced pressure. The crude mixture was purified by flash chromatography (AcOEt/MeOH, 95:05) to obtain pure compound **26** as a white amorphous solid (3.12 g, quantitative). R_f = 0.35. ^{1}H NMR (dmso-d_6, 90 °C, 400 MHz, mixture of rotamers) δ 2.94–3.19 (m, 4H, partially masked by H_2O signal), 4.25 (t, *J* = 6.2 Hz, 1H), 4.39–4.51 (m, 2H), 4.95–5.08 (m, 2H), 5.66 (m, 1H), 6.20–6.37 (m, 1H), 6.96–7.08 (m, 2H), 7.15–7.23 (m, 3H), 7.33 (td, *J* = 1.0, 7.4 Hz, 2H), 7.42 (td, *J* = 1.3, 7.4 Hz, 2H), 7.67 (t, *J* = 7.2 Hz, 2H), 7.87 (d, *J* = 7.5 Hz, 2H), the chemical shift of the acid proton could not be unequivocally assigned; ^{13}C{^{1}H} NMR (dmso-d_6, 90 °C, 100 MHz, only major rotamer peaks were reported) δ 41.6 (t), 42.7 (t), 47.9, 64.1 (s), 66.2 (t), 109.8 (s), 120.8, 125.8, 127.1, 127.8, 128.4, 128.6, 130.7, 141.7 (s), 144.8 (s), 155.0 (s), 174.1 (s); IR (neat, cm^{-1}) 3404, 3067, 3031, 1696, 1686, 1593, 1495, 1448, 1223, 1076; HRMS (ESI) calculated for $C_{27}H_{24}NO_4$ $[M]^-$ 426.1711, found 426.1717 (Δ = 1.4 ppm).

Synthesis of (2*S*,5*R*)-methyl 1-(3-((((9*H*-fluoren-9-yl)methoxy)carbonyl)amino)-3-benzylhexa-1,5-dien-2-yl)-5-ethynylpyrrolidine-2-carboxylate (27)

To a solution of **26** (1.00 g, 2.34 mmol) and **12** (358 mg, 2.34 mmol) in dry THF (47.0 mL, 0.05 M), bis(2-oxo-3-oxazolidinyl)phosphinic chloride (BOP-Cl) (595 mg, 2.34 mmol) and $NaHCO_3$ (197 mg, 2.34 mmol) were added. The reaction mixture was heated to 50 °C and monitored with TLC analysis, R_f = 0.41 (hexane/AcOEt 60:40). Progressive additions of BOP-Cl (up to 1 eq.) and $NaHCO_3$ (up to 2 eq.) were performed. After 48 hours the solvent was evaporated under reduced pressure and the crude mixture was purified by flash chromatography (hexane/AcOEt 65:35) to obtain pure compound **20** as a white amorphous solid (922 mg, 70%). R_f = 0.36. ^{1}H NMR ($CDCl_3$, 400 MHz, mixture of diastereoisomers and rotamers) δ 1.59–1.81 (m, 1.3H), 1.90–2.48 (m, 4.7H), 2.52–2.74 (m, 0.6H) 2.84–3.46 (m, 2.4H), 3.54–4.00 (m, 4H), 4.18–4.30 (m, 1H), 4.32–4.57 (m, 2.6H), 4.65–4.76 (m, 0.4H), 5.04–5.32 (m, 2.3H), 5.64–5.93 (m, 1.4H), 6.03–6.25 (m, 0.3H), 7.02–7.15 (m, 1H), 7.16–7.27 (m, 4H), 7.29–7.37 (m, 2H), 7.38–7.47 (m, 2H), 7.54–7.66 (m, 2H), 7.75–7.84 (m, 2H); ^{13}C{^{1}H} NMR ($CDCl_3$, 100 MHz, mixture of diastereoisomers and rotamers) δ 26.8 (br, t), 34.6 (br, t), 40.0 (t), 40.3 (t), 40.5 (t), 47.6, 50.1, 50.6, 52.7, 61.9 (br), 65.4 (br, s), 66.8 (t), 74.1 (br), 82.5 (s), 119.8 (t), 119.9 (t), 120.4, 125.4, 125.6, 127.2, 127.4, 127.5 (2C), 128.1, 128.2, 128.4, 128.8, 130.1 (br), 130.9, 132.8, 133.0, 136.1 (br, s), 136.9 (s), 141.7 (s), 144.1 (s), 144.3 (2C, s), 155.1 (s), 170.3 (s), 170.6 (s), 172.3 (s); IR (neat, cm^{-1}) 3375, 3286, 3030, 2948, 2254, 2116, 1784, 1754, 1719, 1632, 1495, 1391,

1167, 1077; HRMS (ESI) calculated for $C_{35}H_{34}N_2NaO_5$ $[M+Na]^+$ 585.2360, found 585.2349 (Δ = 1.8 ppm).

General Procedure for domino cross-enyne metathesis/ring-closing metathesis

Compound **27** (1 eq.) and the styrene derivative (2 eq.) were solubilized in Toluene (0.017 M) and the solution was heated to 80 °C. Hoveyda Grubbs II generation catalyst (33.4 mg, 10% mol) was dissolved in Toluene (0.002 M) and slowly added to the reaction mixture over 7 hours using a syringe pump. After 1 hour from the end of the addition the solvent was evaporated under reduced pressure. Formation of the product was monitored by TLC analysis (hexane/AcOEt 60:40).

Synthesis of (3*S*,9a*R*)-methyl 6-((((9*H*-fluoren-9-yl)methoxy)carbonyl)amino)-6-benzyl-9-((*E*)-4-(2-((*tert*-butyldimethylsilyl)oxy)acetamido)styryl)-5-oxo-2,3,5,6,7,9a-hexahydro-1*H*-pyrrolo[1,2-*a*]azepine-3-carboxylate (32)

The title compound was prepared from compound **27** (300 mg, 0.533 mmol) and styrene derivative 2-((tert-butyldimethylsilyl)oxy)-N-(4-vinylphenyl)acetamide (311 mg, 1.07 mmol) according to the general procedure. The crude mixture was purified by flash chromatography to obtain diastereoisomers **32**.

Diastereoisomer 32a: White amorphous solid (109 mg, 25%). R_f = 0.45 (hexane/AcOEt 60:40); $[\alpha]_D^{22}$ +71.76 (c = 1.00, $CDCl_3$) ^{1}H NMR ($CDCl_3$, 400 MHz, mixture of rotamers) δ 0.19 (s, 6H), 1.01 (s, 9H), 2.08–2.23 (m, 3H), 2.64 (m, 1H), 2.86 (d, *J* = 17.6 Hz, 1H), 3.42 (d, *J* = 14.2 Hz, 1H), 3.55 (dd, *J* = 7.3, 17.6 Hz, 1H), 3.70 (d, *J* = 14.1 Hz, 1H), 3.76 (s, 3H), 4.17–4.28 (m, 4H), 4.51 (m, 1H), 4.75 (m, 1H), 4.89 (br s, 1H), 6.14 (br d, *J* = 6.8 Hz, 1H), 6.53–6.65 (m, 3H), 7.00–7.09 (m, 2H), 7.17–7.25 (m, 3H), 7.29–7.35 (m, 2H), 7.37–7.45 (m, 4H), 7.50–7.63 (m, 4H), 7.78 (app d, *J* = 7.6 Hz, 2H), 8.52 (s, 1H); $^{13}C\{^1H\}$ NMR ($CDCl_3$, 100 MHz, mixture of rotamers) δ 1.4, 18.6 (s), 26.2, 26.8 (t), 30.1 (t), 33.9 (t), 36.1 (t), 47.6, 52.8, 62.3, 62.7, 62.9 (s), 63.7 (t), 66.8 (t), 120.0, 120.3 (2C), 125.0, 125.6, 125.7, 125.8, 127.3, 127.4, 127.5, 128.0 (2C), 128.6, 128.7, 128.8, 129.3, 129.4, 129.6, 133.6 (s), 136.8 (s), 137.1 (s), 137.3 (s), 141.6 (s), 141.7 (s), 144.3 (s), 144.5 (s), 154.6 (s), 169.4 (s), 172.3 (s), 172.6 (s); IR (neat, cm^{-1}) 3377, 2952, 2929, 2853, 1742, 1714, 1697, 1630, 1519, 1412, 1249, 1197, 1103, 1070; HRMS (ESI) calculated for $C_{49}H_{55}N_3NaO_7Si$ $[M+Na]^+$ 848.3702, found 848.3687 (Δ = 1.7 ppm).

Diastereoisomer 32b: White amorphous solid (136 mg, 31%). R_f = 0.17 (AcOEt/hexane 60:40); $[\alpha]_D^{22}$ +21.29 (c = 1.20, $CDCl_3$) ^{1}H NMR ($CDCl_3$, 400 MHz, mixture of rotamers) δ 0.19 (s, 6H), 1.01 (s, 9H), 1.95–2.08 (m, 3H), 2.38 (m, 1H), 2.48 (dd, *J* = 6.9, 18.5 Hz, 1H), 2.69 (d, *J* = 18.4 Hz, 1H), 3.06 (d, *J* = 14.1 Hz, 1H), 3.62 (d, *J* = 14.1 Hz, 1H), 3.75 (s, 3H), 4.20–4.26 (m, 3H), 4.39 (m, 1H), 4.65 (app d, *J* = 5.8 Hz, 2H), 4.84 (m, 1H), 5.69 (br d, *J* = 6.3 Hz, 1H), 6.41 (d, *J* = 16.2 Hz, 1H), 6.46 (d, *J* = 16.1 Hz, 1H), 6.98–7.07 (m, 2H), 7.23–7.26 (m, 3H), 7.29–7.35 (m, 4H), 7.38–7.45 (m, 3H), 7.56 (d, *J* = 8.3 Hz, 2H),

7.63 (t, *J* = 6.5 Hz, 2H), 7.77 (t, *J* = 7.0 Hz, 2H), 8.52 (s, 1H); $^{13}C\{^{1}H\}$ NMR ($CDCl_3$, 100 MHz, mixture of rotamers) δ 1.4, 18.6 (s), 26.2, 26.7 (t), 30.1 (t), 33.5 (t), 40.3 (t), 47.9, 52.6, 59.7, 59.8 (s), 62.1, 63.7 (t), 66.3 (t), 120.0, 120.4, 120.5, 121.6, 125.2, 125.3, 125.7, 127.0, 127.4, 127.5, 128.2 (2C), 128.6 (2C), 129.3, 129.4, 131.8, 133.7 (s), 139.9 (s), 137.0 (s), 138.3 (s), 140.4 (s), 141.8 (s), 141.9 (s), 144.1 (s), 155.1 (s), 169.4 (s), 171.7 (s), 173.2 (s); IR (neat, cm^{-1}) 3385, 2948, 2929, 2857, 1720, 1699, 1648, 1519, 1411, 1250, 1197, 1104, 1076; HRMS (ESI) calculated for $C_{49}H_{55}N_3NaO_7Si$ $[M+Na]^+$ 848.3702, found 848.3696 (Δ = 0.6 ppm).

Synthesis of (3*S*,6*R*,9*R*,9a*R*)-methyl 6-((((9*H*-fluoren-9-yl)methoxy)carbonyl)amino)-6-benzyl-9-(4-(2-((*tert*-butyldimethylsilyl)oxy)acetamido)phenethyl)-5-oxooctahydro-1*H*-pyrrolo[1,2-*a*]azepine-3-carboxylate (33)

To a solution of **32a** (215 mg, 0.260 mmol) in dry MeOH (5.20 mL, 0.05 M)), under H_2 (balloon), Pd/C(en) (en = ethylenediamine) was added (43 mg, 20% weight). The reaction mixture was stirred at room temperature for 48 h. Formation of the product was monitored by TLC analysis, R_f = 0.45 (hexane/AcOEt 60:40). The reaction mixture was filtered through a pad of Celite, and the organic phase was evaporated under reduced pressure. The crude mixture was purified by flash chromatography (hexane/AcOEt 65:35) to obtain pure compound **33** as a white amorphous solid (166 mg, 77%). R_f = 0.35. $[\alpha]_D^{22}$ -11.73 (c = 1.50, $CDCl_3$); ^1H NMR (dmso-d_6, 90 °C, 400 MHz, mixture of rotamers) δ 0.15 (s, 6H), 0.96 (s, 9H), 1.60–2.17 (m, 11H), 2.46 (m, 1H), 2.64 (m, 1H), 3.19 (m, 1H), 3.34 (d, *J* = 13.3 Hz, 1H), 3.50–3.63 (m, 3H), 4.13 (dd, *J* = 3.8, 8.5 Hz, 1H), 4.19 (s, 2H), 4.27 (t, *J* = 5.9 Hz, 1H), 4.32–4.45 (m, 2H), 4.54 (dd, *J* = 6.1, 10.6 Hz, 1H), 6.26 (s, 1H), 6.78–6.88 (m, 2H), 7.11–7.23 (m, 5H), 7.30–7.37 (m, 2H), 7.38–7.45 (m, 2H), 7.50 (d, *J* = 8.5 Hz, 2H), 7.65 (t, *J* = 8.0 Hz, 2H), 7.87 (d, *J* = 7.9 Hz, 2H), 9.04 (s, 1H); $^{13}C\{^{1}H\}$ NMR ($CDCl_3$, 100 MHz, mixture of rotamers) δ -5.1, 1.4, 18.6 (s), 26.0, 26.2, 26.7 (t, 2C), 27.6 (t, 2C), 30.1 (t), 32.8 (t), 38.3 (t), 47.7, 52.5, 63.0, 63.4, 63.7 (t), 65.3 8s), 66.7 (t), 120.1, 120.3, 125.5, 125.7, 127.5 82C), 128.0, 128.7, 129.3, 129.9. 135.4 (s), 136.4 (s), 138.5 (s), 141.7 (s), 144.4 (s), 144.5 (s), 154.8 (s), 169.4 (s), 172.0 (s), 172.6 (s); IR (neat, cm^{-1}) 3378, 3064, 3027, 2958, 2929, 2856, 1752, 1718, 1697, 1628, 1524, 1414, 1262, 1106, 1050; HRMS (ESI) calculated for $C_{49}H_{59}N_3NaO_7Si$ $[M+Na]^+$ 852.4015, found 852.4003 (Δ = 1.3 ppm).

Synthesis of methyl (3*S*,6*R*,9*R*,9a*R*)-6-benzyl-6-(((benzyloxy)carbonyl)amino)-9-(4-(2-((*tert*-butyldimethylsilyl)oxy)acetamido)phenethyl)-5-oxooctahydro-1*H*-pyrrolo[1,2-*a*]azepine-3-carboxylate (34)

To a solution of compound **33** (35 mg, 0.042 mmol) in dry THF (0.47 mL, 0.09 M) under nitrogen atmosphere, piperidine (8 µL, 0.08 mmol) was added. Formation of the product was monitored by TLC, R_f = 0.35 (AcOEt/MeOH 95:05). After 6 hours the solvent was evaporated under reduced

pressure and the residue was recovered with a HCl 2N solution and washed with Et_2O. The pH of the aqueous phase was adjusted to 9 with a saturated aqueous solution of Na_2CO_3 and extracted three times with AcOEt. The organic phase was dried with anhydrous Na_2SO_4, filtered, and the solvent was evaporated under reduced pressure. The crude mixture was dissolved in dry CH_2Cl_2 (0.42 mL, 0.10 M) under nitrogen atmosphere and cooled to 0 °C. The reaction mixture was added with benzyl chloroformate (12 µL, 0.084 mmol) and DMAP (10 mg, 0.084 mmol). Formation of the product was monitored by TLC, R_f = 0.50 (hexane/AcOEt 60:40). After 1 hour the reaction mixture was allowed to warm to room temperatue. After 4 hours at rt the solvent was evaporated under reduced pressure and the crude mixture was purified by flash chromatography to obtain compound **34**.
White amorphous solid (21 mg, 66% over two steps). R_f = 0.35 (AcOEt/hexane 65:35); $[\alpha]_D^{22}$ -40.80 (c = 0.5, $CDCl_3$); ^{1}H NMR (dmso-d_6, 500 MHz, mixture of rotamers) δ -0.03 (s, 1.6H), 0.12 (s, 4.3H), 0.85 (s, 2.5H), 0.92 (s, 6.5H), 1.67–2.20 (m, 11H), 2.40 (m, 1H), 2.65 (m, 1H), 3.30 (d, *J* = 13.6 Hz, 1H, partially masked by H_2O signal), 3.43 (d, *J* = 13.7 Hz, 1H), 3.51 (s, 3H), 3.97 (s, 0.6H), 4.14 (dd, *J* = 3.6, 8.9 Hz, 1H), 4.19 (s, 1.4H), 4.38–4.59 (br, 1H), 5.00 (d, *J* = 12.6 Hz, 1H), 5.17 (d, *J* = 12.6 Hz, 1H), 6.36 (s, 1H), 6.76–6.85 (m, 2H), 7.10–7.23 (m, 5H), 7.32–7.45 (m, 5H), 7.51 (d, *J* = 8.4 Hz, 1.4H), 7.59 (d, *J* = 8.4 Hz, 0.6H), 9.36 (s, 0.7H), 9.55 (s, 0.3H); ^{13}C{^{1}H} NMR (dmso-d_6, 125 MHz, mixture of rotamers) δ -4.9, -2.7, 18.6(s), 26.1 (t), 26.3 (3C, including two CH_2), 27.1 (t), 30.1 (t), 32.6 (t), 37.8, 52.0, 62.3 (2C, including one CH_2), 63.2, 63.8 (t), 64.2 (s), 65.5 (t), 120.1, 127.0, 128.3, 128.4, 128.8 (2C), 128.9, 130.0, 136.4 (s), 136.5 (s), 136.7 (s), 137.5 (s), 137.7 (s), 137.9 (s), 153.9 (s), 169.2(s), 171.0 (s), 172.2 (s, 2C); IR (neat, cm^{-1}) 3374, 3028, 2950, 2927, 2855, 1750, 1717, 1696, 1626, 1523, 1412, 1102, 1075. HRMS (ESI) calculated for $C_{42}H_{55}N_3NaO_7Si$ $[M+Na]^+$ 764.3702, found 764.3715 (Δ = 1.8 ppm).

Synthesis of 1-bromo-4-vinylbenzene (43)

To a suspension of 4-bromo-benzaldehyde (1.00 g, 5.40 mmol) and methyltriphenylphosphonium bromide (2.32 g, 6.48 mmol) in dry THF (27 mL, 0.20 M) under nitrogen atmosphere, was added with NaH (584 mg, 24.4 mmol). The reaction mixture is warmed to room temperature and was left stirring overnight. The mixture was washed three times with brine, the organic layer was dried with anhydrous Na_2SO_4, filtered, and evaporated under reduced pressure. The crude mixture was purified by flash chromatography (hexane 100%) to attain pure compound **43** as a colourless oil (620 mg, 62%). R_f = 0.35. The spectroscopic data of compound **52** were matched with literature values.[148]

Synthesis of methyl (3S,9aR)-6-((((9H-fluoren-9-yl)methoxy)carbonyl)amino)-6-benzyl-9-((E)-4-bromostyryl)-5-oxo-2,3,5,6,7,9a-hexahydro-1H-pyrrolo[1,2-a]azepine-3-carboxylate (44)

The title compound was prepared from compound **27** (300 mg, 0.533 mmol) and styrene derivative **43** (195 mg, 1.07 mmol) according to the general procedure. The crude mixture was purified by flash chromatography to obtain diastereoisomers **44**.

Diastereoisomer 44a: White amorphous solid (102 mg, 27%). R_f = 0.40 (hexane/AcOEt 70:30); $[\alpha]_D^{22}$ +49.44 (c = 0.5, $CDCl_3$); ^1H NMR ($CDCl_3$, 400 MHz) δ 2.05–2.22 (m, 3H), 2.55–2.66 (m, 1H), 2.87 (d, *J* = 17.2 Hz, 1H), 3.41 (d, *J* = 13.9 Hz, 1H), 3.49–3.62 (m, 1H), 3.70 (d, *J* = 13.0 Hz, 1H), 3.76 (s, 3H), 4.20–4.29 (m, 2H), 4.45–4.56 (m, 1H), 4.75 (d, *J* = 6.9 Hz, 1H), 4.88 (br s, 1H), 6.16 (br d, *J* = 5.8 Hz, 1H), 6.56 (br s, 1H), 6.59 (d, *J* = 16.1 Hz, 1H), 6.66 (d, *J* = 16.1 Hz, 1H), 7.05 (br s, 2H), 7.18–7.24 (m, 3H), 7.26–7.36 (m, 5H), 7.42 (t, *J* = 7.4 Hz, 2H), 7.48 (d, *J* = 8.4 Hz, 2H), 7.53 (d, *J* = 7.4 Hz, 1H), 7.61 (d, *J* = 7.4 Hz, 1H), 7.78 (d, *J* = 7.5 Hz, 2H); $^{13}C\{^1H\}$ NMR ($CDCl_3$, 100 MHz) δ 26.8 (t), 33.8 (t), 33.9 (t), 36.3 (t), 47.7, 52.8, 62.0, 62.7, 62.9 (s), 66.8 (t), 120.3 (2C), 122.0 (s), 125.6, 125.7, 127.3, 127.4, 127.5, 128.0 (2C), 128.1, 128.3 (2C), 128.8 (3C), 129.6 (2C), 130.1, 132.2 (2C), 136.3 (s), 136.7 (s), 137.2 (s), 141.6 (s), 141.7 (s), 144.3 (s), 144.5 (s), 154.7 (s), 172.2 (s), 172.6 (s); IR (neat, cm^{-1}) 3376, 3023, 2954, 2924, 2854, 1744, 1715, 1630, 1486, 1435, 1365, 1261, 1199, 1177, 1070, 1032;

Diastereoisomer 44b: White amorphous solid (170 mg, 44%). R_f = 0.11 (AcOEt/hexane 70:30); $[\alpha]_D^{22}$ +5.61 (c = 1.0, $CDCl_3$); ^1H NMR ($CDCl_3$, 400 MHz) δ 1.95–2.10 (m, 3H), 2.33–2.37 (m, 1H), 2.43–2.55 (m, 1H); 2.69 (d, *J* = 18.3 Hz, 1H), 3.07 (d, *J* = 14.0 Hz, 1H), 3.61 (d, *J* = 14.0 Hz, 1H), 3.76 (s, 3H), 4.21–4.27 (m, 1H), 4.41 (br s, 1H), 4.61–4.72 (m, 2H), 4.81 (br s, 1H), 4.83–4.90 (m, 1H); 5.71 (br s, 1H), 6.41 (d, *J* = 16.0 Hz, 1H), 6.48 (d, *J* = 16.0 Hz, 1H), 7.03 (br s, 2H), 7.16–7.23 (m, 5H), 7.25–7.28 (m, 4H), 7.29–7.36 (m, 3H), 7.39–7.50 (m, 4H), 7.64 (t, *J* = 6.3 Hz, 2H), 7.75–7.82 (m, 2H); $^{13}C\{^1H\}$ NMR ($CDCl_3$, 100 MHz) δ 26.7 (t), 33.4 (t), 33.6 (t), 40.4 (t), 47.9, 52.6, 59.7, 59.9 (s), 62.1, 66.4 (t), 120.4, 120.5, 121.9 (s), 122.4, 125.2, 125.4, 127.0, 127.1, 127.4, 127.5, 128.2, 128.3 (2C), 128.6 (2C), 128.7, 130.1, 131.8 (2C), 132.2 (2C), 136.4 (s), 136.9 (s), 140.2 (s), 141.8 (s), 142.0 (s), 144.1 (s, 2C), 155.1 (s), 171.7 (s), 173.3 (s); IR (neat, cm^{-1}) 3392, 3306 (broad band), 3023, 2925, 2856, 1721, 1645, 1488, 1449, 1249, 1197, 1179, 1072, 1036.

Synthesis of tert-butyl (4-vinylphenyl)carbamate (47)

To a solution of 4-vinylaniline (800 mg, 6.71 mmol) in dry CH_2Cl_2 (6.7 mL, 1.0 M) under nitrogen atmosphere, was added $(Boc)_2O$ (1.90 g, 8.73 mmol). The After 12 hours the solvent was evaporated under reduced pressure. The crude mixture was purified by flash chromatography (hexane/AcOEt 95:05) to attain pure compound **47** as a white amorphous solid (1.40 g, 95%). R_f = 0.27. ^1H NMR ($CDCl_3$, 400 MHz) δ 1.55 (s, 9H), 5.18 (dd, *J* = 0.8, 10.9 Hz, 1H), 5.68 (dd, *J* = 0.8, 17.6 Hz, 1H), 6.62 (br s, 1H), 6.68 (dd, *J* = 10.9, 17.6 Hz, 1H), 7.32–7.38 (m, 4H); $^{13}C\{^1H\}$ NMR ($CDCl_3$, 100 MHz) δ 28.8, 112.8 (t), 118.9, 127.3 (2C), 132.9 (s), 136.6 (2C), 153.0 (s).

Synthesis of methyl (3S,9aR)-6-((((9H-fluoren-9-yl)methoxy)carbonyl)amino)-6-benzyl-9-((E)-4-((tert-butoxycarbonyl)amino)styryl)-5-oxo-2,3,5,6,7,9a-hexahydro-1H-pyrrolo[1,2-a]azepine-3-carboxylate (48)

The title compound was prepared from compound **27** (300 mg, 0.533 mmol) and styrene derivative 47 (234 mg, 1.07 mmol) according to the general procedure. The crude mixture was purified by flash chromatography to obtain diastereoisomers **48**.

Diastereoisomer 48a: White amorphous solid (96 mg, 24%). R_f = 0.43 (hexane/AcOEt 60:40); $[\alpha]_D^{22}$ +98.88 (c = 1.0, $CDCl_3$); ^1H NMR ($CDCl_3$, 400 MHz) δ 1.55 (s, 9H), 2.04–2.24 (m, 3H), 2.57–2.70 (m, 1H), 2.86 (d, *J* = 17.6 Hz, 1H), 3.42 (d, *J* = 14.1 Hz, 1H), 3.54 (dd, *J* = 8.1, 17.6 Hz, 1H), 3.70 (d, *J* = 14.1 Hz, 1H), 3.76 (s, 3H), 4.18–4.29 (m, 2H), 4.46–4.57 (m, 1H), 4.76 (d, *J* = 6.7 Hz, 1H), 4.88 (br s, 1H), 6.10 (br d, *J* = 7.5 Hz, 1H), 6.56 (d, *J* = 16.0 Hz, 1H), 6.61 (d, *J* = 16.0 Hz, 1H), 6.69 (s, 1H), 7.06 (br s, 2H), 7.15–7.26 (m, 3H), 7.29–7.46 (m, 9H), 7.53 (d, *J* = 7.2 Hz, 1H), 7.62 (d, *J* = 7.3 Hz, 1H), 7.79 (d, *J* = 7.5 Hz, 2H); $^{13}C\{^1H\}$ NMR ($CDCl_3$, 100 MHz) δ 26.8 (t), 28.8 (3C), 33.9 (2C, t), 36.1 (t), 47.6, 52.8, 62.4, 62.8, 63.0 (s), 66.8 (t), 81.1 (s), 119.0 (2C), 120.3 (2C), 124.6, 125.6, 125.8, 127.3, 127.4 (3C), 127.5, 128.0 (2C), 128.1, 128.8 (2C), 129.5, 129.7 (2C), 132.1 (s), 136.9 (s), 137.3 (s), 138.5 (s), 141.6 (s), 141.7 (s), 144.3 (s), 144.5 (s), 153.1 (s), 154.7 (s), 172.3 (s), 172.7 (s); IR (neat, cm^{-1}) 3368, 3029, 2979, 2932, 2848, 1716, 1630, 1587, 1519, 1491, 1411, 1314, 1222, 1154, 1070, 1051;

Diastereoisomer 48b: White amorphous solid (120 mg, 30%). R_f = 0.15 (AcOEt/hexane 60:40); $[\alpha]_D^{22}$ +22.40 (c = 1.0, $CDCl_3$); ^1H NMR ($CDCl_3$, 400 MHz) δ 1.54 (s, 9H), 1.94–2.09 (m, 3H), 2.32–2.41 (m, 1H), 2.46 (dd, *J* = 8.3, 18.4 Hz, 1H), 2.68 (d, *J* = 18.4 Hz, 1H), 3.05 (d, *J* = 14.2 Hz, 1H), 3.62 (d, *J* = 14.2 Hz, 1H), 3.75 (s, 3H), 4.23 (t, *J* = 5.9 Hz, 1H), 4.38 (br s, 1H), 4.64 (d, *J* = 5.9 Hz, 2H), 4.78– 4.91 (m, 2H), 5.66 (br d, *J* = 6.9 Hz, 1H), 6.37 (d, *J* = 16.0 Hz, 1H), 6.43 (d, *J* = 16.0 Hz, 1H), 6.57 (br s, 1H), 6.99–7.06 (m, 2H), 7.22–7.28 (m, 5H), 7.29–7.38 (m, 5H), 7.38–7.46 (m, 2H), 7.62 (t, *J* = 6.5 Hz, 2H), 7.77 (t, *J* = 6.9 Hz, 1H), 7); $^{13}C\{^1H\}$ NMR ($CDCl_3$, 100 MHz) δ 26.7 (t), 28.8 (3C), 33.5 (2C, t), 40.3 (t), 47.9, 52.6, 59.8 (s), 59.9, 62.1, 66.3 (t), 81.2 (s), 118.9 (2C), 120.4, 120.5, 121.2, 125.2, 125.3, 127.0, 127.4 (2C), 127.5, 127.5, 127.9, 128.1, 128.2, 128.6 (2C), 129.5, , 131.8 (2C), 132.3 (s), 136.9 (s), 138.3 (s), 138.5 (s), 140.5 (s), 141.8 (s), 141.9 (s), 144.1 (s), 153.0 (s), 155.1 (s), 171.7 (s), 173.3 (s); IR (neat, cm^{-1}) 3323, 3026, 2963, 2927, 2854, 1721, 1638, 1589, 1520, 1496, 1411, 1315, 1262, 1156, 1103, 1028.

Synthesis of methyl (3S,6R,9S,9aR)-6-((((9H-fluoren-9-yl)methoxy)carbonyl)amino)-6-benzyl-9-(4-((tert-butoxycarbonyl)amino)phenethyl)-5-oxooctahydro-1H-pyrrolo[1,2-a]azepine-3-carboxylate (49)

To a solution of **48a** (365 mg, 0.484 mmol) in dry MeOH (9.7 mL, 0.05 M), under H_2 (balloon), PtO_2 (platinum oxide) was added (4 mg, 1% weight). The reaction mixture was stirred at room temperature for 24 h. Formation of the product was monitored by TLC analysis, R_f = 0.48

(hexane/AcOEt 60:40). The reaction mixture was filtered through a pad of Celite, and the organic phase was evaporated under reduced pressure. The crude mixture was purified by flash chromatography (hexane/AcOEt 70:30) to obtain pure compound **49** as a white amorphous solid (334 mg, 91%). R_f = 0.31. $[\alpha]_D^{22}$ -10,80 (c = 1.0, $CDCl_3$); ^{1}H NMR (dmso-d_6, 80 °C, 400 MHz) δ 1.49 (s, 9H), 1.63–2.18 (m, 11H), 2.35–2.45 (m, 1H), 2.58–2.69 (m, 1H), 3.18 (br s, 1H), 3.33 (d, *J* = 12.5 Hz, 1H), 3.53 (s, 3H), 4.11 (dd, *J* = 3.8, 8.6 Hz, 1H), 4.27 (t, *J* = 5.9 Hz, 1H), 4.31–4.46 (m, 2H), 4.54 (dd, *J* = 5.8, 10.5 Hz, 1H), 6.26 (br s, 1H), 6.82 (br s, 2H), 7.10 (d, *J* = 8.4 Hz, 2H), 7.13–7.19 (m, 3H), 7.31–7.38 (m, 4H), 7.39–7.45 (m, 2H), 7.65 (t, *J* = 8.2 Hz, 2H), 7.87 (d, *J* = 8.2 Hz, 2H), 8.89 (s, 1H); ^{13}C{^{1}H} NMR (dmso-d_6, 80 °C, 100 MHz) δ 26.7 (t), 27.0 (t), 27.6 (t), 27.7 (t), 29.1, 30.5 (t), 33.2 (t), 36.5 (t), 38.6, 47.9, 52.2, 62.6, 63.7, 64.7 (s), 66.2 (t), 79.7 (s), 119.5 (2C), 120.8 (2C), 125.6, 125.7, 127.3, 127.8 (2C), 127.9 (2C), 128.4 (2C), 128.7 (2C), 129.1 (2C), 130.3 (2C), 136.7 (s), 137.0 (s), 138.1 (s), 141.8 (s, 2C), 144.8 (s), 144.9 (s), 153.8 (s), 154.4 (s), 171.6 (s), 172.5 (s); IR (neat, cm^{-1}) 3364, 3029, 2978, 2932, 2877, 1719, 1626, 1594, 1521, 1486, 1448, 1412, 1366, 1313, 1225, 1155, 1077, 1050.

Synthesis of methyl (3S,6R,9S,9aR)-6-amino-6-benzyl-9-(4-((tert-butoxycarbonyl)amino) phenethyl)-5-oxooctahydro-1H-pyrrolo[1,2-a]azepine-3-carboxylate (50)

To a solution of compound **49** (275 mg, 0.363 mmol) in dry THF (4.1 mL, 0.090 M) under nitrogen atmosphere, piperidine (36 µL, 0.36 mmol) was added. Formation of the product was monitored by TLC, R_f = 0.34 (AcOEt/MeOH 95:05). After 6 hours the solvent was evaporated under reduced pressure and the crude mixture was purified by flash chromatography (AcOEt/MeOH 95:05) to obtain compound **50** as a white amorphous solid (167 mg, 85%). R_f = 0.34.

Synthesis of (3S,6R,9S,9aR)-6-benzyl-6-(((benzyloxy)carbonyl)amino)-9-(4-((tert-butoxycarbonyl) amino)phenethyl)-5-oxooctahydro-1H-pyrrolo[1,2-a]azepine-3-carboxylic acid (52)

Compound **50** (71 mg, 0.13 mmol) was dissolved in dry THF (1.3 mL, 0.10 M) under nitrogen atmosphere and cooled to 0 °C. The reaction mixture was added with $(Cbz)_2O$ (49 mg, 0.17 mmol) and, after 2 hours, was warmed to room temperature. After 16 hour the reaction mixture was added with a 1.6 M aqueous solution of LiOH (166 µL, 0.265 mmol). If needed, MeOH can be added to homogenise the solution and, afterwards, the reaction mixture was heated to 60 °C. After 16 hours the solvent was evaporated under reduced pressure, the residue was recovered with water, the pH was adjusted to 2 by addition of a 0.01 M HCl aqueous solution and the aqueous layer was extracted three times with AcOEt. The organic phase was dried with anhydrous Na_2SO_4, filtered, and the solvent was evaporated under reduced pressure. The crude mixture was purified by flash chromatography (AcOEt/MeOH 99:01) to obtain compound **52** as a white amorphous solid (82 mg, 96%). R_f = 0.45. $[\alpha]_D^{22}$ -82,94 (c = 1.0, $CDCl_3$); ^{1}H NMR ($CDCl_3$, 400 MHz) δ 1.54 (s, 9H), 1.56–1.67 (m,

2H), 1.69–1.80 (m, 1H), 1.81–2.14 (m, 6H), 2.32–2.47 (m, 2H), 2.66–2.76 (m, 1H), 2.89 (br s, 1H), 3.38 (d, *J* = 13.9 Hz, 1H), 3.61 (d, *J* = 13.9 Hz, 1H), 4.29 (br s, 1H), 4.43 (d, *J* = 7.2 Hz, 1H), 5.08 (d, *J* = 12.4 Hz, 1H), 5.24 (d, *J* = 12.4 Hz, 1H), 6.56 (br s, 2H), 6.86 (d, *J* = 6.9 Hz, 2H), 7.07 (d, *J* = 8.4 Hz, 2H), 7.14–7.30 (m, 5H), 7.32–7.45 (m, 5H), 10.85 (br s, 1H); $^{13}C\{^{1}H\}$ NMR ($CDCl_3$, 100 MHz) δ 26.1 (t), 26.7 (t), 26.8 (t), 28.8 (3C), 30.1 (t), 30.3 (t), 32.3 (t), 32.4 (t), 36.5, 64.4, 65.3 (s), 66.6 (t), 81.0 (s), 119.4 (2C), 127.6, 128.5, 128.8 (2C), 128.9 (2C), 129.1 (2C), 129.7 (2C), 136.1 (s), 136.2 (s), 136.8 (s), 137.2 (s), 153.5 (s), 154.6 (s), 172.0 (s), 174.9 (s); IR (neat, cm^{-1}) 3600–2600 (broad band), 3354, 2961, 2929, 2856, 1716, 1624, 1593, 1520, 1485, 1447, 1412, 1366, 1313, 1227, 1156, 1075, 1049, 1026.

Synthesis of methyl N^2-((benzyloxy)carbonyl)- N^{ω} -((2,2,4,6,7-pentamethyl-2,3-dihydrobenzo furan-5-yl)sulfonyl)-L-arginylglycinate (55)

To a solution of Z-Arg(Pbf)-OH (1.03 g, 1.84 mmol) in dry THF (18 mL, 0.10 M) under nitrogen atmosphere NMM (0.81 mL, 7.3 mmol) was added. The reaction mixture was cooled to -20 °C and isobutyl chloroformate (0.29 mL, 2.2 mmol) was added. After 20 minutes H_2N-Gly-OMe*HCl (346 mg, 2.76 mmol) was also added and the reaction mixture was warmed at room temperature and left stirring for 15 hours. Afterwards, the suspension was filtered through a pad of Celite, and the organic phase was evaporated under reduced pressure. The residue was recovered with AcOEt and was washed with water. The organic phase was dried with anhydrous Na_2SO_4, filtered, and the solvent was evaporated under reduced pressure. The crude mixture was purified by flash chromatography (CH_2Cl_2/acetone 70:30) to obtain compound **55** as a white amorphous solid (930 mg, 80%). R_f = 0.33. The spectroscopic data of compound **52** were matched with literature values.[112]

Synthesis of methyl N^{ω} -((2,2,4,6,7-pentamethyl-2,3-dihydrobenzofuran-5-yl)sulfonyl)-L-arginyl glycinate (56)

To a solution of compound **55** (682 mg, 1.08 mmol) in dry MeOH (11 mL, 0.10 M), under H_2 (balloon), $Pd(OH)_2$/C (68 mg, 10% weight) was added. The reaction mixture was stirred at room temperature for 2 h. Afterwards, it was filtered through a pad of Celite and the organic phase was evaporated under reduced pressure. Compound **56** was isolated as a white amorphous solid without the need of further purifications (537 mg, quantitative). The spectroscopic data of compound **52** were matched with literature values.[112]

Synthesis of methyl N^2-((3S,6R,9S,9aR)-6-benzyl-6-(((benzyloxy)carbonyl)amino)-9-(4-((tert-butoxycarbonyl)amino)phenethyl)-5-oxooctahydro-1H-pyrrolo[1,2-a]azepine-3-carbonyl)-N^{ω}-((2,2,4,6,7-pentamethyl-2,3-dihydrobenzofuran-5-yl)sulfonyl)-L-arginylglycinate (57)

Compound **52** (85 mg, 0.13 mmol) and compound **56** (128 mg, 0.259 mmol) were dissolved in dry THF (1.3 mL, 0.10 M). The reaction mixture was added with HATU (98 mg, 0.26 mmol) and DIPEA (47 µL, 0.26 mmol) and was left stirring for 3 hours. Afterwards, the solvent was evaporated under reduced pressure, the residue was recovered with CH_2Cl_2 and was washed with a 1 M $KHSO_4$ aqueous solution and a saturated $NaHCO_3$ aqueous solution. The organic phase was dried with anhydrous Na_2SO_4, filtered, and the solvent was evaporated under reduced pressure. The crude mixture was purified by flash chromatography (AcOEt/hexane 90:10) to obtain compound **57** as a white amorphous solid (148 mg, quantitative). R_f = 0.34. $[\alpha]_D^{22}$ -28,86 (c = 1.0, $CDCl_3$); ^{1}H NMR ($CDCl_3$, 400 MHz) δ 1.46 (s, 6H), 1.54 (s, 9H), 1.55–2.15 (m, 11H), 2.09 (s, 3H), 2.23 (br s, 1H), 2.31–2.43 (m, 2H), 2.49–2.66 (m, 2H), 2.53 (s, 3H), 2.61 (s, 3H), 2.86–2.94 (m, 1H), 2.95 (s, 2H), 3.26 (br s, 1H), 3.38 (d, *J* = 13.8 Hz, 1H), 3.56 (d, *J* = 13.8 Hz, 1H), 3.68 (s, 3H), 3.90 (dd, *J* = 5.6, 17.6 Hz, 1H), 4.01 (dd, *J* = 5.6, 17.6 Hz, 1H), 4.35 (br s, 2H), 4.53 (d, *J* = 6.9 Hz, 1H), 5.03 (d, *J* = 12.3 Hz, 1H), 5.24 (d, *J* = 12.3 Hz, 1H), 5.95 (br s, 1H), 6.15 (br s, 2H), 6.68 (br s, 1H), 6.77 (br s, 1H), 6.84 (d, *J* = 6.7 Hz, 2H), 7.08 (d, *J* = 7.9 Hz, 2H), 7.12–7.25 (m, 5H), 7.32–7.45 (m, 5H), 7.48 (br s, 1H), 7.82 (br s, 1H); ^{13}C{^{1}H} NMR ($CDCl_3$, 100 MHz) δ 12.9, 18.3, 19.7, 25.9 (br t), 26.3 (br t), 26.9 (t), 27.7 (2C, br t), 28.8 (3C), 29.0 (2C), 29.9 (t), 30.1 (t), 30.8 (t), 33.5 (t), 38.1, 39.0, 39.7 (br t), 41.4 (t), 43.6 (t), 52.6, 63.4 (br), 64.3, 65.1 (s), 66.6 (t), 81.0 (s), 86.9 (s), 118.0 (s), 120.9, 125.1 (s), 127.5, 128.4 (2C), 128.6 (2C), 128.8 (2C), 128.9 (2C), 129.4 (2C), 129.9 (2C), 132.9 (s), 135.9 (s), 136.3 (s), 137.1 (s), 137.8 (s), 138.9 (s), 154.4 (s), 155.1 (s), 156.5 (s), 159.3 (s), 166.2 (s), 170.9 (s), 171.2 (s), 172.7 (s), 173.4 (s); IR (neat, cm^{-1}) 3600–2600 (broad band), 3329, 2963, 2928, 2855, 1720, 1664, 1613, 1522, 1449, 1411, 1367, 1313, 1304, 1261, 1234, 1157, 1090, 1049, 1026.

Synthesis of tert-butyl (S)-4-(((3S,6R,9S,9aR)-6-benzyl-9-(4-((tert-butoxycarbonyl) amino) phenethyl)-3-(((S)-1-((2-methoxy-2-oxoethyl)amino)-1-oxo-5-(3-((2,2,4,6,7-pentamethyl-2,3-dihydrobenzofuran-5-yl)sulfonyl)guanidino)pentan-2-yl)carbamoyl)-5-oxooctahydro-1H-pyrrolo[1,2-a]azepin-6-yl)amino)-3-(((benzyloxy)carbonyl)amino)-4-oxobutanoate (58)

To a solution of compound **57** (130 mg, 0.115 mmol) in dry MeOH (1.2 mL, 0.10 M), under H_2 (balloon), $Pd(OH)_2$/C (13 mg, 10% weight) was added. The reaction mixture was stirred at room temperature for 24 h. Afterwards, it was filtered through a pad of Celite and the organic phase was evaporated under reduced pressure. The crude mixture was dissolved in dry THF (1.2 mL, 0.10 M) under nitrogen atmosphere and was added with Z-L-Asp(O*t*Bu)-OH (74 mg, 0.23 mmol), HATU (98 mg, 0.26 mmol) and DIPEA (47 µL, 0.26 mmol. After 3 hours, the solvent was evaporated under reduced pressure, the residue was recovered with CH_2Cl_2 and was washed with a 1 M $KHSO_4$ aqueous solution and a saturated $NaHCO_3$ aqueous solution. The organic phase was dried with anhydrous Na_2SO_4, filtered, and the solvent was evaporated under reduced pressure. The crude mixture was purified by flash chromatography (AcOEt/hexane 80:20) to obtain compound **58** as a

white amorphous solid (125 mg, 83%). R_f = 0.35. $[\alpha]_D^{22}$ -42,84 (c = 1.0, $CDCl_3$); ^1H NMR (dmso-d_6, 400 MHz) δ 1.29–1.43 (m, 3H), 1.38 (s, 9H), 1.40 (s, 6H), 1.47 (s, 9H), 1.50–1.61 (m, 2H), 1.64–1.76 (m, 2H), 1.78–2.06 (m, 7H), 1.98 (s, 3H), 2.27–2.38 (m, 1H), 2.40 (s, 3H), 2.42–2.45 (m, 1H), 2.46 (s, 3H), 2.54–2.63 (m, 1H), 2.69 (dd, *J* = 5.5, 15.8 Hz, 1H), 2.79 (br s, 1H), 2.86–3.03 (m, 4H), 3.41 (d, *J* = 13.6 Hz, 1H), 3.51 (d, *J* = 13.6 Hz, 1H), 3.60 (s, 3H), 3.74–3.89 (m, 2H), 4.10–4.19 (m, 1H), 4.20–4.27 (m, 1H), 4.32–4.43 (m, 2H), 4.97 (d, *J* = 12.6 Hz, 1H), 5.05 (d, *J* = 12.6 Hz, 1H), 6.39 (br s, 1H), 6.63 (br s, 1H), 6.92 (d, *J* = 6.1 Hz, 2H), 7.04 (d, *J* = 8.4 Hz, 2H), 7.10–7.22 (m, 3H), 7.22–7.38 (m, 7H), 7.77 (d, *J* = 8.4 Hz, 1H), 7.84–7.92 (m, 2H), 8.23 (t, *J* = 5.6 Hz, 1H), 9.18 (s, 1H); $^{13}C\{^1H\}$ NMR ($CDCl_3$, 100 MHz) δ 12.3, 17.9, 19.3, 25.0 (br t), 26.1 (t), 27.1 (br t), 27.3 (br t), 27.9 (3C), 28.3 (3C), 28.5 (2C), 29.2 (t), 29.5 (t), 29.6 (t), 32.3 (t), 36.5 (t), 38.7, 51.2, 52.2, 52.9, 60.0 (br), 64.0, 65.3 (s), 67.1 (t), 80.2 (s), 81.5 (s), 86.6 (s), 117.7 (s), 119.4 (2C), 124.9 (s), 127.5, 127.9 (2C), 128.2, 128.5 (6C), 130.0 (2C), 133.3 (s), 134.7 (s), 136.0 (s), 136.2 (s), 136.4 (s), 139.3 (s), 153.3 (s), 155.2 (s), 156.8 (s), 159.5 (s), 169.9 (s), 170.2 (s), 171.0 (s), 171.7 (s), 173.0 (s), 173.5 (s); IR (neat, cm^{-1}) 3600–2600 (broad band), 3336, 2977, 2928, 2869, 1723, 1665, 1616, 1525, 1453, 1411, 1367, 1294, 1235, 1158, 1108, 1088, 1051.

Synthesis of tert-butyl (S)-4-(((3S,6R,9S,9aR)-6-benzyl-3-(((S)-1-((2-(benzyloxy)-2-oxoethyl) amino)-1-oxo-5-(3-((2,2,4,6,7-pentamethyl-2,3-dihydrobenzofuran-5-yl) sulfonyl)guanidino) pentan-2-yl)carbamoyl)-9-(4-((tert-butoxycarbonyl)amino) phenethyl)-5-oxooctahydro-1H-pyrrolo[1,2-a]azepin-6-yl)amino)-3-(((benzyloxy) carbonyl)amino)-4-oxobutanoate (59)

To a solution of compound **58** (115 mg, 0.088 mmol) in dry THF (0.88 mL, 0.10 M), under nitrogen atmosphere, BnOH (0.91 mL, 8.8 mmol), Ti(*i*PrO)$_4$ (13 µL, 0.044 mmol) and 4 Å molecular sieves (192 mg) were added. The reaction mixture was heated to 90 °C and was left stirring for 16 hours. Afterwards, the mixture was filtered through a pad of Celite and the organic phase was evaporated under reduced pressure. The residue was recovered with CH_2Cl_2 and was washed two times with a 2 M HCl aqueous solution. The organic phase was dried with anhydrous Na_2SO_4, filtered, and the solvent was evaporated under reduced pressure. The crude mixture was purified by flash chromatography (CH_2Cl_2/MeOH 95:05) to obtain compound **59** as a white amorphous solid (94 mg, 77%). R_f = 0.38. $[\alpha]_D^{22}$ -42,20 (c = 1.0, $CDCl_3$); ^1H NMR (dmso-d_6, 60 °C, 400 MHz) δ 1.31–1.44 (m, 3H), 1.39 (s, 9H), 1.40 (s, 6H), 1.48 (s, 9H), 1.53–1.64 (m, 2H), 1.68–2.03 (m, 9H), 2.00 (s, 3H), 2.30–2.39 (m, 1H), 2.43 (s, 3H), 2.44–2.49 (m, 1H), 2.48 (s, 3H), 2.53–2.62 (m, 1H), 2.70 (dd, *J* = 5.5, 15.8 Hz, 1H), 2.74–2.81 (m, 1H), 2.89–3.01 (m, 4H), 3.41 (d, *J* = 13.7 Hz, 1H), 3.53 (d, *J* = 13.7 Hz, 1H), 3.81–3.95 (m, 2H), 4.14–4.22 (m, 1H), 4.23–4.29 (m, 1H), 4.30–4.42 (m, 2H), 4.99 (d, *J* = 12.6 Hz, 1H), 5.04 (d, *J* = 12.6 Hz, 1H), 5.11 (s, 2H), 6.42 (br s, 1H), 6.54 (br s, 1H), 6.95 (d, *J* = 6.3 Hz, 2H), 7.04 (d, *J* = 8.4 Hz, 2H), 7.13–7.22 (m, 3H), 7.24–7.39 (m, 12H), 7.54 (br s, 1H), 7.73 (d, *J* = 8.1 Hz, 1H), 7.81–7.89 (m, 1H), 8.10 (t, *J* = 5.7 Hz, 1H), 8.97 (s, 1H); $^{13}C\{^1H\}$ NMR (dmso-d_6, 60 °C, 100 MHz) δ 12.0, 17.4,

18.7, 25.2 (t), 26.1 (t), 26.2 (t), 26.8 (t), 27.8 (3C), 28.2 (5C), 28.6 (t), 28.9 (t), 29.3 (t), 29.6 (t), 32.3 (t), 34.5 (t), 37.0, 38.7, 37.6 (t), 40.8 (t), 42.7 (t), 52.3, 53.1, 61.8, 63.5, 64.9 (s), 65.7 (t), 65.9 (t), 78.8 (s), 80.1 (s), 86.1 (s), 116.2 (s), 118.6 (2C), 124.3 (s), 126.5, 127.4 (2C), 127.6, 127.8 (2C), 127.8 (2C), 127.9, 128.2 (2C), 128.2 (2C), 128.3 (2C), 129.6 (2C), 131.5 (s), 134.5 (s), 135.6 (s), 135.9 (s), 136.3 (s), 136.8 (s), 137.2 (s), 152.9 (s), 155.6 (s), 156.1 (s), 157.5 (s), 169.2 (s), 169.4 (s), 169.5 (s), 170.7 (s), 171.3 (s), 171.8 (s); IR (neat, cm^{-1}) 3600–2600 (broad band), 3327, 2970, 2927, 2869, 1722, 1663, 1615, 1523, 1454, 1411, 1367, 1236, 1156, 1108, 1089, 1051, 1028.

Synthesis of compound 60

To a solution of compound **59** (134 mg, 0.0970 mmol) in dry MeOH (1.9 mL, 0.050 M), under H_2 (balloon), $Pd(OH)_2/C$ (13 mg, 10% weight) was added. The reaction mixture was stirred at room temperature for 12 h. Afterwards, it was filtered through a pad of Celite and the organic phase was evaporated under reduced pressure. The crude mixture was dissolved in dry THF (24 mL, 0.0040 M) under nitrogen atmosphere and was added with HATU (74 mg, 0.19 mmol) and DIPEA (35 µL, 0.19 mmol. After 24 hours, the solvent was evaporated under reduced pressure and the crude mixture was purified by flash chromatography (AcOEt/MeOH 98:02) to obtain compound **58** as a white amorphous solid (81 mg, 73%). R_f = 0.30. $[\alpha]_D^{22}$ -21.60 (c = 1.3, $CDCl_3$); IR (neat, cm^{-1}) 3600–2600 (broad band), 3327, 2925, 2854, 1722, 1657, 1622, 1520, 1453, 1411, 1368, 1296, 1236, 1155, 1107, 1090, 1052, 1028.

Synthesis of 3a-RGD

Compound **60** (106 mg, 0.0929 mmol) was dissolved in a 90:05:03:02 TFA/thioanisole/1,2-ethanedithiol/anisole solution (9.3 mL, 0.010 M) and the reaction mixture was stirred at room temperature for 3 h. Afterwards, the solvent was evaporated under reduced pressure, the residue was recovered with water and washed with Et_2O. The aqueous layer was evaporated under reduced pressure and the crude mixture was purified by semipreparative HPLC (Atlantis prep T3 5 µm 10x150 mm, stationary phase: C18, mobile phase: 75:25:0.1 H_2O:CH_3CN:TFA) to obtain **3a-RGD** (di-trifluoroacetate salt) as a white amorphous solid (61 mg, 68%). ^1H NMR (D_2O, 400 MHz) δ 1.69–1.82 (m, 3H), 1.38–1.95 (m, 1H), 1.96–2.33 (m, 7H), 2.38–2.49 (m, 1H), 2.50–2.59 (m, 1H), 2.72 (br s, 2H), 2.88–3.00 (m, 1H), 3.08–3.22 (m, 2H), 3.27 (dd, *J* = 6.6, 16.9 Hz, 1H), 3.33–3.48 (m, 2H), 3.55 (d, *J* = 13.5 Hz, 1H), 3.83 (d, *J* = 13.5 Hz, 1H), 3.89 (d, *J* = 14.7 Hz, 1H), 4.12 (br s, 1H), 4.31 (d, *J* = 14.7 Hz, 1H), 4.43 (t, *J* = 8.9 Hz, 1H), 4.63–4.69 (m, 1H), 5.18 (t, *J* = 6.2 Hz, 1H), 7.40 (d, *J* = 6.3 Hz, 2H), 7.59–7.69 (m, 5H), 7.71 (d, *J* = 7.9 Hz, 2H). MALDI TOF/TOF™ 5800 System (ABSciex) m/z: 732.4 $[M+H]^+$.

Synthesis of methyl 5-azidopentanoate (62)

To a solution of 5-Bromopentanoic acid (1.00 g, 5.52 mmol) in dry MeOH (6.9 mL, 0.80 M) at 0 °C under nitrogen atmosphere, $SOCl_2$ (1.20 mL, 16.6 mmol) was added drop-wise. After 30 minutes, the reaction has warmed to room temperature. After 1 hour, the solvent was remove under reduced pressure and the residue was recovered with 7 mL of AcOEt. The organic layer was washed three times with 5 mL of a $NaHCO_3$ saturated aqueous solution, three times with 5 mL of H_2O and once with 4 mL of brine. The organic phase was dried with anhydrous Na_2SO_4, filtered, and the solvent was evaporated under reduced pressure. The crude mixture of compound **61** was dissolved in dry DMF (7.4 mL, 0.75 M) under nitrogen atmosphere and was added with NaN3 (719 mg, 11.0 mmol). The reaction was heated to 80 °C through microwave irradiation for 20 minutes. The residue was recovered with AcOEt and was washed three times with a $NaHCO_3$ saturated aqueous solution, three times with H_2O and once with brine. The organic phase was dried with anhydrous Na_2SO_4, filtered, and the solvent was evaporated under reduced pressure. The crude mixture was purified by flash chromatography (toluene/AcOEt 95:05) to obtain compound **62** as a pale yellow oil (756 mg, 87% over two steps). R_f = 0.37. ^{1}H NMR ($CDCl_3$, 400 MHz) δ 1.59–1.68 (m, 2H), 1.69–1.78 (m, 2H), 2.36 (t, *J* = 7.1 Hz, 2H), 3.30 (t, *J* = 6.7 Hz, 2H), 3.68 (s, 3H); $^{13}C\{^1H\}$ NMR ($CDCl_3$, 100 MHz) δ 22.5 (t), 28.7 (t), 33.8 (t), 51.4 (t), 52.0, 174.0 (s).

Synthesis of 5-azidopentanoic acid (63)

To a solution of compound **62** (500 mg, 3.18 mmol) in dry MeOH (3.2 mL, 1.0 M) under nitrogen atmosphere, a 1.6 M aqueous solution of LiOH (1.06 mL, 6.36 mmol) was added. After 2 hours the solvent was evaporated under reduced pressure, the residue was recovered with water, the pH was adjusted to 2 by addition of a 1 M HCl aqueous solution and the aqueous layer was extracted three times with AcOEt. The organic phase was dried with anhydrous Na_2SO_4, filtered, and the solvent was evaporated under reduced pressure to afford compound **63** as a colourless oil without the need of further purifications (454 mg, quantitative). R_f = 0.55 (AcOEt/MeOH 90:10). ^{1}H NMR ($CDCl_3$, 400 MHz) δ 1.62–1.79 (m, 4H), 2.42 (t, *J* = 7.1 Hz, 2H), 3.32 (t, *J* = 6.5 Hz, 2H), 9.70 (br s, 1H); $^{13}C\{^1H\}$ NMR ($CDCl_3$, 100 MHz) δ 22.2 (t), 28.6 (t), 33.8 (t), 51.4 (t), 180.0 (s).

Synthesis of 2-(prop-2-yn-1-yloxy)acetic acid (64)

Prop-2-yn-1-ol (400 mg, 7.14 mmol) was added drop-wise in a solution of NaH (747 mg, 17.1 mmol) in dry THF (24 mL, 0.30 M) at 0°C under nitrogen atmosphere. Afterwards, 2-chloroacetic acid (742 mg, 7.85 mmol) was added in 2 hours and the reaction has warmed to room temperature. After 12 hours, the pH was adjusted to 2 by addition of a 0.02 M H_2SO_4 aqueous solution and the aqueous layer was extracted three times with AcOEt. The organic phase was dried with anhydrous Na_2SO_4, filtered, and the solvent was evaporated under reduced pressure. The crude mixture was purified

by flash chromatography (CH_2Cl_2/MeOH 95:05) to obtain compound **52** as a white amorphous solid (82 mg, 96%). R_f = 0.27. The spectroscopic data of compound **52** were matched with literature values.[127b]

Synthesis of 2-(prop-2-yn-1-yloxy)acetic acid (65)

To a solution of compound **64** (100 mg, 0.88 mmol) in dry CH_2Cl_2 (1.8 mL, 0.50 M) under nitrogen atmosphere, N-hydroxysuccinimide (102 mg, 0.89 mmol) and EDC*HCl (252 mg, 1.32 mmol) were added. After 1 hour, H_2O was added and the mixture was extracted three times with AcOEt. The organic phases were dried with anhydrous Na_2SO_4, filtered, and the solvent was evaporated under reduced pressure to afford compound **65**, which was reacted in the next step without further purifications.

Synthesis of 2,5-dioxopyrrolidin-1-yl 5-azidopentanoate (66)

To a solution of compound **63** (50 mg, 0.35 mmol) in dry CH_2Cl_2 (0.7 mL, 0.5 M) under nitrogen atmosphere, N-hydroxysuccinimide (41 mg, 0.35 mmol) and EDC*HCl (101 mg, 0.53 mmol) were added. After 1 hour, H_2O was added and the mixture was extracted three times with AcOEt. The organic phases were dried with anhydrous Na_2SO_4, filtered, and the solvent was evaporated under reduced pressure to afford compound **66** without the need of further purifications (83 mg, quantitative). R_f = 0.30 (hexane/AcOEt 60:40). ^{1}H NMR ($CDCl_3$, 400 MHz) δ 1.68–1.79 (m, 2H), 1.82–1.91 (m, 2H), 2.68 (t, *J* = 7.1 Hz, 2H), 2.82–2.90 (m, 4H), 3.36 (t, *J* = 6.6 Hz, 2H); ^{13}C{^{1}H} NMR ($CDCl_3$, 100 MHz) δ 22.3 (t), 26.0 (t), 28.3 (t), 30.8 (t), 51.2 (t), 168.6 (s), 170.0 (s).

Functionalisation of fibroin nanoparticles with linker 65

Fibroin nanoparticles (20 mg, Lys: 80 nmol/mg) were suspended in phosphate buffer (1 mL, pH: 7.4) for 1 hour to hydrate. A 10 mg/mL solution of compound **65** was added (50 µL, 0.0017 mmol). After 24 hours the nanoparticles were dialysed.

Bioconjugation of modified nanoparticles with Azide-fluor 545

Modified fibroin nanoparticles (20 mg, Lys: 80 nmol/mg) were suspended in phosphate buffer (1 mL, pH: 7.4) for 1 hour to hydrate. Azide-fluor 545 (1.4 mg, 0.0024 mmol), a 12 mg/mL solution of $CuSO_4$ (100 µL, 0.000481 mmol) and a 52 mg/mL solution of sodium L-ascorbate (100 µL,0.00262 mmol) were added. After 72 hours the nanoparticles were dialysed.

Bioconjugation of modified nanoparticles with compound 67

3a-RGD (5 mg, 0.00521 mmol) was dissolved in phosphate buffer (0.1 mL, 0.05 M) and a 5 mg/mL solution of compound **66** in CH_3CN (50 µL, 0.010 mmol) was added. After 36 hours the pH of the aqueous layer was adjusted to 3with TFA and the mixture was washed twice with CH_2Cl_2. The crude mixture containing compound **67** is then added to a previously prepared suspension of modified fibroin nanoparticles (20 mg, Lys: 80 nmol/mg) in phosphate buffer (1 mL, pH: 7.4). Afterwards, a 12 mg/ml solution of $CuSO_4$ (100 µL, 0.000481 mmol) and a 52 mg/ml solution of sodium L-ascorbate (100 µL, 0.00262 mmol) were added. After 72 hours the nanoparticles were dialysed.

Synthesis of 5-(4-(4-((methylsulfonyl)diazenyl)phenyl)-1H-1,2,3-triazol-1-yl)pentanoic acid (70)

To a solution of compound **63** (14 mg, 0.096 mmol) and azosulfone **69** (20 mg, 0.096 mmol) in dry THF (0.5 mL, 0.2 M) under nitrogen atmosphere, CuI (1 mg, 0.005 mmol) and NEt_3 (7 µL, 0.048 mmol) were added. After 1 hour the solvent was evaporated under reduced pressure and the crude mixture was submitted to the next synthetic step without further purifications.

Synthesis of 2,5-dioxopyrrolidin-1-yl 5-(4-(4-((methylsulfonyl)diazenyl)phenyl)-1H-1,2,3-triazol-1-yl)pentanoate (71)

To a solution of crude compound **70** (0.096 mmol) in dry CH_2Cl_2 (0.2 mL, 0.5 M) under nitrogen atmosphere, EDC*HCl (28 mg, 0.14 mmol) and NHS (11 mg, 0.097 mmol) were added. After 1 hour the solvent was evaporated under reduced pressure, the residue was recovered with water and extracted three times with AcOEt. The organic phase was dried with anhydrous Na_2SO_4, filtered, and the solvent was evaporated under reduced pressure to obtain compound **70** as a yellow amorphous solid without further purification required. (42 mg, quantitative). ^{1}H NMR (dmso-d6, 400 MHz) δ 1.59–1.70 (m, 2H), 1.94–2.05 (m, 2H), 2.78 (t, *J* = 7.4 Hz, 2H), 2.81 (br s, 4H), 3.44 (s, 3H), 4.51 (t, *J* = 6.9, 2H), 8.07 (d, *J* = 8.6, 2H), 8.18 (d, *J* = 8.6, 2H), 8.87 (s, 1H); ^{13}C{^{1}H} NMR (dmso-d_6, 100 MHz) δ 22.1 (t), 26.3 (t), 29.4 (t), 30.4 (t), 35.7, 50.1 (t), 124.3, 126.1 (2C), 127.2 (2C), 138.4 (s), 145.7 (s), 148.6 (s), 169.7 (s), 171.1 (s); IR (neat, cm^{-1}) 3133, 3038, 3022, 2929, 2859, 1808, 1777, 1734, 1608, 1472, 1413, 1326, 1210, 1145, 1094, 1048.

Synthesis of 2-benzyl-2-(((benzyloxy)carbonyl)amino)but-3-enoic acid (72)

A suspension of quaternary amino acid **89** (100 mg, 0.52 mmol) in dry CH_3CN (5.2 mL, 0.10 M) under nitrogen atmosphere, was added with tetramethylammonium hydroxide pentahydrate (188 mg, 1.04 mmol). The reaction mixture was stirred for 45 minutes, then $(Cbz)_2O$ (298 mg, 1.04 mmol) was added. After 12 hours, the solvent was evaporated under reduced pressure. The residue was

recovered with a saturated aqueous solution of Na_2CO_3 and washed three times with AcOEt. The pH of the aqueous phase was adjusted to 1, with a HCl 1N solution, and extracted three times with AcOEt. The organic layer was dried with anhydrous Na_2SO_4, filtered, and evaporated under reduced pressure. The crude mixture was purified by Kugelrohr distillation (110°C, 0.01 mmHg) to obtain **72** as a yellow oil (162 mg, 96%). R_f = 0.53 (CH_2Cl_2/MeOH 90:10 with 1% AcOH). The spectroscopic data of compound **72** were matched with literature values.[132]

Synthesis of methyl (2*S*,5*R*)-1-((*S*)-2-benzyl-2-(((benzyloxy)carbonyl)amino)but-3-enoyl)-5-ethynylpyrrolidine-2-carboxylate (73)

To a solution of **72** (212 mg, 0.652 mmol) and **12** (100 mg, 0.652 mmol) in dry THF (2.2 mL, 0.30 M), HATU (273 mg, 0.718 mmol) and DIPEA (0.17 mL, 0.98 mmol) were added. The reaction was heated at 60 °C and was left stirring for 26 hours. Afterwards, the solvent was evaporated under reduced pressure and the crude mixture was purified by flash chromatography (hexane/AcOEt 70:30) to obtain diastereoisomers **73**.

Diastereoisomer **73a**. White amorphous solid; (123 mg, 41%). R_f = 0.31 (hexane/AcOEt 70:30); $[\alpha]_D^{22}$ +18.70 (c = 0.25, $CDCl_3$); ^{1}H NMR (dmso-d_6, 400 MHz) δ 1.69 (m, 1H), 1.84–2.00 (m, 2H), 2.29 (m, 1H), 3.07 (d, *J* = 13.0 Hz, 1H), 3.22 (d, *J* = 1.8 Hz, 1H), 3.49 (d, *J* = 13.1 Hz, 1H), 3.66 (s, 3H), 4.30 (m, 1H), 4.85 (d, *J* = 12.3 Hz, 1H), 4.86 (m, 1H), 5.03 (d, *J* = 17.8 Hz, 1H), 5.14 (d, *J* = 10.9 Hz, 1H), 5.26 (d, *J* = 12.3 Hz, 1H), 5.84 (dd, *J* = 10.9, 17.7 Hz, 1H), 6.89–7.05 (m, 2H), 7.11–7.25 (m, 3H), 7.29–7.49 (m, 5H), 7.71 (s, 1H); ^{13}C{^{1}H} NMR (dmso-d_6, 100 MHz) δ 27.6 (t), 33.9 (t), 42.5 (t), 50.4, 52.4, 61.4, 64.5 (s), 66.2 (t), 74.5, 83.7 (s), 115.1 (t), 127.1, 128.5, 128.7, 129.2, 131.7, 137.1 (s), 138.0 (s), 139.0, 155.0 (s), 170.5 (s), 172.5 (s); IR (neat, cm^{-1}) 3292, 2952, 2925, 2855, 1722, 1638, 1495, 1454, 1255, 1197, 1166; HRMS (ESI) calculated for $C_{27}H_{28}KN_2O_5$ $[M+K]^+$ 499.1630, found 499.1625 (Δ = 1.1 ppm).

Diastereoisomer **73b**. White amorphous solid; (120 mg, 40%). R_f = 0.4 (hexane/AcOEt 70:30); $[\alpha]_D^{22}$ -10.50 (c = 0.25, $CDCl_3$); ^{1}H NMR (dmso-d6, 120°C, 400 MHz) mixture of conformers δ 1.84–2.19 (m, 3H), 2.48 (br, 1H,), 2.96 (m, 1H), 3.18–3.30 (m, 2H,), 3.61 (m, 3H), 4.43–4.56 (m, 1.7 H), 4.94–5.11 (m, 2.2 H), 5.16–5.29 (m, 1.5 H), 5.42 (d, *J* = 10.6 Hz, 0.3H), 5.50 (d, *J* = 17.1 Hz, 0.3H) , 6.02 (dd, *J* = 10.8, 17.5 Hz, 0.7H), 6.11 (dd, *J* = 10.5, 17.1 Hz, 0.7H), 6.96 (m, 0.6H), 7.07 (m, 1.4H), 7.13–7.25 (m, 3H), 7.26–7.41 (m, 6H); ^{13}C{^{1}H} NMR (dmso-d_6, 100 MHz) δ 26.2 (t), 29.5 (t), 29.8 (t), 33.5 (t), 41.3 (t), 41.4 (t), 41.8 (t), 49.1, 49.6, 51.6, 51.7, 60.0, 60.2, 62.9 (t), 63.6 (s), 64.0 (s), 65.4 (t), 65.5 (t), 68,7 (s), 72.4 (s), 74.5 (s), 82.4 (s), 84.2 (s), 115.0 (t), 117.1 (t), 117.7 (t), 126.1, 126.3, 126.4, 126.6, 127.6 (2C), 127.7, 128.0 (2C), 128.1, 128.3, 128.4, 130.2, 130.8 (2C), 133.5 (s), 134.6, 135.8 (s), 136.2 (s), 136.5 (s), 136.8 (s), 137.7 (s), 142.5 (s), 150.1 (s), 154.0 (s), 168.8 (s), 169.9 (s), 170.5 (s), 171.5 (s), 171.6 (s); IR (neat, cm^{-1}) 3382, 3289, 2955, 1720, 1637, 1496, 1481, 1454, 1393, 1259, 1199, 1168, 1075, 1025.

Synthesis of 4-benzyl-2-phenyl-4-vinyloxazol-5(4*H*)-one (75)

To a solution of 4-benzyl-2-phenyloxazol-5(4H)-one (**22**) (100 mg, 0.40 mmol) in dry THF (0.67 mL, 0.60 M) under nitrogen atmosphere, Et_3N (28 µL, 0.20 mmol) was added and the reaction mixture was cooled at –10°C. A solution of 2-(phenylselenyl)acetaldehyde (83 mg, 0.42 mmol) in dry THF (0.70 mL, 0.60 M) was added and the reaction mixture was stirred for 0.5 h. Formation of the aldol adducts was monitored by TLC analysis, R_f = 0.36 and R_f = 0.29 (hexane/AcOEt 85:15). Afterwards, methanesulfonyl chloride (46 µL, 0.60 mmol) and NEt_3 (56 µL, 0.40 mmol) were added in three portions at 10-minute intervals. After each addition, the pH was monitored with litmus paper and, if necessary, NEt_3 was added to basify the solution. Formation of mesylates was monitored with TLC analysis, R_f = 0.28 and R_f = 0.23 (hexane/AcOEt 80:20). After 10 minutes from the last addition, tetrabutylammonium iodide (145 mg, 0.40 mmol) was added and the reaction mixture was heated in a microwave oven at 110°C for 10 minute. After reaction completion, monitored by TLC analysis, the mixture was washed with phosphate buffer saturated with NaCl. The organic layer was dried with anhydrous Na_2SO_4, filtered, and evaporated under reduced pressure. The crude mixture was purified by flash chromatography to obtain **75** as a yellow oil (89 mg, 82 %).
Chiral procedure: ($(DHQD)_2PHAL$ (0.10 eq) was used in the aldol condensation step in place of NEt_3 (87 mg, 78 %). R_f = 0.63 (hexane/AcOEt 95:05); ^1H NMR ($CDCl_3$, 400 MHz) δ 3.29 (s, 2H), 5.35 (d, *J* = 10.7 Hz, 1H), 5.55 (d, *J* = 17.2 Hz, 1H), 6.14 (dd, *J* = 10.5, 17.2 Hz, 1H), 7.14–7.25 (m, 5H), 7.45 (app t, *J* = 7.8 Hz, 2H), 7.56 (app t, *J* = 7.5 Hz, 1H), 7.91 (app d, *J* = 7.8 Hz, 2H); ^{13}C NMR ($CDCl_3$, 100 MHz) δ 44.6 (t), 75.7 (s), 117.9 (t), 126.1 (s), 127.7, 128.3, 128.6, 129.1, 130.7, 133.1, 134.4 (s), 135.0, 160.5 (s), 177.8 (s); IR (neat, cm^{-1}) 3031, 2917, 2848, 1815, 1654, 1580, 1450, 965; HRMS (ESI) calculated for $C_{18}H_{15}NNaO_2$ $[M+Na]^+$ 300.09950, found 300.10005 (Δ = 1.8 ppm).

Synthesis of methyl (3S,6S,8aR)-6-benzyl-6-(((benzyloxy)carbonyl)amino)-5-oxo-8-vinyl-1,2,3,5,6, 8a-hexahydroindolizine-3-carboxylate (77a)

To a solution of compound **73a** (38 mg, 0.085 mmol) in dry toluene (4.0 mL, 0.021 M) under nitrogen atmosphere, Hoveyda Grubbs II generation catalyst (1.3 mg, 0.0021 mmol) was added and the reaction mixture was heated at 65 °C. Hoveyda Grubbs II generation catalyst (6.7 mg, 0.011 mmol) was dissolved in Toluene (4.5 mL, 0.0024 M) and slowly added to the reaction mixture over 16 hours using a syringe pump. Afterwards, the solvent was evaporated under reduced pressure and the crude mixture was purified by flash chromatography (cyclohexane/AcOEt 60:40) to obtain compound **77a** as a white amorphous solid (18 mg, 46 %). R_f = 0.35. $[\alpha]_D^{22}$ +66.45 (c = 1.1, $CDCl_3$); ^1H NMR (dmso-d_6, 80 °C, 400 MHz) δ 1.54–1.67 (m, 1H), 1.84–1.93 (m, 1H), 1.94–2.07 (m, 1H), 2.13–2.22 (m, 1H), 2.96 (d, *J* = 13.0 Hz, 1H), 3.13 (d, *J* = 13.0 Hz, 1H), 3.24–3.30 (m, 1H), 3.53 (s, 3H), 4.12 (d, *J* = 9.5 Hz, 1H), 5.01 (d, *J* = 12.7 Hz, 1H), 5.09 (d, *J* = 12.7 Hz, 1H), 5.11 (d, *J* = 11.2 Hz, 1H), 5.25 (d, *J* = 17.7 Hz, 1H), 6.06 (s, 1H), 6.24 (dd, *J* = 11.2, 17.7 Hz, 1H), 6.70 (s, 1H), 7.02–7.09 (m, 2H), 7.16–

7.25 (m, 3H), 7.27–7.44 (m, 5H); $^{13}C\{^{1}H\}$ NMR ($CDCl_3$, 100 MHz) δ 28.1 (t), 29.1 (t), 44.1 (t), 52.2, 57.3, 59.2, 60.5 (s), 66.3 (t), 115.7 (t), 125.2, 126.9, 127.6, 127.9 (2C), 128.4, 130.7, 133.6, 134.7 (s), 136.3 (s), 136.4 (s), 154.8 (s), 167.3 (s), 171.6 (s). IR (neat, cm^{-1}) 3392, 3030, 2951, 2927, 2853, 1721, 1653, 1489, 1451, 1371, 1240, 1201, 1175, 1088, 1077, 1042, 1014.

Synthesis of methyl (3S,6R,8aR)-6-benzyl-6-(((benzyloxy)carbonyl)amino)-5-oxo-8-vinyl-1,2,3,5,6, 8a-hexahydroindolizine-3-carboxylate (77b)

To a solution of compound **73b** (70 mg, 0.152 mmol) in dry toluene (7.2 mL, 0.021 M) under nitrogen atmosphere, Hoveyda Grubbs II generation catalyst (2.3 mg, 0.0037 mmol) was added and the reaction mixture was heated at 65 °C. Hoveyda Grubbs II generation catalyst (12 mg, 0.011 mmol) was dissolved in Toluene (3.5 mL, 0.0024 M) and slowly added to the reaction mixture over 16 hours using a syringe pump. Afterwards, the solvent was evaporated under reduced pressure and the crude mixture was purified by flash chromatography (hexane/AcOEt 60:40) to obtain compound **77b** as a white amorphous solid (26 mg, 37 %). R_f = 0.24. ^{1}H NMR (dmso-d_6, 80 °C, 400 MHz, mixture of rotamers, only major rotamer peaks were reported) δ 1.32–1.42 (m, 1H), 1.81–1.89 (m, 1H), 2.11–2.18 (m, 1H), 2.21–2.28 (m, 1H), 3.07 (d, *J* = 13.4 Hz, 1H, partially masked by H_2O signal), 3.21 (d, *J* = 13.4 Hz, 1H), 3.62 (s, 3H), 4.15–4.25 (m, 2H), 4.98 (s, 2H), 5.06 (d, *J* = 10.6 Hz, 1H), 5.22 (d, *J* = 17.7 Hz, 1H), 5.50 (d, *J* = 1.9 Hz, 1H), 6.17 (dd, *J* = 11.2, 17.7 Hz, 1H), 7.16–7.25 (m, 5H), 7.30–7.39 (m, 6H); $^{13}C\{^{1}H\}$ NMR (dmso-d_6, 80 °C, 100 MHz, only major rotamer peaks were reported) δ 28.6 (t), 30.6 (t), 44.6 (t), 52.4, 58.0, 58.6 (s), 60.7 (t), 66.5 (t), 116.0 (t), 127.3, 128.0, 128.5, 128.6, 128.7, 129.2, 131.6, 135.5, 136.4 (s), 137.7 (s), 144.2, 155.8 (s), 168.0 (s), 172.3 (s); IR (neat, cm^{-1}) 3284, 3030, 2924, 2853, 1742, 1719, 1655, 1641, 1496, 1455, 1399, 1361, 1244, 1201, 1079, 1016.

Synthesis of methyl (2S,5R)-1-((S)-2-benzyl-2-(((benzyloxy)carbonyl)amino)but-3-enoyl)-5-(buta-1,3-dien-2-yl)pyrrolidine-2-carboxylate (78a)

Ethylene was bubbled for 15 minutes into a solution of compound **73a** (74 mg, 0.16 mmol) in dry toluene (1.6 mL, 0.10 M). Afterwards, Hoveyda Grubbs II generation catalyst (10 mg, 0.016 mmol) was added and the reaction mixture was heated at 40 °C while maintaining ethylene atmosphere (balloon). Every hour ethylene was bubbled into the reaction mixture for 15 minutes. After 8 hours the solvent was evaporated under reduced pressure and the crude mixture was purified by flash chromatography (hexane/AcOEt 65:35) to obtain compound **78a** as a white amorphous solid (51 mg, 65 %). R_f = 0.35.

Synthesis of methyl (2S,5R)-1-((S)-2-benzyl-2-(((benzyloxy)carbonyl)amino)but-3-enoyl)-5-(buta-1,3-dien-2-yl)pyrrolidine-2-carboxylate (78b)

Ethylene was bubbled for 15 minutes into a solution of compound **73b** (100 mg, 0.22 mmol) in dry toluene (2.2 mL, 0.10 M). Afterwards, Hoveyda Grubbs II generation catalyst (14 mg, 0.022 mmol) was added and the reaction mixture was heated at 40 °C while maintaining ethylene atmosphere (balloon). Every hour ethylene was bubbled into the reaction mixture for 15 minutes. After 8 hours the solvent was evaporated under reduced pressure and the crude mixture was purified by flash chromatography (hexane/AcOEt 75:25) to obtain compound **78b** as a white amorphous solid (36 mg, 33 %). R_f = 0.34.

Synthesis of methyl (3S,6S,9aR)-6-benzyl-6-(((benzyloxy)carbonyl)amino)-9-methylene-5-oxo-2,3,5,6,9,9a-hexahydro-1H-pyrrolo[1,2-a]azepine-3-carboxylate (79a)

Compound **78a** (48 mg, 0.094 mmol) was dissolved in dry toluene (9.4 mL, 0.010 M) under nitrogen atmosphere and was heated to 80 °C. Hoveyda Grubbs II generation catalyst (6.0 mg, 0.0094 mmol) was added portion-wise in 24 hours. Afterwards, the solvent was evaporated under reduced pressure and the crude mixture was purified by flash chromatography (toluene/AcOEt 85:15) to obtain compound **79a** as a white amorphous solid (31 mg, 70 %, conversion: 89%). R_f = 0.34. $[\alpha]_D^{22}$ +18.00 (c = 1.0, $CDCl_3$); ^{1}H NMR ($CDCl_3$, 400 MHz) δ 2.07–2.17 (m, 1H), 2.17–2.28 (m, 1H), 2.36–2.46 (m, 2H), 3.33 (d, *J* = 14.4 Hz, 1H), 3.67 (s, 3H), 3.98 (d, *J* = 14.3 Hz, 1H), 4.54 (dd, *J* = 4.2, 8.2 Hz, 1H), 5.10 (br s, 1H), 5.11 (d, *J* = 12.5 Hz, 1H), 5.17 (d, *J* = 1.4 Hz, 1H), 5.20–5.27 (m, 2H), 6.27 (s, 2H), 6.69 (br s, 1H), 6.89–6.95 (m, 2H), 7.16–7.23 (m, 3H), 7.34–7.44 (m, 5H); ^{13}C{^{1}H} NMR ($CDCl_3$, 100 MHz) δ 27.7 (t), 30.3 (t), 40.6 (t), 52.7, 58.7, 62.7, 64.7 (s), 66.5 (t), 117.1 (t), 124.5, 127.6, 128.3, 128.7, 128.9, 129.8, 130.2, 130.5, 135.7 (s), 137.3 (s), 141.5 (s), 154.7 (s), 169.3 (s), 172.3 (s); IR (neat, cm^{-1}) 3374, 3029, 2925, 2853, 1739, 1695, 1669, 1645, 1484, 1451, 1436, 1381, 1298, 1240, 1170, 1082, 1047.

Synthesis of methyl (3S,6R,9aR)-6-benzyl-6-(((benzyloxy)carbonyl)amino)-9-methylene-5-oxo-2,3,5,6,9,9a-hexahydro-1H-pyrrolo[1,2-a]azepine-3-carboxylate (79b)

Compound **78b** (35 mg, 0.072 mmol) was dissolved in dry toluene (7.2 mL, 0.010 M) under nitrogen atmosphere and was heated to 80 °C. Hoveyda Grubbs II generation catalyst (4.5 mg, 0.0072 mmol) was added portion-wise in 24 hours. Afterwards, the solvent was evaporated under reduced pressure and the crude mixture was purified by flash chromatography (hexane/AcOEt 60:40) to obtain compound **79b** as a white amorphous solid (21 mg, 61 %, conversion: 84%). R_f = 0.40. ^{1}H NMR ($CDCl_3$, 400 MHz) δ 1.86–2.34 (m, 4H), 3.15 (d, *J* = 14.2 Hz, 1H), 3.68 (d, *J* = 14.2 Hz, 1H), 3.71 (s, 3H), 4.71 (br s, 1H), 4.85 (br s, 1H), 5.05 (t, *J* = 6.3 Hz, 1H), 5.08–5.15 (m, 3H), 5.16–5.26 (m, 1H), 5.74 (d, *J* = 11.6 Hz, 1H), 6.25 (d, *J* = 11.6 Hz, 1H), 7.10 (br s, 2H), 7.24 (br s, 3H) 7.34–7.48 (m, 5H); ^{13}C{^{1}H} NMR ($CDCl_3$, 100 MHz) δ 27.1 (t), 31.0 (t), 39.5 (t), 52.2, 57.6, 59.7 (s), 61.1, 67.0 (t), 118.1 (t), 126.2, 126.7, 128.2, 128.5, 128.6, 128.7, 131.4, 135.8, 136.5 (s), 143.4 (s), 153.9 (s), 168.8 (s), 172.8 (s); IR

(neat, cm^{-1}) 3320, 3027, 2952, 2921, 2850, 1718, 1654, 1494, 1452, 1402, 1376, 1254, 1196, 1171, 1073, 1026.

Synthesis of methyl (2R,3'S,6'S,9a'R)-6'-benzyl-6'-(((benzyloxy)carbonyl)amino)-5'-oxo-1',2',3',5',6',9a'-hexahydrospiro[oxirane-2,9'-pyrrolo[1,2-a]azepine]-3'-carboxylate (80)

A solution of compound **79a** (50 mg, 0.109 mmol) in dry CH_2Cl_2 (1.1 mL, 0.10 M) under nitrogen atmosphere was cooled to 0 °C and *m*CPBA (23 mg, 0.13 mmol) was added. The reaction was warmed to room temperature and, after 4 hours, AcOEt was added and the reaction was quenched with a 1 M NaOH aqueous solution. The aqueous layer was extracted three times with AcOEt. The organic phases were collected, washed with a NaCl saturated solution, dried with anhydrous Na_2SO_4, filtered, and evaporated under reduced pressure. The crude mixture was purified by flash chromatography (hexane/AcOEt 60:40) to obtain diastereoisomers **80**.

Diastereoisomer **80a**. White amorphous solid; (22 mg, 42%). R_f = 0.27 (hexane/AcOEt 60:40); $[\alpha]_D^{22}$ -42.18 (c = 1.0, $CDCl_3$); ^{1}H NMR ($CDCl_3$, 400 MHz) δ 1.69–1.81 (m, 1H), 1.88–2.08 (m, 2H), 2.11–2.23 (m, 1H), 2.84 (br s, 1H), 3.13 (d, *J* = 3.8 Hz, 1H), 3.35 (d, J = 13.9 Hz, 1H), 3.70 (s, 3H), 3.82 (d, *J* = 13.8 Hz, 1H), 4.48 (dd, J = 5.2, 8.5 Hz, 1H), 4.57 (br s, 1H), 5.11 (d, *J* = 12.4 Hz, 1H), 5.19 (d, *J* = 12.4 Hz, 1H), 5.41 (d, *J* = 12.7 Hz, 1H), 6.45 (br s, 1H), 6.58 (d, *J* = 12.7 Hz, 1H), 6.92–6.98 (m, 2H), 7.18–7.25 (m, 3H), 7.31–7.43 (m, 5H); IR (neat, cm^{-1}) 3379, 3030, 2952, 2924, 2851, 1745, 1718, 1645, 1483, 1430, 1392, 1367, 1244, 1200, 1176, 1072, 1043. MS (ESI): 499.21 [M+Na^+].

Diastereoisomer **80b**. White amorphous solid; (21 mg, 40%). R_f = 0.16 (hexane/AcOEt 60:40); $[\alpha]_D^{22}$ -34.16 (c = 1.0, $CDCl_3$); ^{1}H NMR ($CDCl_3$, 400 MHz) δ 1.89–2.12 (m, 3H), 2.18 (m, 1H), 2.79 (d, *J* = 4.3 Hz, 1H), 2.83 (d, *J* = 4.3 Hz, 1H), 3.30 (d, J = 14.5 Hz, 1H), 3.69 (s, 3H), 3.99 (d, *J* = 14.5 Hz, 1H), 4.54 (dd, J = 3.9, 8.0 Hz, 1H), 5.00 (t, J = 6.9 Hz, 1H), 5.09 (d, *J* = 12.5 Hz, 1H), 5.22 (d, *J* = 12.5 Hz, 1H), 5.23 (d, *J* = 12.5 Hz, 1H), 6.63 (d, *J* = 12.5 Hz, 1H), 6.74 (s, 1H), 6.88 (d, *J* = 6.8 Hz, 2H), 7.13–7.23 (m, 3H), 7.31–7.42 (m, 5H); $^{13}C\{^1H\}$ NMR ($CDCl_3$, 100 MHz) δ 25.4 (t), 27.4 (t), 39.8 (t), 52.6 (t), 52.8, 54.5 (s), 57.8, 62.2, 64.3 (s), 66.6 (t), 127.7, 128.4 (2C), 128.8, 128.9, 129.1, 129.7, 135.4 (s), 136.2, 137.2 (s), 154.7 (s), 169.2 (s), 171.7 (s); IR (neat, cm^{-1}) 3375, 3029, 2953, 2924, 2854, 1715, 1640, 1480, 1429, 1396, 1367, 1247, 1215, 1198, 1175, 1070, 1043; MS (ESI).

Synthesis of methyl (3S,6S,9aR)-6-benzyl-6-(((benzyloxy)carbonyl)amino)-9-(4-nitrobenzylidene)-5-oxo-2,3,5,6,9,9a-hexahydro-1H-pyrrolo[1,2-a]azepine-3-carboxylate (81)

To a solution of compound **79a** (22 mg, 0.048 mmol) in dry EtOH (0.47 mL, 0.10 M), under nitrogen atmosphere, 4-bromo-nitrobenzene (11 mg, 0.053 mmol), PdEnCat 30 (6 mg, 0.002 mmol) and Bu_4NOAc (43 mg, 0.14 mmol) were added. The reaction was heated to 120 °C through microwave irradiation for 3 hours. The reaction mixture was filtered through a Gooch apparatus and the solvent was evaporated under reduced pressure. The crude mixture was purified by flash chromatography

(toluene/AcOEt 80:20) to obtain compound **81** as a white amorphous solid (13 mg, 47 %). R_f = 0.37; ^{1}H NMR ($CDCl_3$, 400 MHz) ^{1}H NMR ($CDCl_3$, 400 MHz) mixture of *E* and *Z* diastereoisomers, major diastereoisomer δ 2.15 (m, 1H), 2.43–2.64 (m, 2H), 2.55 (m, 1H), 3.40 (d, J = 14.1 Hz, 1H), 3.67 (s, 3H), 3.90 (d, J = 14.2 Hz, 1H), 4.58 (dd, J = 5.2, 8.2 Hz, 1H); 4.94–5.05 (m, 1H), 5.12 (d, J = 12.4 Hz, 1H), 5.22 (d, J = 12.4 Hz, 1H), 6.45 (d, J = 12.4 Hz, 1H), 6.51 (d, J = 12.5 Hz, 1H), 6.52–6.63 (br s, 1H), 6.58 (s, 1H), 6.93–7.01 (m, 2H), 7.18–7.26 (m, 3H), 7.32–7.44 (m, 5H), 7.49 (d, J = 8.4 Hz, 2H), 8.23 (d, J = 8.5 Hz, 2H); ^{13}C{^{1}H} NMR ($CDCl_3$, 75 MHz) δ 27.2 (t), 29.2 8t), 29.6 (t), 52.3, 59.8, 61.9, 64.6 (s), 66.2 (t), 123.4, 124.0, 125.5, 125.6, 127.7, 127.9, 128.3, 128.4, 129.5, 130.4, 132.7, 134.8 (s), 135.9 (s), 136.6 (s), 142.6 (s), 146.8 (s), 154.3 (s), 168.7 (s), 171.8 (s).

Synthesis of methyl (3S,6R,8aR)-6-benzyl-6-(((benzyloxy)carbonyl)amino)-8-((E)-4-nitrostyryl)-5-oxo-1,2,3,5,6,8a-hexahydroindolizine-3-carboxylate (82)

To a solution of compound **77a** (30 mg, 0.065 mmol) in dry EtOH (0.65 mL, 0.10 M), under nitrogen atmosphere, 4-bromo-nitrobenzene (14 mg, 0.072 mmol), PdEnCat 30 (8 mg, 0.003 mmol) and Bu_4NOAc (59 mg, 0.19 mmol) were added. The reaction was heated to 80 °C for 12 hours. The reaction mixture was filtered through a Gooch apparatus and the solvent was evaporated under reduced pressure. The crude mixture was purified by flash chromatography (toluene/AcOEt 75:25) to obtain compound **82** as a white amorphous solid (21 mg, 55 %). R_f = 0.34. $[\alpha]_D^{22}$ +125.56 (c = 1.0, $CDCl_3$); ^{1}H NMR ($CDCl_3$, 400 MHz) δ 1.75–2.10 (m, 3H), 2.13–2.22 (m, 1H), 2.79–2.86 (m, 1H), 3.24 (d, *J* = 12.9 Hz, 1H), 3.44 (d, *J* = 12.6 Hz, 1H), 3.71 (s, 3H), 4.30 (dd, *J* = 2.2, 7.9 Hz, 1H), 5.17 (s, 2H), 6.17 (bs, 1H), 6.63 (d, *J* = 16.4 Hz, 1H), 6.67 (d, *J* = 16.3 Hz, 1H), 6.92 (bs, 1H), 7.10 (d, *J* = 7.1 Hz, 2H), 7.17–7.27 (m, 3H), 7.33–7.43 (m, 5H), 7.53 (d, *J* = 8.6 Hz, 2H), 8.23 (d, *J* = 8.3 Hz, 2H). ^{13}C{^{1}H} NMR ($CDCl_3$, 100 MHz) δ 28.6 (t), 29.7 (t), 44.5 (t), 52.8, 57.9, 59.7, 61.2 (s), 67.0 (t), 124.1, 124.6, 127.3, 127.6, 128.2, 128.3, 128.4, 128.5, 128.9, 130.0, 131.2, 135.0 (s), 136.0 (s), 136.8 (s), 143.5 (s), 147.4 (s), 155.4 (s), 167.6 (s), 172.0 (s); IR (neat, cm^{-1}) 3391, 2960, 2923, 2852, 1746, 1712, 1649, 1592, 1512, 1447, 1362, 1339, 1260, 1197, 1175, 1156, 1088, 1022.

Synthesis of methyl (3S,6R,8aR)-6-benzyl-6-(((benzyloxy)carbonyl)amino)-8-((E)-5-cyanopent-1-en-1-yl)-5-oxo-1,2,3,5,6,8a-hexahydroindolizine-3-carboxylate (83)

To a solution of compound **77a** (30 mg, 0.065 mmol) in dry toluene (0.65 mL, 0.10 M), under nitrogen atmosphere, Hoveyda Grubbs II generation catalyst (2 mg, 0.003 mmol) and 5-hexenenitrile (7.4 mg, 0.078 mmol) were added. The reaction was heated to 60 °C for 6 hours. Afterwards, the solvent was evaporated under reduced pressure and the crude mixture was purified by flash chromatography (hexane/AcOEt 70:30) to obtain compound **83** as a yellow amorphous solid (15 mg, 43 %). R_f = 0.37. ^{1}H NMR ($CDCl_3$, 400 MHz) δ 1.64–1.75 (m, 2H), 1.80 (quintuplet, *J* = 7.1 Hz, 2H), 1.91–2.07 (m, 2H), 2.29 (q, *J* = 7.1 Hz, 2H), 2.38 (t, *J* = 7.2 Hz, 2H), 2.64–2.72 (m, 1H), 3.19 (d, *J* = 12.9 Hz, 1H), 3.40 (d, *J*

= 12.8 Hz, 1H), 3.70 (s, 3H), 4.25 (dd, *J* = 1.5, 8.4 Hz, 1H), 5.14 (s, 2H), 5.69 (td, *J* = 7.2, 15.8 Hz, 1H), 5.93 (d, *J* = 15.8 Hz, 1H), 6.17 (s, 1H), 6.61 (s, 1H), 7.04–7.09 (m, 2H), 7.16–7.25 (m, 3H), 7.33–7.42 (m, 5H); $^{13}C\{^{1}H\}$ NMR ($CDCl_3$, 100 MHz) δ 16.9 (t), 25.1 (t), 28.6 (t), 30.1 (t), 32.0 (t), 44.5 (t), 52.7, 58.0, 60.0, 61.0 (s), 66.8 (t), 119.7 (s), 124.1, 127.4, 128.1, 128.4 (2C), 128.8, 128.9, 130.1, 131.2, 135.3 (s), 136.1 (s), 136.9 (s), 155.3 (s), 167.8 (s), 172.1 (s); IR (neat, cm^{-1}) 3392, 2957, 2922, 2853, 2245, 1740, 1650, 1493, 1454, 1376, 1260, 1201, 1175, 1154, 1087, 1017.

General procedure for the synthesis of the allyl enol carbonates

The amino acid derivative (1.0 equiv.) was dissolved in a 3 N aqueous solution of NaOH (0.10 M) at 0 °C and benzoylated under Schotten-Baumann conditions by performing three sequential additions of benzoyl chloride (1.0 eq) and 6 N aqueous NaOH (3.0 eq) at 30 minutes intervals. Afterwards, the reaction mixture was stirred for 1 hour at 0 °C and filtered through a Gooch apparatus. The solid residue was washed with cold water and dried under reduced pressure for 12 hours. The *N*-benzoyl amino acid (1 equiv.) was added portionwise over 20 min to a stirred solution of DCC (1 equiv.) in dry CH_2Cl_2 (0.30 M) under a nitrogen atmosphere at 0 °C. The progress of the reaction was monitored by TLC analysis. While the reaction mixture was kept at 0°C, a vacuum filtration with a Gooch apparatus was performed. The solvent from the filtrate was evaporated under reduced pressure to obtain the desired azlactones as white amorphous solids. To a solution of crude oxazolone (1.0 equiv.) in dry THF (0.10 M) under nitrogen atmosphere at 0°C, NEt_3 (1.1 equiv.) and allyl chloroformate (1.1 equiv.) were added. Afterwards, the reaction mixture was warmed to room temperature and the formation of the product was monitored by TLC analysis. After 12 hours, H_2O was added, the organic solvent was evaporated under reduced pressure and the aqueous layer was extracted three times with Et_2O. The organic phases were collected, dried with anhydrous Na_2SO_4, filtered, and the solvent was evaporated under reduced pressure.

Allyl (4-benzyl-2-phenyloxazol-5-yl) carbonate (23)

The title compound was prepared from L-phenylalanine (1.00 g, 6.05 mmol) according to the general procedure. The product was purified by flash chromatography to give **23** as a pale yellow amorphous solid (1.40 g, 69% over three steps). The spectroscopic data of compound **23** were matched with literature values.[118]

Allyl (2,4-diphenyloxazol-5-yl) carbonate (96)

The title compound was prepared from L-α-phenylglycine (1.00 g, 8.68 mmol) according to the general procedure. The product was purified by flash chromatography to give **2g** as a pale yellow amorphous solid (1.68 g, 60% over three steps). R_f = 0.27 (hexane/AcOEt 97:03); ^{1}H NMR ($CDCl_3$, 400

MHz) δ 4.85 (dt, *J* = 1.3, 5.9 Hz, 2 H), 5.42 (dq, *J* = 1.2, 10.4 Hz, 1 H), 5.50 (dq, *J* = 1.3, 17.2 Hz, 1 H), 6.03 (ddt, *J* = 5.9, 10.4, 17.2 Hz, 1 H), 7.35 (t, *J* = 7.3 Hz, 1 H), 7.43–7.52 (m, 5 H), 7.85 (d, *J* = 7.3 Hz, 2 H), 8.05–8.11 (m, 2 H); $^{13}C\{^{1}H\}$ NMR ($CDCl_3$, 100 MHz) δ 71.2 (t), 121.0 (t), 124.1 (s), 126.3, 126.6, 127.4 (s), 128.4, 129.1, 129.2, 130.2 (s), 130.5, 130.9, 145.6 (s), 151.5 (s), 155.6 (s); IR (neat, cm^{-1}) 3031, 2950, 1781, 1752, 1649, 1201; HRMS (ESI) calcd. for $C_{19}H_{15}NO_4Na$ $[M + Na]^+$ 344.0899; found 344.0900 (Δ = 0.3 ppm).

Allyl (4-isopropyl-2-phenyloxazol-5-yl) carbonate (97)

The title compound was prepared from L-valine (1.00 g, 8.54 mmol) according to the general procedure. The product was purified by flash chromatography to give **97** as a colourless oil (1.52 g, 62% over three steps). R_f = 0.24 (hexane/AcOEt 90:10); ^{1}H NMR ($CDCl_3$, 400 MHz) δ 1.31 (d, *J* = 6.9 Hz, 6 H), 2.92 (septuplet, *J* = 6.9 Hz, 1 H), 4.81 (dt, *J* = 1.3, 5.9 Hz, 2 H), 5.39 (dq, *J* = 1.3, 10.4 Hz, 1 H), 5.48 (dq, *J* = 1.3, 17.1 Hz, 1 H), 6.02 (ddt, *J* = 5.9, 10.4, 17.1 Hz, 1 H), 7.41–7.47 (m, 3 H), 7.95–8.02 (m, 2 H); $^{13}C\{^{1}H\}$ NMR ($CDCl_3$, 100 MHz) δ 21.4, 25.8, 70.8 (t), 120.7 (t), 126.4, 127.7 (s), 129.0, 129.9 (s), 130.5, 130.7, 144.9 (s), 152.1 (s), 155.2 (s); IR (neat, cm^{-1}) 3062, 2968, 2875, 1783, 1654, 1198; HRMS (ESI) calcd. for $C_{16}H_{18}NO_4$ $[M + H]^+$ 288.1236; found 288.1225 (Δ = –3.8 ppm).

Allyl (4-methyl-2-phenyloxazol-5-yl) carbonate (98)

The title compound was prepared from L-alanine (1.00 g, 11.2 mmol) according to the general procedure. The product was purified by flash chromatography to give **98** as a white amorphous solid (2.60 g, 89% over three steps). The spectroscopic data of compound **98** were matched with literature values.[149]

Allyl (4-(2-(methylthio)ethyl)-2-phenyloxazol-5-yl) carbonate (99)

The title compound was prepared from L-methionine (1.00 g, 6.70 mmol) according to the general procedure. The product was purified by flash chromatography to give **99** as a pale yellow amorphous solid (1.46 g, 68% over three steps). R_f = 0.29 (hexane/AcOEt 90:10); IR (neat, cm^{-1}) 3074, 2916, 1785, 1664, 1243, 1209; ^{1}H NMR ($CDCl_3$, 400 MHz) δ 2.15 (s, 3 H), 2.77–2.89 (m, 4 H), 4.81 (d, *J* = 5.9 Hz, 2 H), 5.39 (d, *J* = 10.4 Hz, 1 H), 5.48 (d, *J* = 17.1 Hz, 1 H), 6.01 (ddt, *J* =5.9, 10.4, 17.1 Hz, 1 H), 7.40–7.48 (m, 3 H), 7.92–7.99 (m, 2 H); $^{13}C\{^{1}H\}$ NMR ($CDCl_3$, 100 MHz) δ 15.9, 25.6 (t), 32.7 (t), 71.0 (t), 120.9 (t), 123.3 (s), 126.3, 127.4 (s), 129.1, 130.6, 130.8, 146.6 (s),151.7 (s), 155.5 (s); HRMS (ESI) calcd. for $C_{16}H_{17}NO_4SNa$ $[M + Na]^+$ 342.0776; found 342.0778 (Δ = 0.6 ppm).

Allyl (4-benzyl-2-(4-methoxyphenyl)oxazol-5-yl) carbonate (100)

The title compound was prepared from L-phenylalanine (1.00 g, 6.05 mmol) according to the general procedure. The product was purified by flash chromatography to give **100** as pale yellow amorphous solid (0.98 g, 44% over three steps). R_f = 0.33 (hexane/AcOEt 85:15); IR (neat, cm^{-1}) 3063, 2944, 2839, 1782, 1663, 1206, 1166; ^1H NMR ($CDCl_3$, 400 MHz) δ 3.87 (s, 3H), 3.88 (s, 2 H), 4.71 (dt, *J* = 1.3, 5.9 Hz, 2 H), 5.38 (dq, *J* = 1.2, 10.4 Hz, 1 H), 5.44 (dq, *J* = 1.3, 17.2 Hz, 1 H), 5.95 (ddt, *J* = 5.9, 10.4, 17.2 Hz, 1 H), 6.95 (d, *J* = 8.9 Hz, 2 H), 7.24 (m, 1 H), 7.30–7.33 (m, 4 H), 7.90 (d, *J* = 8.9 Hz, 2 H); $^{13}C\{^1H\}$ NMR ($CDCl_3$, 100 MHz) δ 31.9 (t), 55.8, 70.8 (t), 114.5, 120.2 (s), 120.8 8t), 123.4 (s), 126.9, 128.1, 128.8, 129.3, 130.6, 138.0 (s), 146.3 (s), 151.7 (s), 155.7 (s), 161.7 (s); HRMS (ESI) calcd. for $C_{21}H_{19}NO_5Na$ $[M + Na]^+$ 388.1161; found 388.1165 (Δ = 1.0 ppm).

Allyl (4-benzyl-2-(4-chlorophenyl)oxazol-5-yl) carbonate (101)

The title compound was prepared from L-phenylalanine (1.00 g, 6.05 mmol) according to the general procedure. The product was purified by flash chromatography to give **101** as a yellow amorphous solid (0.74 g, 33% over three steps). R_f = 0.27 (hexane/AcOEt 90:10); ^1H NMR ($CDCl_3$, 400 MHz) δ 3.89 (s, 2 H), 4.72 (dt, *J* = 1.1, 6.0 Hz, 2 H), 5.39 (dq, *J* = 1.1, 10.4 Hz, 1 H), 5.45 (dq, *J* = 1.3, 17.2 Hz, 1 H), 5.96 (ddt, *J* = 5.9, 10.4, 17.2 Hz, 1 H), 7.25 (m, 1 H), 7.30–7.36 (m, 4 H), 7.42 (d, *J* = 8.7 Hz, 2 H), 7.90 (d, *J* = 8.7 Hz, 2 H); $^{13}C\{^1H\}$ NMR ($CDCl_3$, 100 MHz) δ 31.8 (t), 70.9 (t), 120.9 (t), 124.1 (s), 126.0 (s), 127.0, 127.7, 128.9, 129.2, 129.4, 130.5, 136.8 (s), 137.8 (s), 146.8 (s), 151.6 (s), 154.6 (s); IR (neat, cm^{-1}): 3060, 2927, 2902, 1780, 1668, 1206, 1166, 1093; HRMS (ESI) calcd. for $C_{20}H_{16}NO_4NaCl$ $[M + Na]^+$ 392.0666; found 392.0674 (Δ = 2.0 ppm).

General procedure for the asymmetric Tsuji decarboxylative allylation

To a solution of Pd catalyst (0.01 eq) and chiral phosphine (0.04 eq) in dry CH_3CN (0.015 M), a solution of allyl enol carbonate (1.0 eq) in dry CH_3CN (0.03 M) was added over 5 minutes by using a syringe-pump. After 30 minutes, phosphate buffer (pH 7.4) was added and the organic solvent was evaporated at reduced pressure. The aqueous layer was extracted with CH_2Cl_2 and the organic phases were collected, dried with anhydrous Na_2SO_4, filtered, and evaporated under reduced pressure.

4-allyl-4-benzyl-2-phenyloxazol-5(4*H*)-one (24)

The title compound was prepared from **23** (1.0 g, 2.98 mmol) according to the general procedure. The product was purified by flash chromatography to give **24** as a colourless oil (851 mg, 98%). The spectroscopic data of compound **24** were matched with literature values.[118]

4-allyl-2,4-diphenyloxazol-5(4*H*)-one (102)

The title compound was prepared from **96** (50 mg, 0.16 mmol) according to the general procedure. The product was purified by flash chromatography to give **102** as a colourless oil (38 mg, 86%). The spectroscopic data of compound **102** were matched with literature values.[150]

4-allyl-4-isopropyl-2-phenyloxazol-5(4*H*)-one (103)

The title compound was prepared from **97** (50 mg, 0.17 mmol) according to the general procedure. The product was purified by flash chromatography to give **103** as a colourless oil (34 mg, 83%). The spectroscopic data of compound **103** were matched with literature values.[150]

4-allyl-4-methyl-2-phenyloxazol-5(4*H*)-one (104)

The title compound was prepared from **98** (50 mg, 0.19 mmol) according to the general procedure. The product was purified by flash chromatography to give **104** as a colourless oil (34 mg, 83%). The spectroscopic data of compound **104** were matched with literature values.[142]

4-allyl-4-(2-(methylthio)ethyl)-2-phenyloxazol-5(4*H*)-one (105)

The title compound was prepared from **99** (50 g, 0.16 mmol) according to the general procedure. The product was purified by flash chromatography to give **105** as a colourless oil (38 g, 86%). R_f = 0.30 (hexane/AcOEt 90:10); $[\alpha]_D^{22}$ –23.5 (c = 1.0, $CDCl_3$); ^{1}H NMR ($CDCl_3$, 400 MHz) δ 2.07 (s, 3 H), 2.23–2.29 (m, 2 H), 2.40 (m, 1 H), 2.50 (m, 1 H), 2.59 (ddt, *J* = 0.9, 7.8, 13.6 Hz, 1 H), 2.67 (ddt, *J* = 1.1, 6.9, 13.6 Hz, 1 H), 5.14 (dq, *J* = 0.9, 10.1 Hz, 1 H), 5.20 (dq, *J* = 1.2, 17.1 Hz, 1 H), 5.67 (dddd, *J* = 6.9, 7.8, 10.1, 17.1 Hz, 1 H), 7.51 (t, *J* = 7.5 Hz, 2 H), 7.60 (tt, *J* = 1.3, 7.5 Hz, 1 H), 7.99–8.05 (m, 2 H); ^{13}C{^{1}H} NMR ($CDCl_3$, 100 MHz) δ 15.6, 29.1 (t), 36.3 (t), 42.3 (t), 73,1 (s), 121.3 (t), 126.1 (s), 128.4, 129.2, 130.6, 132.2, 161.0 (s), 180.0 (s); IR (neat, cm^{-1}) 3076, 2917, 2852, 1813, 1651, 1290; HRMS (ESI) calcd. for $C_{15}H_{17}NO_2NaS$ $[M + Na]^+$ 298.0878; found 298.0883 (Δ = 1.7 ppm).

4-allyl-4-benzyl-2-(4-methoxyphenyl)oxazol-5(4*H*)-one (106)

The title compound was prepared from **100** (50 mg, 0.14 mmol) according to the general procedure. The product was purified by flash chromatography to give **106** as a colourless oil (41 mg, 90%). The spectroscopic data of compound **106** were matched with literature values.[151]

4-allyl-4-benzyl-2-(4-chlorophenyl)oxazol-5(4*H*)-one (107)

The title compound was prepared from **101** (50 mg, 0.14 mmol) according to the general procedure. The product was purified by flash chromatography to give **107** as a colourless oil (44 g, 96%). The spectroscopic data of compound **107** were matched with literature values.[151]

4-benzyl-4-(2-methylallyl)-2-phenyloxazol-5(4*H*)-one (108)

The title compound was prepared from **109** (50 mg, 0.14 mmol) according to the general procedure. The product was purified by flash chromatography to give **108** as a colourless oil (28 mg, 64%). R_f = 0.33 (hexane/AcOEt 97:03); ^{1}H NMR ($CDCl_3$, 400 MHz) δ 1.77 (s, 3 H), 2.73 (d, *J* = 13.4 Hz, 1 H), 2.79 (d, *J* = 13.4 Hz, 1 H), 3.19 (d, *J* = 13.4 Hz, 1 H), 3.26 (d, *J* = 13.4 Hz, 1 H), 4.86 (s, 2 H), 7.12–7.22 (m, 5 H), 7.44 (t, *J* = 7.6 Hz, 2 H), 7.54 (t, *J* = 7.5 Hz, 1 H), 7.85 (d, *J* = 7.5 Hz, 2 H); ^{13}C{^{1}H} NMR ($CDCl_3$, 100 MHz) δ 24.6, 44.2 (t), 45.3 (t), 75.9 (s), 116.4 (t), 126.2 (s), 127.6, 128.2, 128.5, 129.1, 130.6, 132.8, 134.7 (s), 140.3 (s), 160.1 (s), 179.7 (s); IR (neat, cm^{-1}): 3063, 2923, 2854, 1815, 1652, 1290, 1096; HRMS (ESI) calcd. for $C_{20}H_{19}NO_2Na$ $[M + Na]^+$ 328.1313; found 328.1309 (Δ = –1.2 ppm).

4-benzyl-2-phenyloxazol-5-yl (2-methylallyl) carbonate (109)

2-Methylprop-2-en-1-ol (172 mg, 2.39 mmol) was dissolved in dry toluene (3.0 ml, 0.80 M) at 0 ºC, under a nitrogen atmosphere, and K_2CO_3 (396 mg, 2.87 mmol) was added to the reaction mixture. Then, a solution of triphosgene (508 mg, 1.71 mmol) in dry toluene (1.8 ml, 0.66 M) was added drop-wise. After 2 h the reaction was bubbled with nitrogen to remove the excess of phosgene, and was transferred via cannula into a round-bottom flask containing 4-benzyl-2-phenyloxazol-5(4H)-one **22** (300 mg, 1.19 mmol) and Et_3N (0.500 ml, 3.74 mmol) in dry THF (5.42 ml, 0.22 M) cooled at 0 °C. After 12 hours, H_2O was added, the organic solvent was evaporated under reduced pressure and the aqueous layer was extracted three times with Et_2O. The organic phases were collected, dried with anhydrous Na_2SO_4, filtered, and the solvent was evaporated under reduced pressure. The crude mixture was purified by flash chromatography to give a white amorphous solid (242 mg, 58%). R_f = 0.26 (hexane/AcOEt 95:05); ^{1}H NMR ($CDCl_3$, 400 MHz) δ 1.80–1.83 (m, 3 H), 3.91 (s, 2 H), 4.63–4.65 (m, 2 H), 5.05 (m, 1 H), 5.09 (quintuplet, *J* = 1.1 Hz, 1 H), 7.25 (m, 1 H), 7.30–7.34 (m, 4 H), 7.42–7.47 (m, 3 H), 7.94–8.00 (m, 2 H); ^{13}C{^{1}H} NMR ($CDCl_3$, 100 MHz) δ 19.7, 31.9 (t), 73.6 (t), 115.5 (t), 126.4, 126.9, 127.5 (s), 128.9, 129.1, 129.2, 130.7, 137.9 (s), 138.5 (s), 146.7 (s), 151.7 (s), 155.5 (s); IR (neat, cm^{-1}): 3030, 2944, 2926, 1778, 1665, 1209; HRMS (ESI) calcd. for $C_{21}H_{19}NO_4Na$ $[M + Na]^+$ 372.1212; found 372.1212 (Δ = 0.0 ppm).

Synthesis of methyl 2-benzamido-2-benzyl-5-(4-nitrophenyl)pent-4-enoate (111)

To a solution of **24** (50 mg, 0,17 mmol) in dry MeOH (1.7 mL, 0.10 M) under nitrogen atmosphere, 1-bromo-4-nitrobenzene (38 mg, 0.19 mmol), tetrabutylammonium acetate (0.16 g, 0.52 mmol) and Pd EnCat 30® (43 mg, 10% mmol) were added.

The reaction mixture was heated at 120°C for 15 minute by microwave irradiation. Reaction completion was monitored by TLC analysis, R_f = 0.26 (hexane/AcOEt 80:20). The reaction mixture was filtered with a Gooch apparatus to remove Pd EnCat 30®. The solvent was evaporated under reduced pressure, and the residue was recovered with AcOEt and washed two times with water. The organic layer was dried with anhydrous Na_2SO_4, filtered, and evaporated under reduced pressure. The crude mixture was purified by flash chromatography to give **111** as a yellow solid (57 mg, 75%). R_f = 0.20 (hexane/AcOEt 80:20); IR (neat, cm^{-1}): 3030, 2951, 2854, 1734, 1660, 1512, 1338, 1221; ^1H NMR ($CDCl_3$, 400 MHz, mixture of E/Z diastereoisomers). The integral of the isolated signal at 6.22 ppm, belonging to the major diastereoisomer, was arbitrarily assigned the value of one proton: δ 2.98 (dd, *J* = 7.5, 14.1 Hz, 1 H), 3.10 (ddd, *J* = 1.3, 8.1, 15.1 Hz, 0.5 H), 3.18 (d, *J* = 13.5 Hz, 0.5 H), 3.27 (d, *J* = 13.5 Hz, 1 H), 3.72 (s, 1.5 H), 3.81–3.94 (m, 4.5 H), 3.98 (d, *J* = 13.5 Hz, 0.5 H), 4.03 (d, *J* = 13.5 Hz, 1 H), 5.75 (ddd, *J* = 6.6, 8.1, 11.9 Hz, 0.5 H), 6.22 (dt, *J* = 7.6, 15.4 Hz, 1 H), 6.54–6.61 (m, 1.5 H), 6.97–7.03 (m, 2.5 H), 7.05–7.10 (m, 2 H), 7.17–7.25 (m, 4.5 H), 7.36–7.47 (m, 6 H), 7.49–7.56 (m, 1.5 H), 7.65–7.72 (m, 3 H), 8.12 (d, *J* = 8.8 Hz, 2 H), 8.22 (d, *J* = 8.8 Hz, 1 H); $^{13}C\{^1H\}$ NMR ($CDCl_3$, 100 MHz, mixture of E/Z diastereoisomers) δ 34.5 (t), 39.3 (t), 40.8 (t), 41.1 (t), 53.2, 53.4, 66.5 (s), 67.0 (s), 124.0, 124.3, 127.1, 127.2 (2C), 127.5, 127.6, 128.7, 128.8, 129.0, 129.1, 129.3, 129.6, 129.8, 129.9, 130.0, 130.8, 132.1 (2C), 132.6, 135.2 (s), 135.5 (s), 136.1 (s), 136.2 (s), 143.8 (s), 144.0 (s), 147.3 (s), 167.2 (s), 167.5 (s), 173.5 (s); HRMS (ESI) calcd. for $C_{26}H_{24}N_2O_5Na$ $[M + Na]^+$ 467.1583; found 467.1586 (Δ = 0.6 ppm).

Synthesis of (*E*)-7-(4-benzyl-5-oxo-2-phenyl-4,5-dihydrooxazol-4-yl)hept-5-enenitrile (112)

Compound **24** (50 mg, 0,17 mmol) and 5-hexenenitrile (49 mg, 0.51 mmol) were dissolved in dry toluene (1.7 mL, 0.10 M) under nitrogen atmosphere. Afterward, Hoveyda-Grubbs II generation catalyst (11 mg, 10% mol) was added and the reaction mixture was heated at 60 °C. Reaction completion was monitored by TLC analysis, R_f = 0.25 (hexane/AcOEt 80:20). After 5 hours the solvent was evaporated under reduced pressure and the crude mixture was purified by flash chromatography to give **112** as a pale yellow oil (50 mg, 81%). R_f = 0.19 (hexane/AcOEt 80:20); IR (neat, cm-1): 3031, 2922, 2851, 2246, 1814, 1654; ^1H NMR ($CDCl_3$, 400 MHz, mixture of E/Z diastereoisomers). The integral of the isolated quartet at 2.19 ppm, belonging to the major diastereoisomer, was arbitrarily assigned the value of two protons: δ 1.63 (quintuplet, *J* = 7.1 Hz, 2 H), 1.72 (quintuplet, *J* = 7.2 Hz, 0.6 H), 2.11 (q, *J* = 7.1 Hz, 2 H), 2.19 (t, *J* = 7.1 Hz, 2 H), 2.26 (q, *J* = 7.2 Hz, 0.6 H), 2.34 (t, *J* = 7.2 Hz, 0.6 H), 2.65–2.87 (m, 2.6 H), 3.12–3.32 (m, 2.6 H), 5.37–5.50 (m, 1.6 H), 5.55 (dt, *J* = 7.0, 15.2 Hz, 1 H), 7.14–7.23 (m, 6.5 H), 7.42–7.49 (m, 2.6 H), 7.52–7.58 (m, 1.3 H),

7.84–7.90 (m, 2.6 H); $^{13}C\{^{1}H\}$ NMR ($CDCl_3$, 75 MHz, mixture of E/Z diastereoisomers) δ 16.4 (t), 16.9 (t), 25.1 (t), 25.5 (t), 26.7 (t), 31.5 (t), 35.3 (t), 40.7 (t), 43.5 (t), 43.7 (t), 75.2 (s), 75.3 (s), 119.7 (s), 119.9 (s), 123.9, 124.9, 125.7 (s), 125.8 (s), 127.7, 128.2, 128.6, 129.1, 129.2, 130.5, 132.9, 133.1, 133.2, 134.5, 134.6 (2C), 160.5 (s, 2C), 179.2 (s), 179.4 (s); HRMS (ESI) calcd. for $C_{23}H_{22}N_2O_2Na$ $[M + Na]^+$ 381.1579; found 381.1581 (Δ = 0.5 ppm).

General procedure for the ring-opening of azlactone ring under acidic conditions

The allyl oxazolone (1.0 eq) was dissolved in TFA/water 90:10 (0.1 M), and the solution was heated at 100 °C for 12 h. After evaporation of the solvent under reduced pressure, water was added to the residue, and the mixture was washed three times with CH_2Cl_2. The aqueous phase was evaporated under reduced pressure to give the fully deprotected quaternary amino acid.

2-ammonio-2-benzylpent-4-enoate (25)

The title compound was prepared from compound **24** (85 mg, 0.29 mmol), **106** (36 mg, 0.19 mmol) and **107** (34 mg, 0.10 mmol) according to the general procedure for the ring-opening of azlactone ring under acidic conditions. The crude mixture was purified by ion-exchange chromatography with Amberlite IR-120 (Plus)® resin as the stationary phase. After the crude mixture was loaded onto the column, the resin was washed with H_2O until the eluted solution turned neutral, then it was eluted with NH_3 (10 % aqueous solution). The fractions containing the product were evaporated under reduced pressure to give **25** (58 mg, 98 % starting from **24**; 34 mg, 87 % starting from **106**; 17 mg, 79 % starting from **107**) as a white solid. The spectroscopic data of compound **25** were matched with literature values.[145]

2-ammonio-2-isopropylpent-4-enoate (114)

The title compound was prepared from compound **103** (63 mg, 0.26 mmol) according to the general procedure for the ring-opening of azlactone ring under acidic conditions. The crude mixture was purified by ion-exchange chromatography with Amberlite IR-120 (Plus)® resin as the stationary phase. After the crude mixture was loaded onto the column, the resin was washed with H_2O until the eluted solution turned neutral, then it was eluted with NH_3 (10 % aqueous solution). The fractions containing the product were evaporated under reduced pressure to give **114** (35 mg, 86 %) as a white solid. The spectroscopic data of compound **114** were matched with literature values.[145]

Methyl 2-ammonio-2-phenylpent-4-enoate (115)

The title compound was prepared from compound **102** (80 mg, 0.28 mmol) according to the general procedure for the ring-opening of azlactone ring under acidic conditions. The crude mixture was dissolved in dry methanol (2.8 ml, 0.10 M) and, afterwards, a 0.30 M solution of diazomethane in Et_2O (0.93 ml, 0.28 mmol) was added.

After 3 hours, the solvent was evaporated under reduced pressure and the residue was recovered with a 1.0 M solution of HCl. The aqueous layer was washed with CH_2Cl_2, basified to pH 12 with a 3.0 M aqueous solution of NaOH and extracted three times with AcOEt. The organic phases were collected, dried with anhydrous Na_2SO_4, filtered, and evaporated under reduced pressure to afford compound 7 was obtained as a pale yellow amorphous solid.

The spectroscopic data of compound 115 were matched with literature values.[145]

Synthesis of 2-benzamido-2-methylpent-4-enoic acid (116)

To a solution of **104** (22 mg, 0,10 mmol) in dry THF (1.0 mL, 0.10 M), a 1.6 M aqueous solution of LiOH was added (5.0 µL, 1.2 mmol).

After 2 h the organic solvent was evaporated under reduced pressure and the residue was washed two times with CH_2Cl_2. Then, the aqueous phase was acidified to pH 1 with a 6 M aqueous solution of HCl and was extracted three times with CH_2Cl_2. The organic layer was dried with anhydrous Na_2SO_4, filtered, and evaporated under reduced pressure to give **116** as a yellow solid (20 mg, 84%) without the need of further purifications. The spectroscopic data of compound **116** were matched with literature values.[145]

Synthesis of methyl 2-benzamido-2-phenylpent-4-enoate (117)

Compound **102** (50 mg, 0.18 mmol) was dissolved in dry MeOH (1.8 ml, 0.10 M) and a saturated HCl methanolic solution (50 µl) was added. Afterwards the reaction mixture was heated at 120 °C for 1.5 hours by microwave irradiation. The solvent was evaporated under reduced pressure and the crude mixture was purified by flash chromatography to give compound **117** as a pale yellow amorphous solid (48 mg, 86%).

R_f = 0.31 (hexane/AcOEt 85:15); ^{1}H NMR ($CDCl_3$, 400 MHz) δ 3.32 (dd, *J* = 7.6, 13.6 Hz, 1 H), 3.76 (s, 3 H), 3.84 (dd, *J* = 6.9, 13.6 Hz, 1 H), 5.15 (dd, *J* = 1.7, 10.2 Hz, 1 H), 5.21 (dd, *J* = 1.7, 17.1 Hz, 1 H), 5.73 (dddd, *J* = 6.9, 7.6, 10.2, 17.1 Hz, 1 H), 7.32 (t, *J* = 7.2 Hz, 1 H), 7.39 (t, *J* = 7.1 Hz, 2 H), 7.47 (t, *J* = 7.2 Hz, 2 H), 7.50–7.57 (m, 3 H), 7.74 (s, 1 H), 7.85 (d, *J* = 7.1 Hz, 1 H); ^{13}C{^{1}H} NMR ($CDCl_3$, 100 MHz) δ 37.6 (t), 53.8, 66.2 (s), 120.1 (t), 126.4, 127.4, 128.4, 129.0 (2C), 132.1, 132.7, 135.0 (s), 139.5 (s), 166.0 (s), 173.6 (s); IR (neat, cm^{-1}): 3413, 3062, 2952, 1731, 1667, 1480, 1230; HRMS (ESI) calcd. for $C_{19}H_{19}NO_3Na$ $[M + Na]^+$ 332.1263; found 332.1270 (Δ = 2.1 ppm).

Synthesis of methyl 2-benzamido-2-(2-(methylthio)ethyl)pent-4-enoate (118)

Compound **105** (50 mg, 0.18 mmol) was dissolved in dry MeOH (1.8 ml, 0.10 M) and a saturated HCl methanolic solution (50 µl) was added. Afterwards the reaction mixture was heated at 120 °C for 1.5 hours by microwave irradiation. The solvent was evaporated under reduced pressure and the crude mixture was purified by flash chromatography to give compound **118** as a pale yellow amorphous solid (50 mg, 91%). R_f = 0.27 (hexane/AcOEt 80:20); ^{1}H NMR ($CDCl_3$, 400 MHz) δ 2.07 (s, 3 H), 2.19–2.36 (m, 2 H), 2.51 (m, 1 H), 2.60 (dd, *J* = 7.5, 13.8 Hz, 1 H), 3.02 (m, 1 H), 3.41 (dd, *J* = 7.3, 13.8 Hz, 1 H), 3.84 (s, 3 H), 5.04–5.15 (m, 2 H), 5.63 (ddt, *J* = 7.4, 10.1, 17.4 Hz, 1 H), 7.26 (s, 1 H), 7.64 (t, *J* = 7.4 Hz, 2 H), 7.54 (t, *J* = 7.3 Hz, 1 H), 7.81 (d, *J* = 7.3 Hz, 2 H); ^{13}C{^{1}H} NMR ($CDCl_3$, 100 MHz) δ 16.0, 29.5 (t), 34.6 (t), 40.0 (t), 53.4, 64.9 (s), 119.8 (t), 127.3, 129.0, 132.0, 132.3, 135.1 (s), 166.7 (s), 174.4 (s); IR (neat, cm^{-1}) 3407, 3321, 3063, 2950, 2917, 1735, 1643, 1226; HRMS (ESI) calcd. for $C_{16}H_{21}NO_3NaS$ $[M + Na]^+$ 330.1140; found 330.1143 (Δ = 0.9 ppm).

4. Appendix of NMR and HPLC data

^{1}H NMR (400 MHz), ^{13}C NMR and DEPT 135 spectra of compound 26

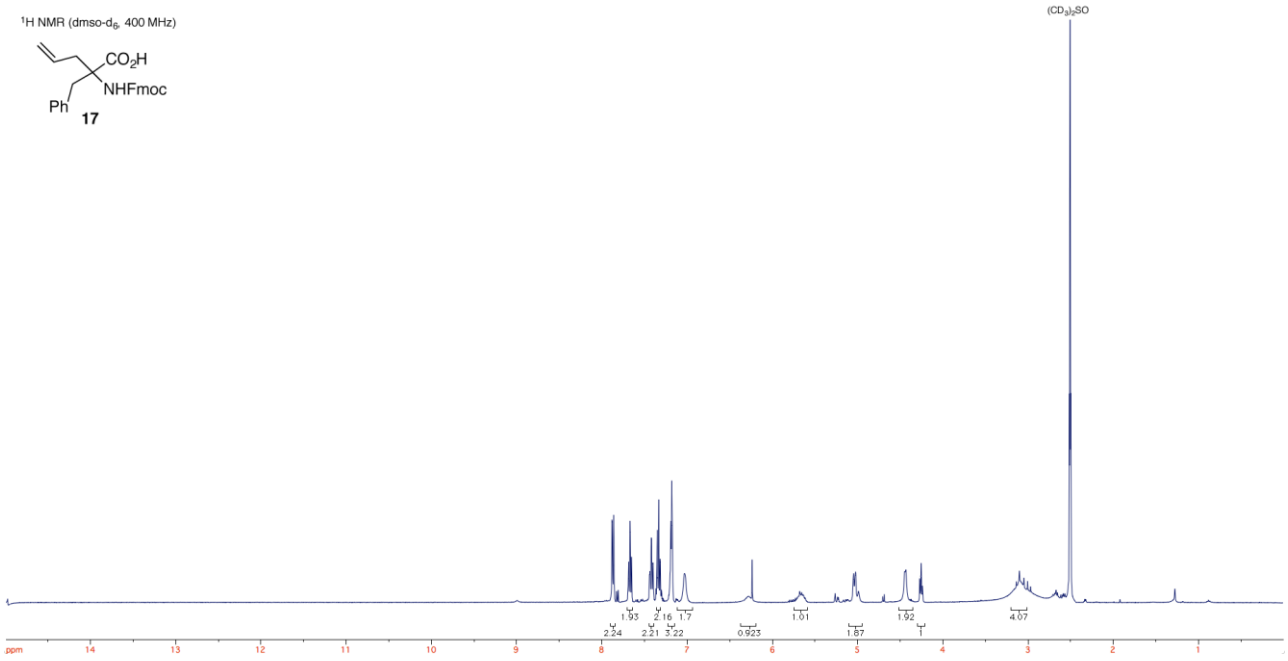

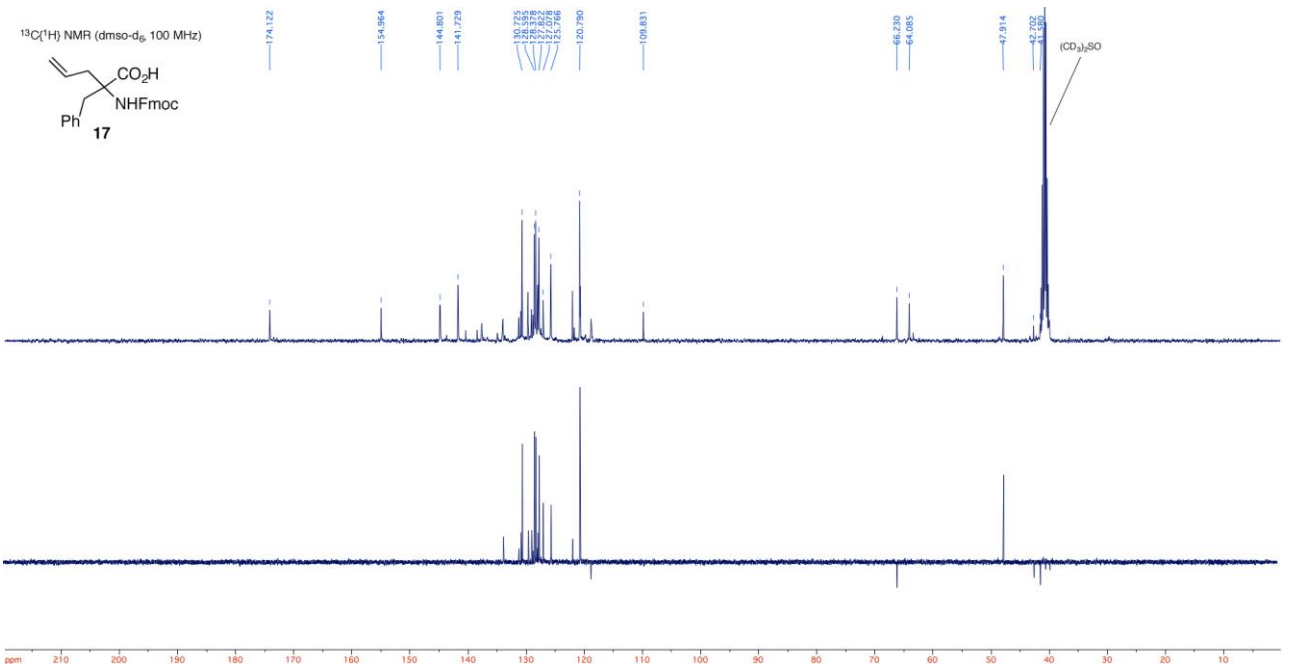

^{1}H NMR (400 MHz), ^{13}C NMR and DEPT 135 spectra of compound 27

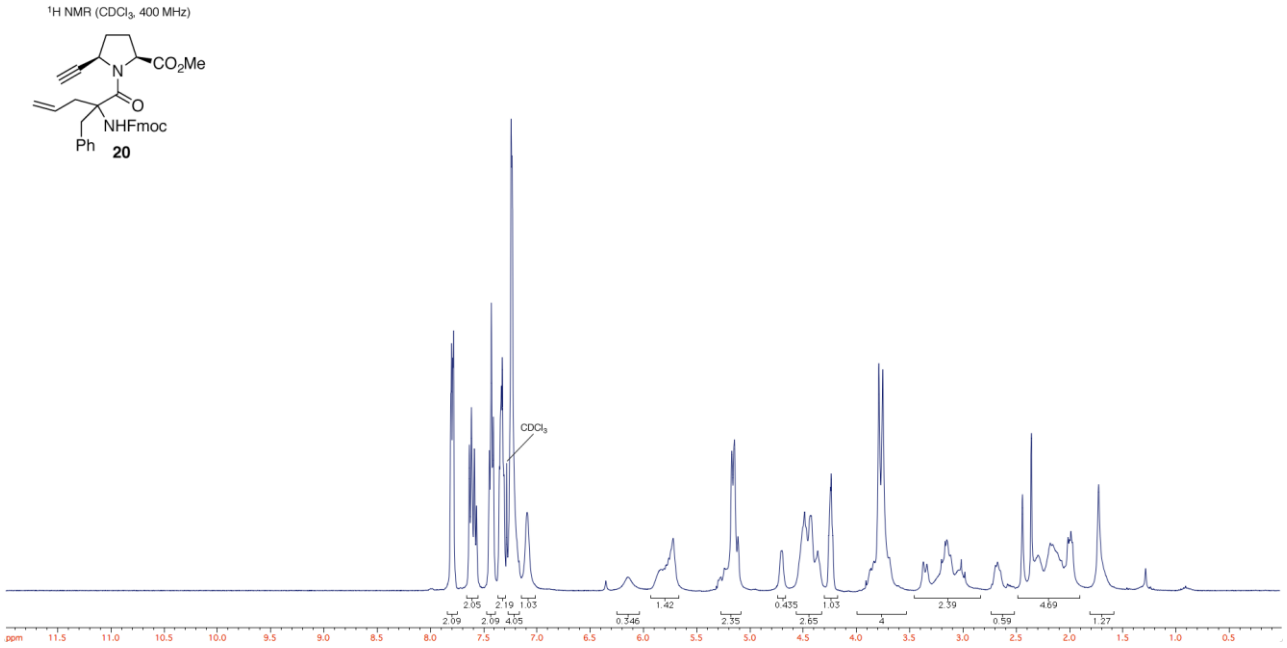

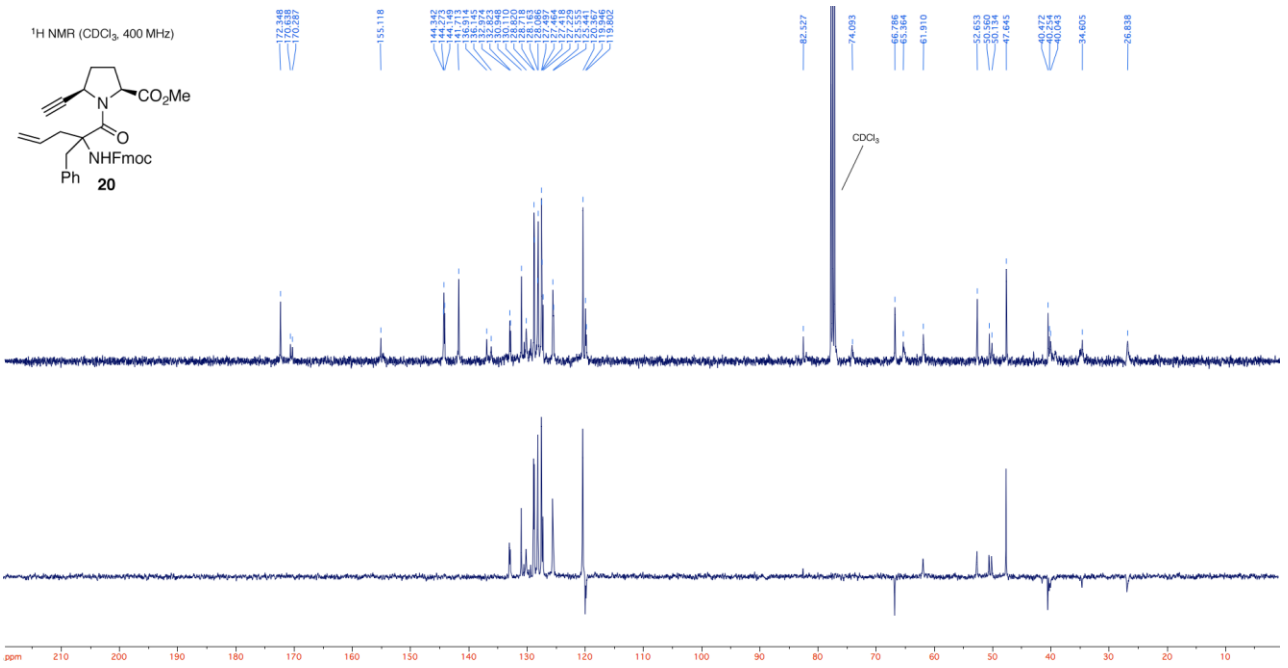

^{1}H NMR (400 MHz), ^{13}C NMR and DEPT 135 spectra of compound 32a

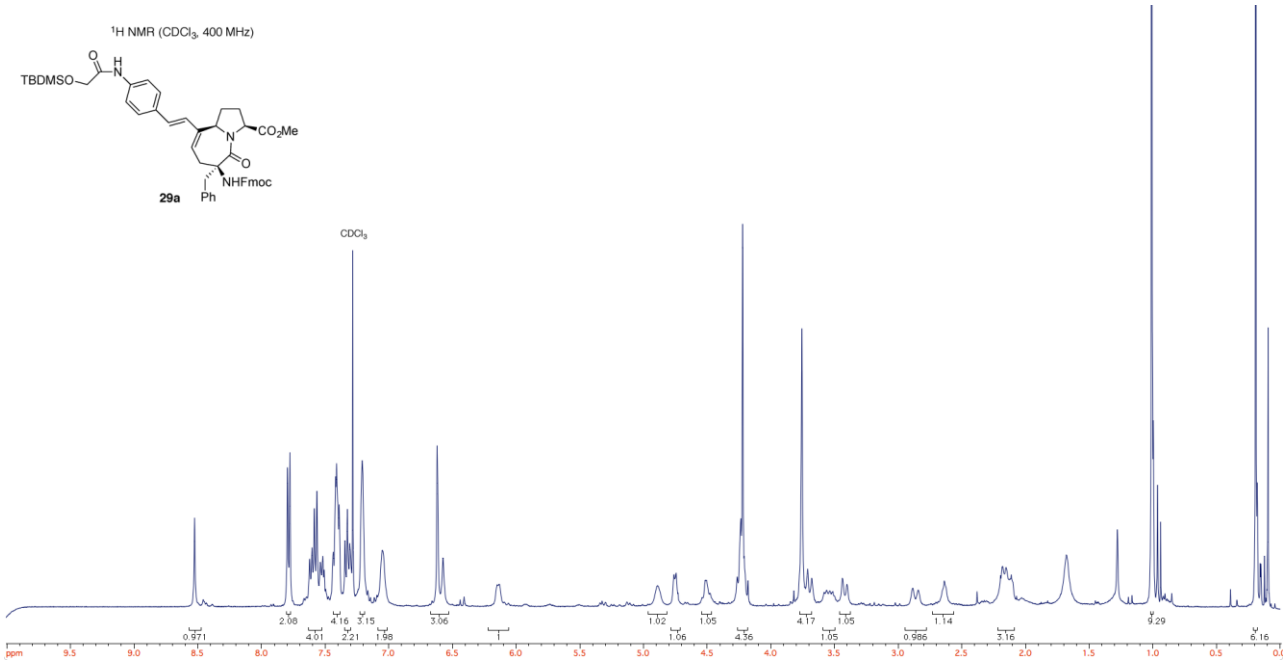

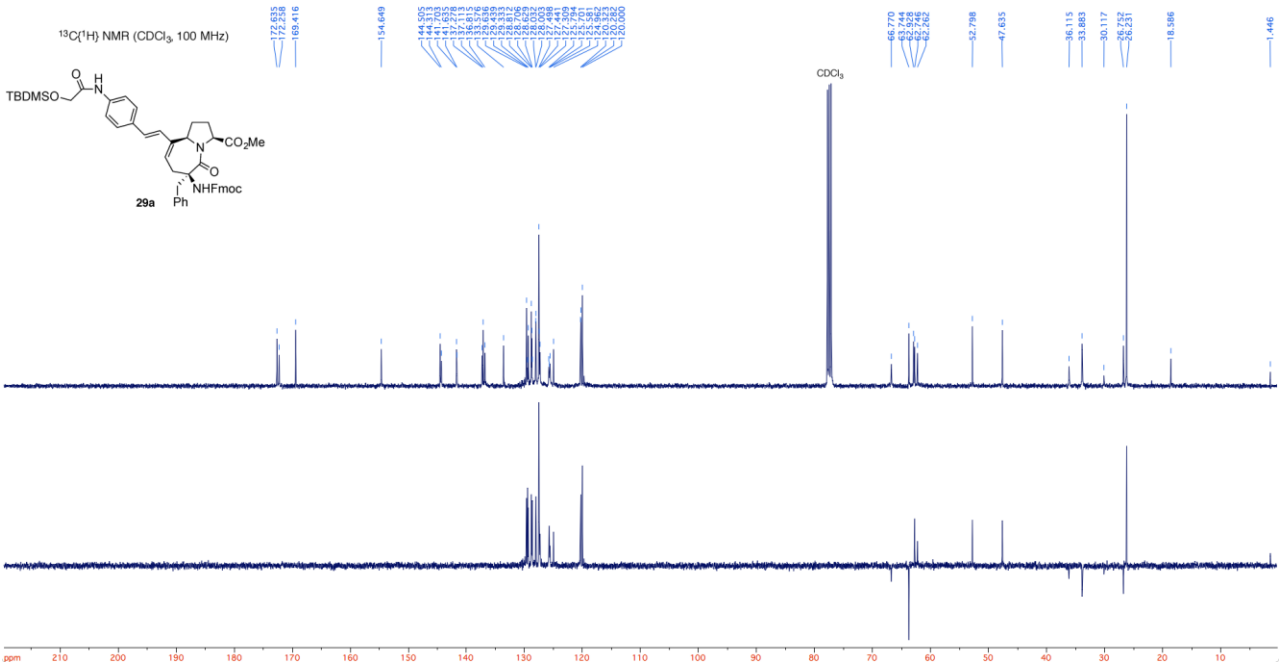

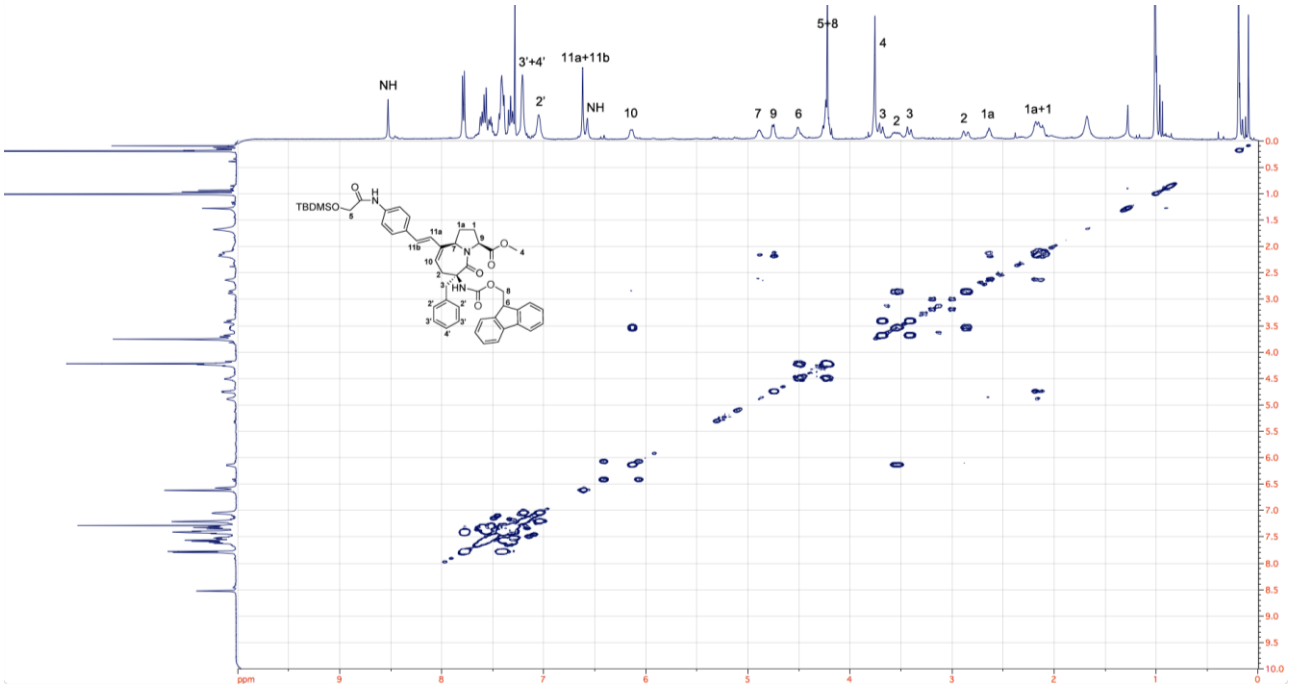

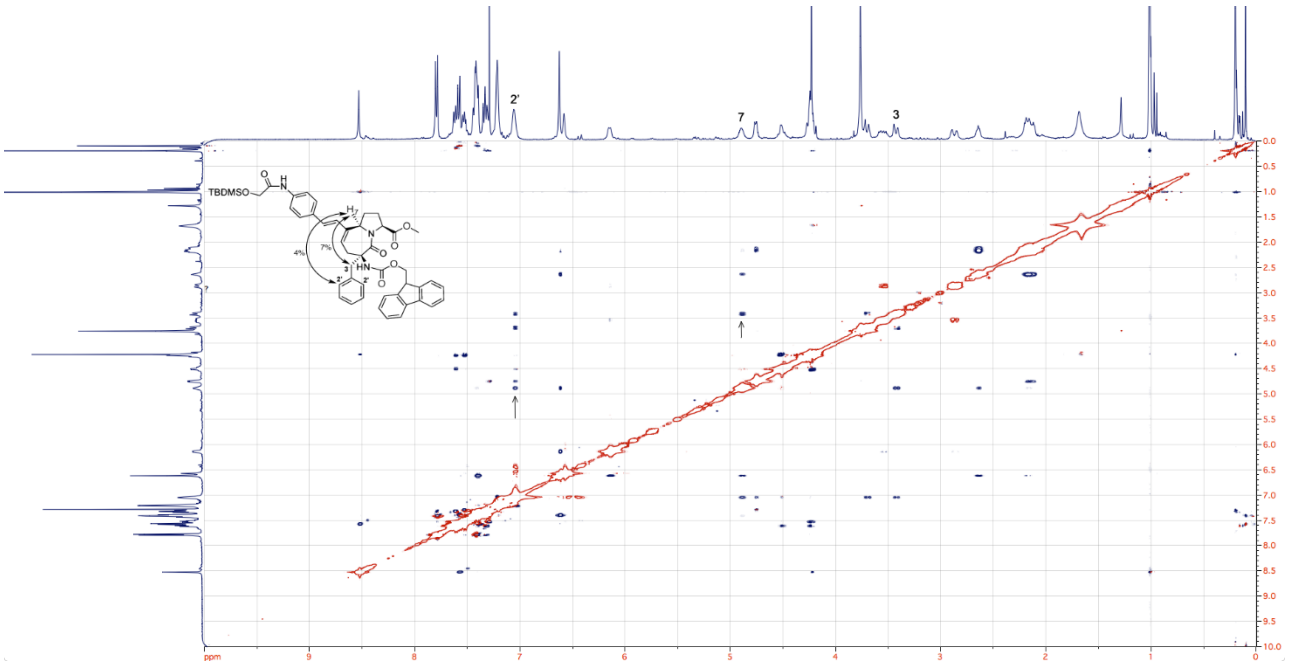

NOEs of H_7 with $H_{2'}$ and H_3 are diagnostic for the (*R*) absolute configuration of the C3 quaternary stereocenter.

^{1}H NMR (400 MHz), ^{13}C NMR and DEPT 135 spectra of compound 32b

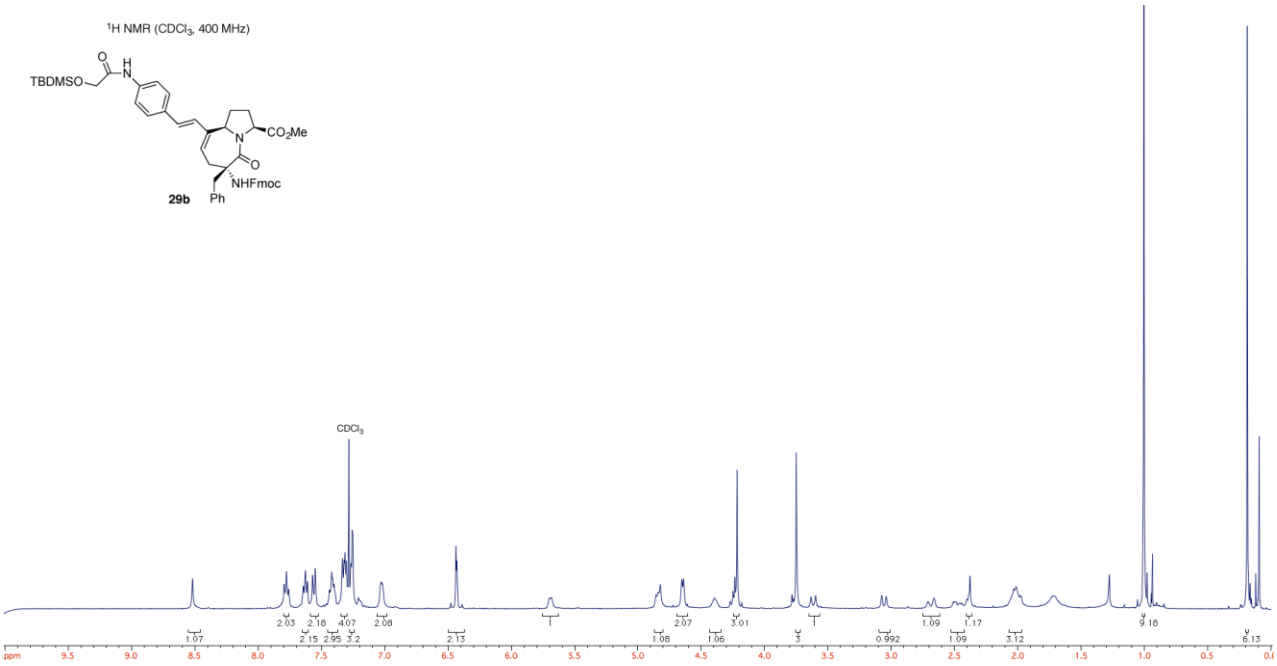

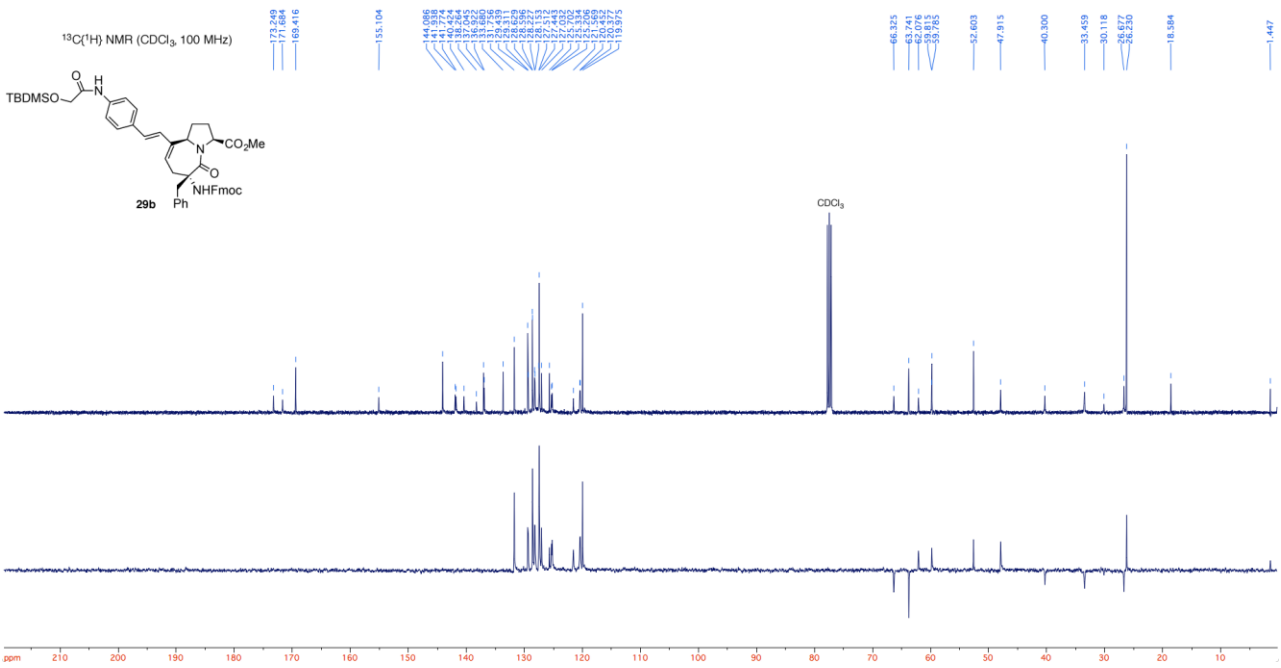

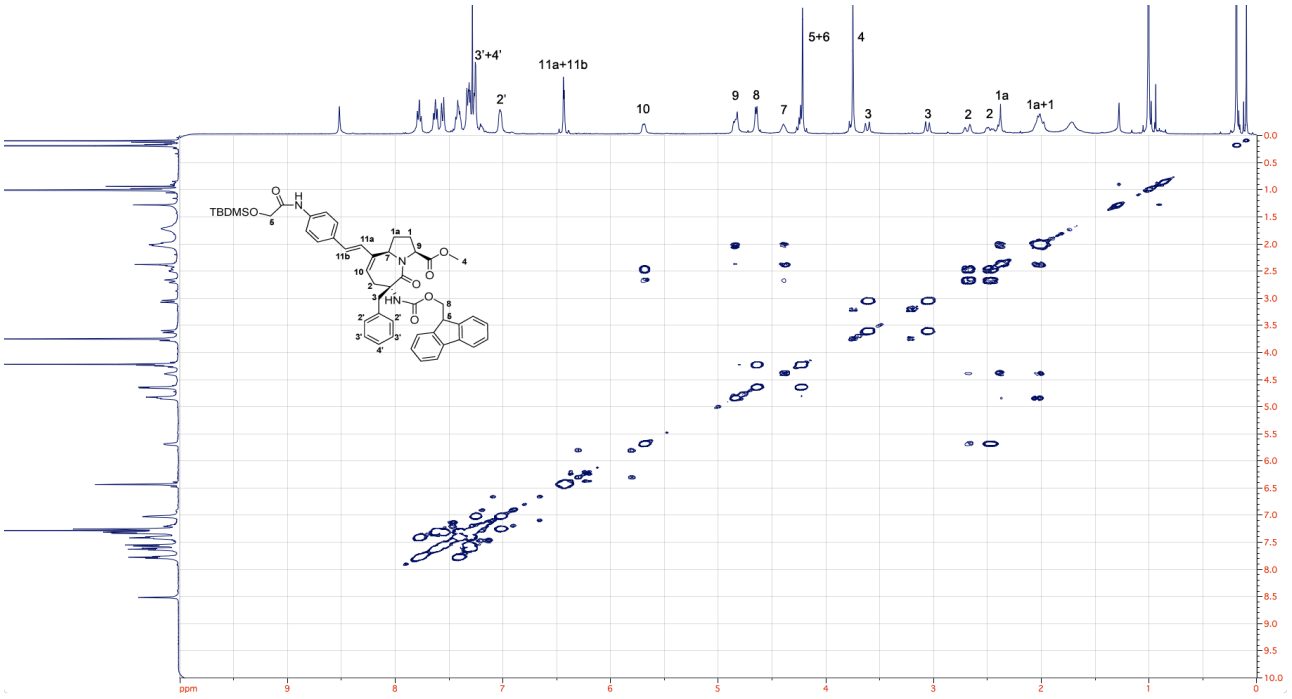

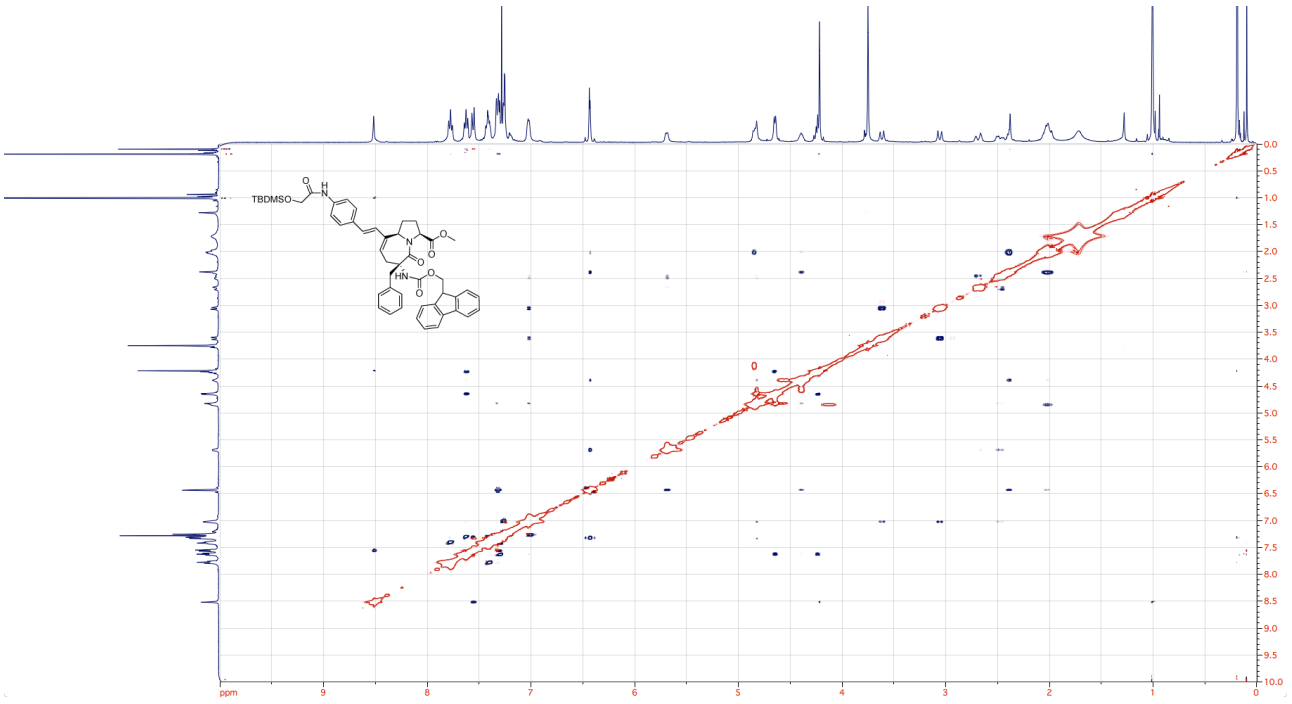

^{1}H NMR (400 MHz), ^{13}C NMR and DEPT 135 spectra of compound 33

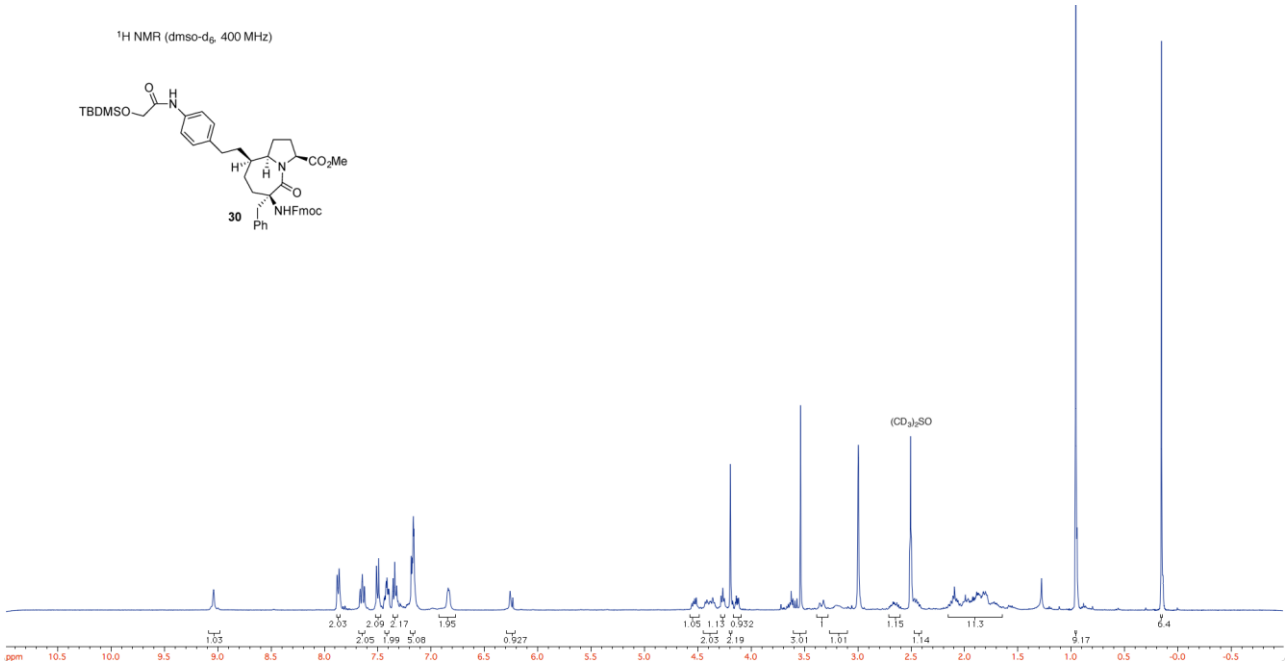
^{1}H NMR (dmso-d$_6$, 400 MHz)
TBDMSO
CO_2Me
NHFmoc
Ph
30
$(CD_3)_2SO$

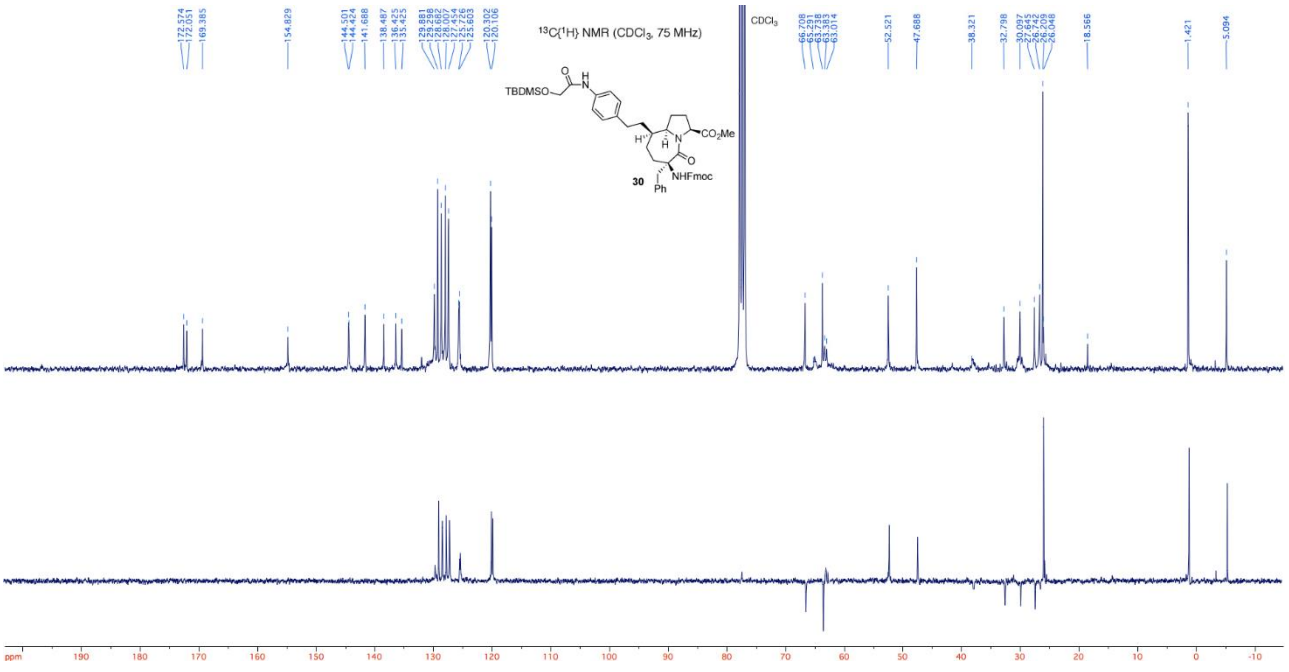
$^{13}C\{^1H\}$ NMR ($CDCl_3$, 75 MHz)
$CDCl_3$
TBDMSO
CO_2Me
NHFmoc
Ph
30

^{1}H NMR (500 MHz), ^{13}C NMR, DEPT 135, 2D-COSY, HSQC-DEPT, and 2D-NOESY spectra of compound 31

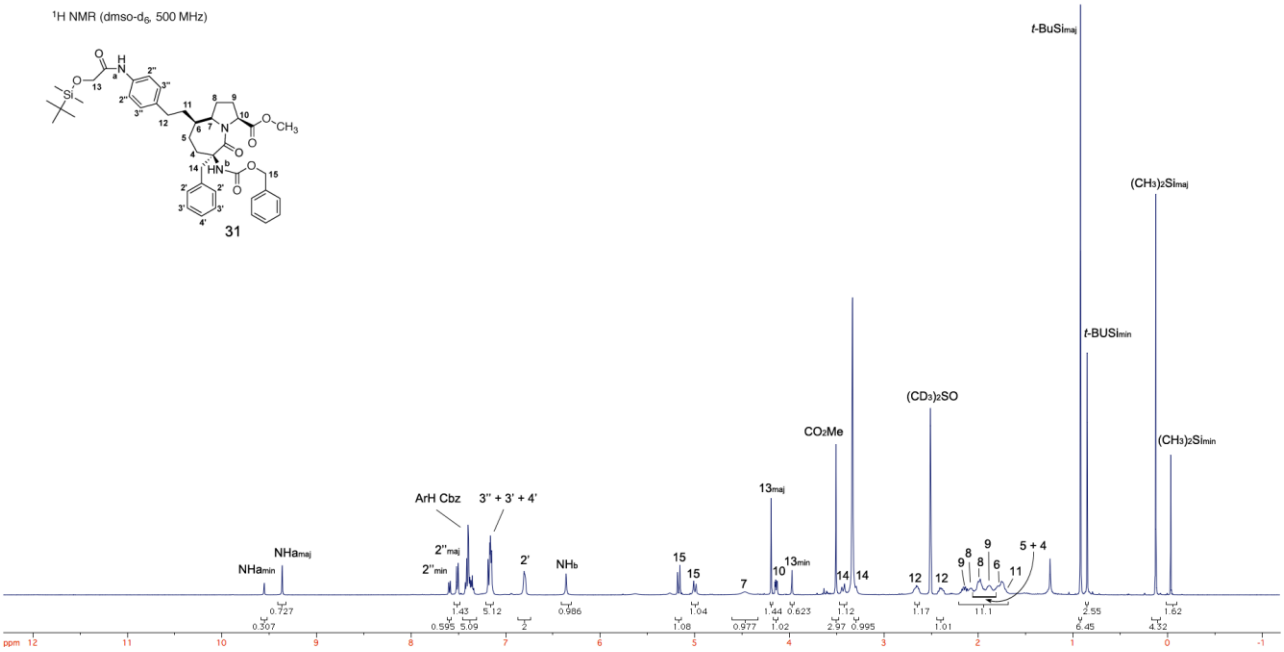

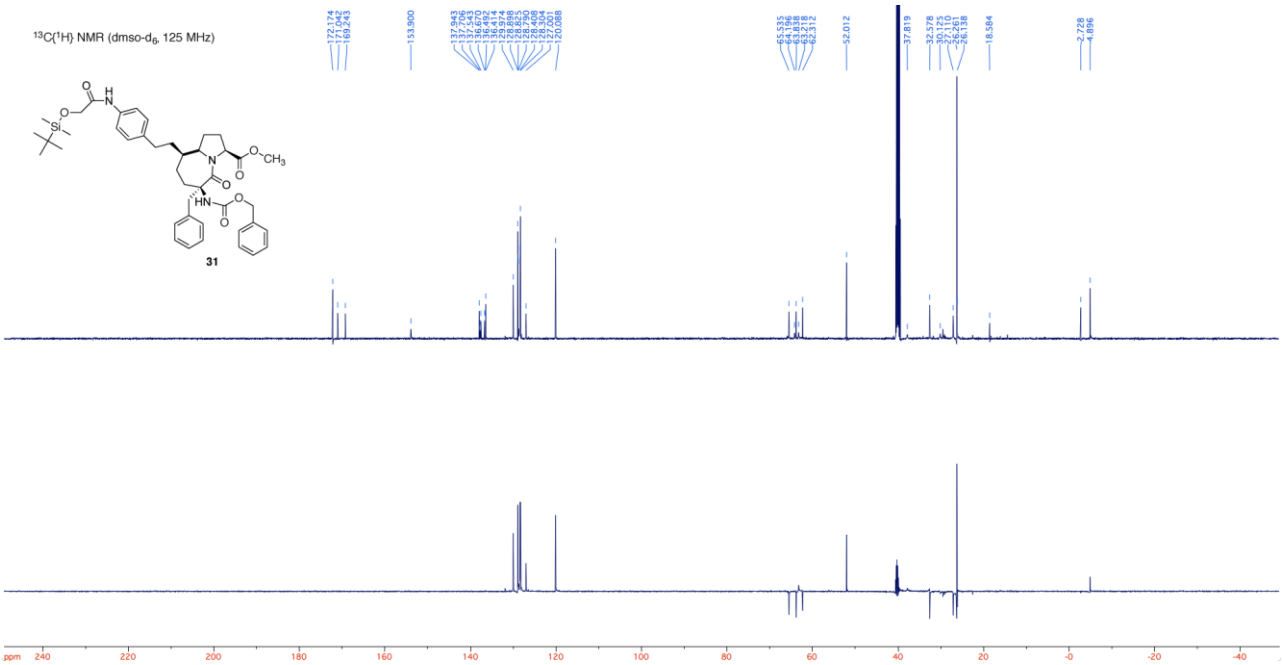

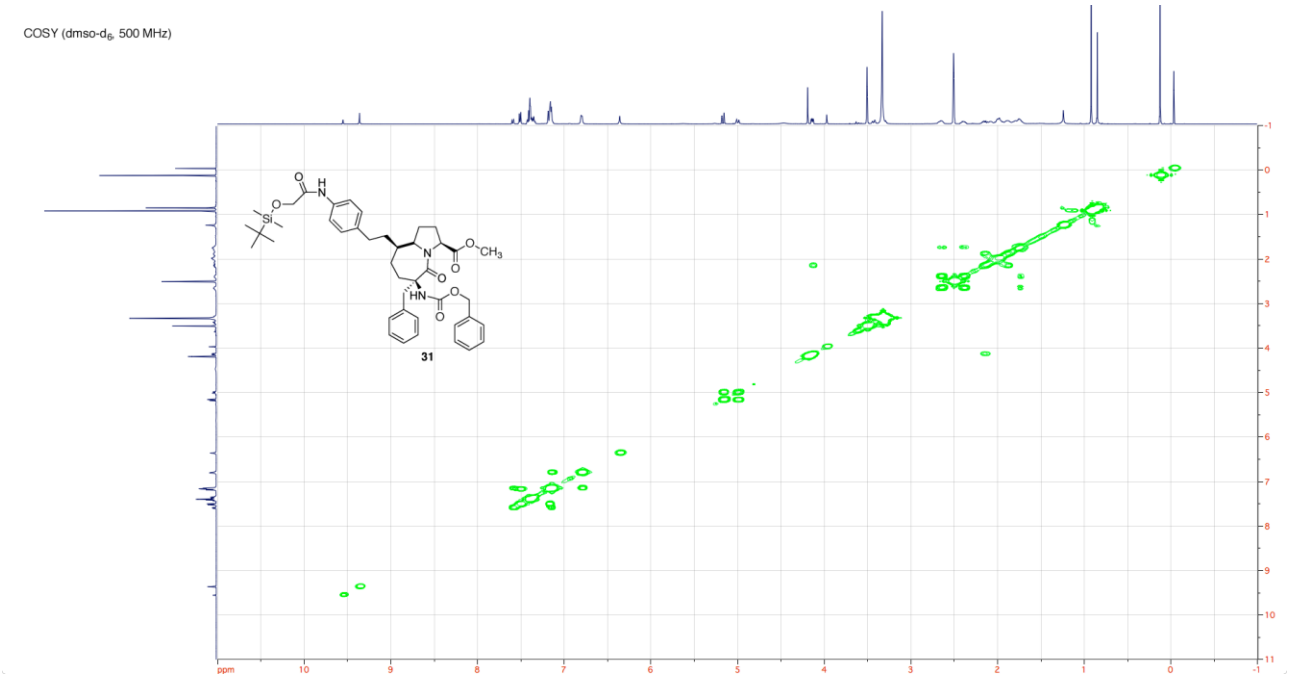
COSY (dmso-d6, 500 MHz)
31

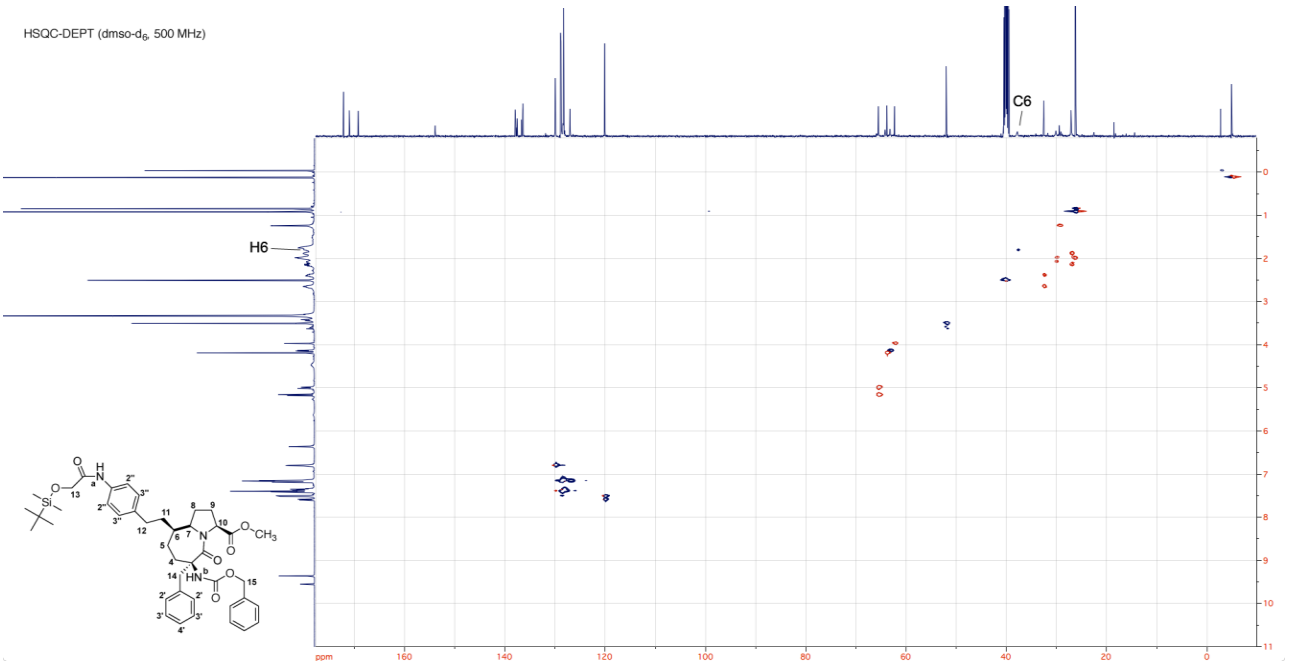
HSQC-DEPT (dmso-d6, 500 MHz)
C6
H6

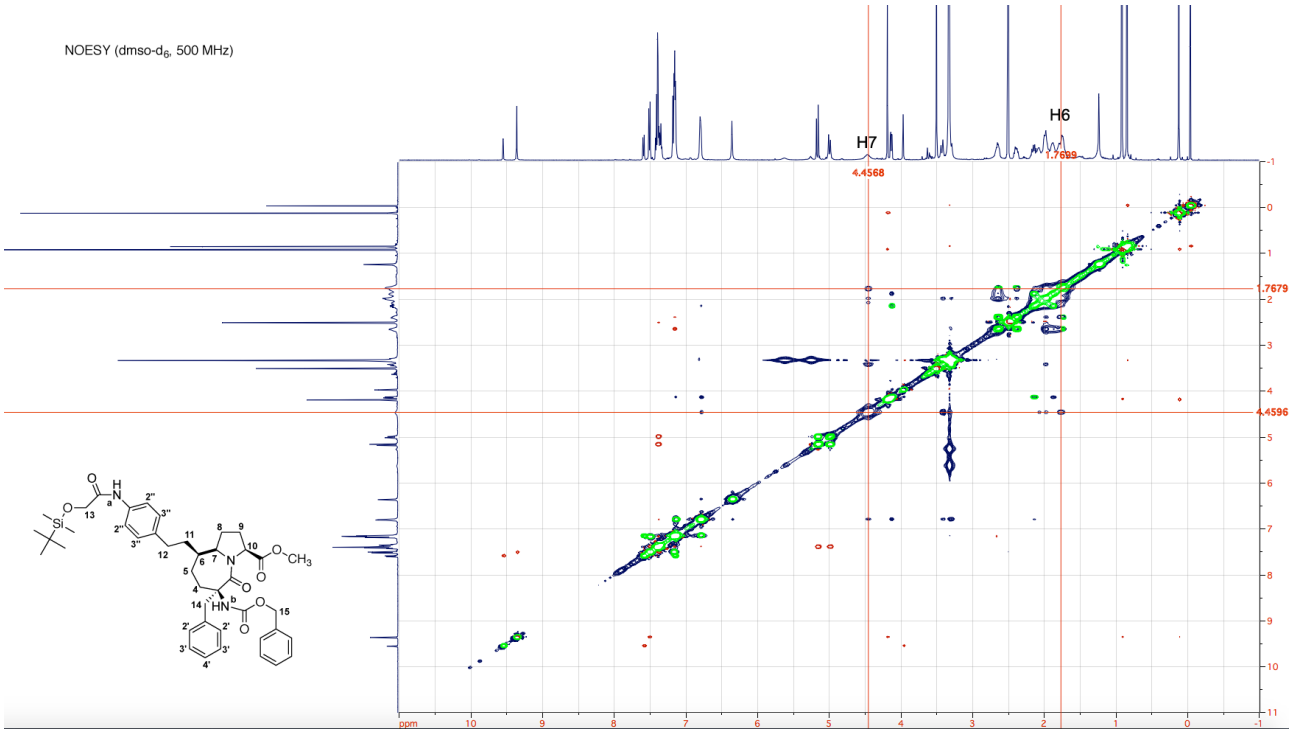
NOESY (dmso-d6, 500 MHz)
H7
H6
4.4568
1.7699
1.7679
4.4596
ppm

^{1}H NMR (400 MHz), ^{13}C NMR and DEPT 135 spectra of compound 44a

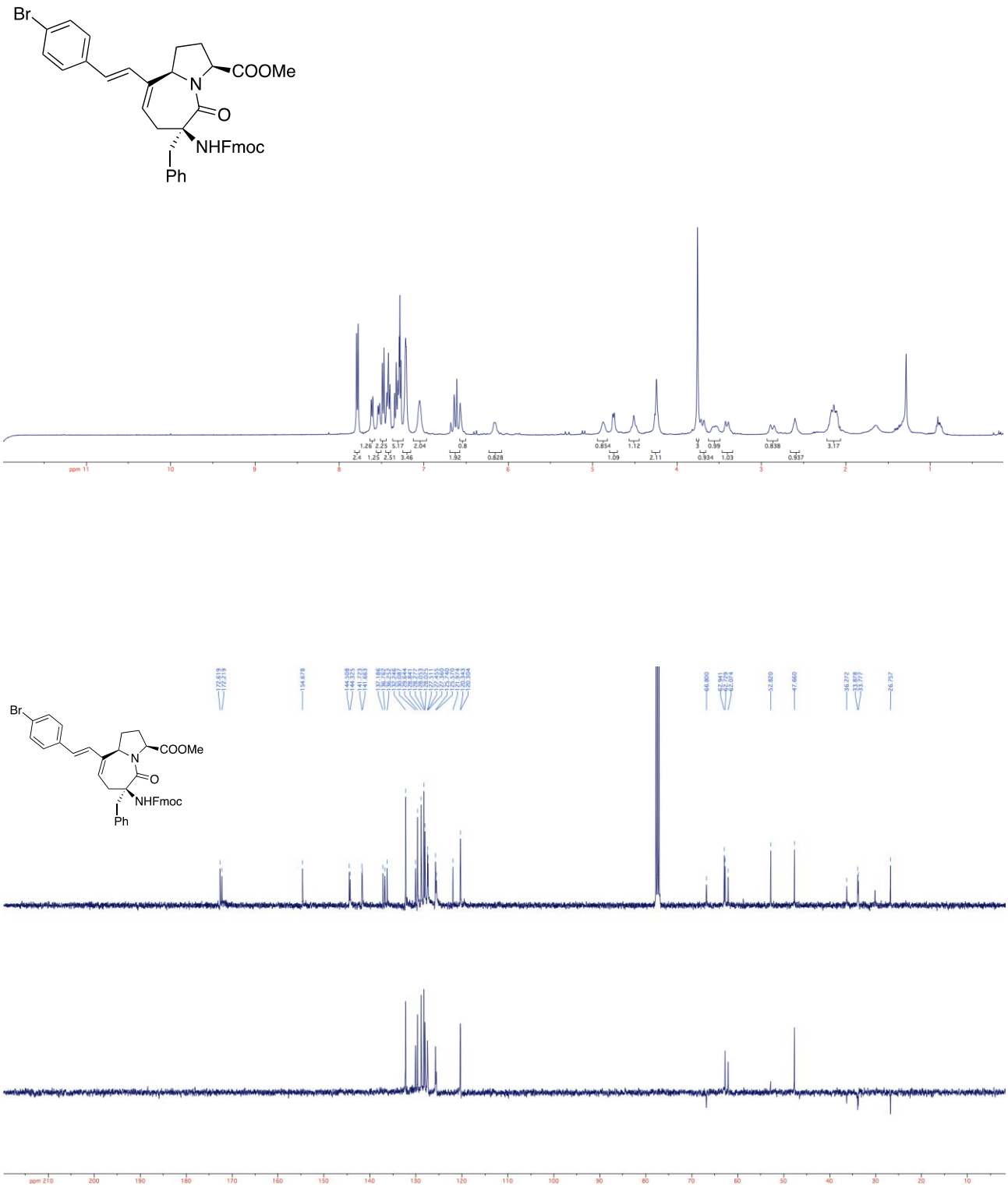

^{1}H NMR (400 MHz), ^{13}C NMR and DEPT 135 spectra of compound 44b

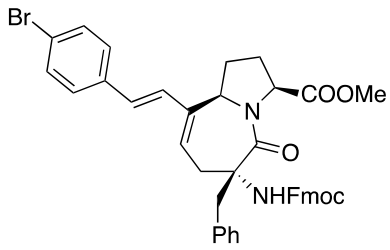

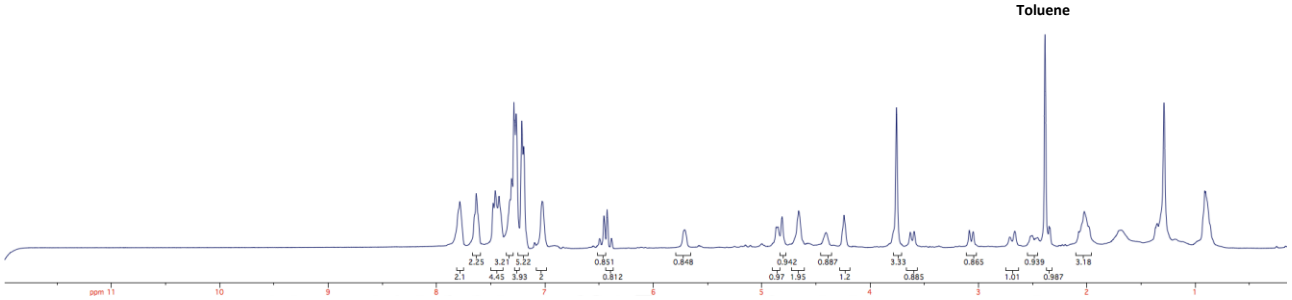

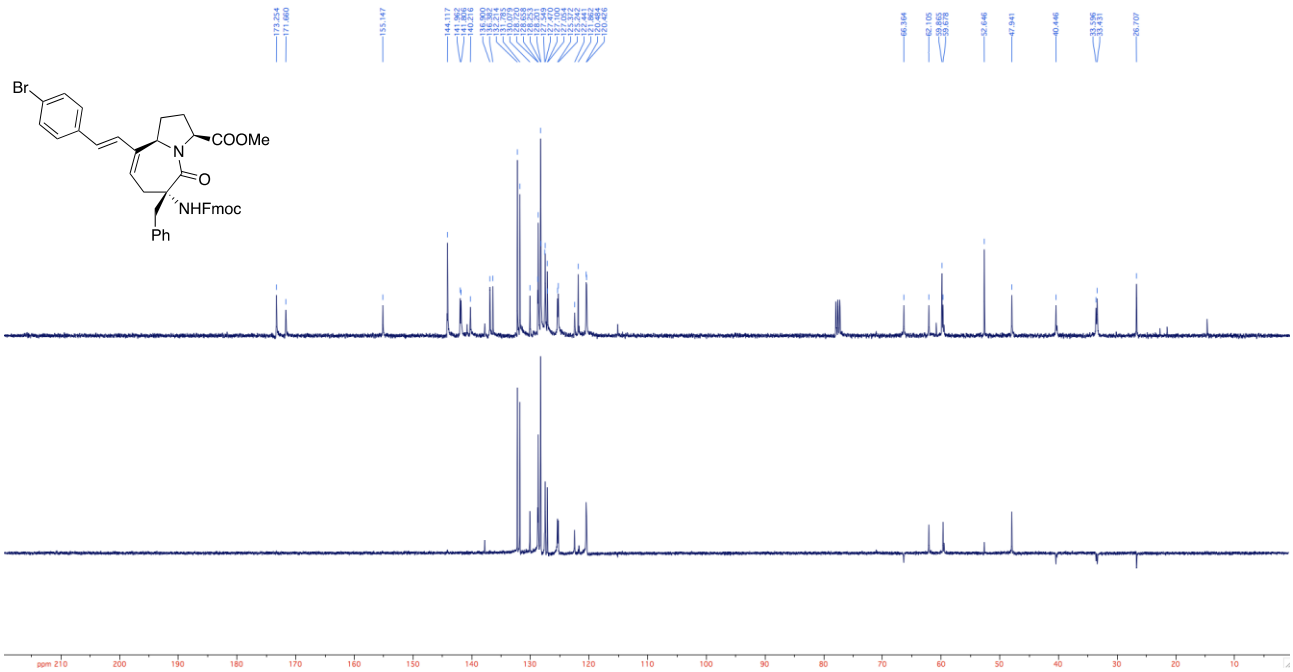

^{1}H NMR (400 MHz), ^{13}C NMR and DEPT 135 spectra of compound 47

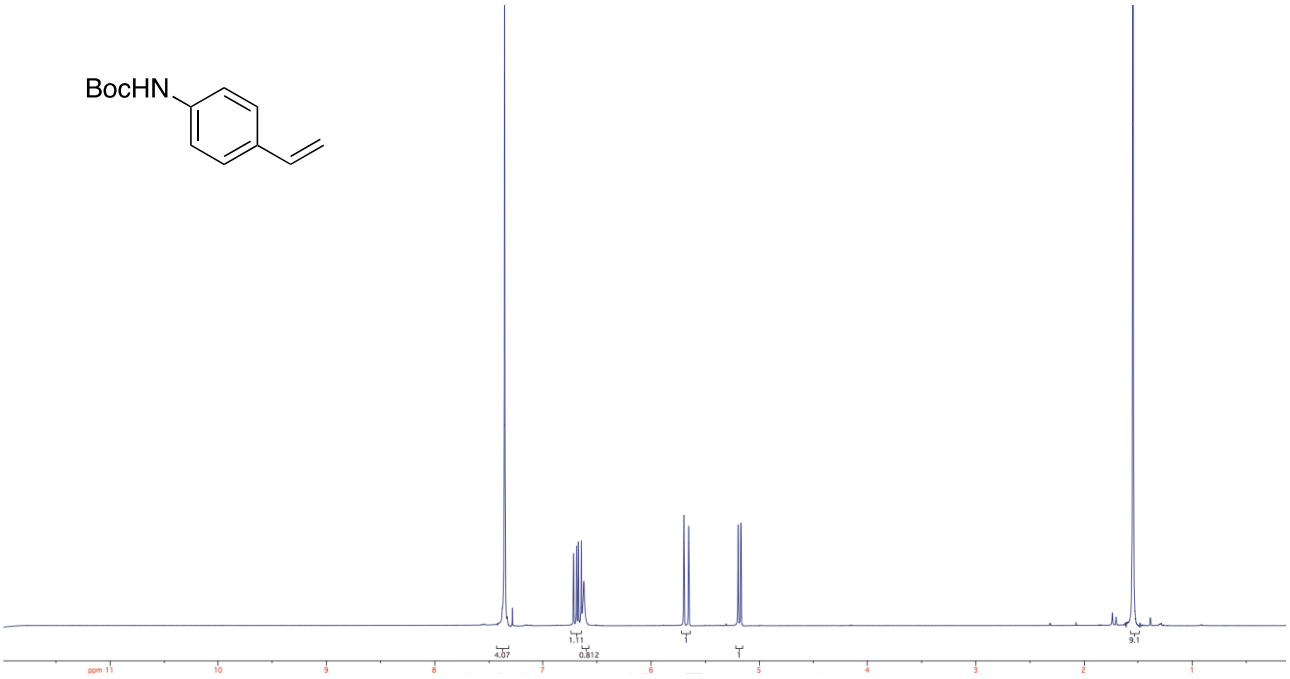

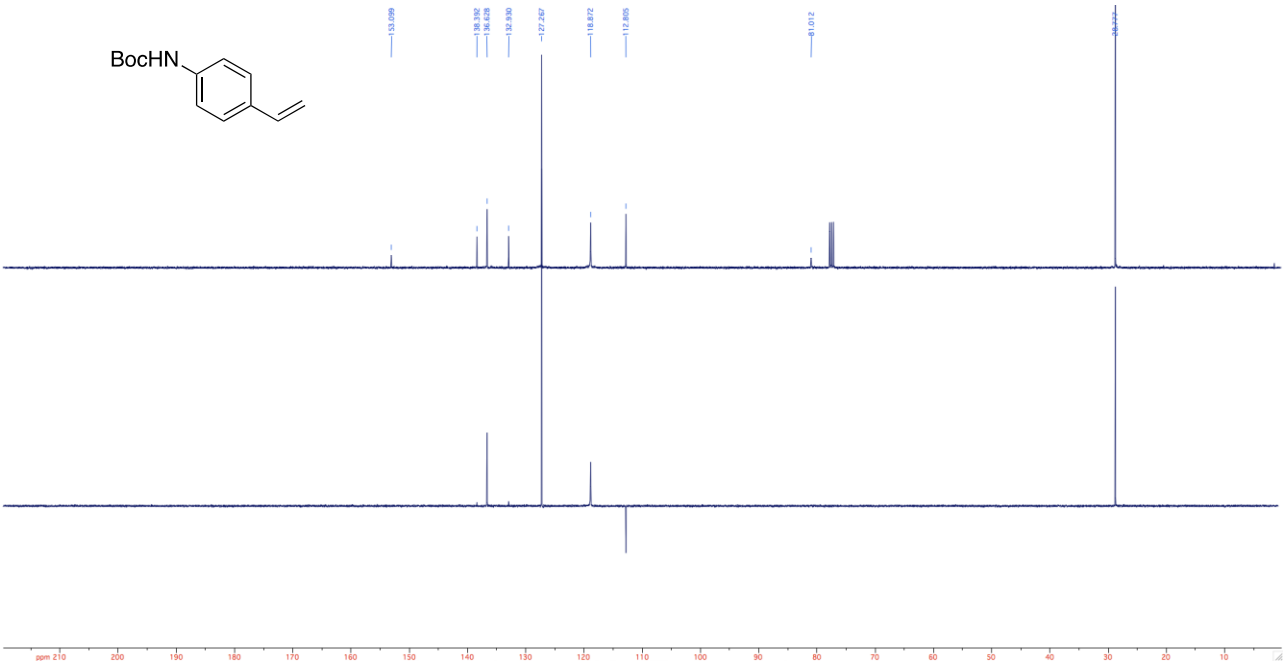

^{1}H NMR (400 MHz), ^{13}C NMR and DEPT 135 spectra of compound 48a

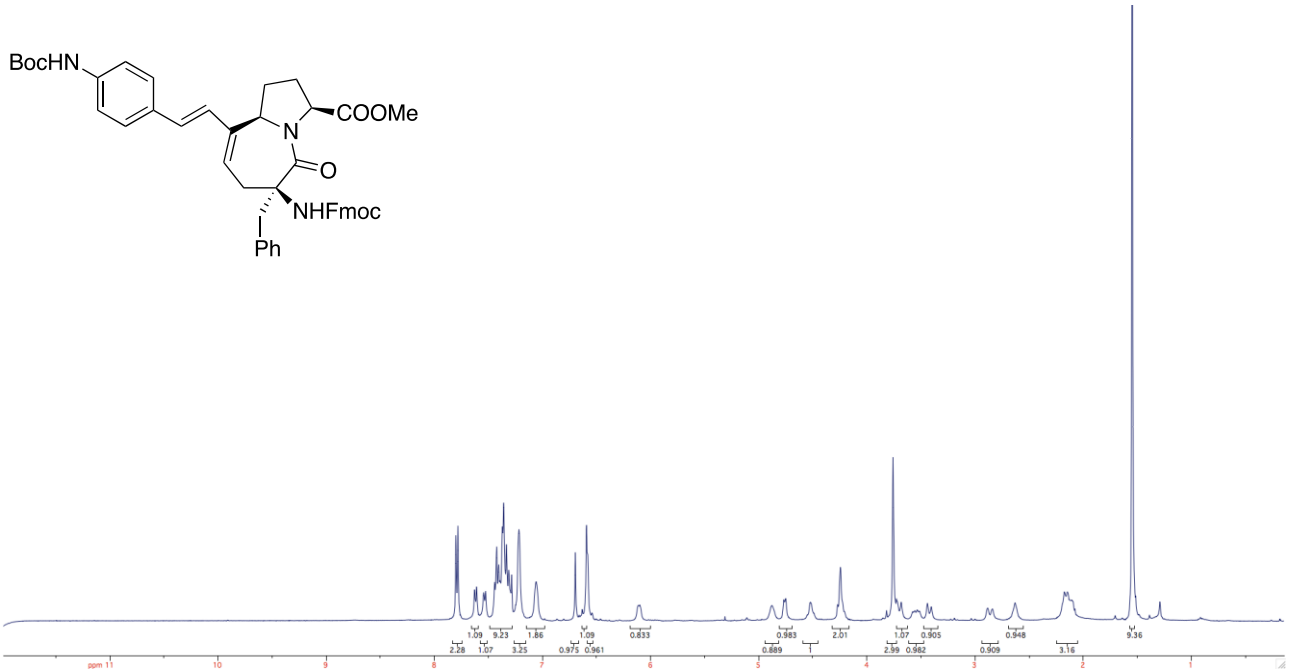

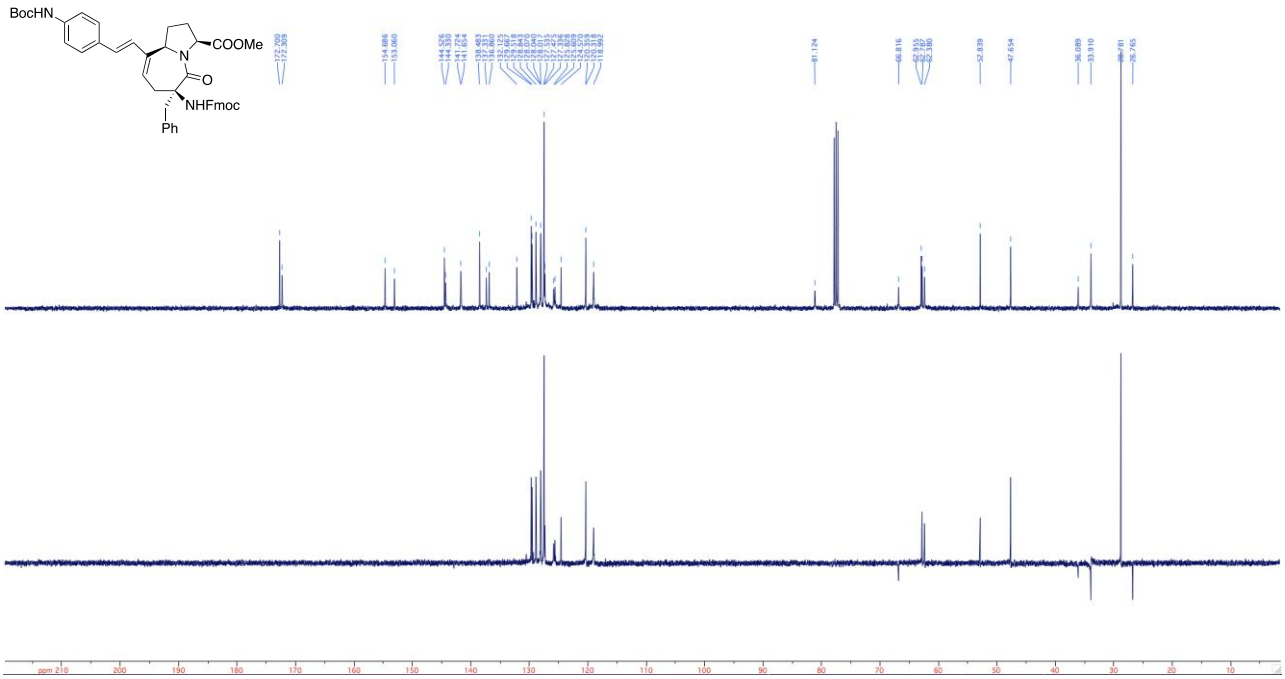

^{1}H NMR (400 MHz), ^{13}C NMR and DEPT 135 spectra of compound 48b

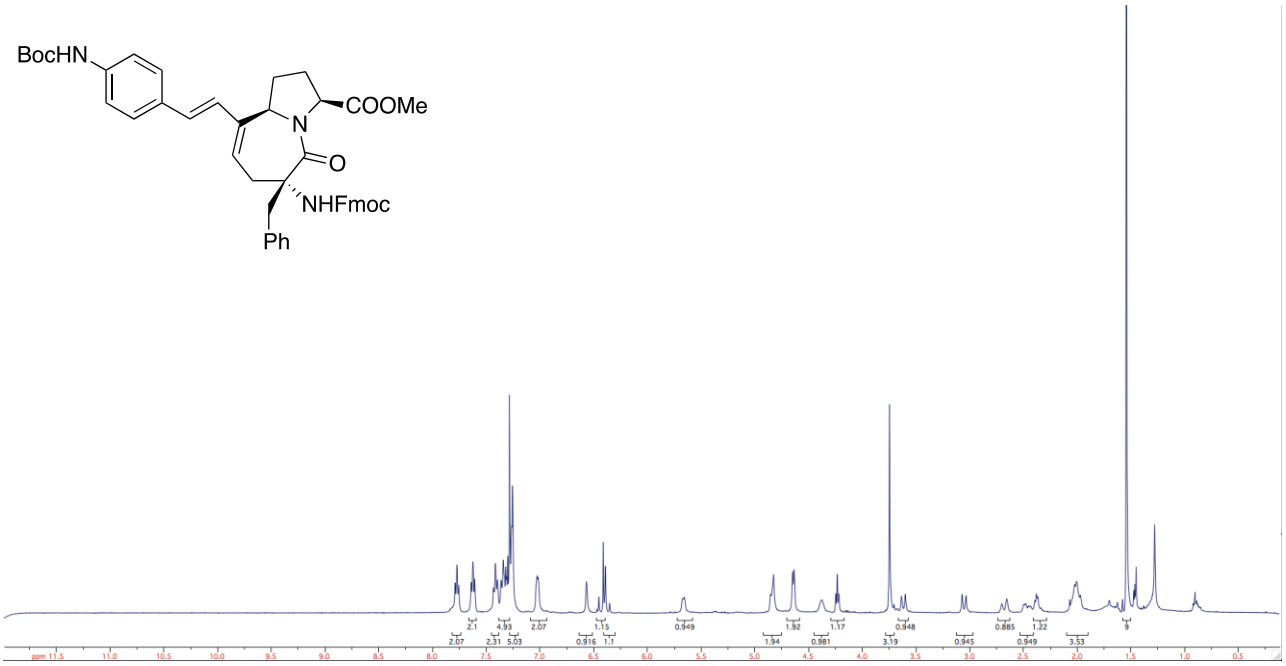

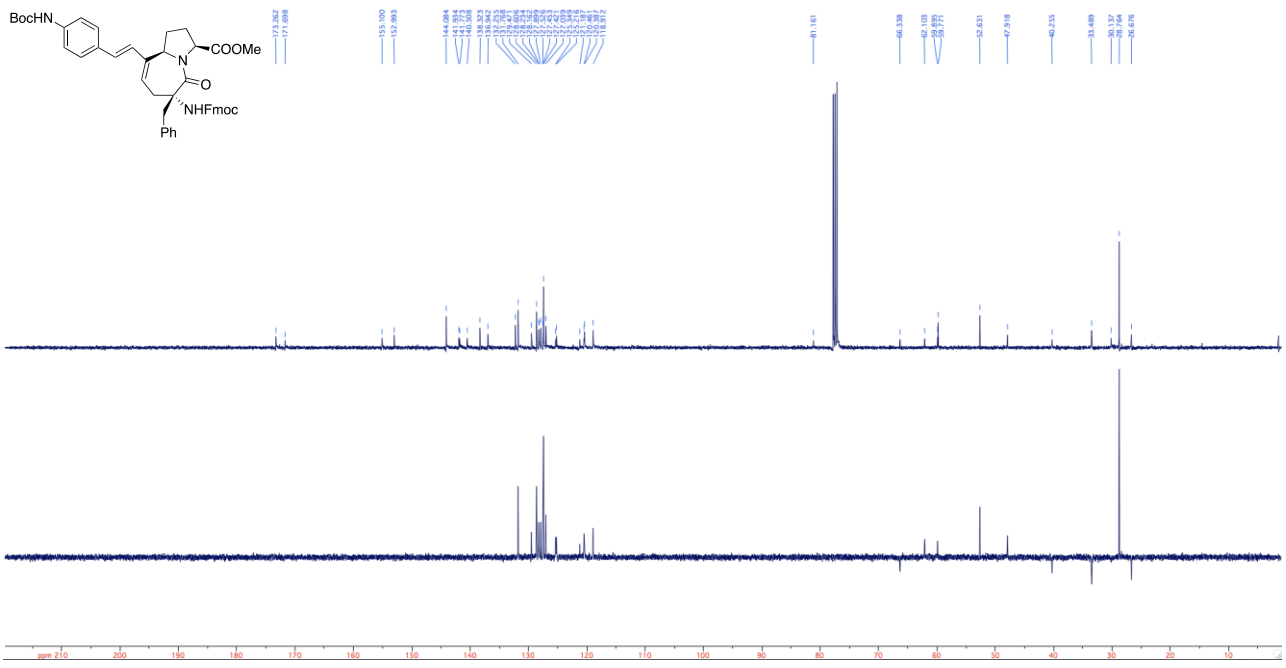

^{1}H NMR (400 MHz), ^{13}C NMR and DEPT 135 spectra of compound 49

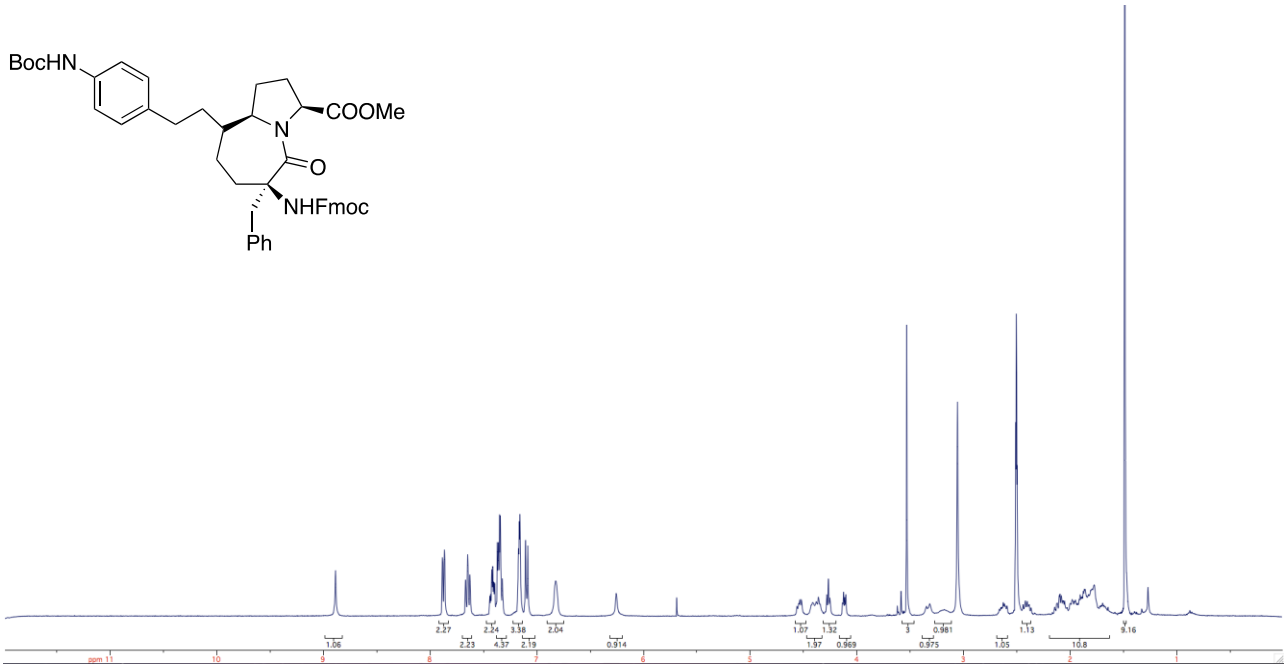

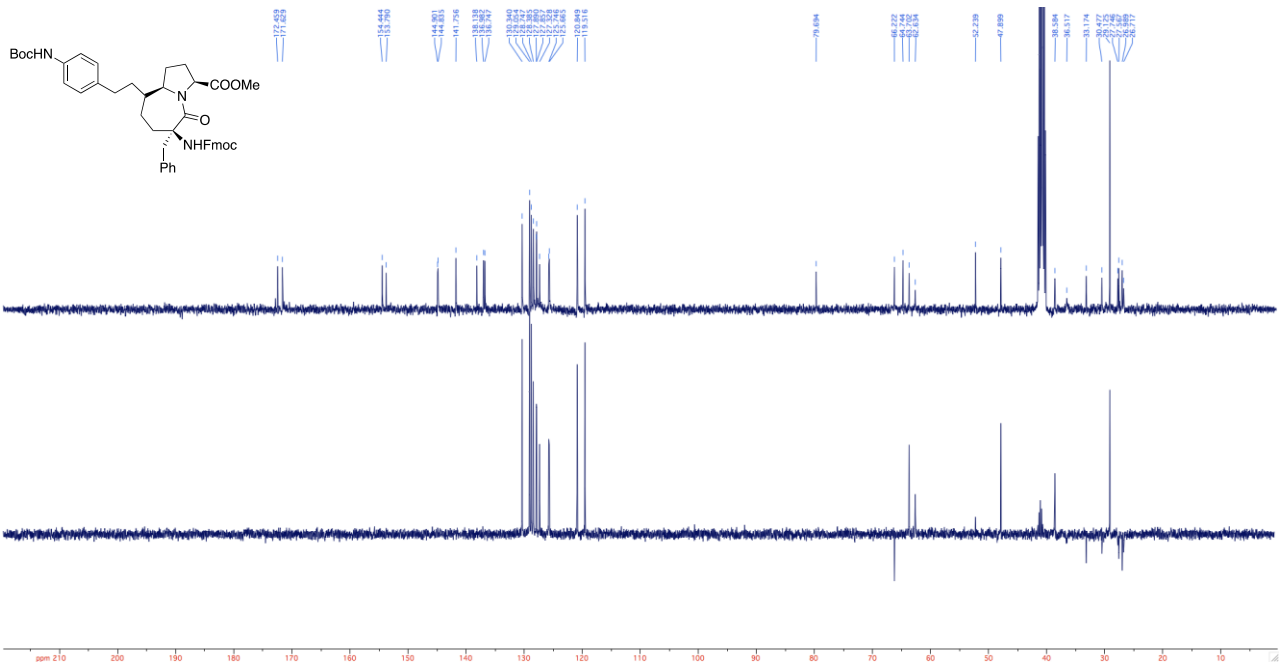

^{1}H NMR (400 MHz), ^{13}C NMR and DEPT 135 spectra of compound 52

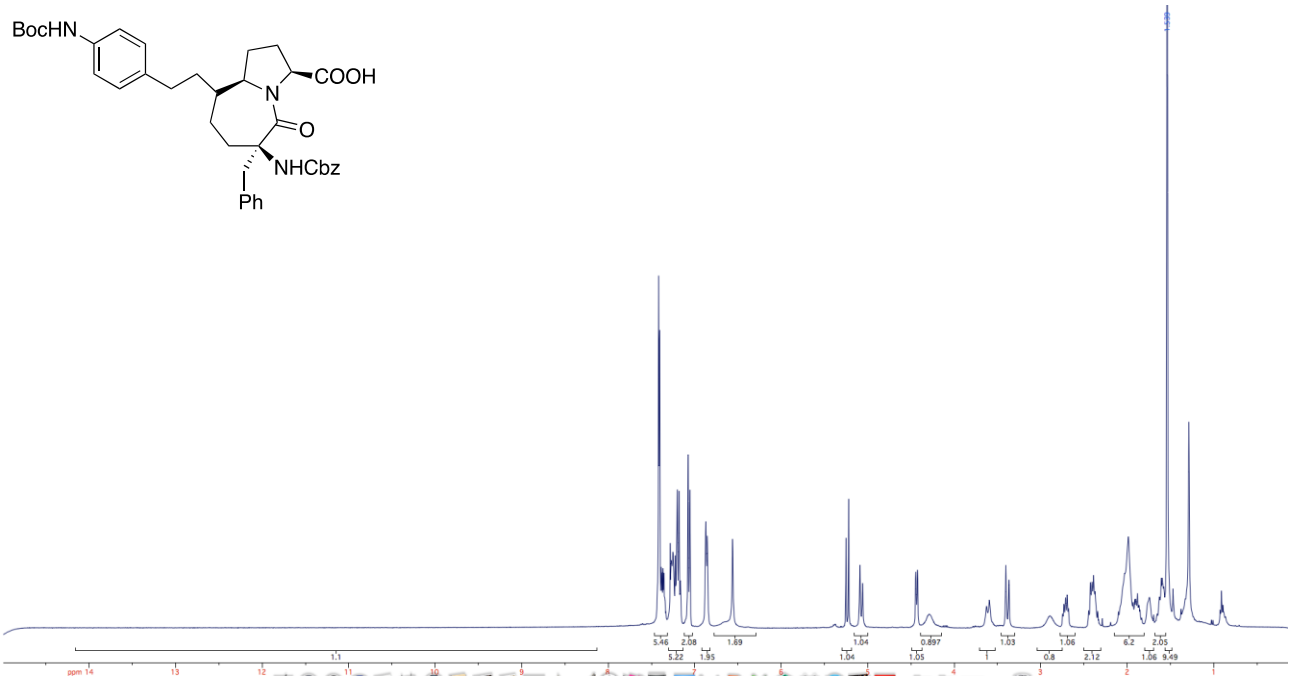

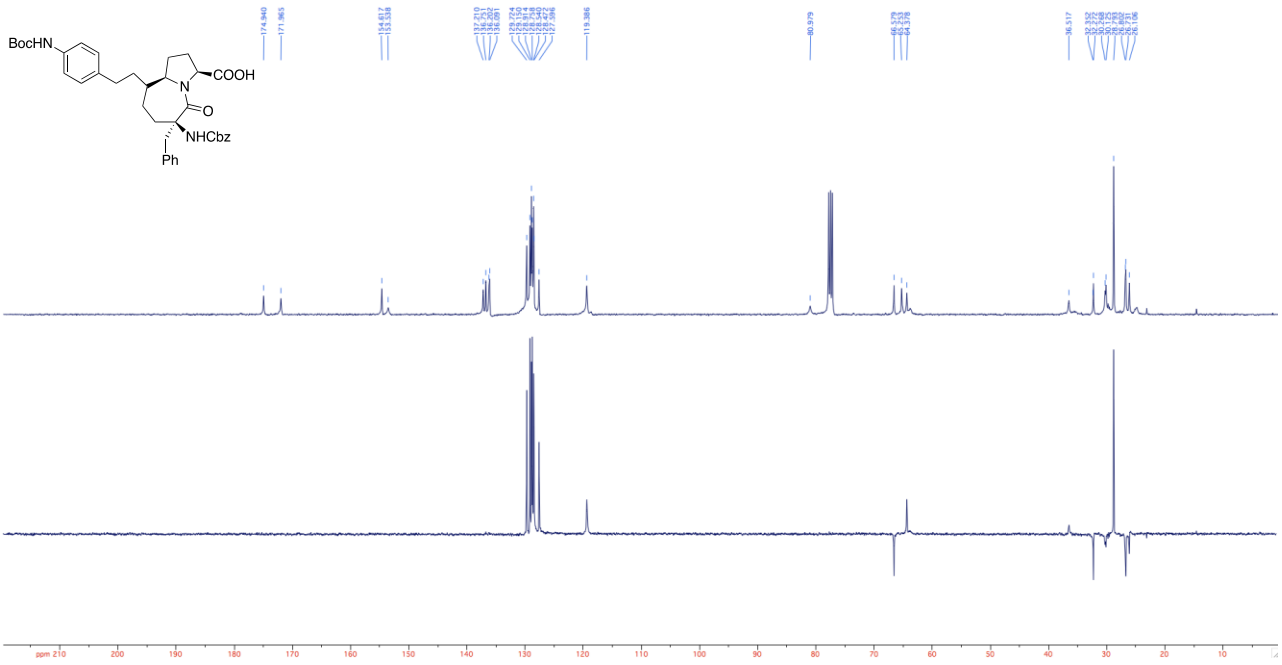

^{1}H NMR (400 MHz), ^{13}C NMR and DEPT 135 spectra of compound 57

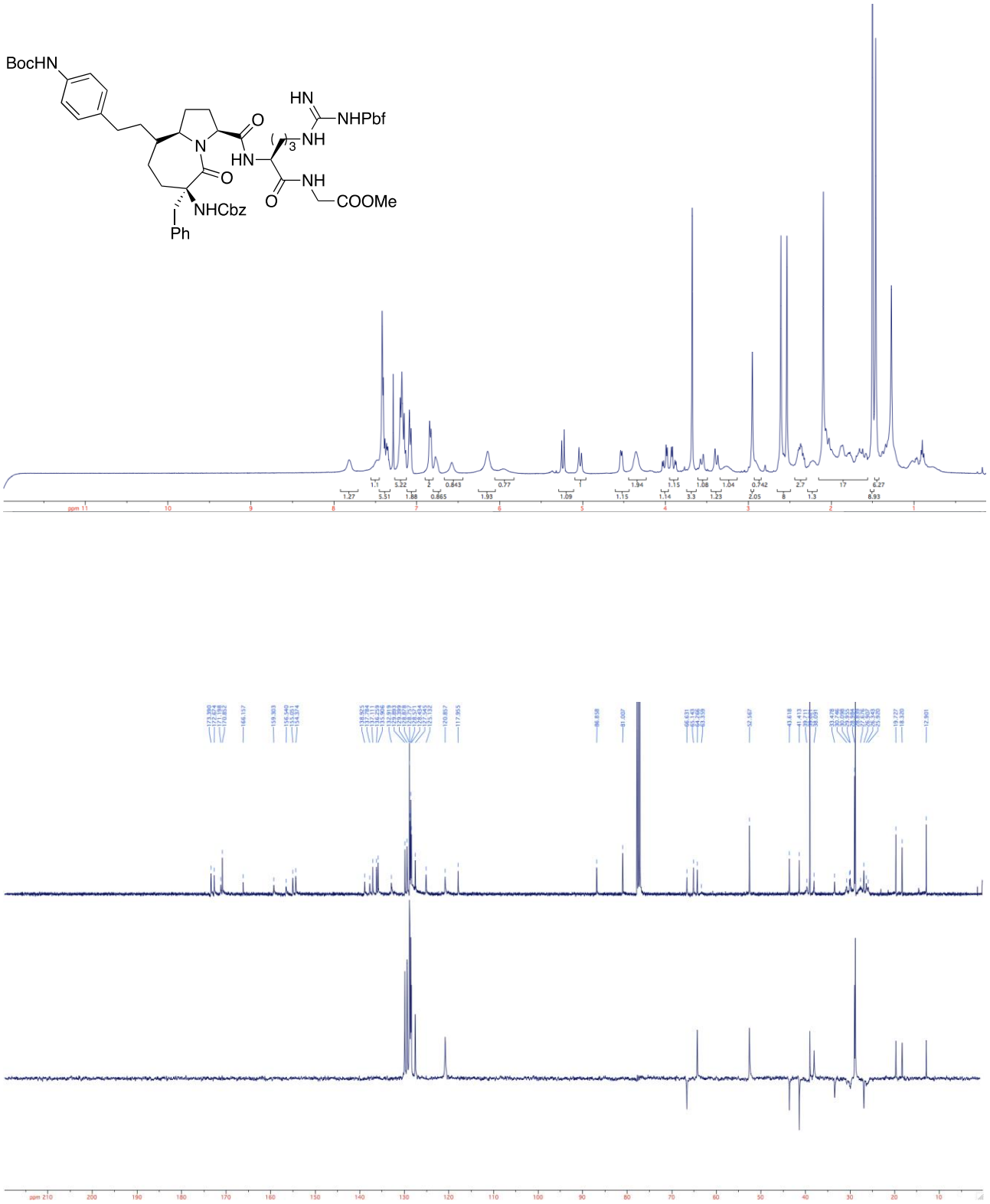

^{1}H NMR (400 MHz), ^{13}C NMR and DEPT 135 spectra of compound 58

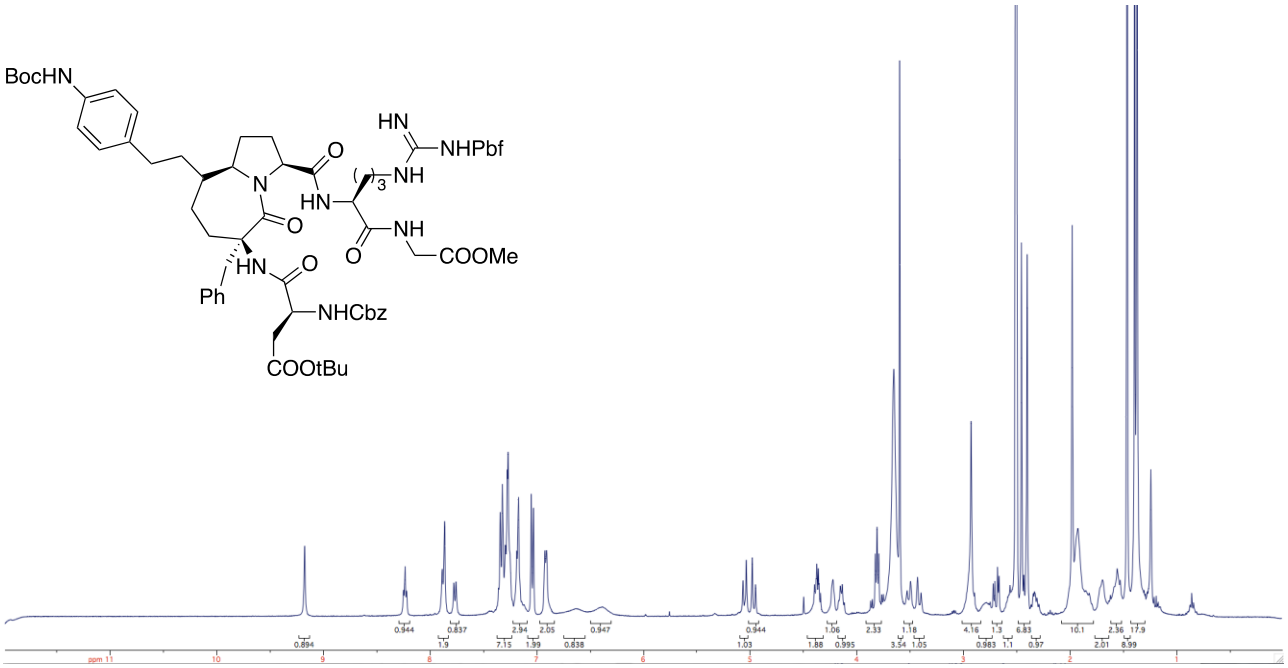

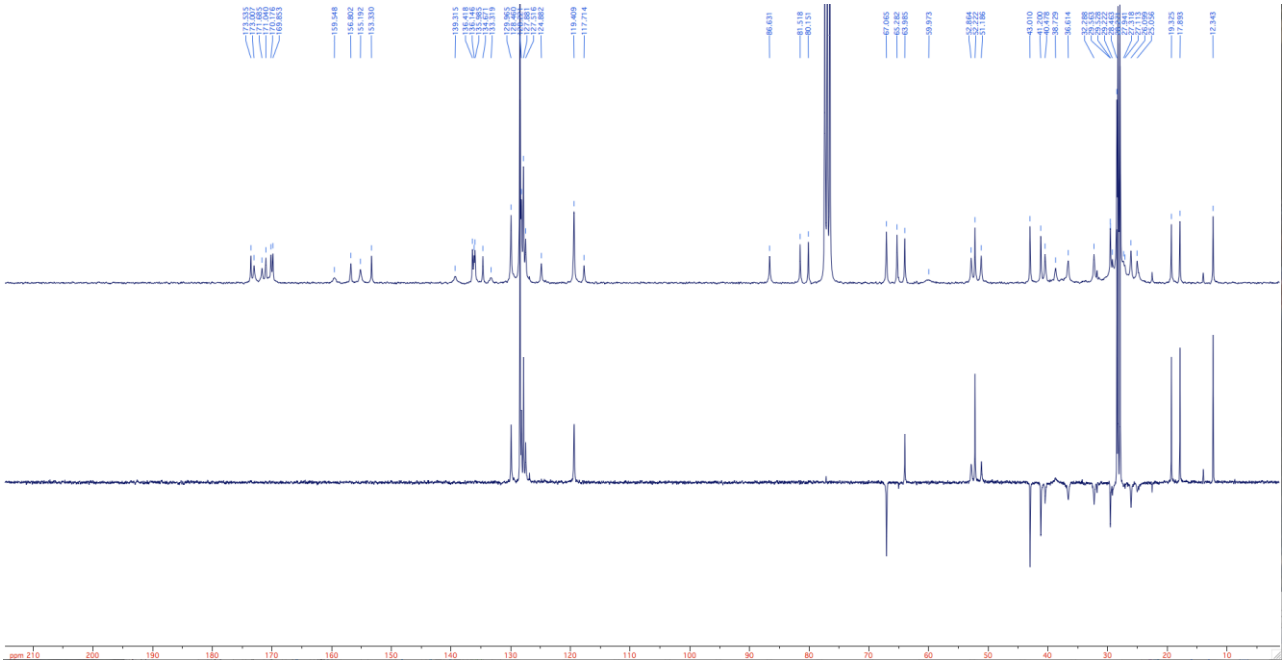

^{1}H NMR (400 MHz), ^{13}C NMR and DEPT 135 spectra of compound 59

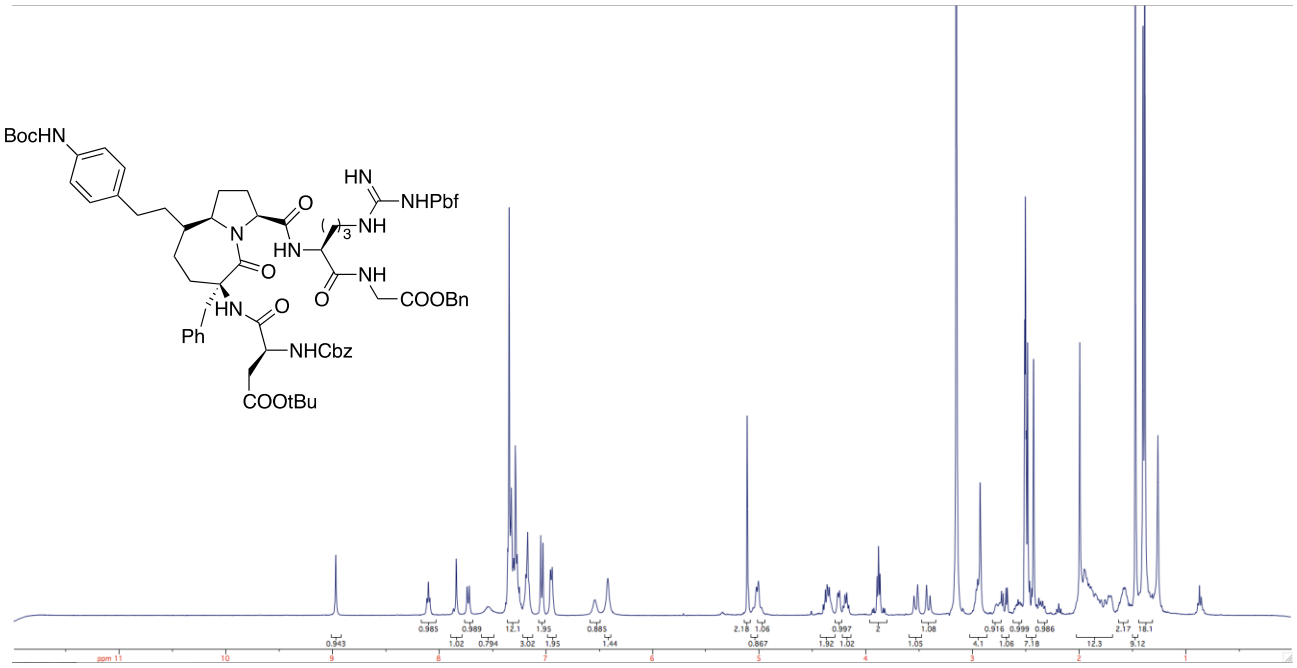

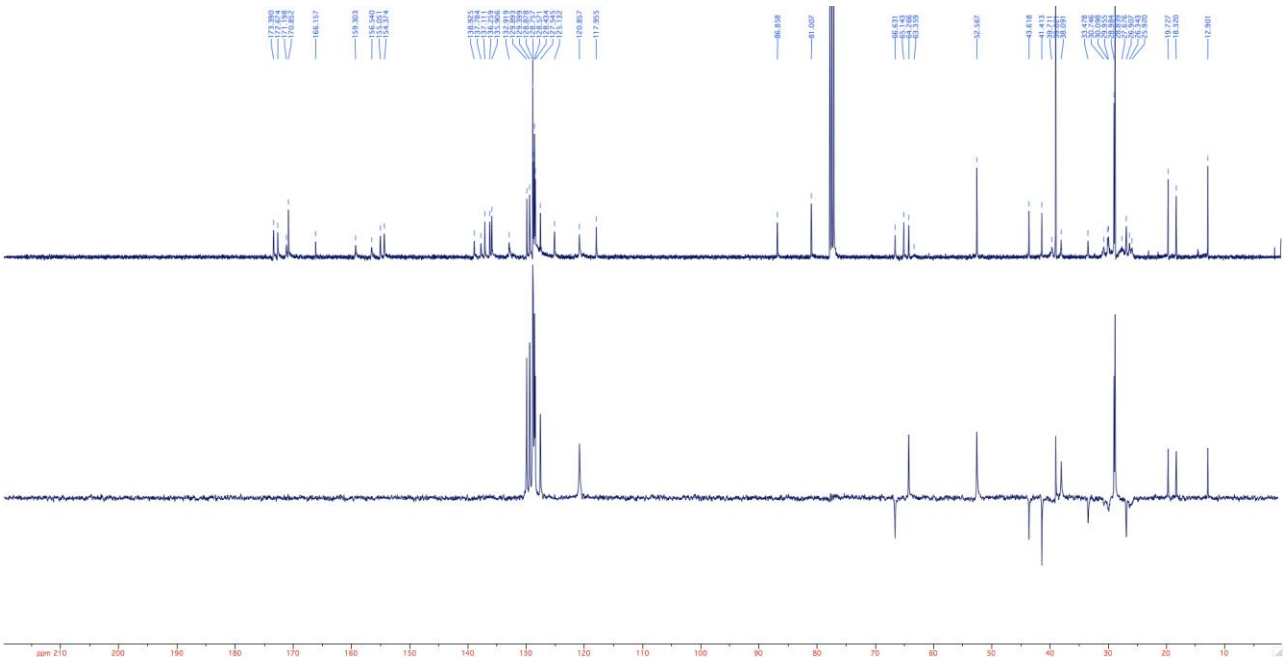

^{1}H NMR (400 MHz) spectra of 3a-RGD

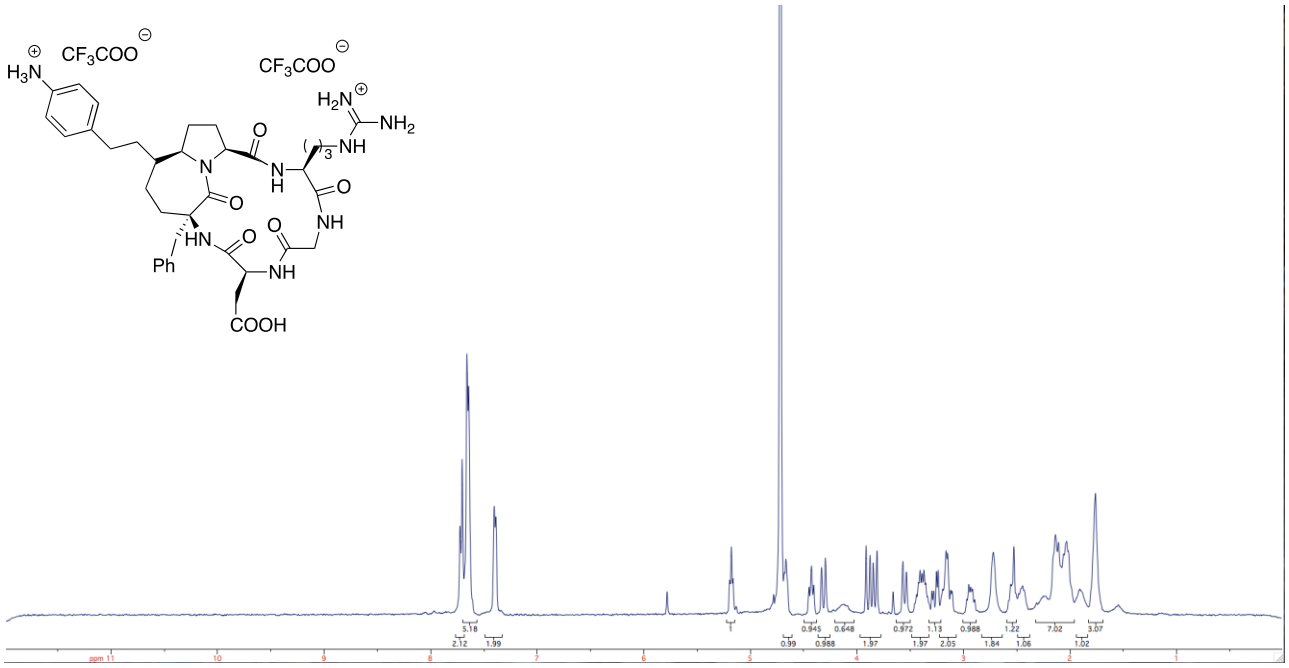

^{1}H NMR (400 MHz), ^{13}C NMR and DEPT 135 spectra of compound 62

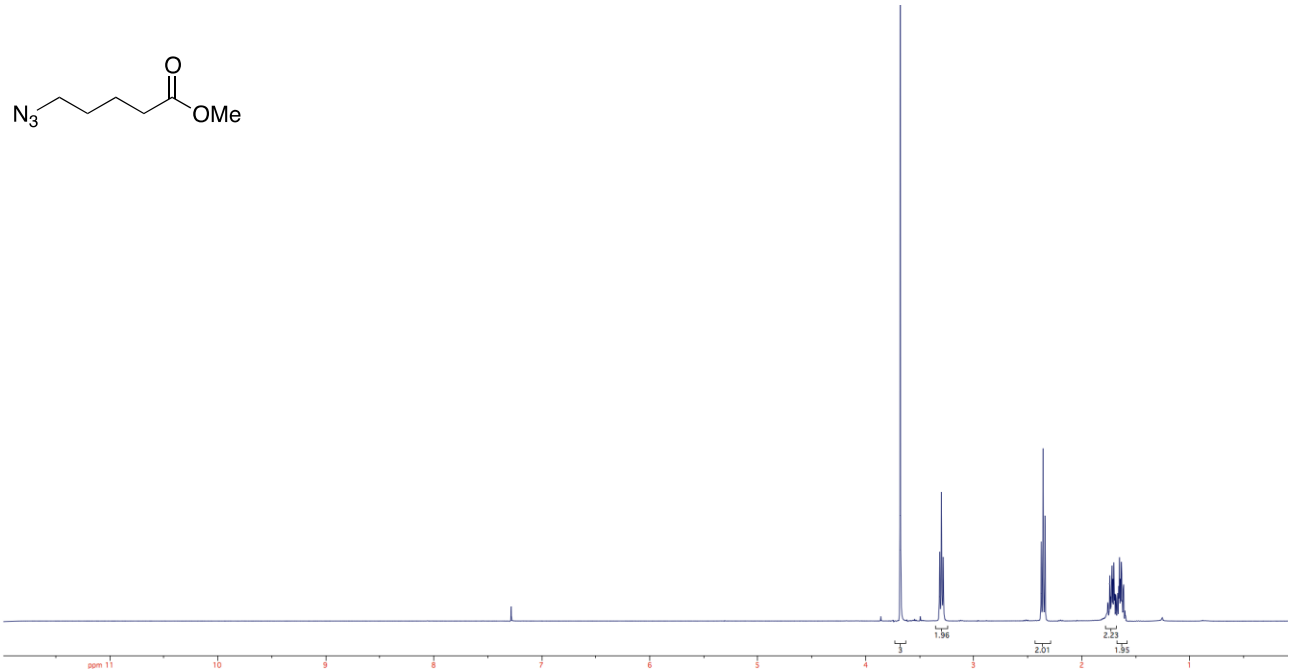

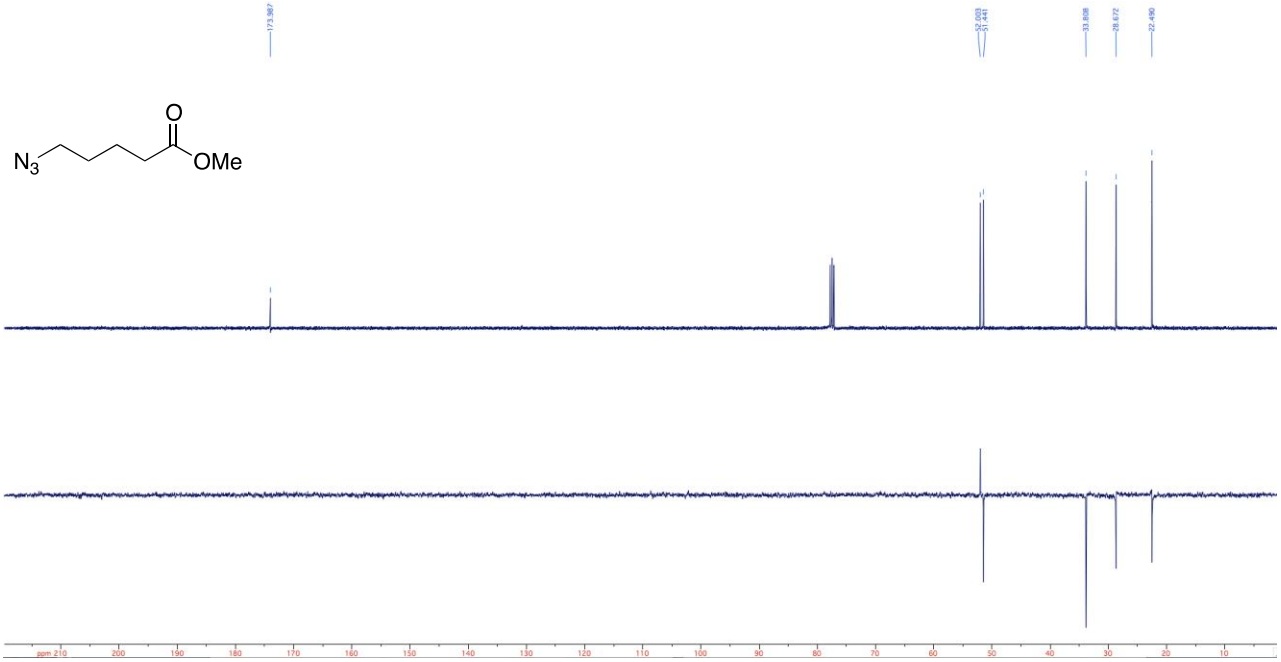

^{1}H NMR (400 MHz), ^{13}C NMR and DEPT 135 spectra of compound 63

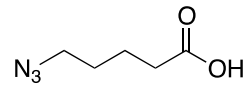

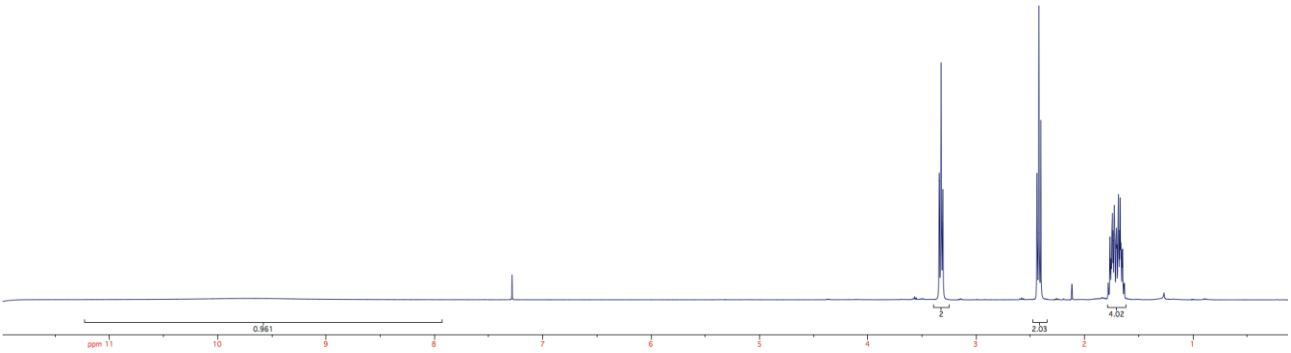

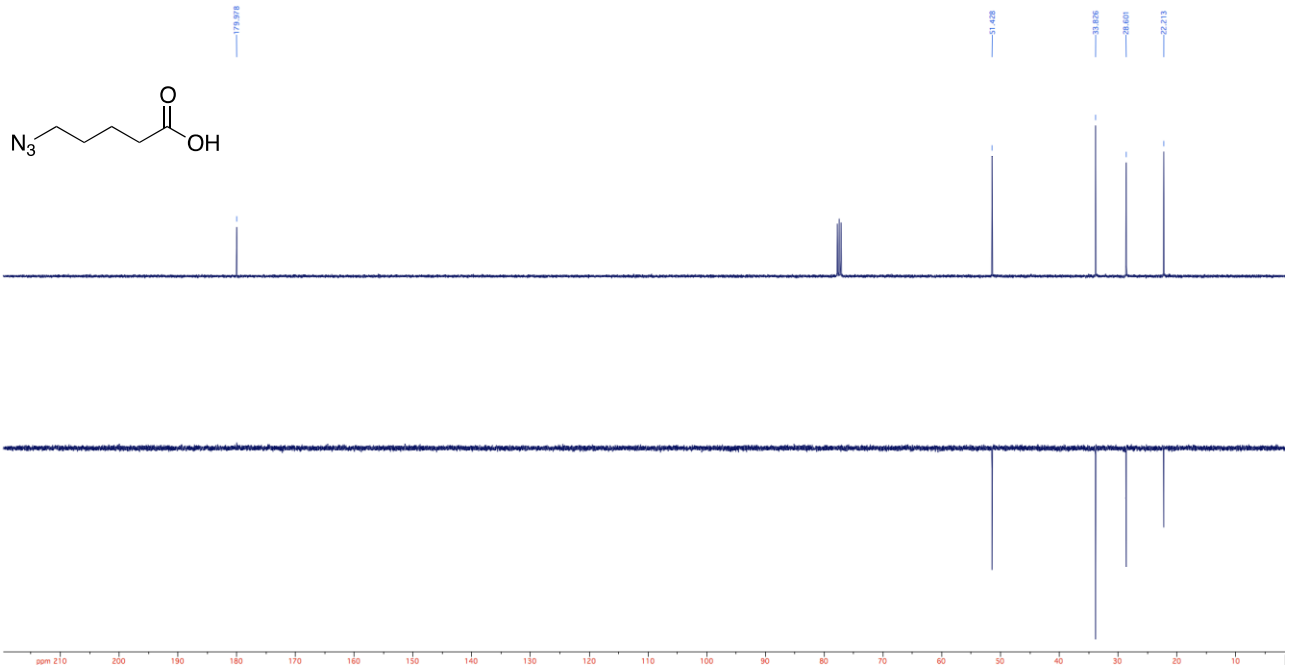

^{1}H NMR (400 MHz), ^{13}C NMR and DEPT 135 spectra of compound 66

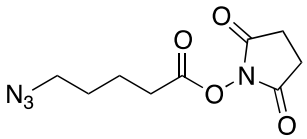

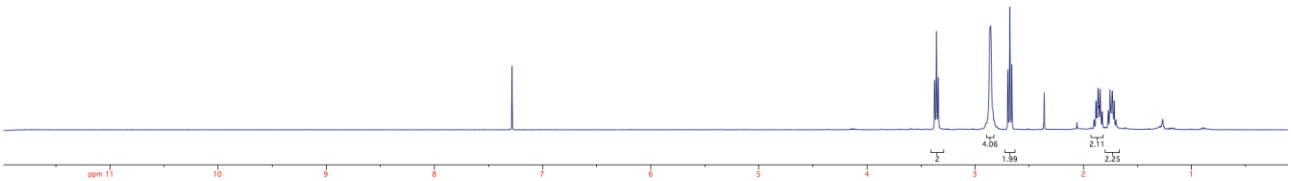

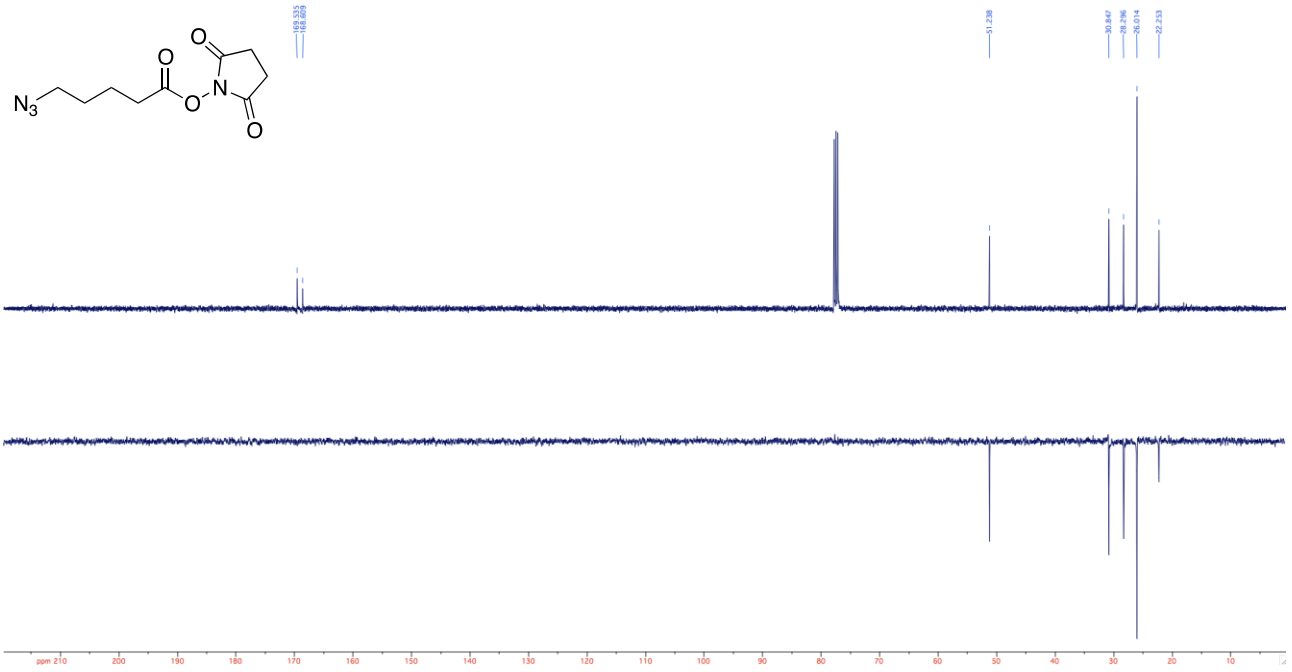

^{1}H NMR (400 MHz), ^{13}C NMR and DEPT 135 spectra of compound 71

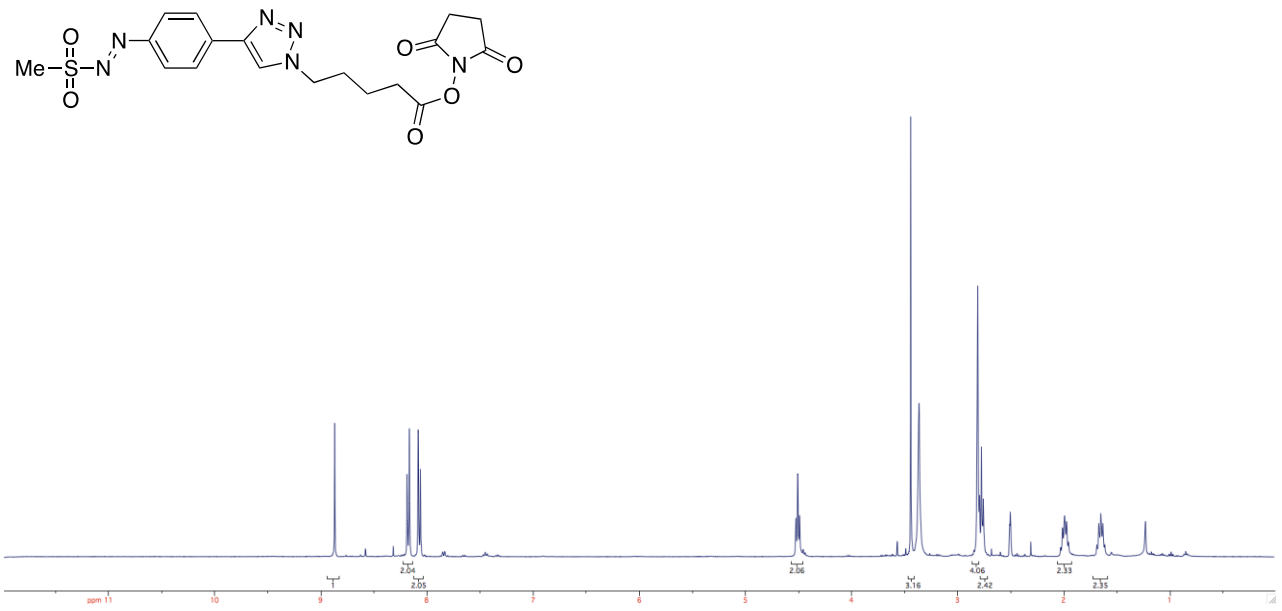

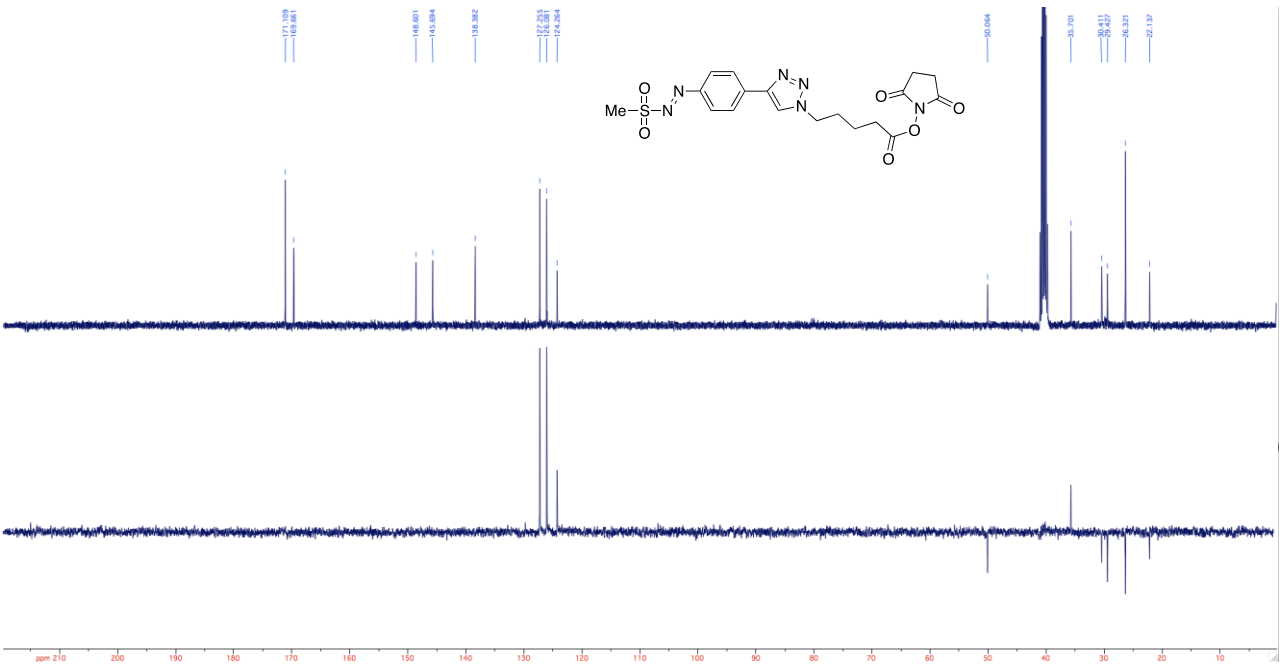

^{1}H NMR (400 MHz), ^{13}C NMR and DEPT 135 spectra of compound 72

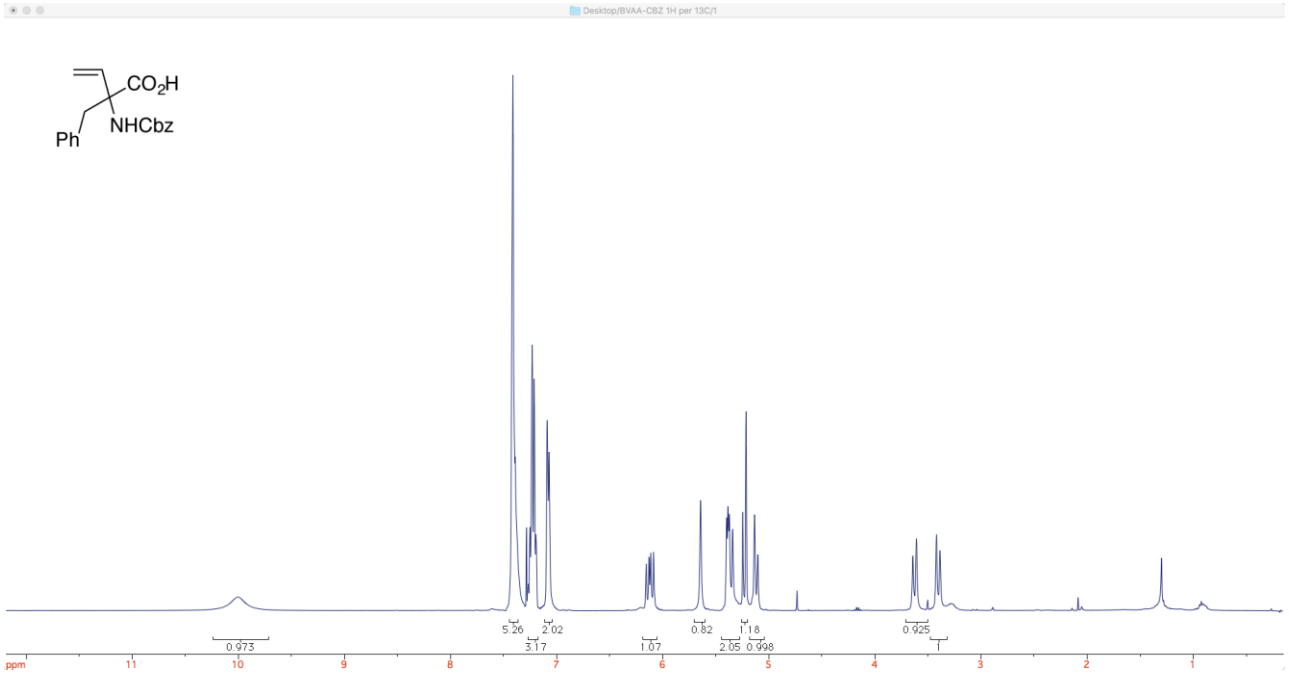

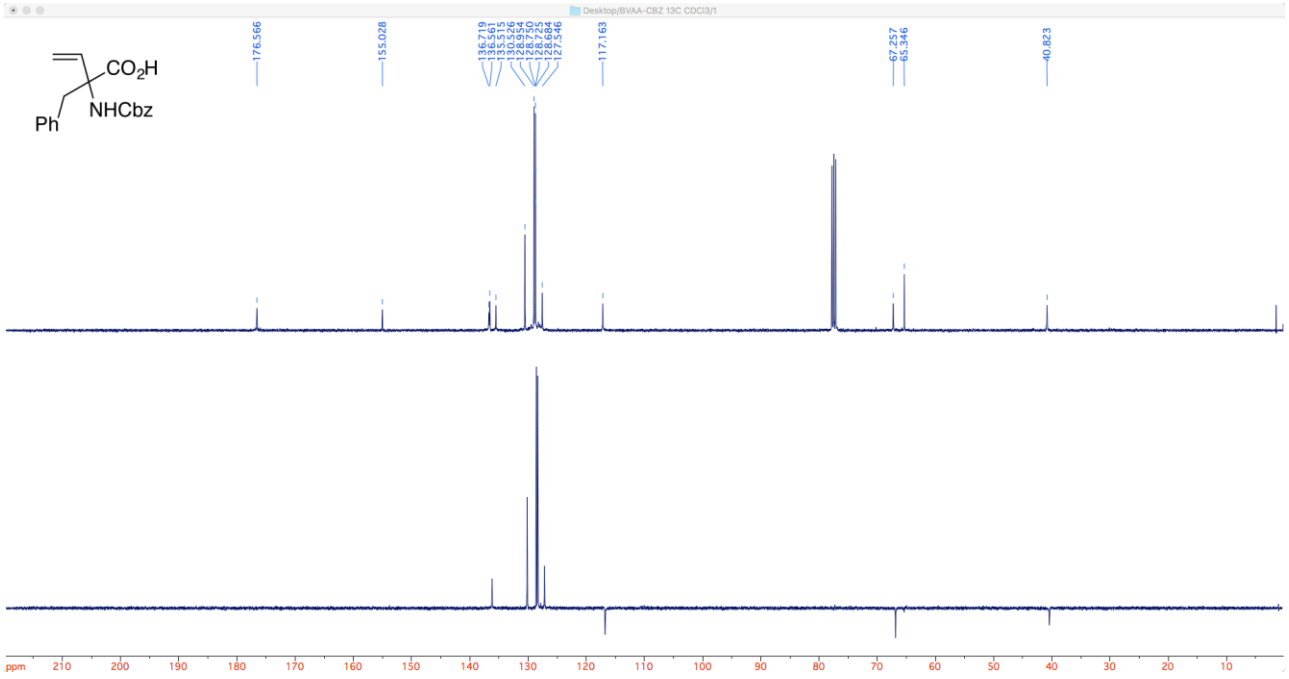

^{1}H NMR (400 MHz), ^{13}C NMR and DEPT 135 spectra of compound 73a

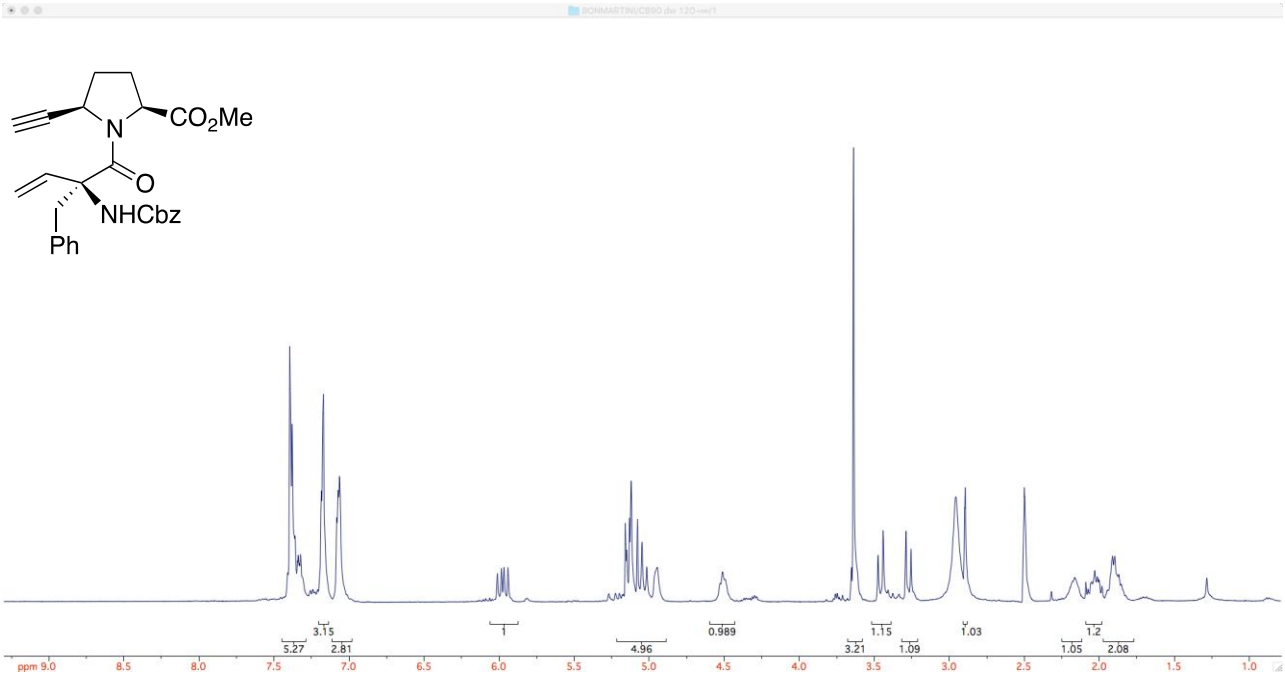

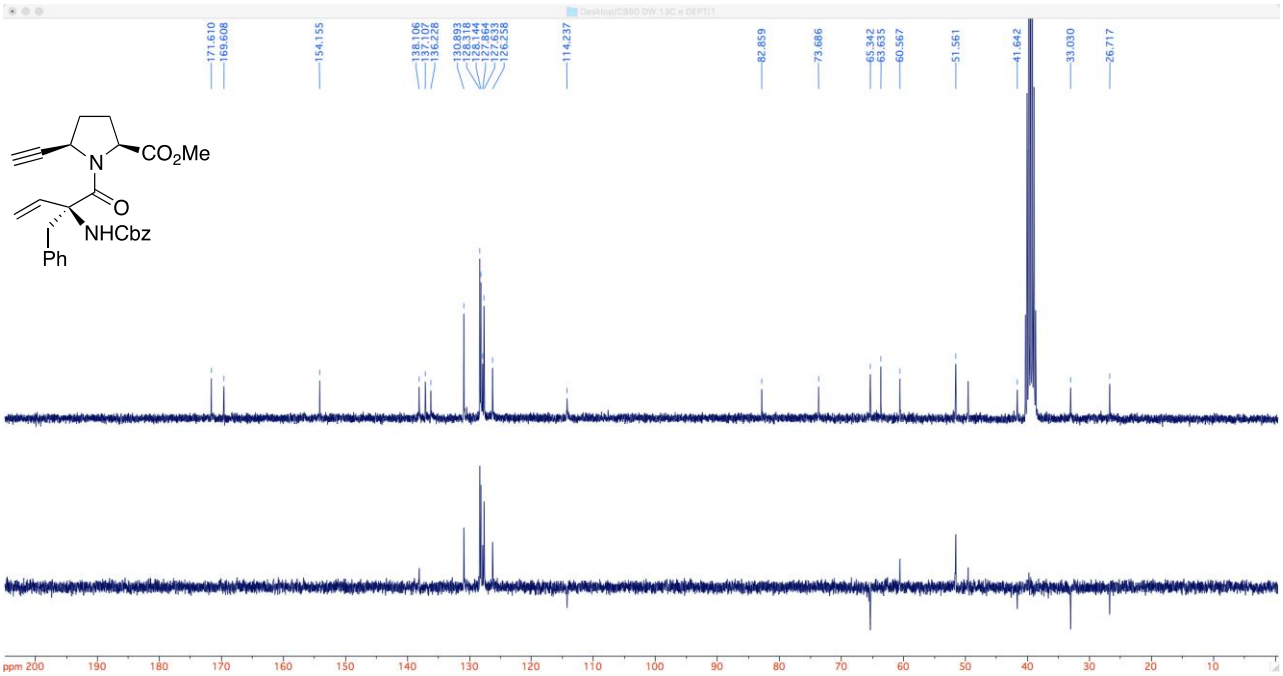

^{1}H NMR (400 MHz), ^{13}C NMR and DEPT 135 spectra of compound 73b

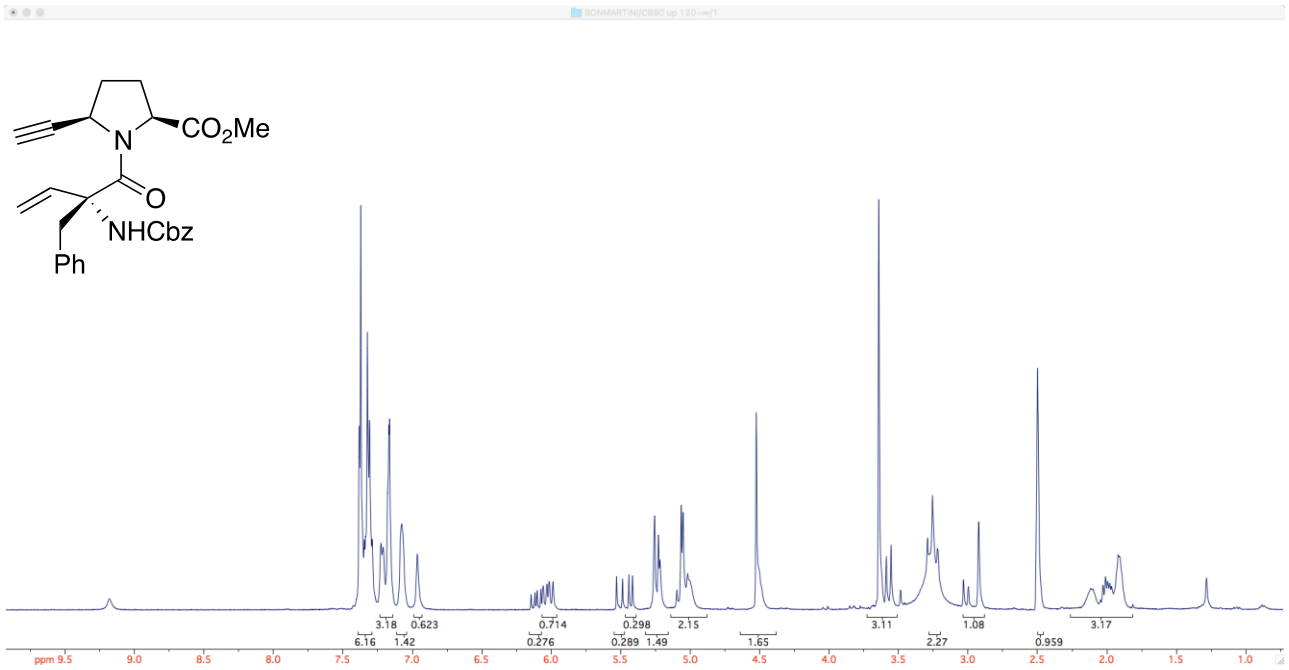

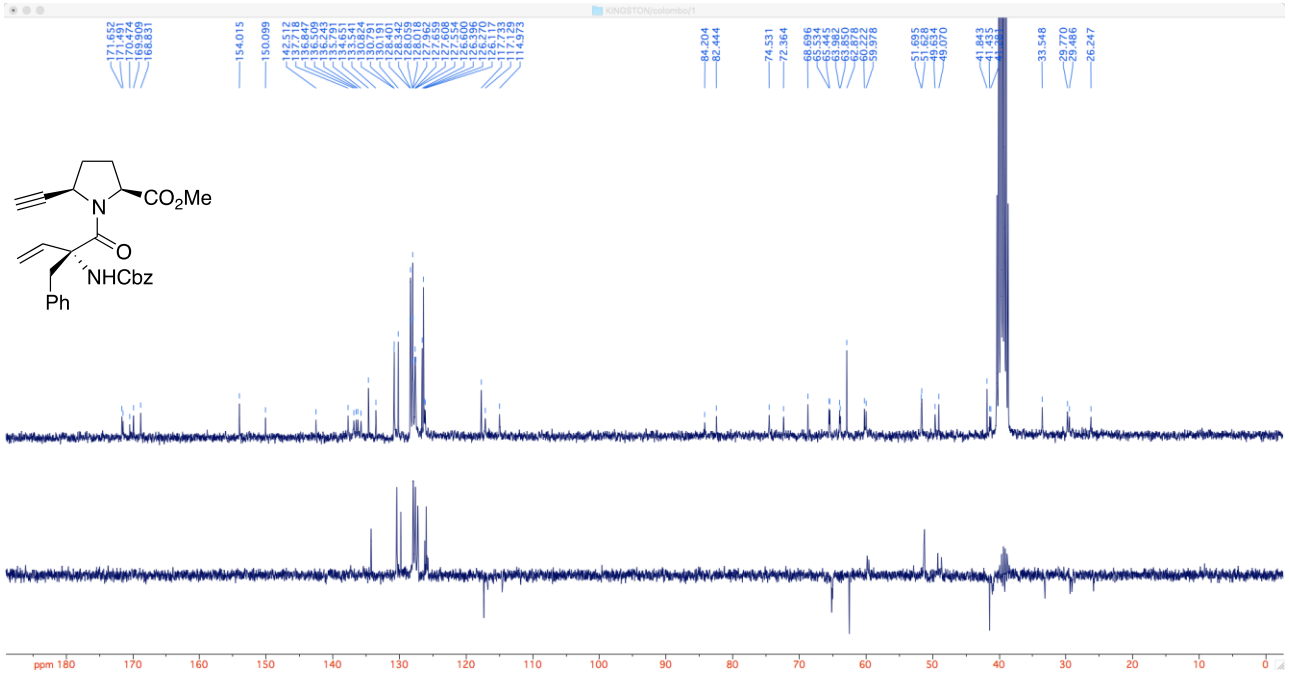

^{1}H NMR (400 MHz), ^{13}C NMR and DEPT 135 spectra of compound 75

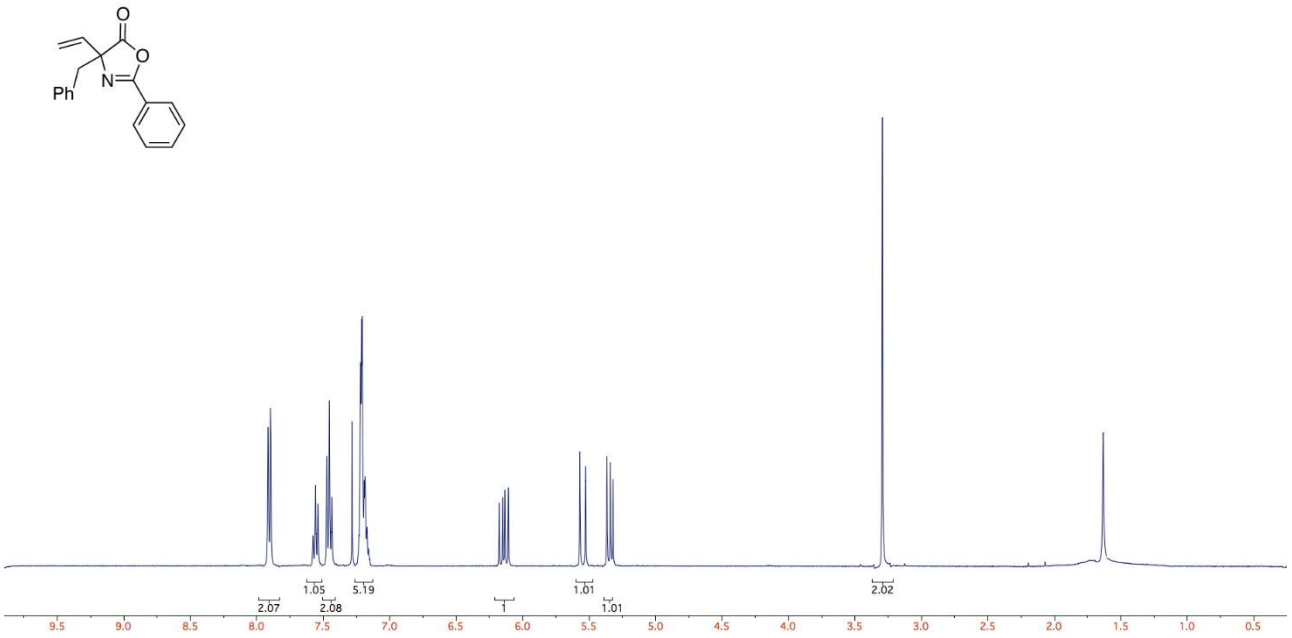

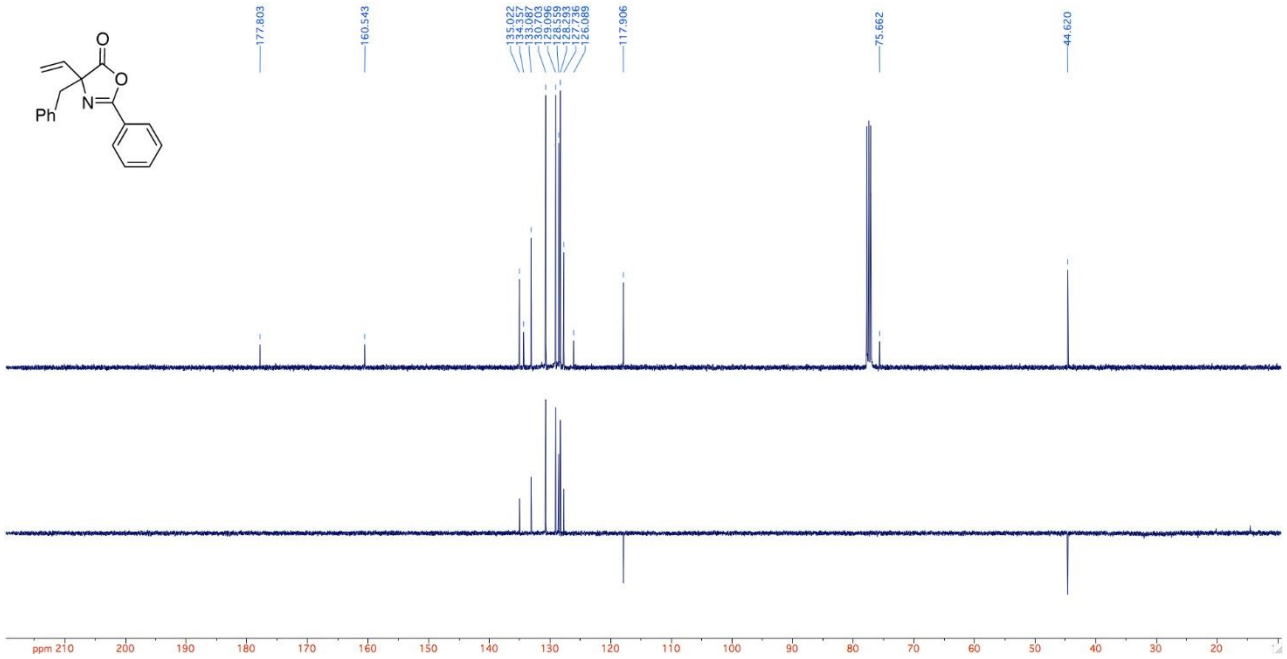

^{1}H NMR (400 MHz), ^{13}C NMR and DEPT 135 spectra of compound 77a

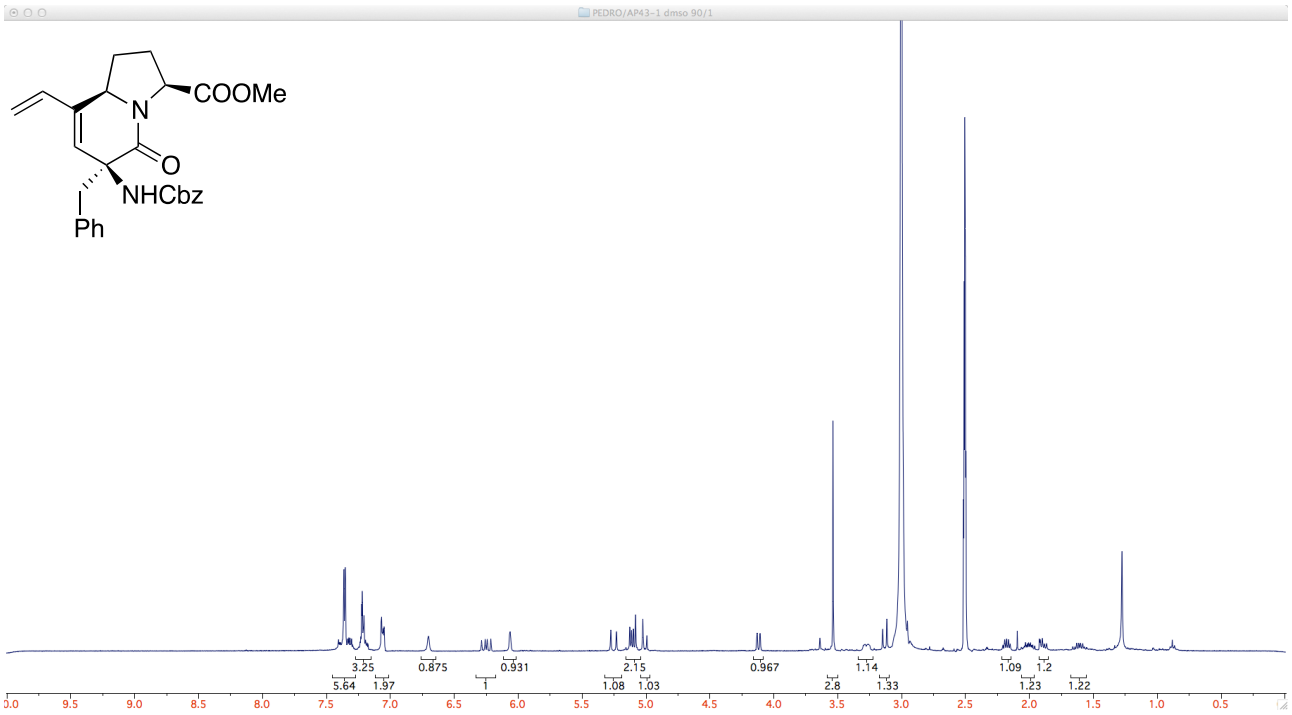

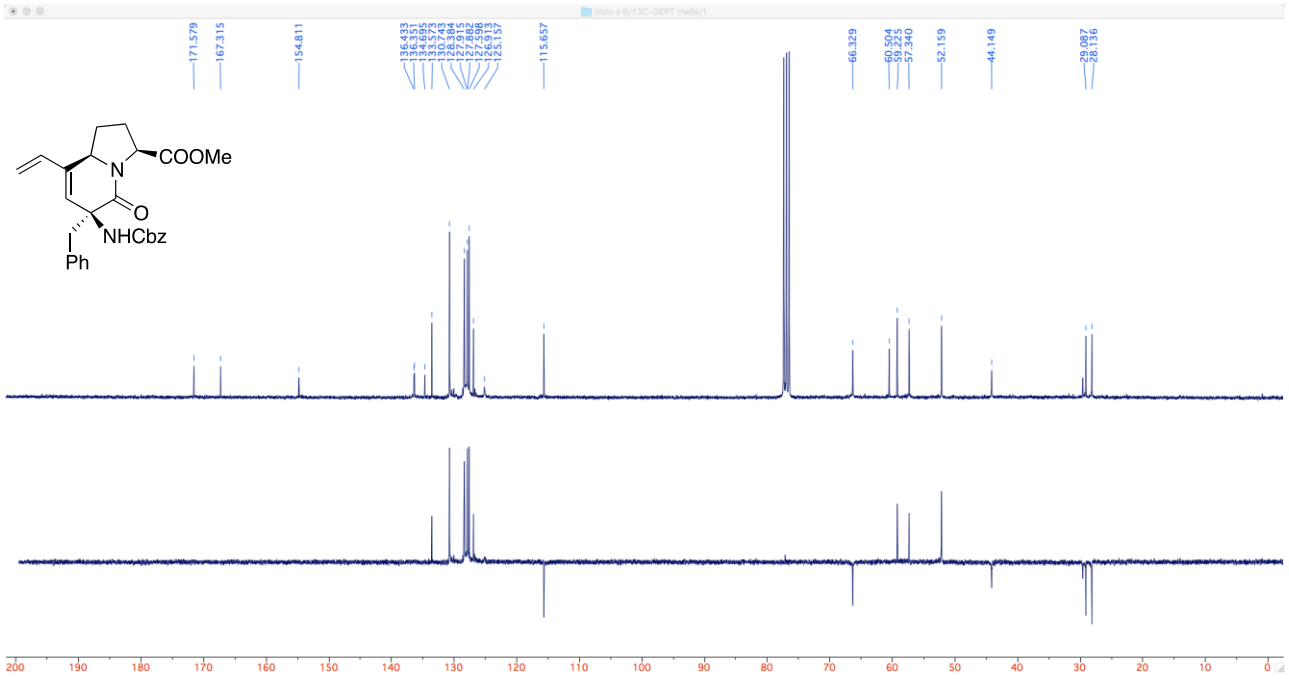

^{1}H NMR (400 MHz), ^{13}C NMR and DEPT 135 spectra of compound 77b

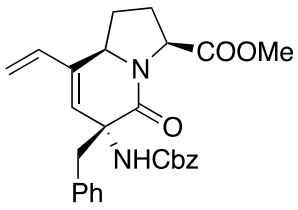

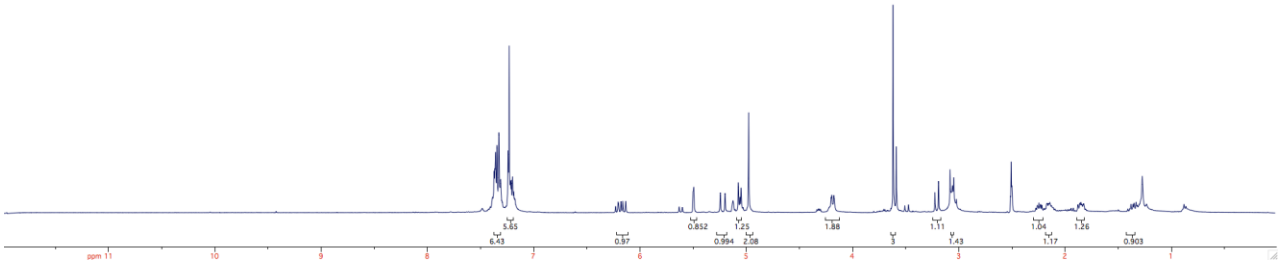

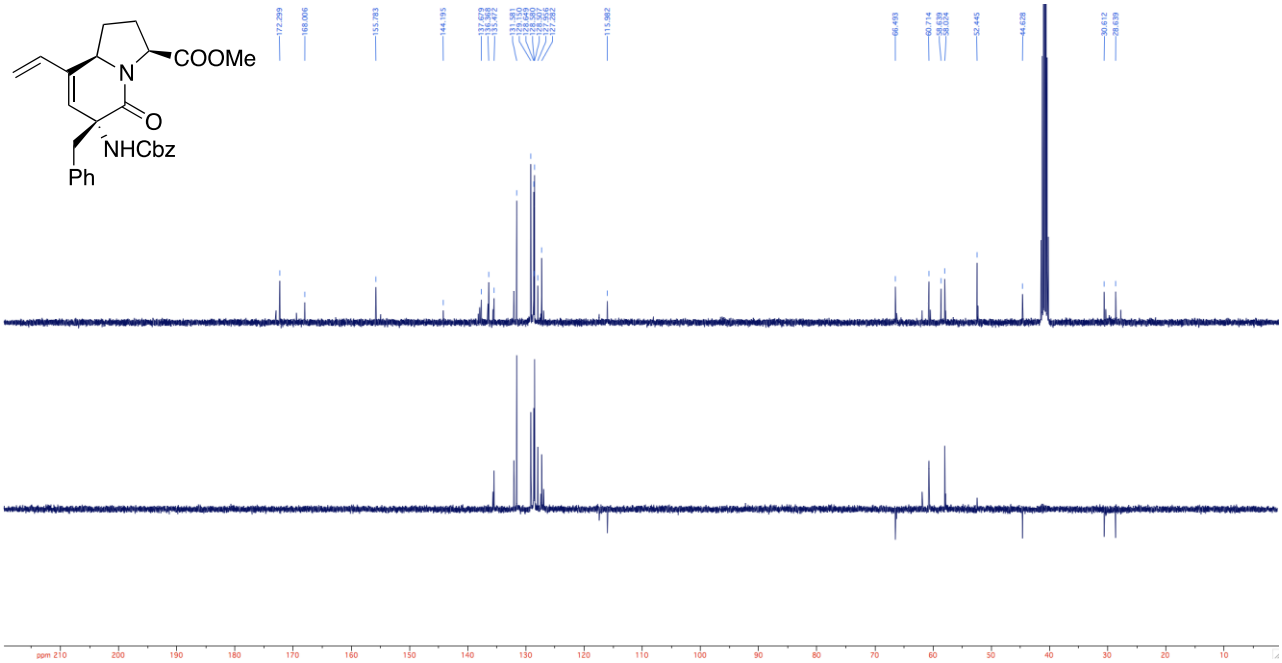

^{1}H NMR (400 MHz), ^{13}C NMR and DEPT 135 spectra of compound 79a

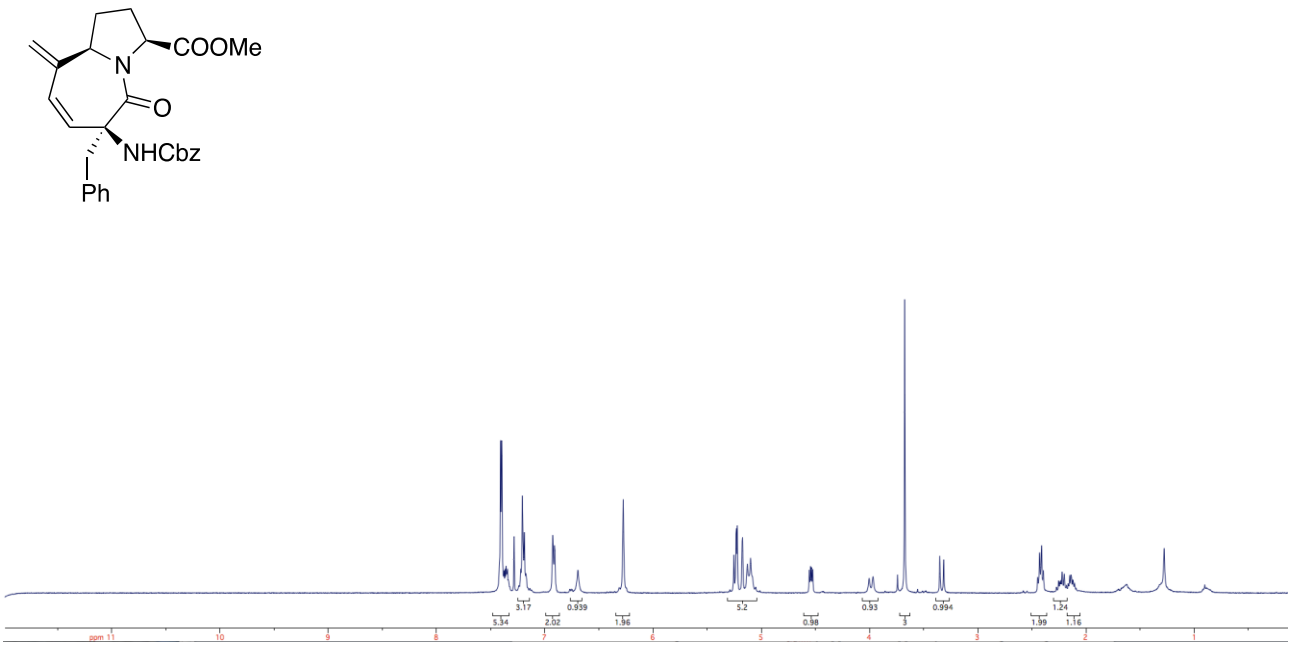

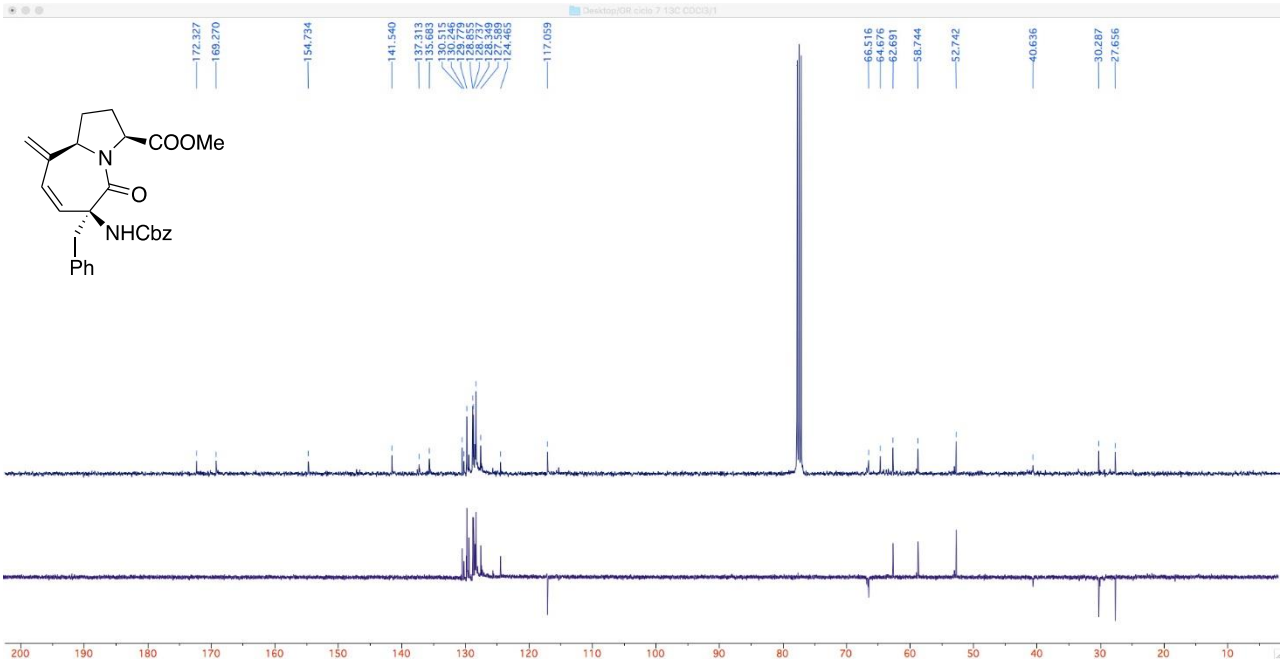

^{1}H NMR (400 MHz), ^{13}C NMR and DEPT 135 spectra of compound 79b

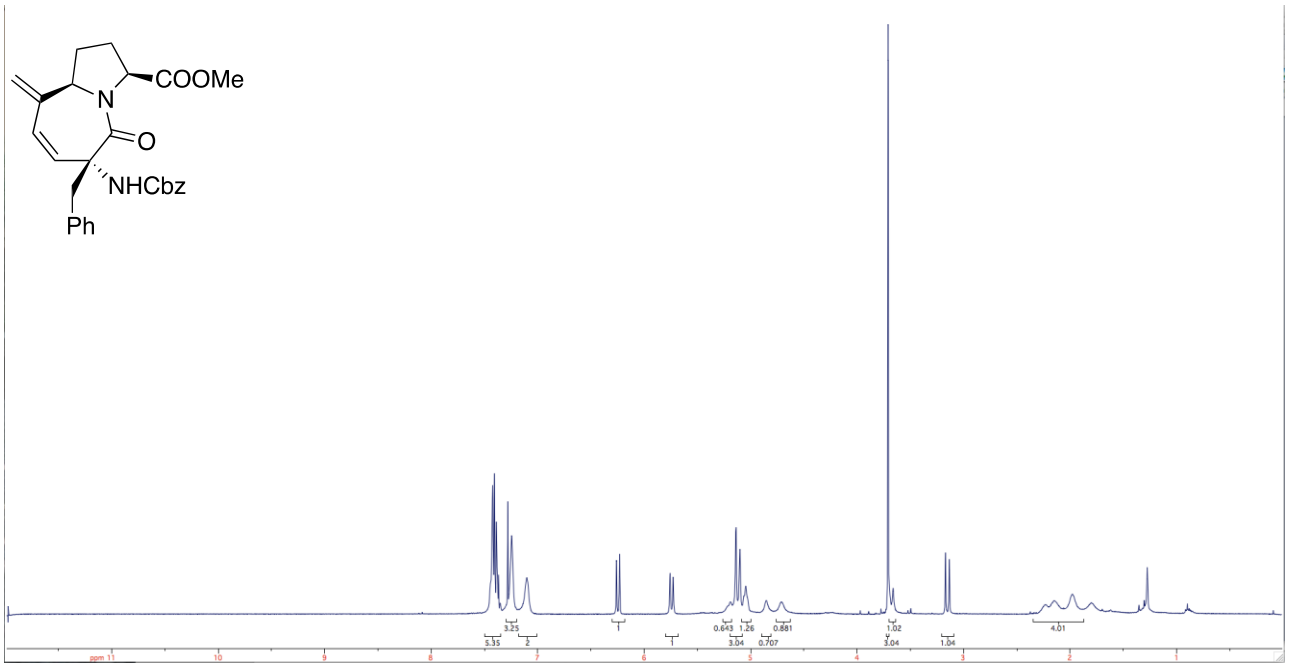

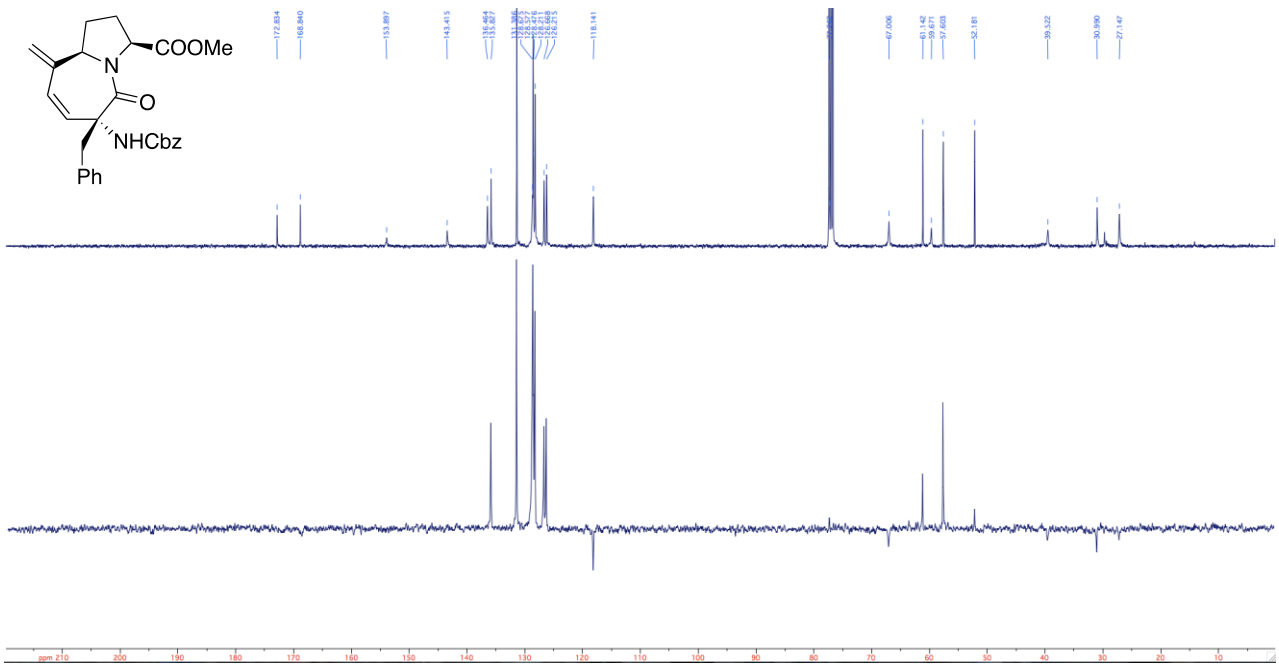

^{1}H NMR (400 MHz) spectra of compound 80a

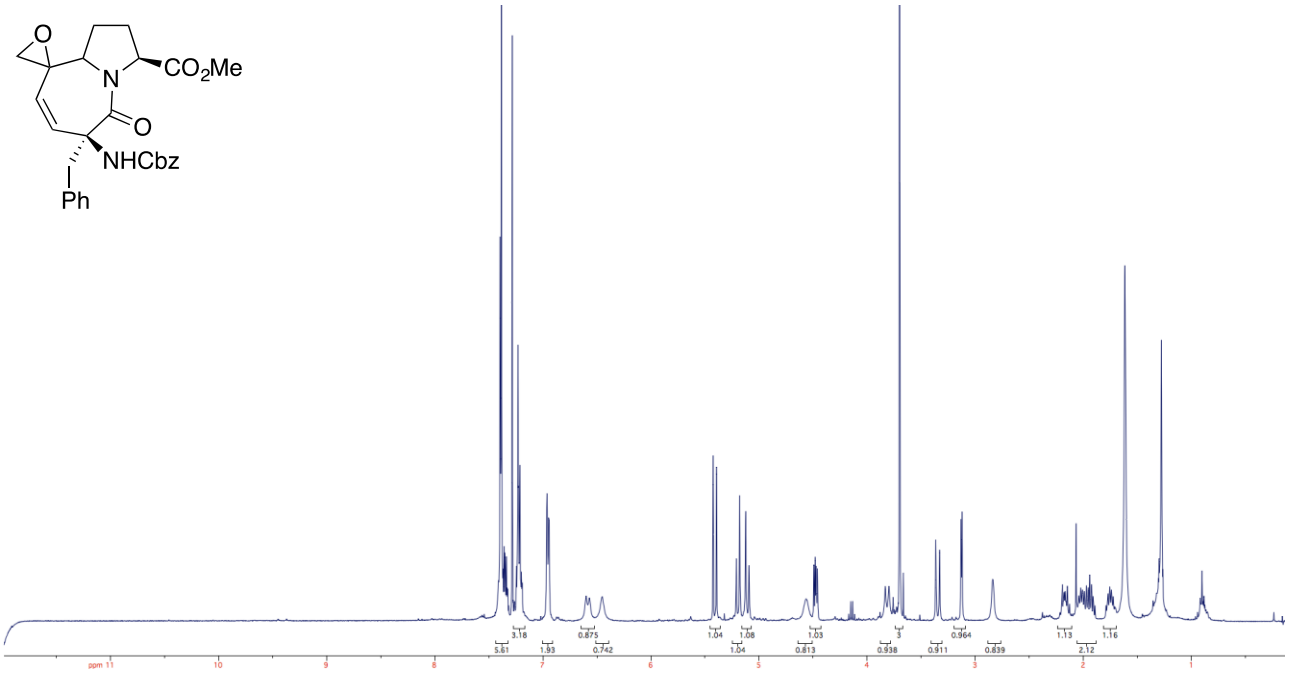

^{1}H NMR (400 MHz), ^{13}C NMR and DEPT 135 spectra of compound 80b

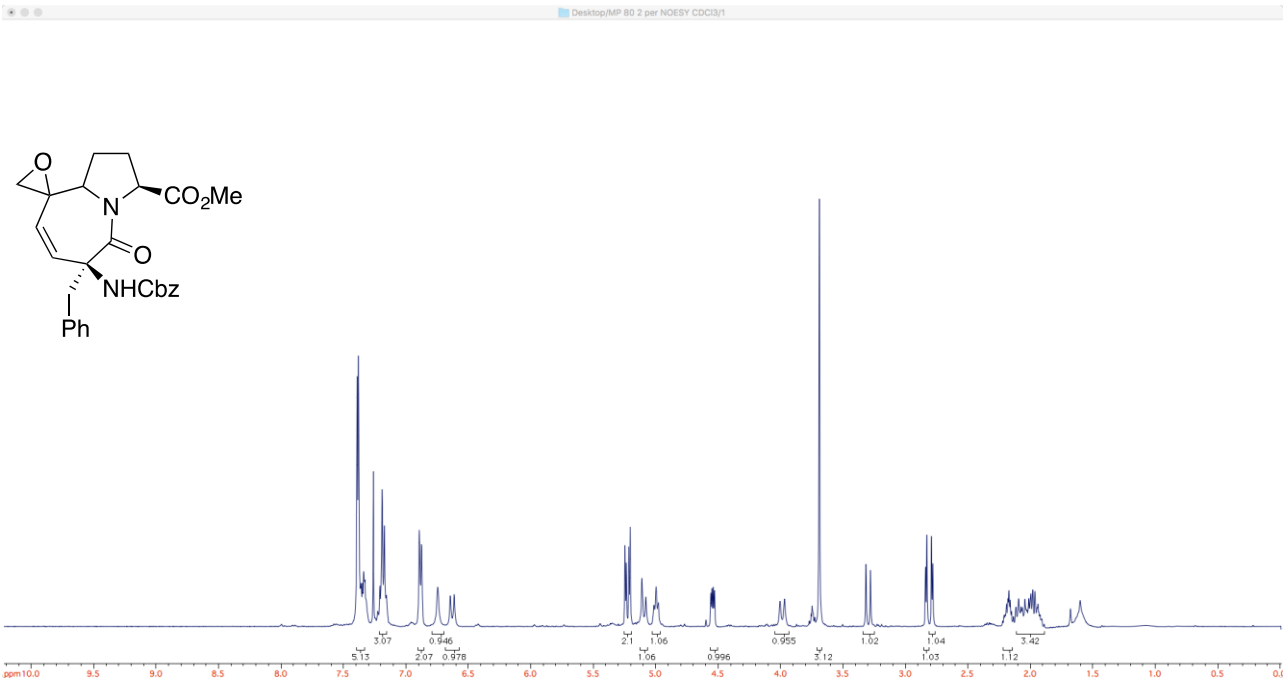

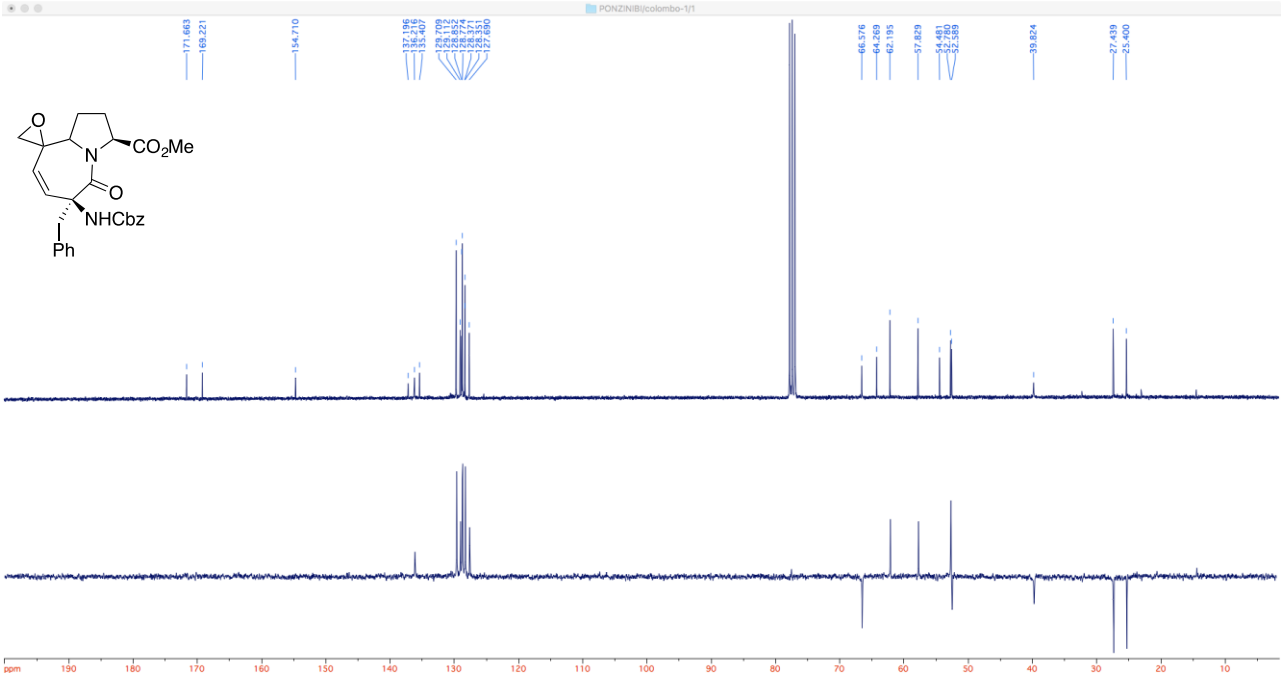

^{1}H NMR (400 MHz), ^{13}C NMR and DEPT 135 spectra of compound 81

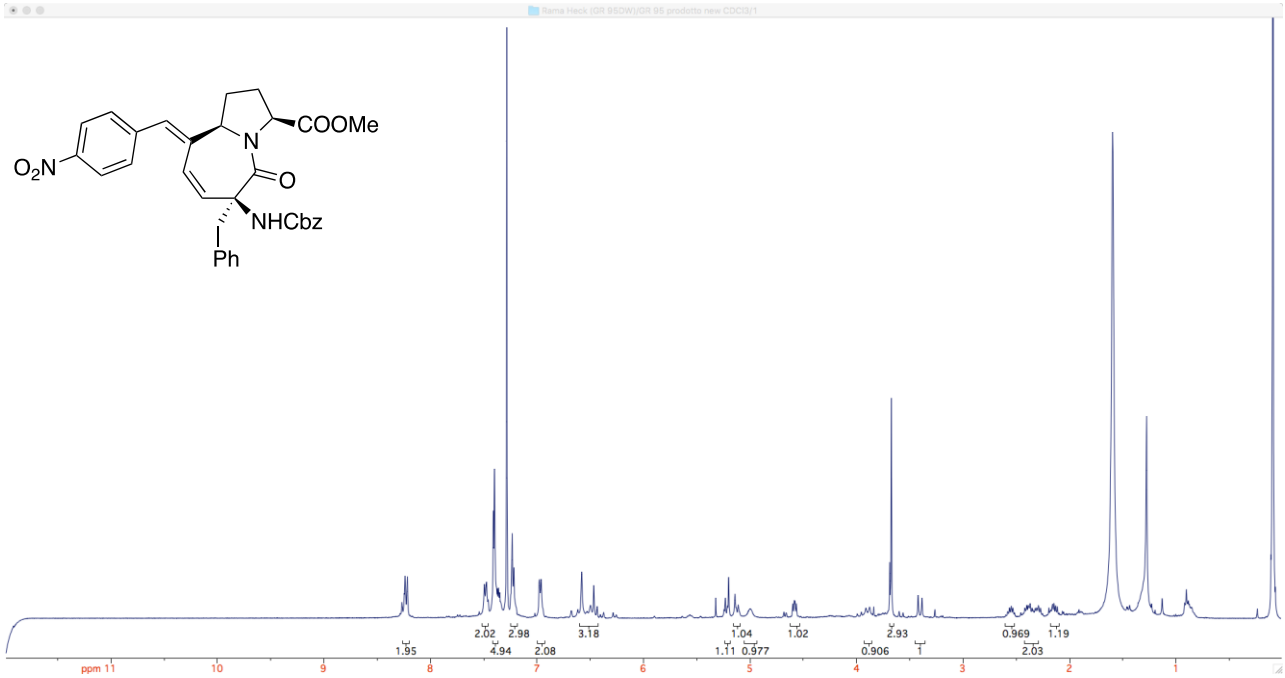

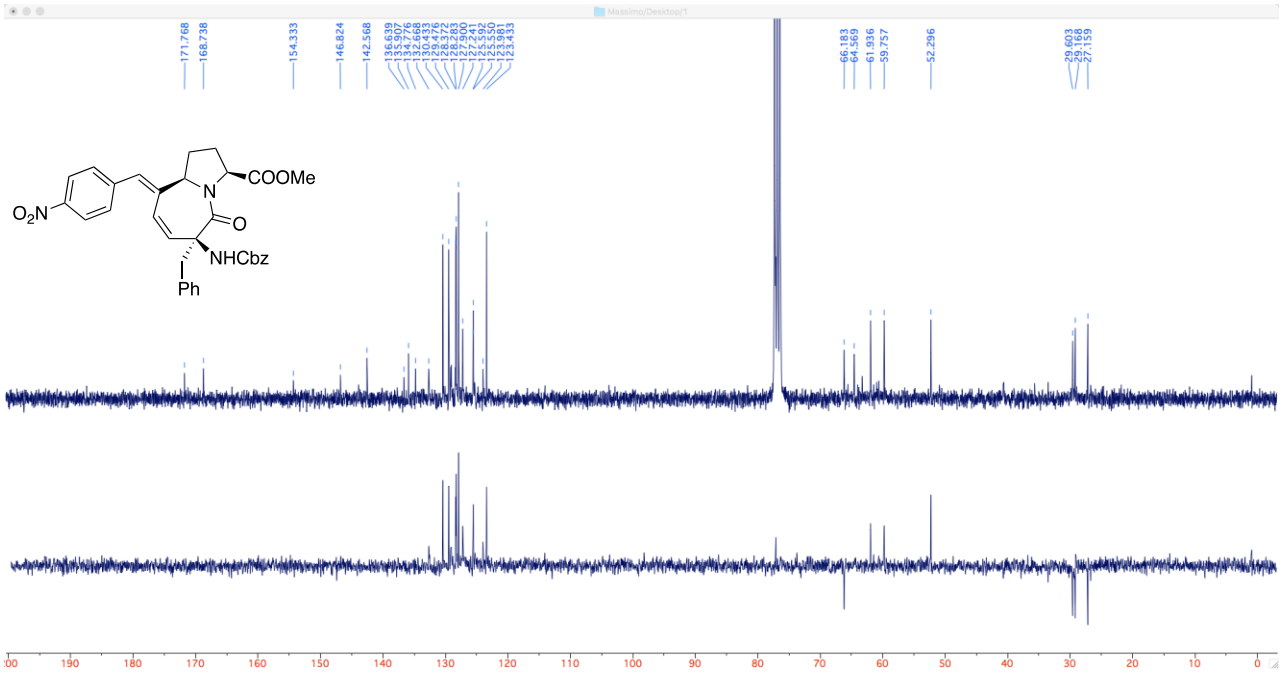

^{1}H NMR (400 MHz), 2D-NOESY spectra of compound 81

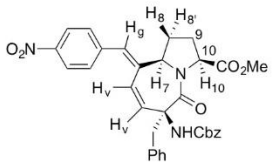

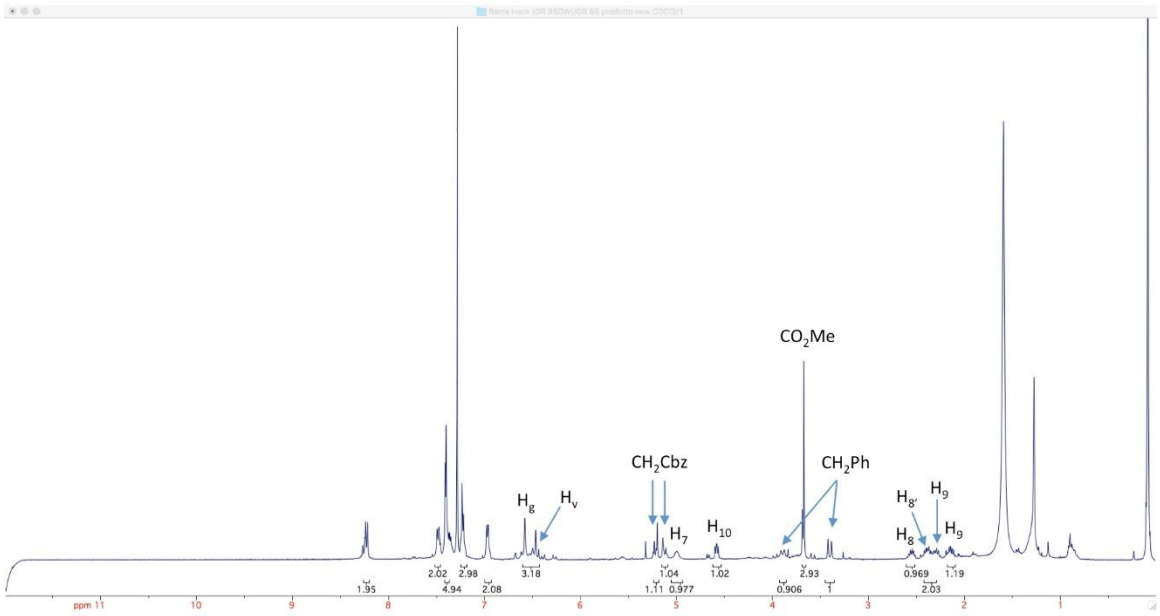

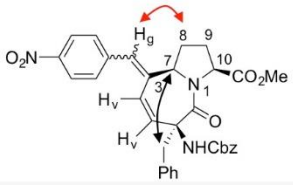

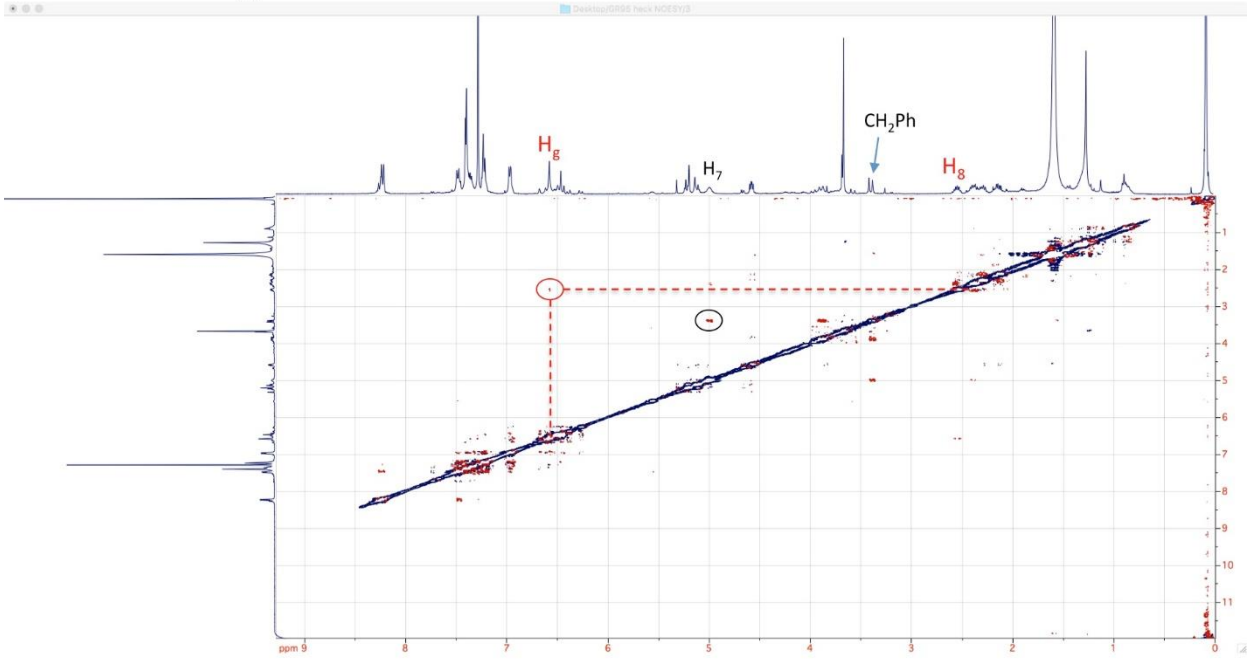

^{1}H NMR (400 MHz), ^{13}C NMR and DEPT 135 spectra of compound 82

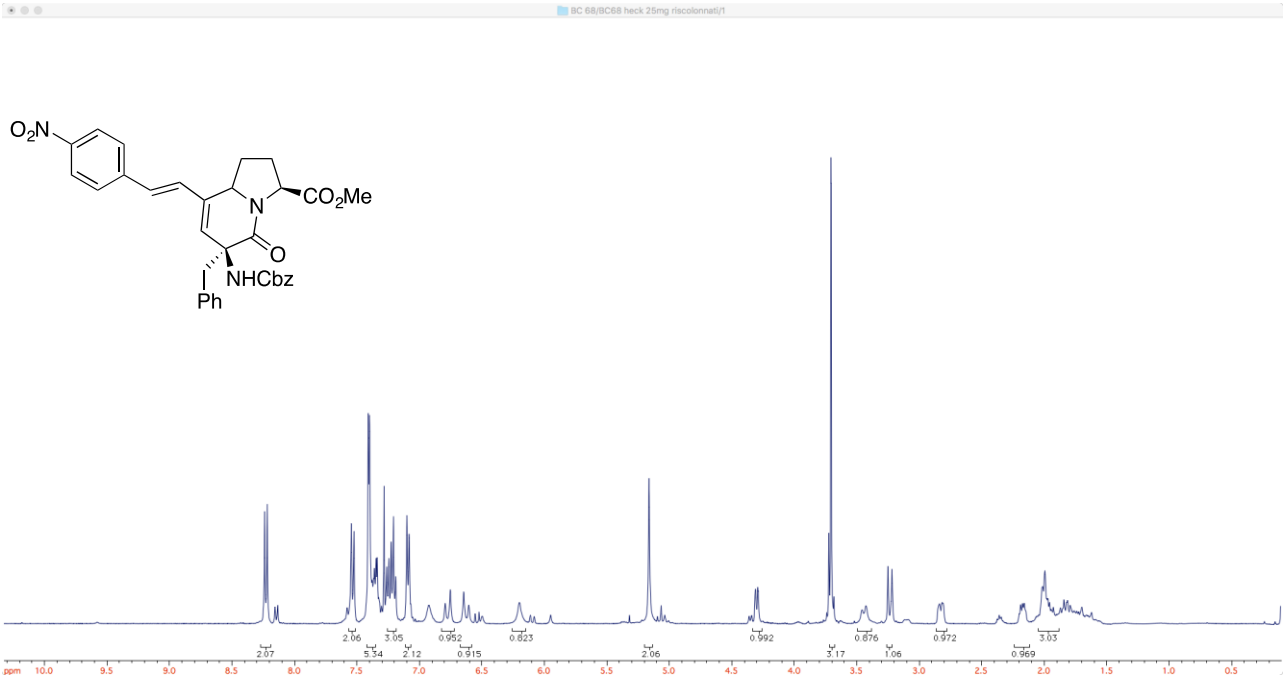

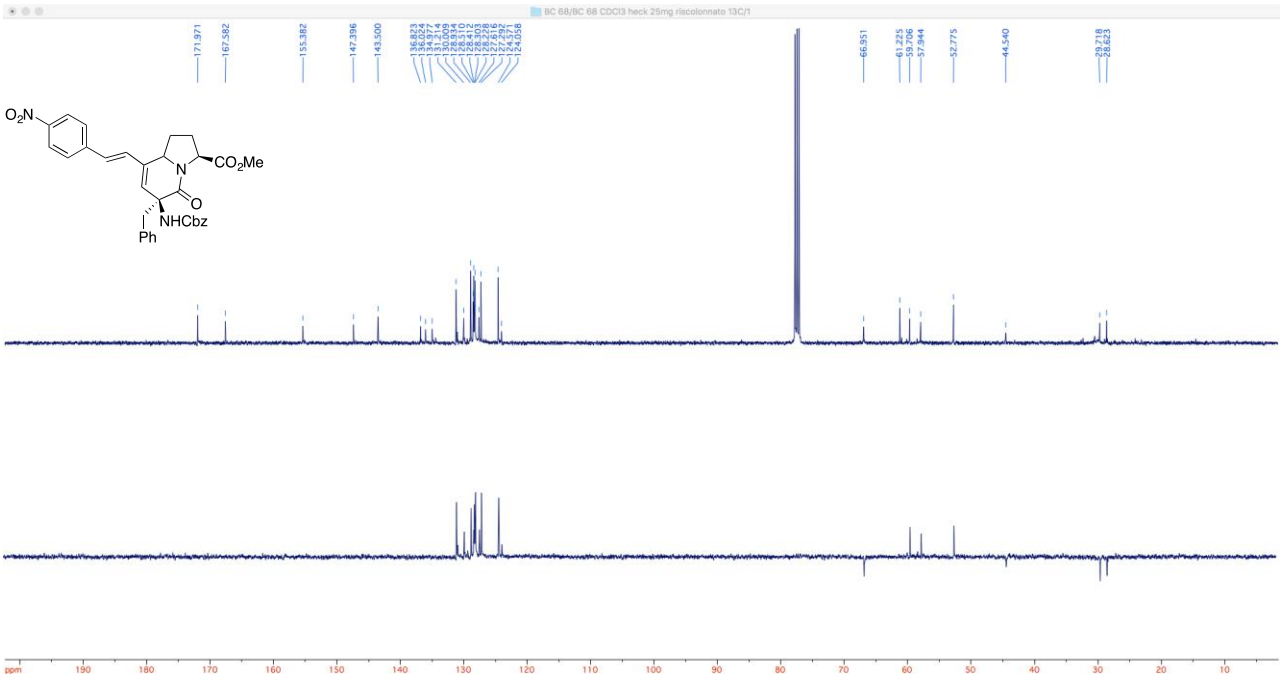

^{1}H NMR (400 MHz), ^{13}C NMR and DEPT 135 spectra of compound 83

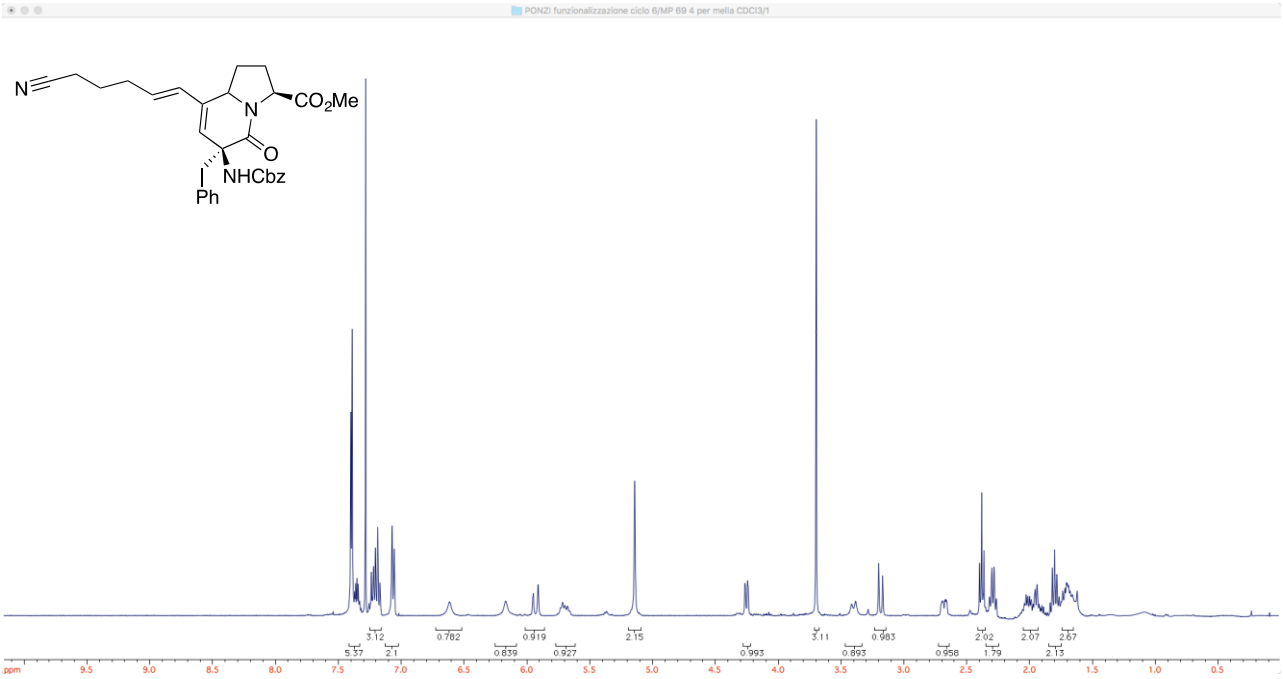

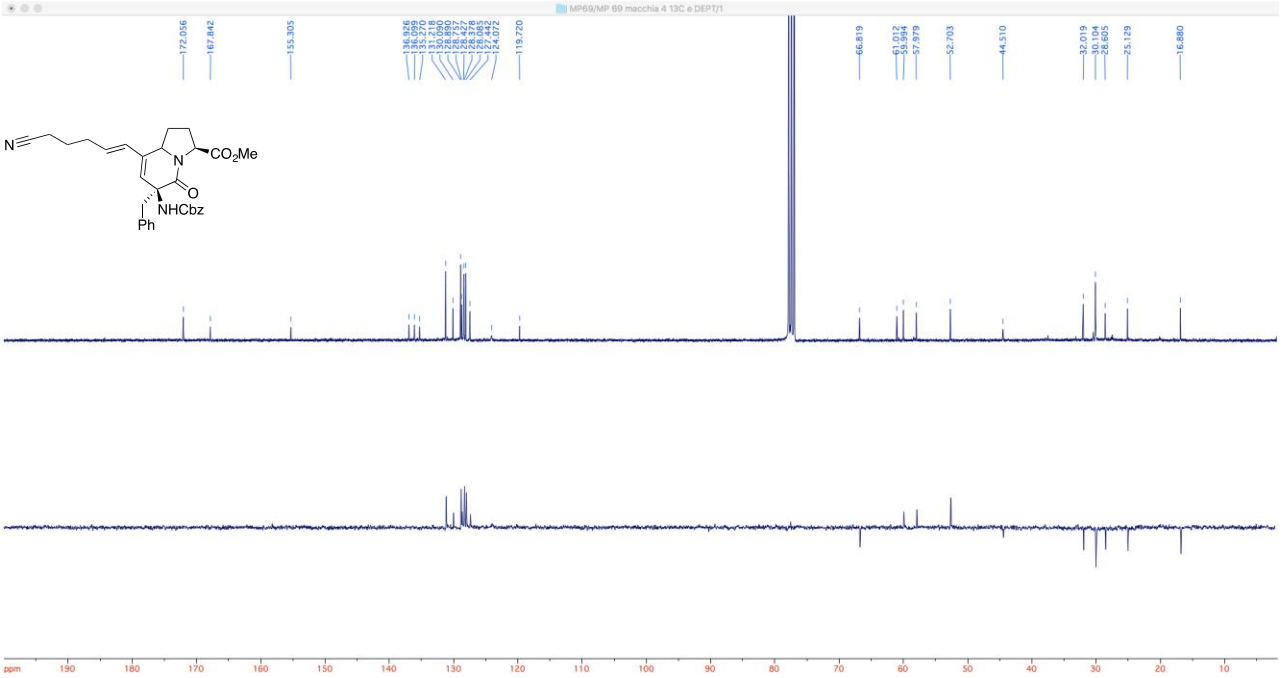

^{1}H NMR (400 MHz), ^{13}C NMR and DEPT 135 spectra of compound 96

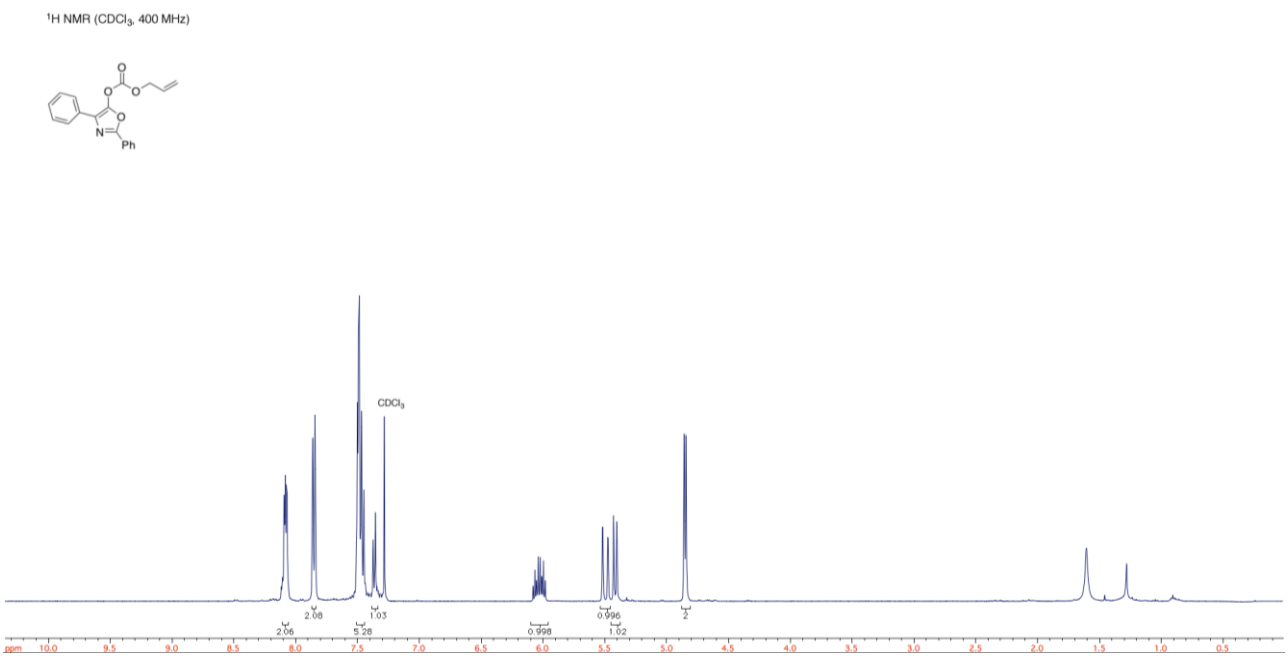

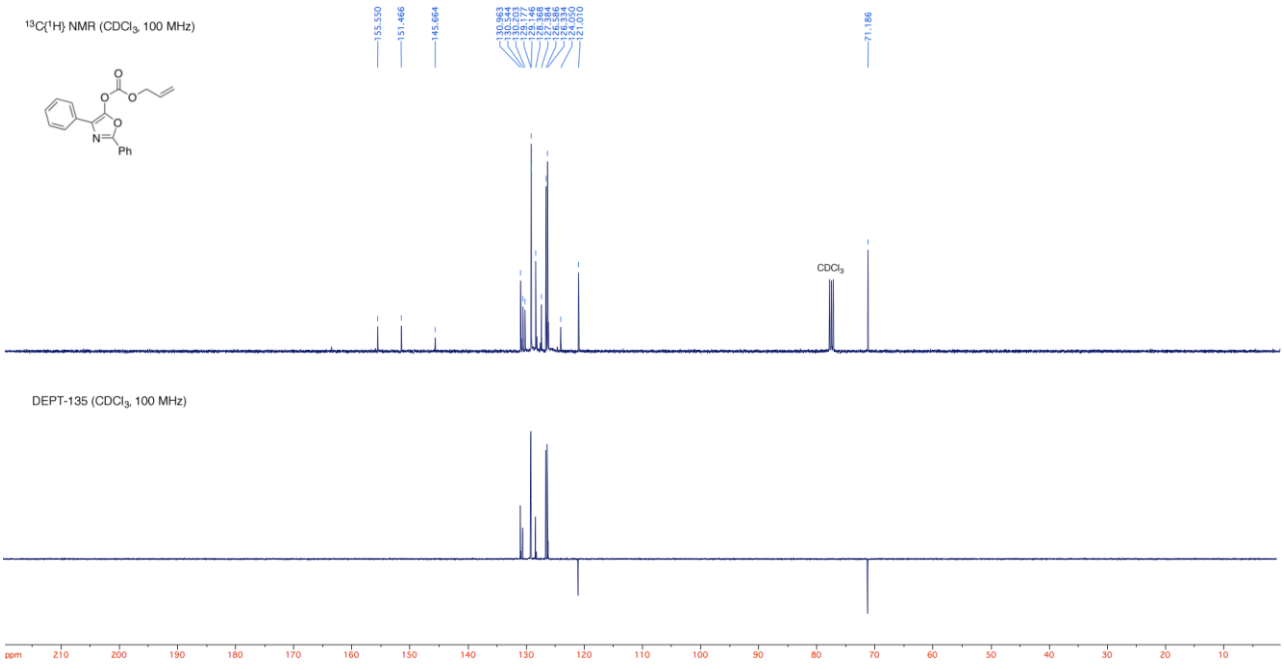

^{1}H NMR (400 MHz), ^{13}C NMR and DEPT 135 spectra of compound 97

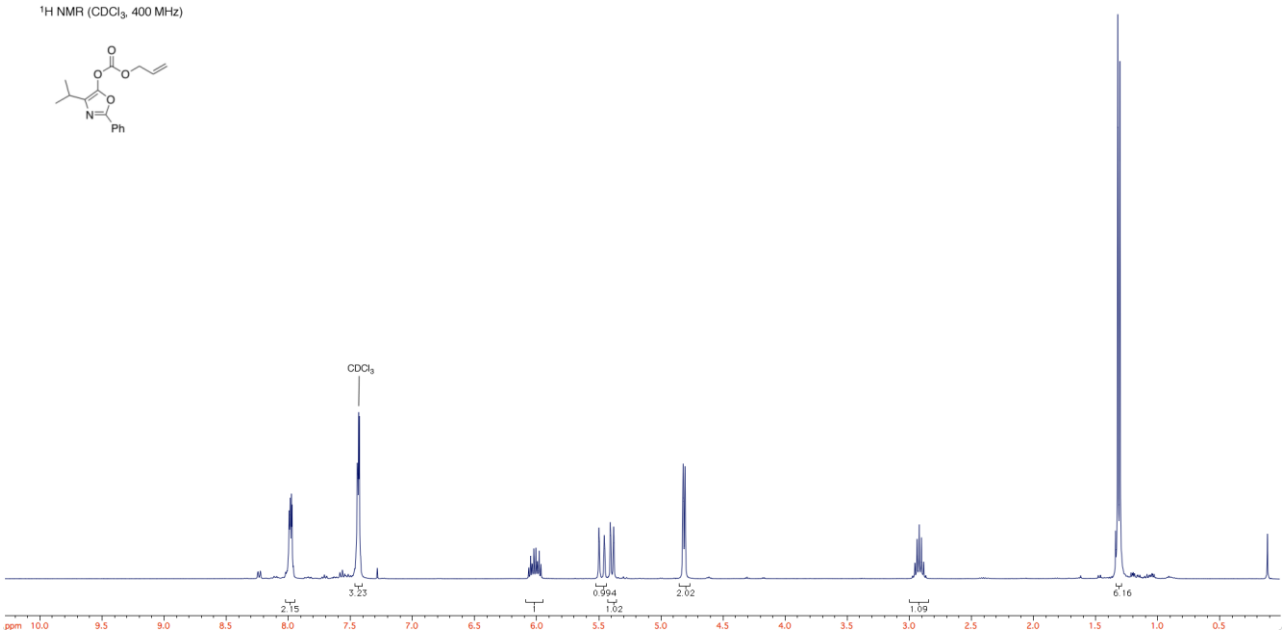

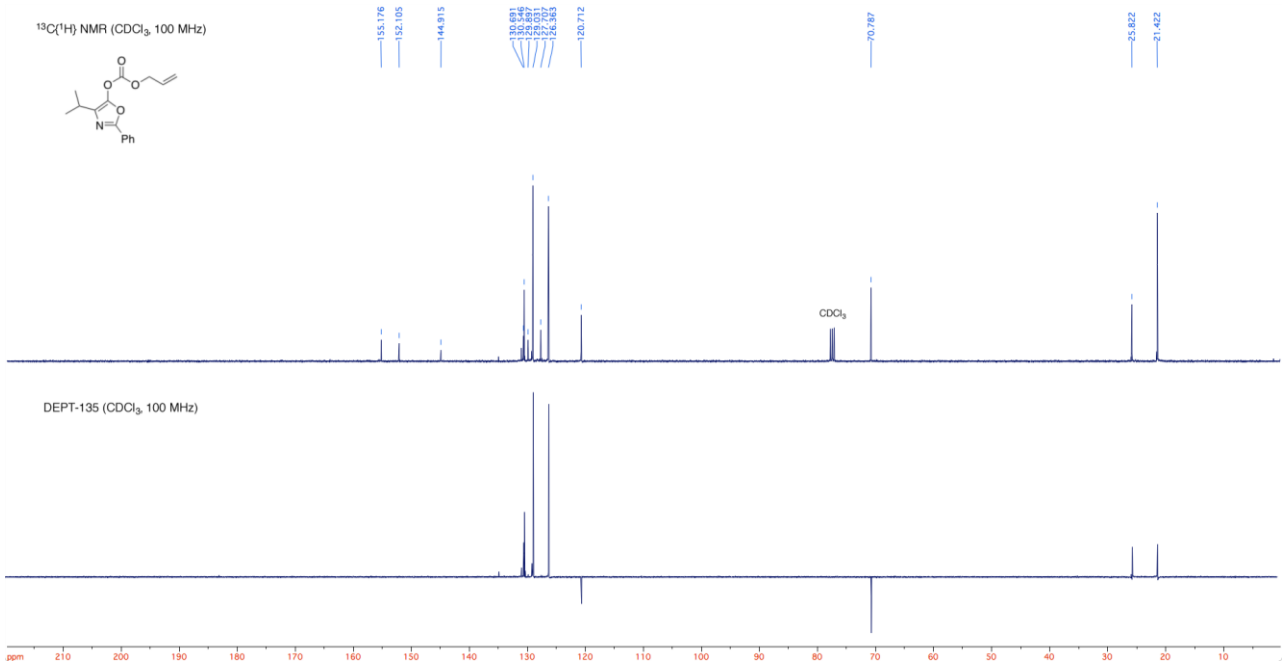

^{1}H NMR (400 MHz), ^{13}C NMR and DEPT 135 spectra of compound 98

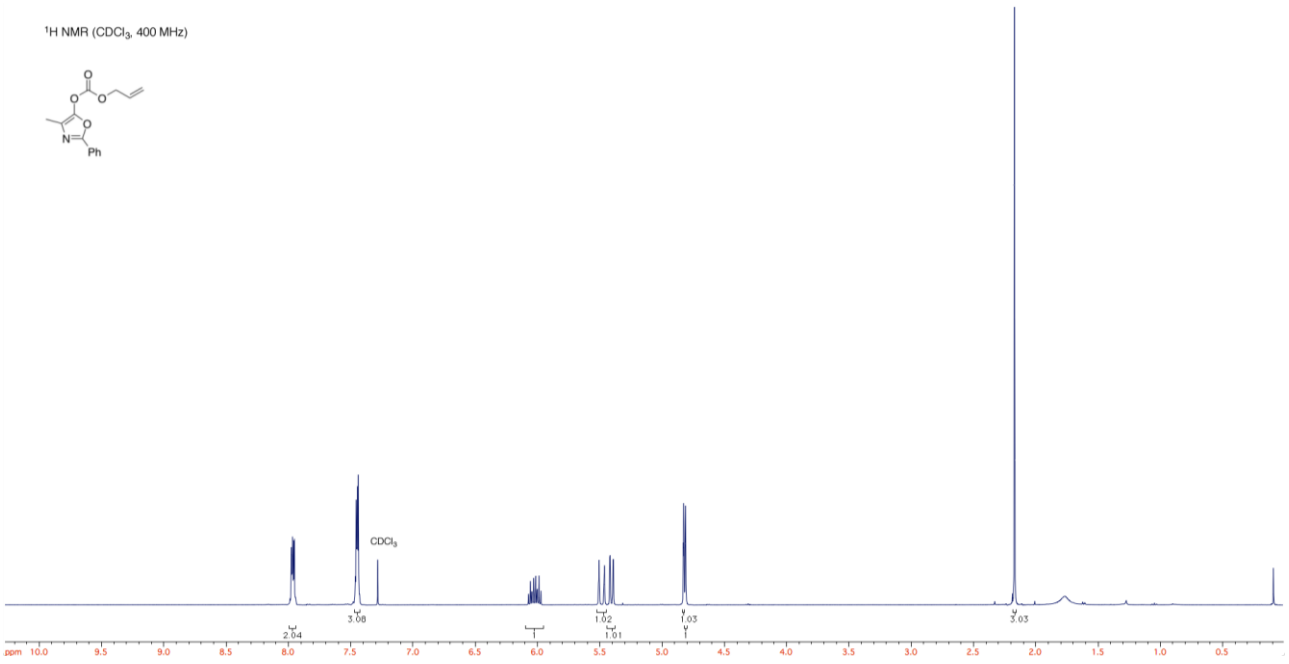

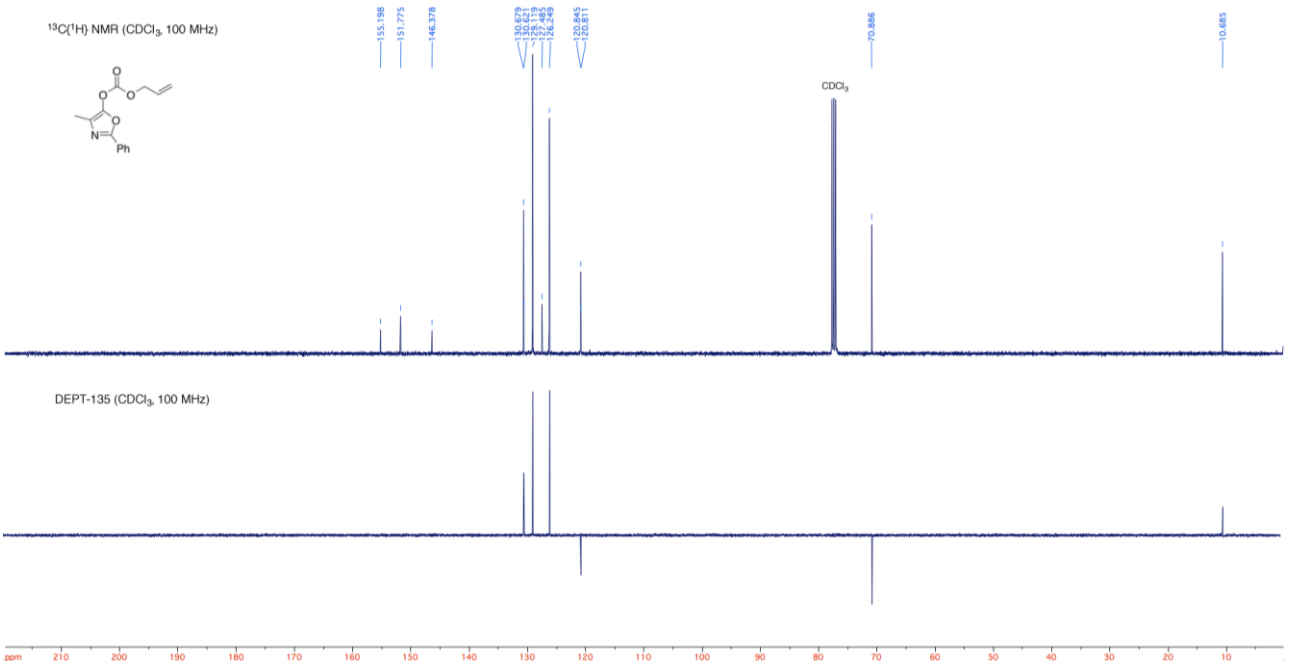

^{1}H NMR (400 MHz), ^{13}C NMR and DEPT 135 spectra of compound 99

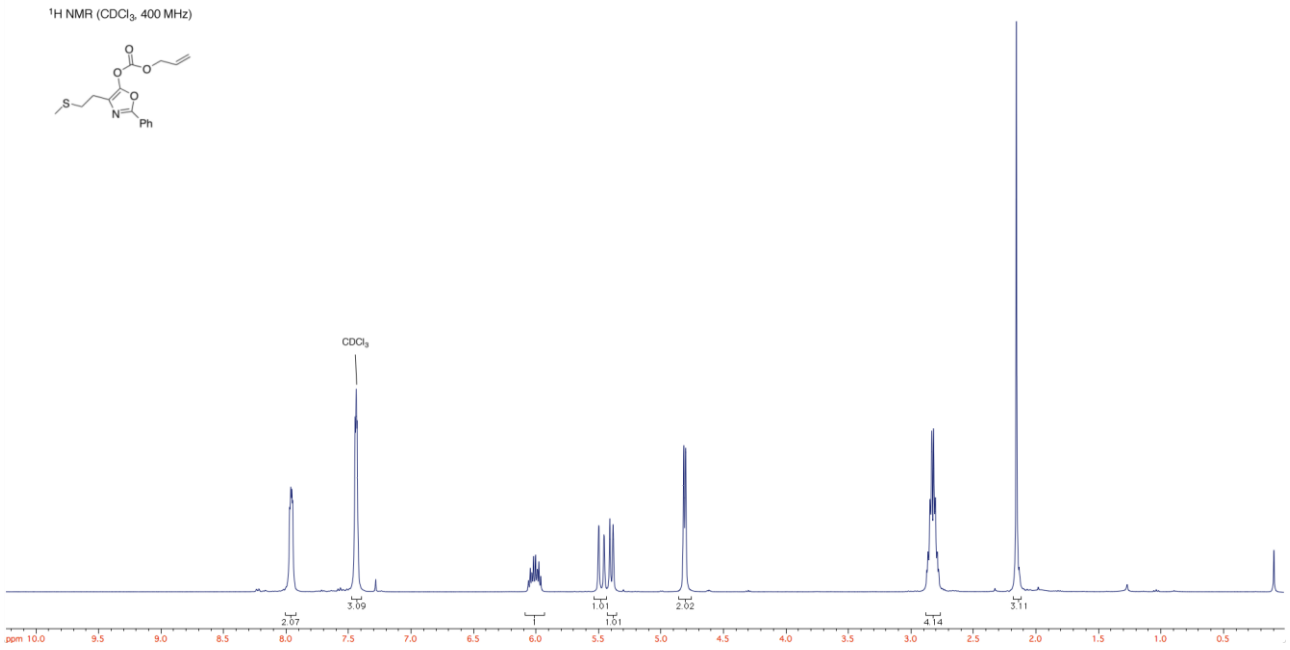

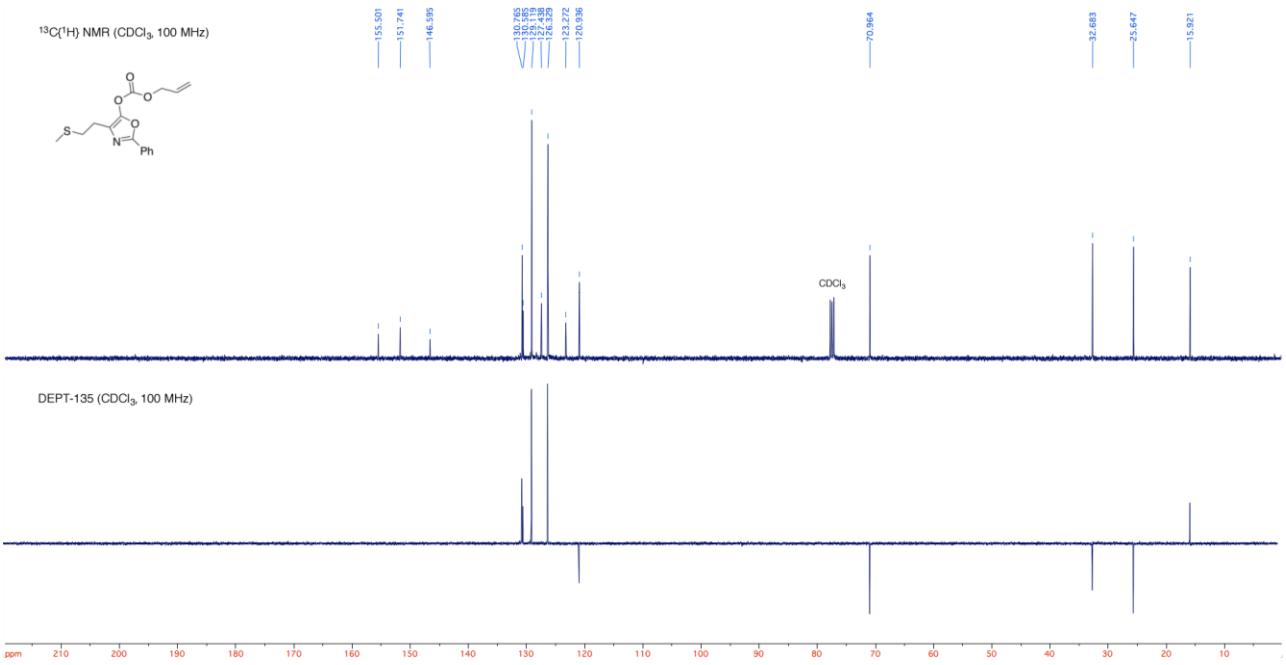

^{1}H NMR (400 MHz), ^{13}C NMR and DEPT 135 spectra of compound 100

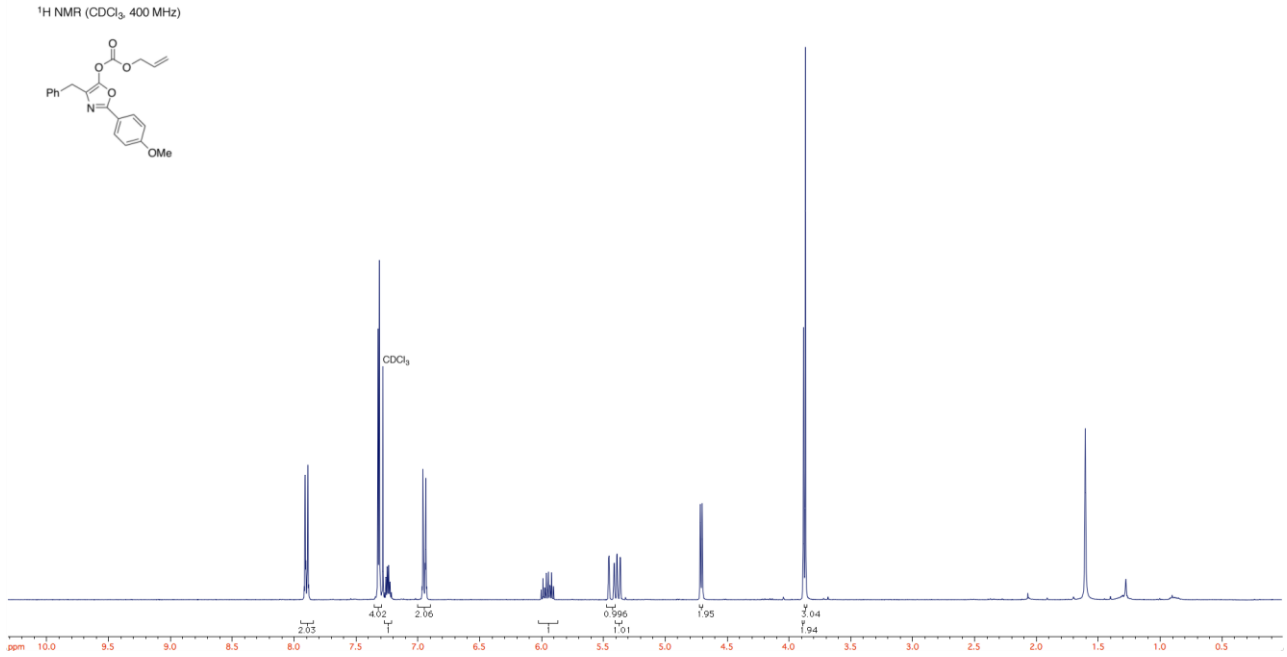

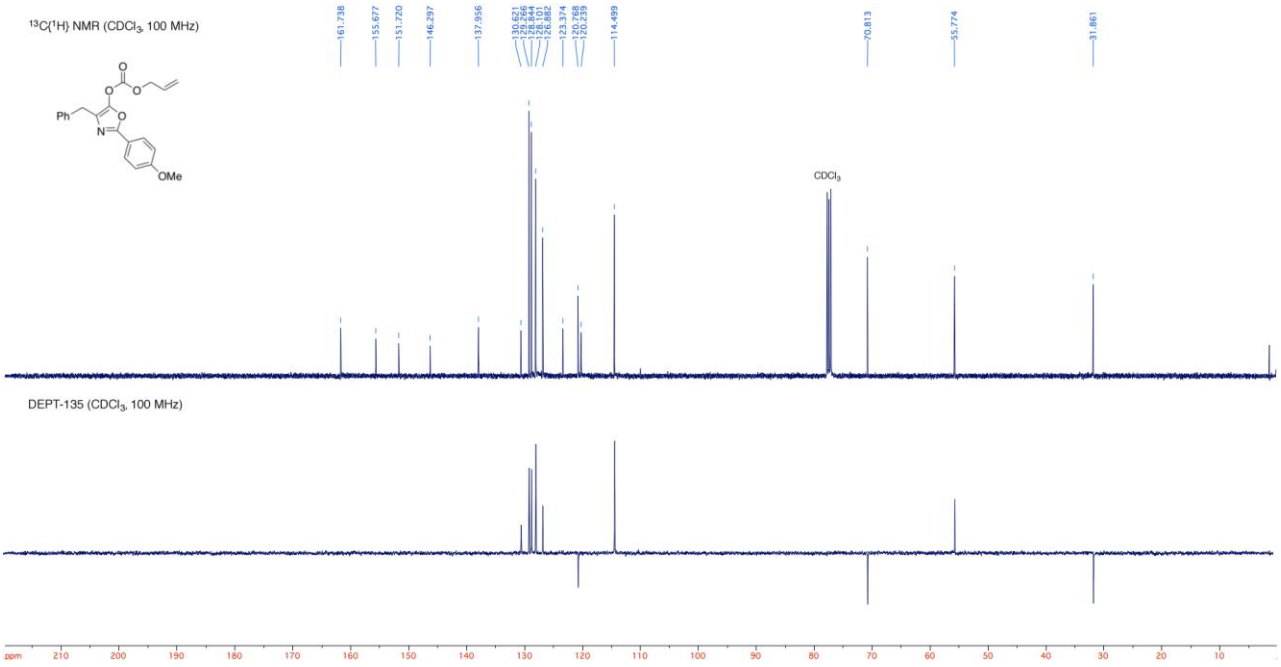

^{1}H NMR (400 MHz), ^{13}C NMR and DEPT 135 spectra of compound 101

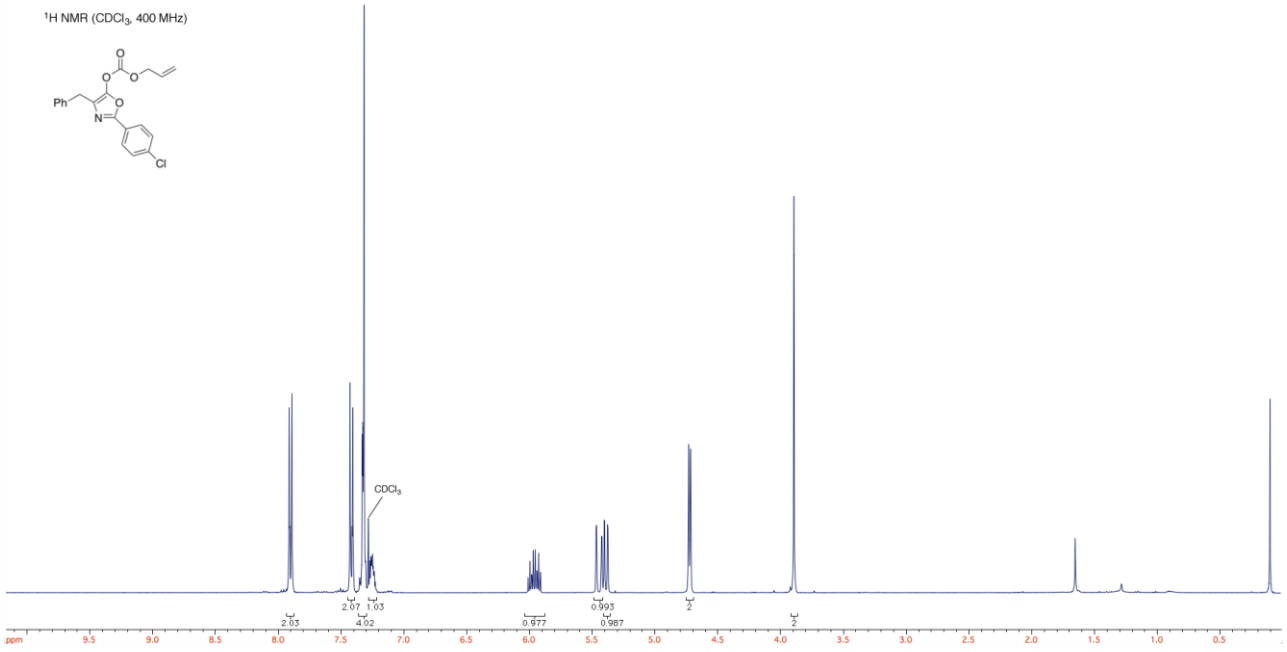

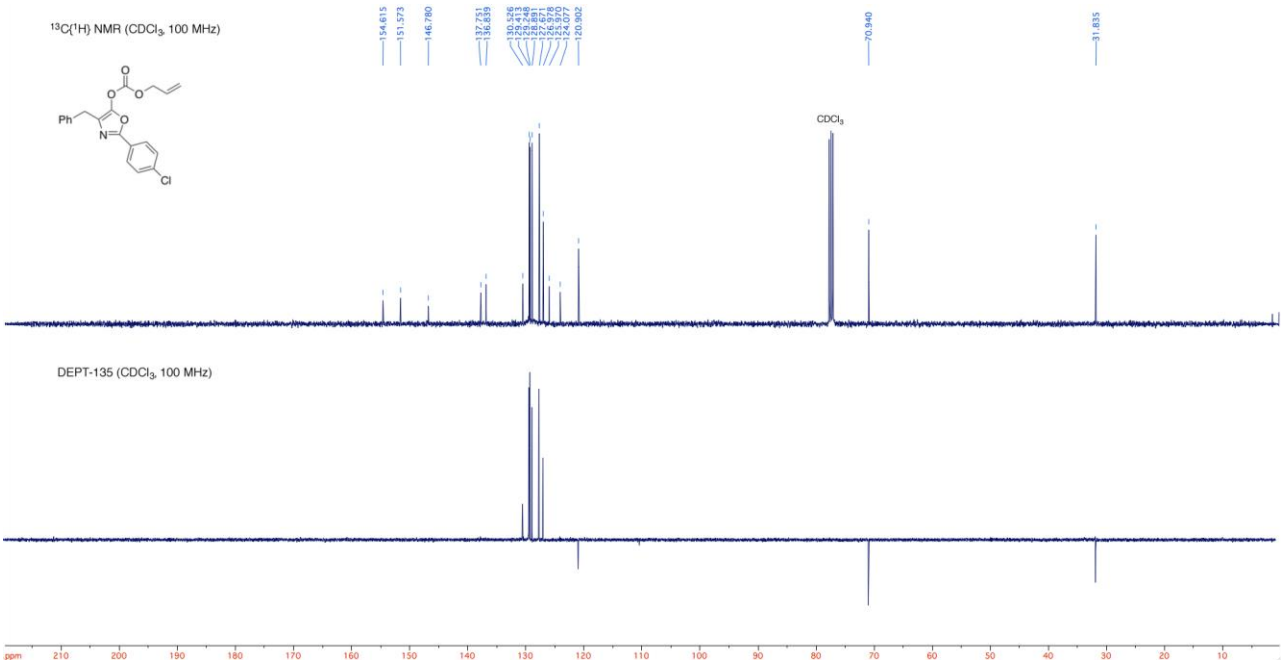

^{1}H NMR (400 MHz), ^{13}C NMR and DEPT 135 spectra of compound 102

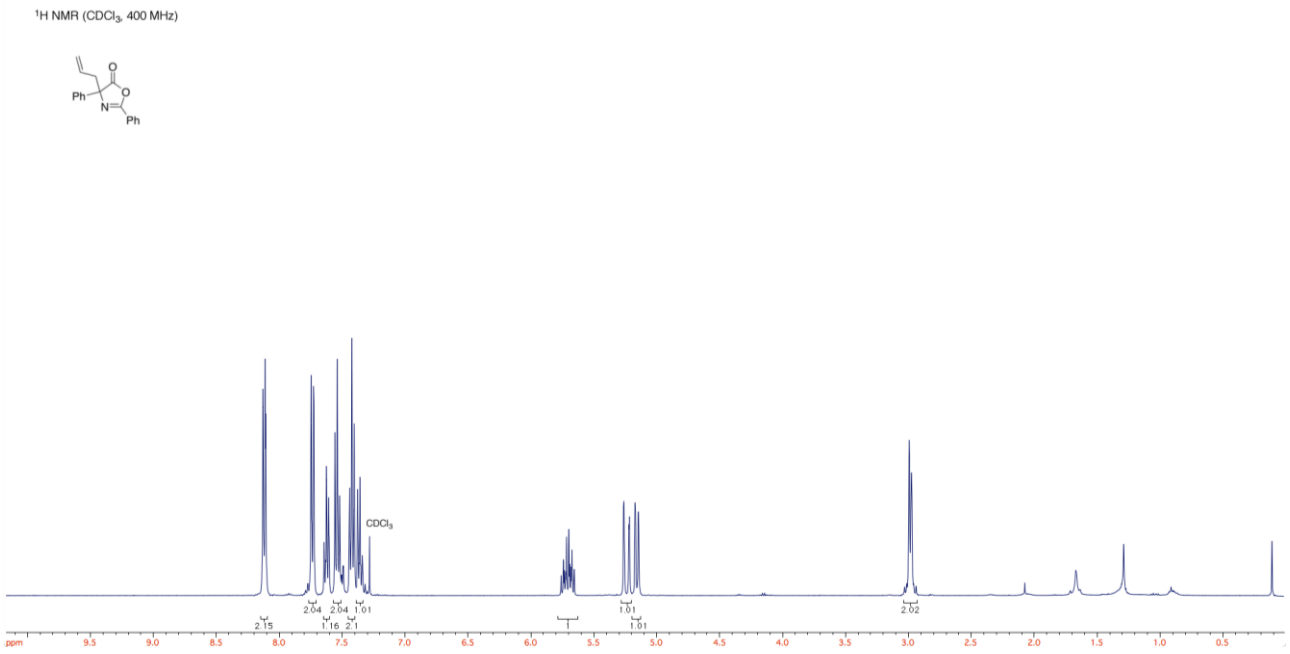

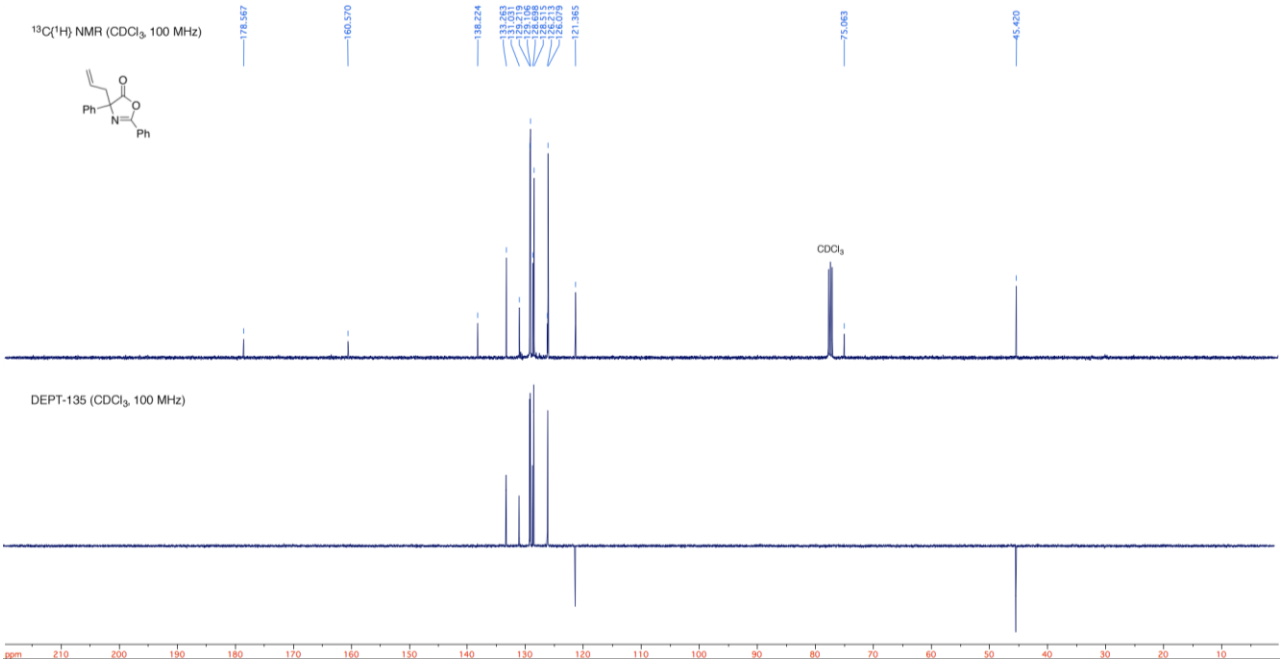

^{1}H NMR (400 MHz), ^{13}C NMR and DEPT 135 spectra of compound 103

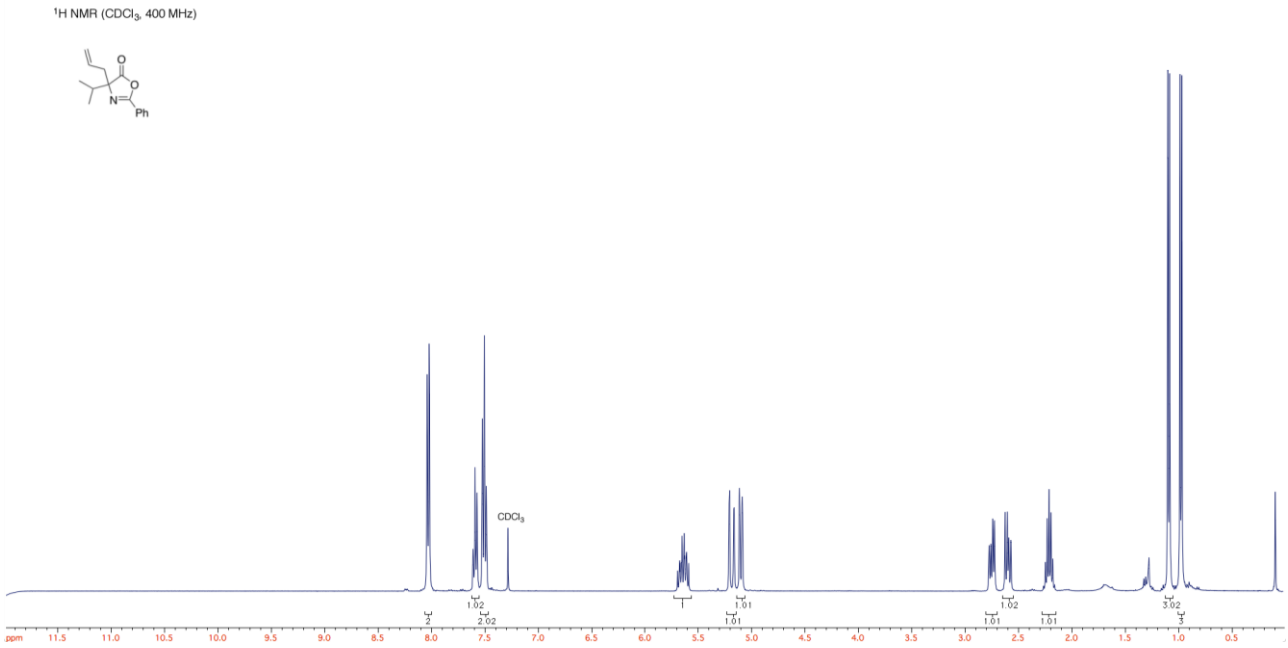

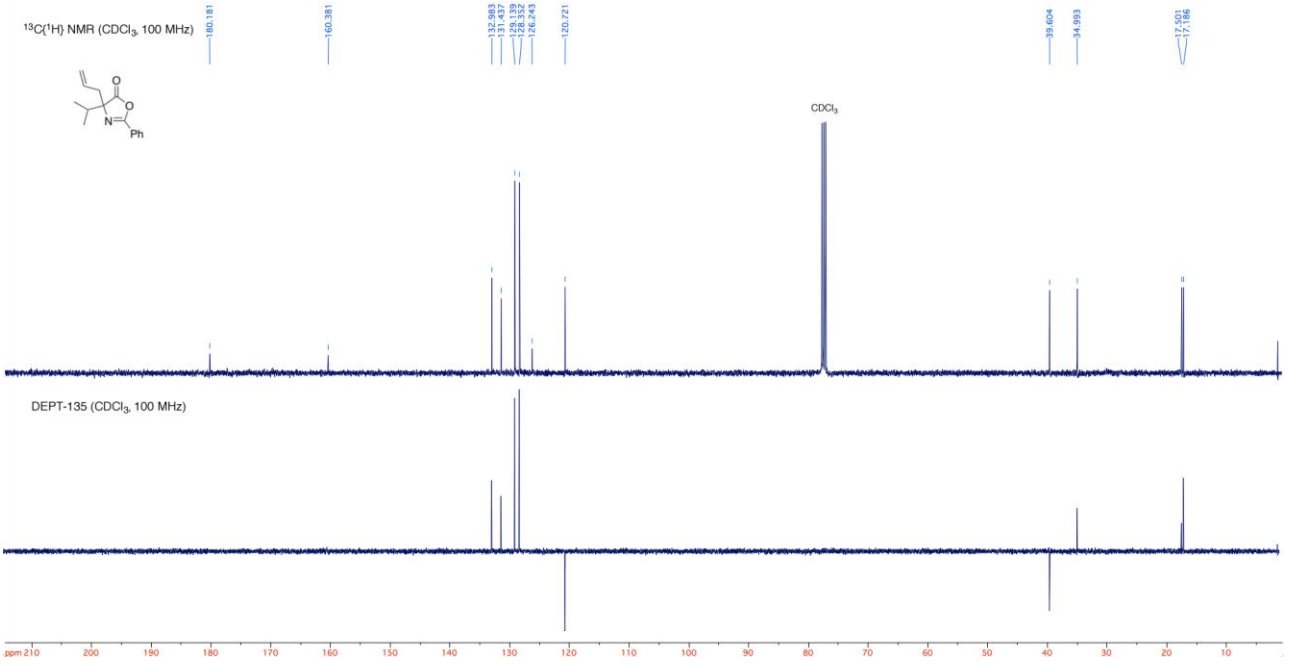

^{1}H NMR (400 MHz), ^{13}C NMR and DEPT 135 spectra of compound 104

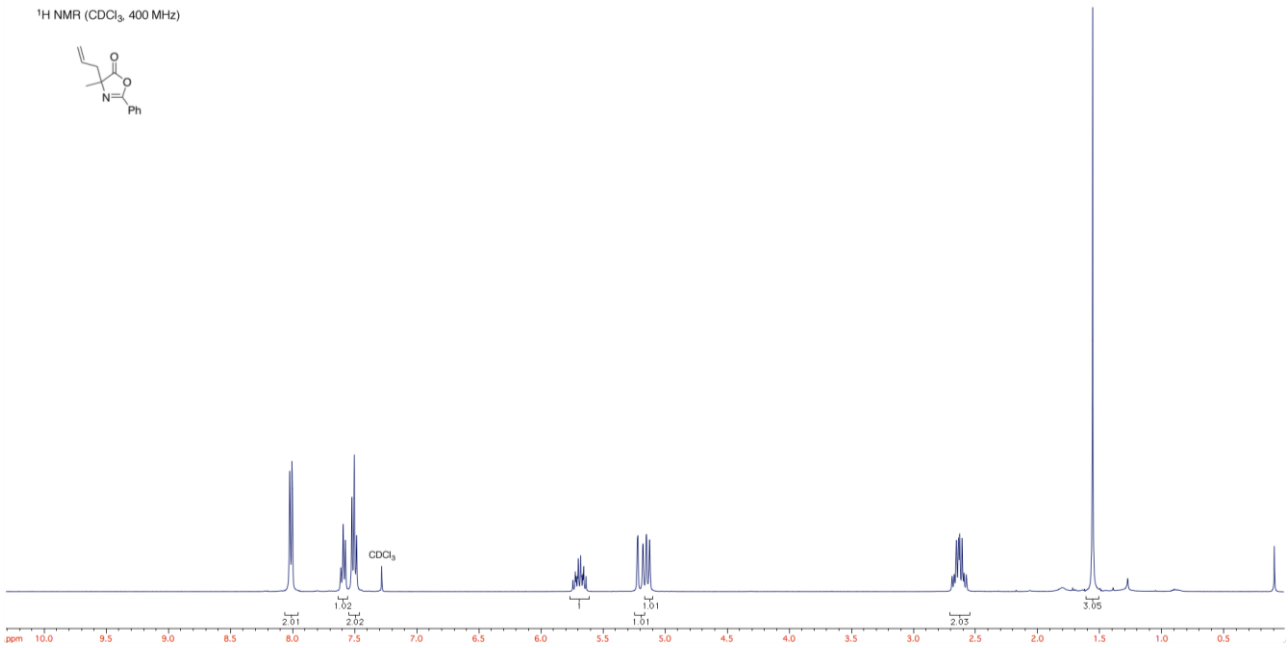

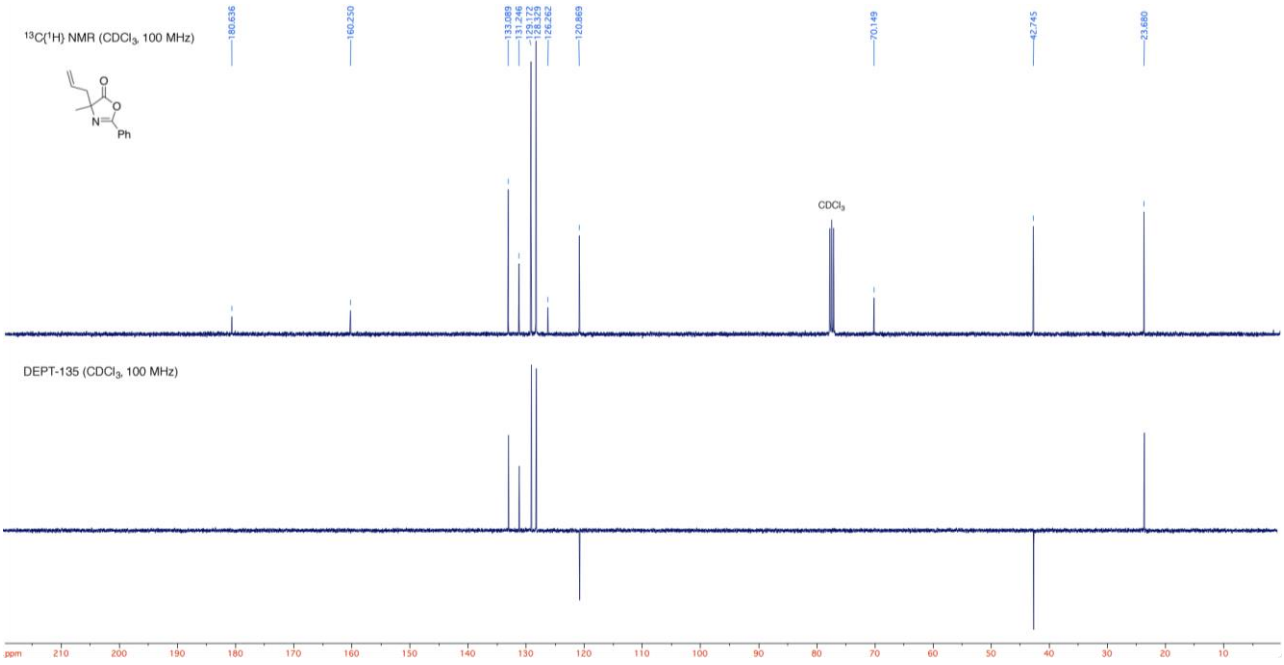

^{1}H NMR (400 MHz), ^{13}C NMR and DEPT 135 spectra of compound 105

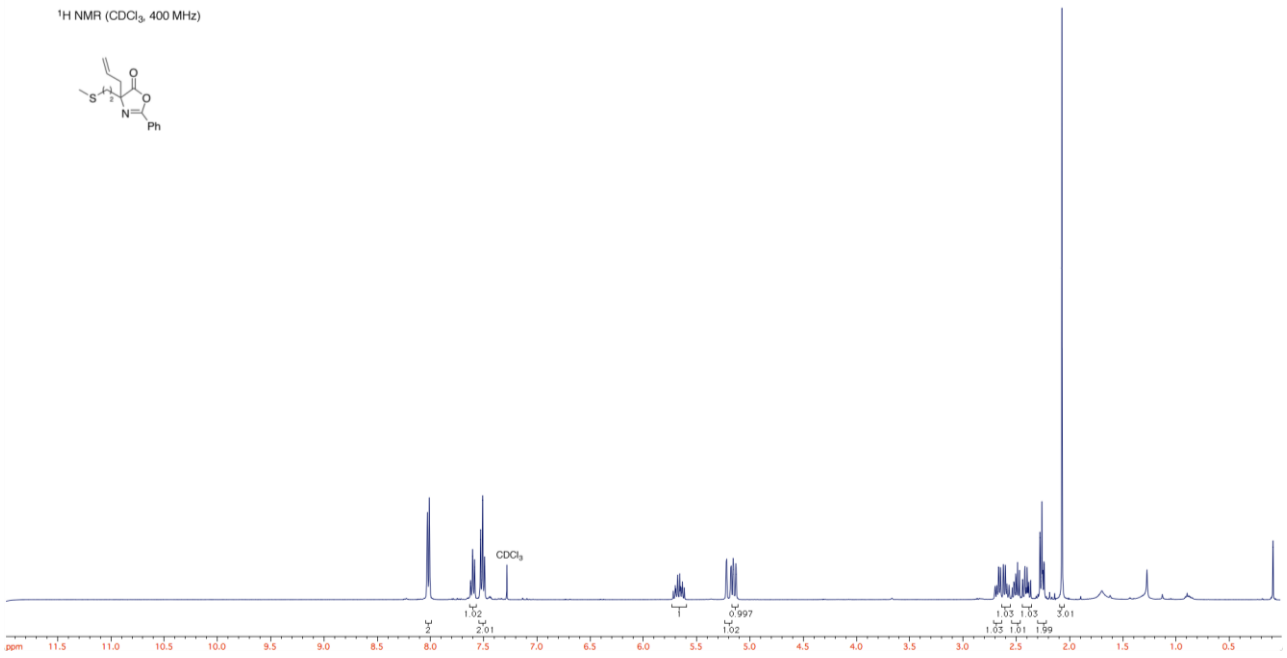

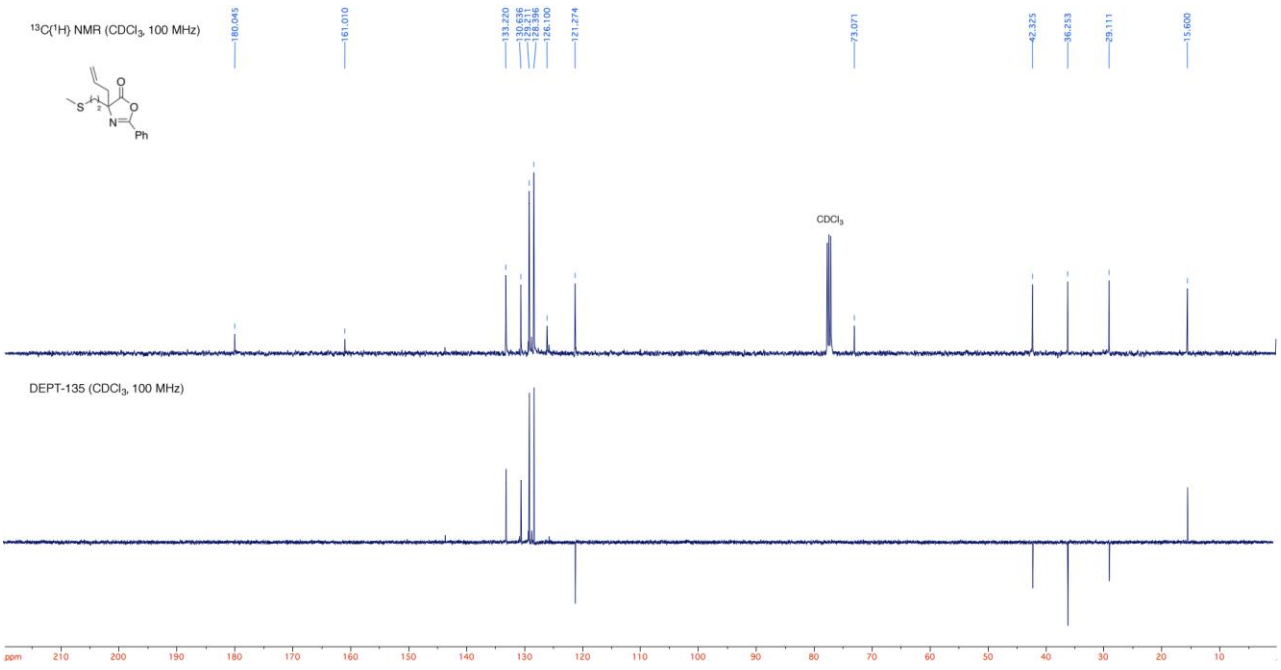

^{1}H NMR (400 MHz), ^{13}C NMR and DEPT 135 spectra of compound 106

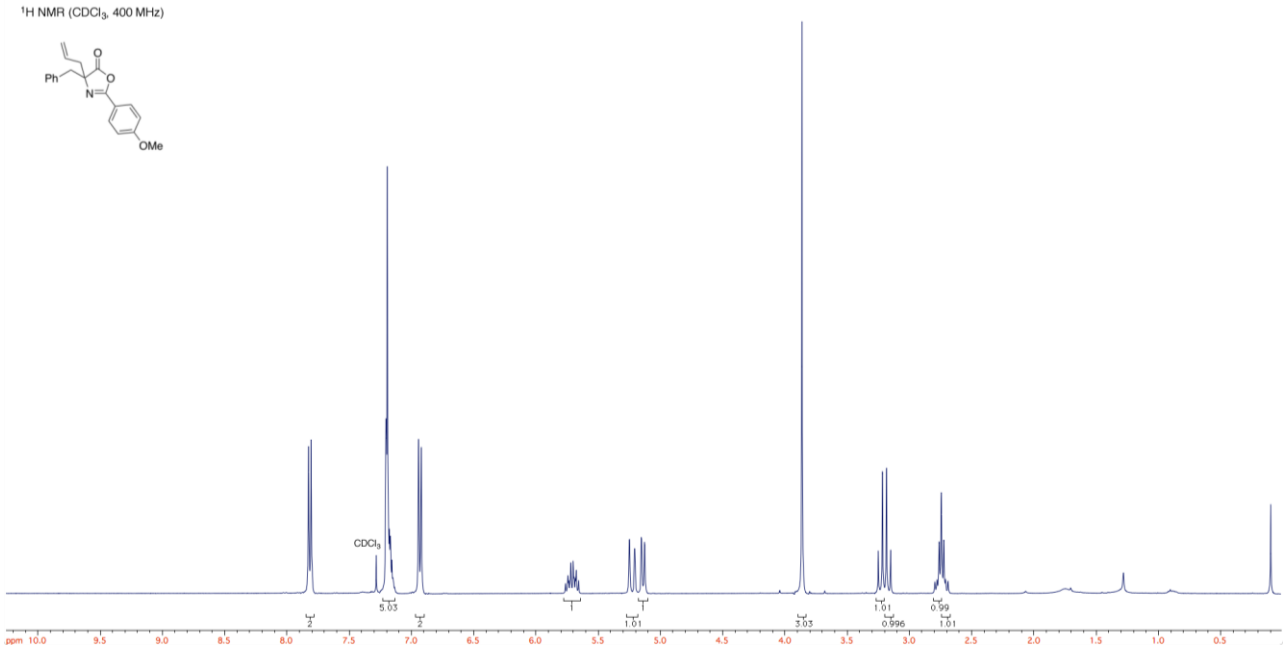

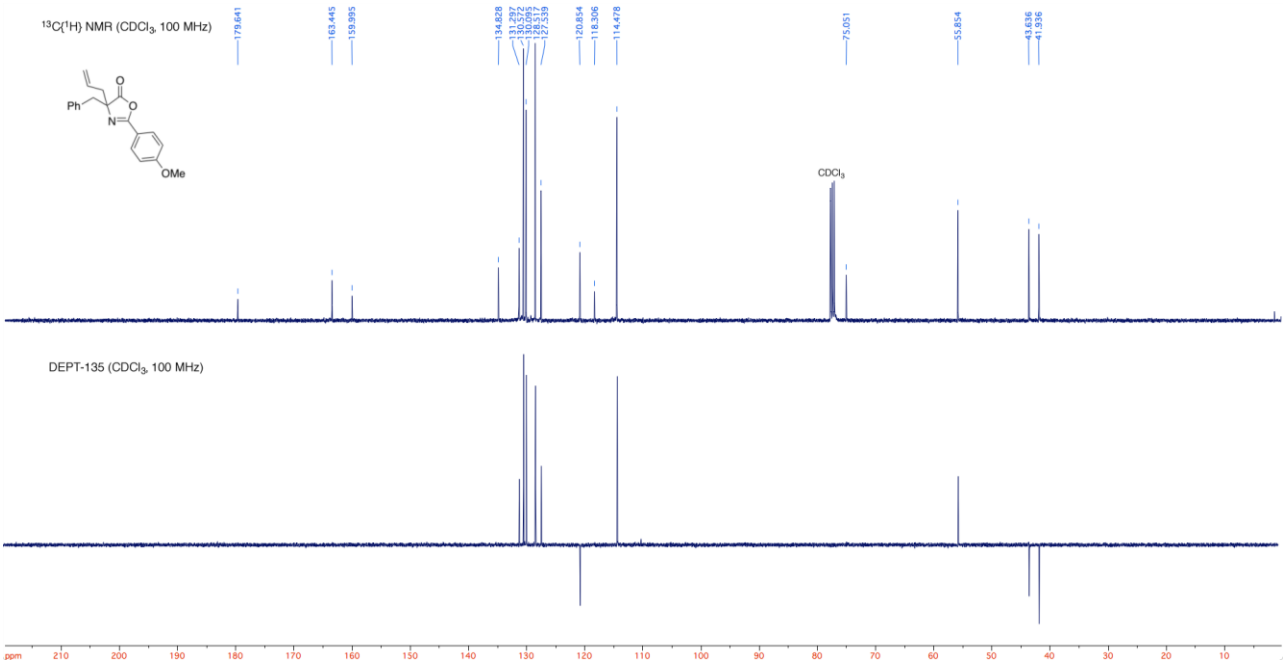

^{1}H NMR (400 MHz), ^{13}C NMR and DEPT 135 spectra of compound 107

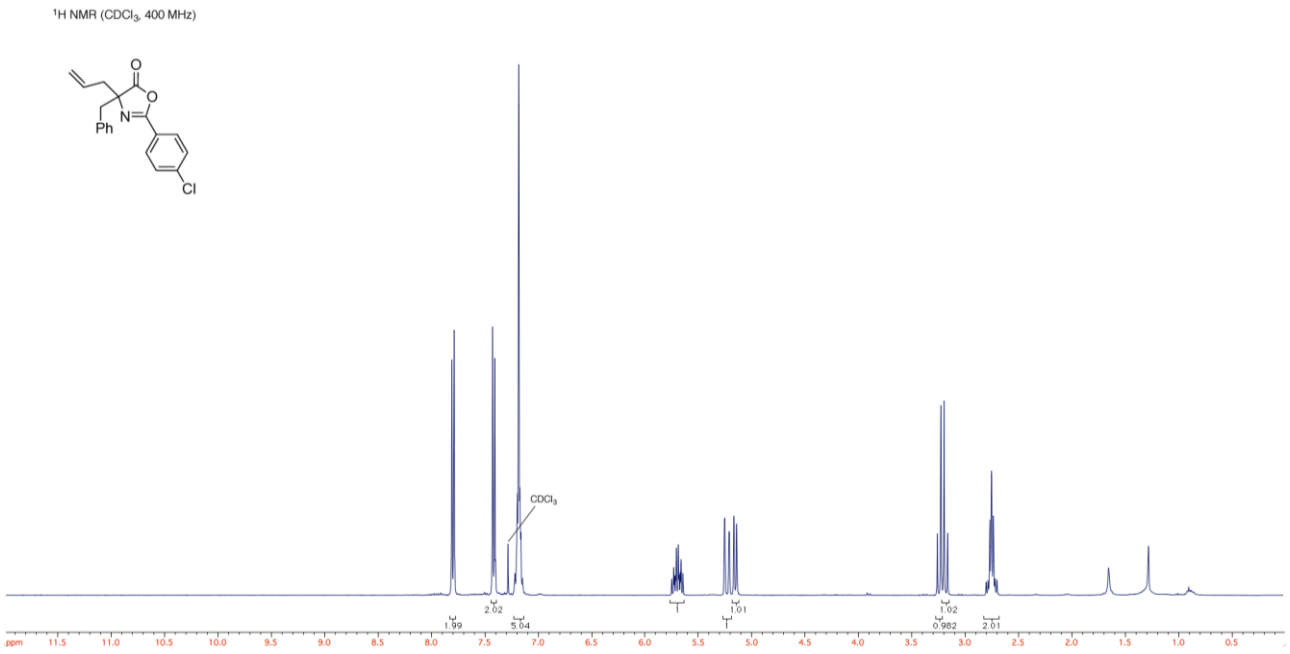

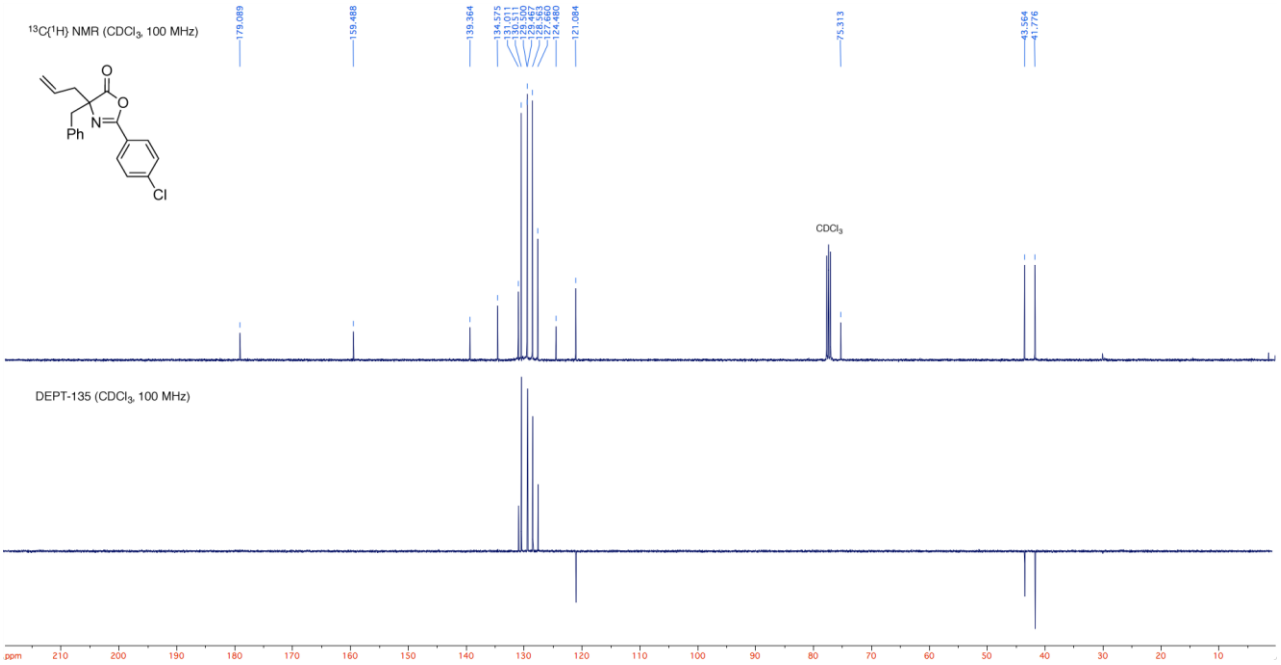

^{1}H NMR (400 MHz), ^{13}C NMR and DEPT 135 spectra of compound 108

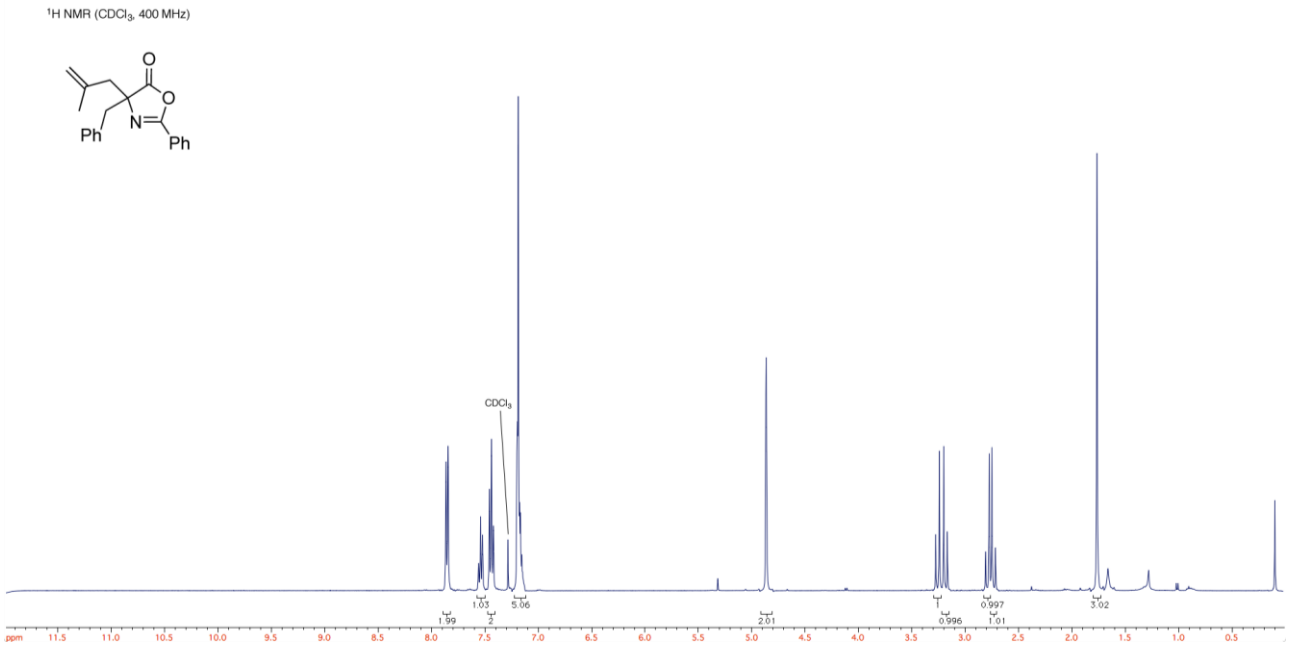

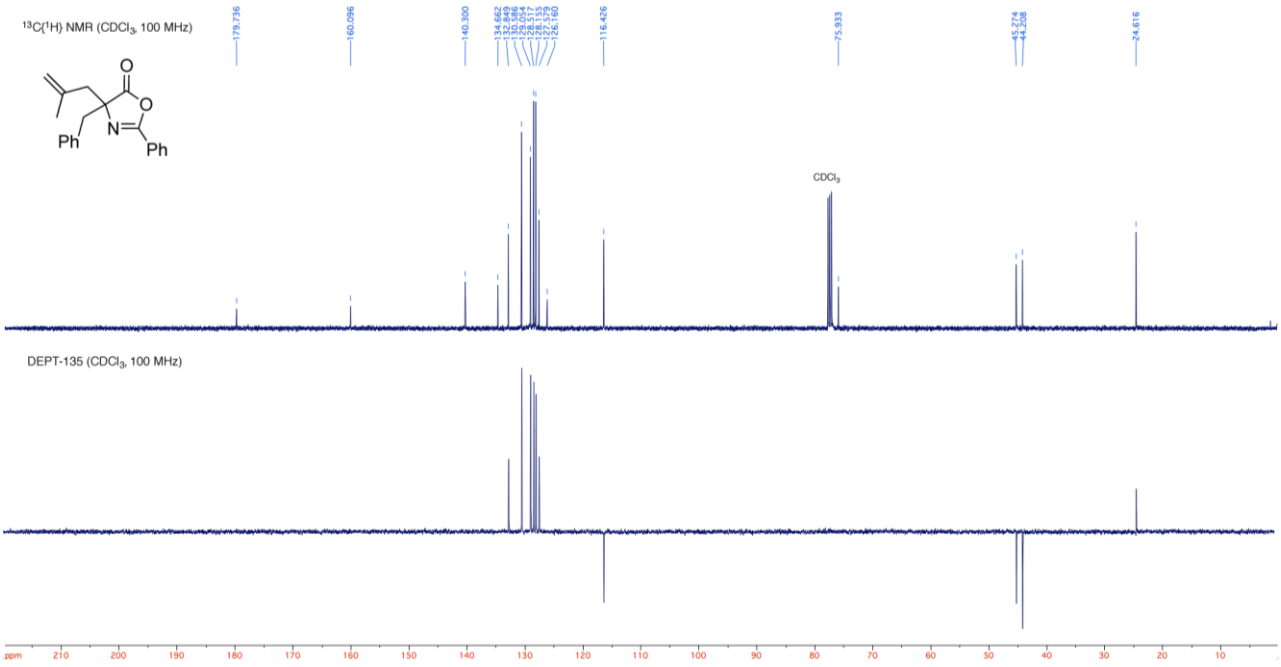

^{1}H NMR (400 MHz), ^{13}C NMR and DEPT 135 spectra of compound 109

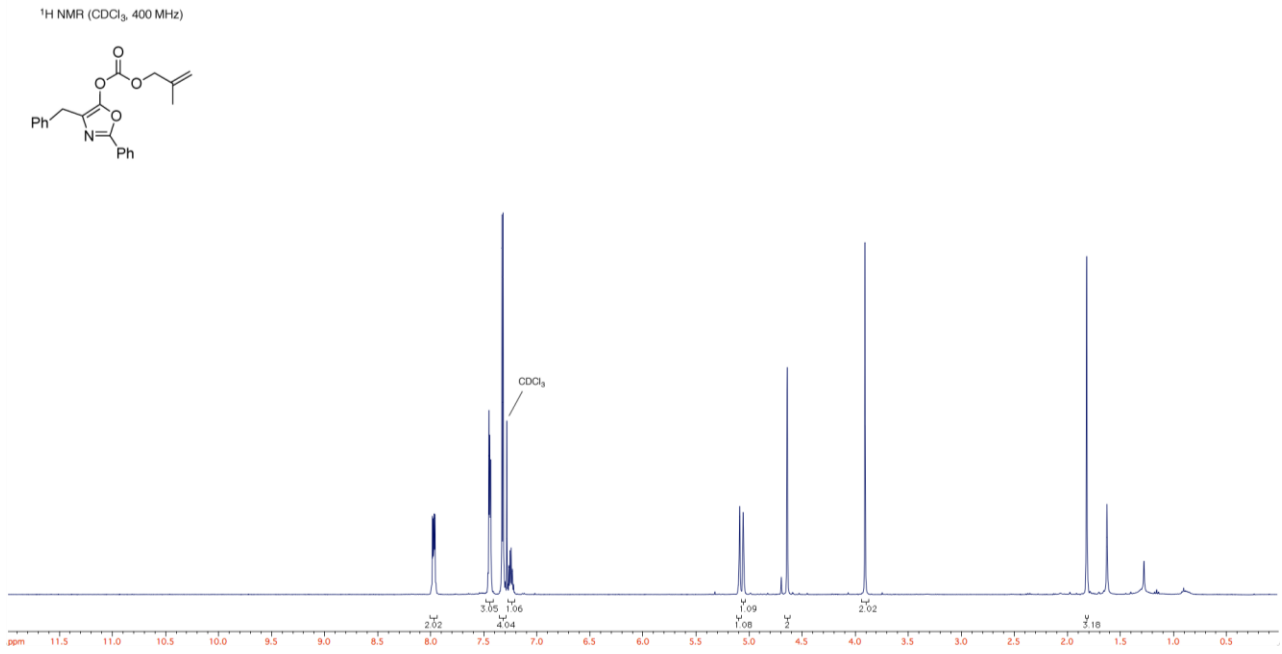

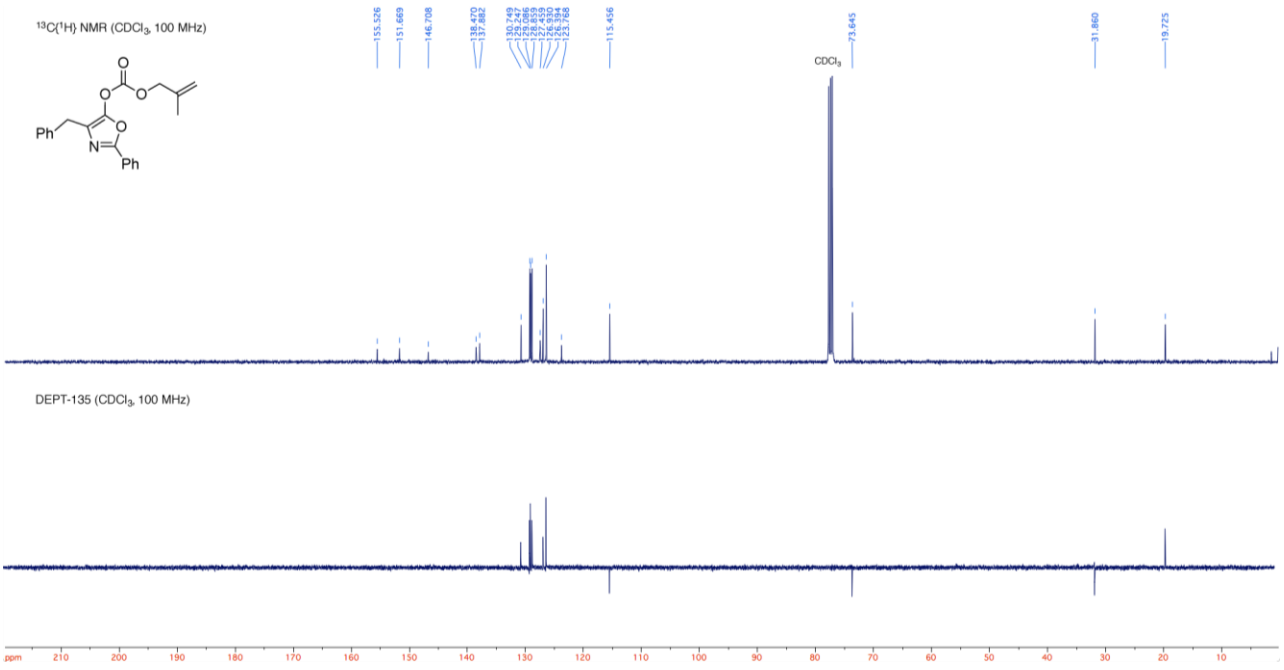

^{1}H NMR (400 MHz), ^{13}C NMR and DEPT 135 spectra of compound 111

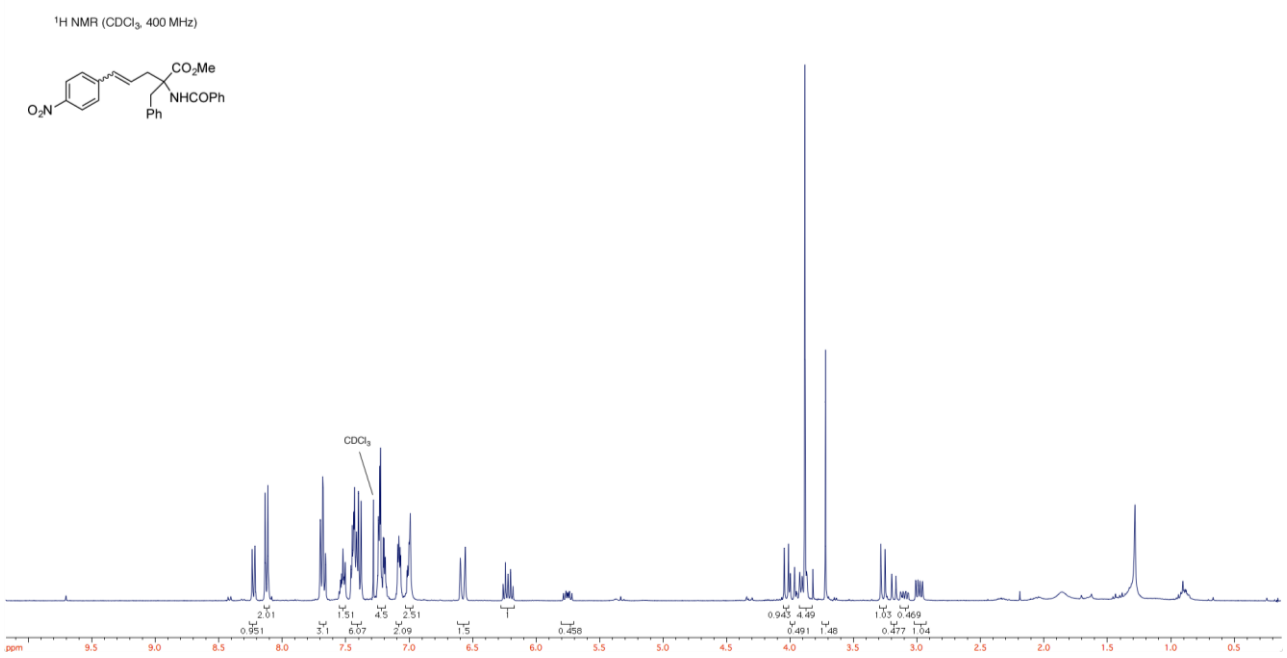

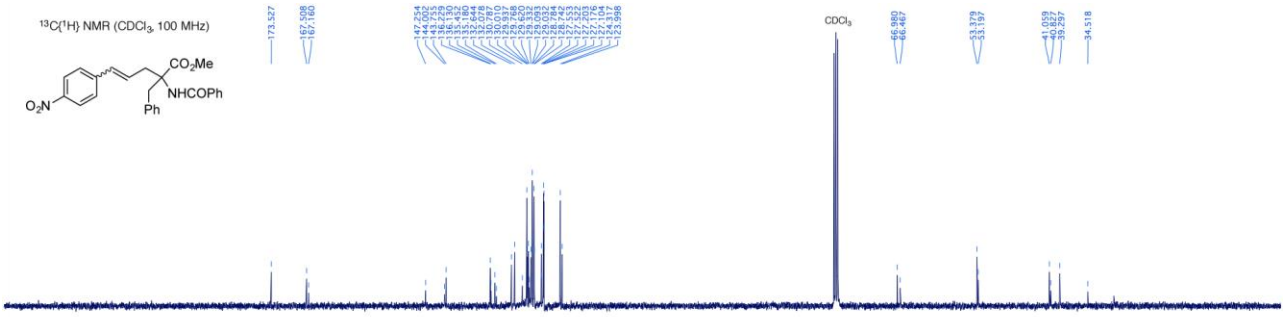

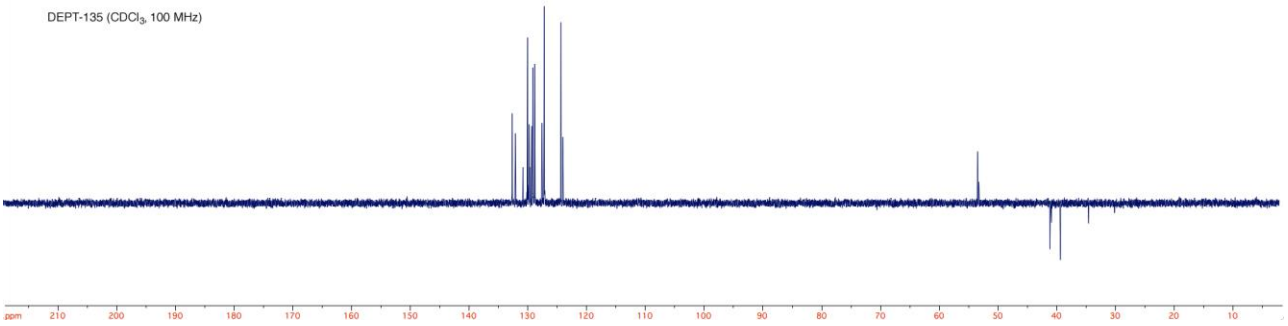

^{1}H NMR (400 MHz), ^{13}C NMR and DEPT 135 spectra of compound 112

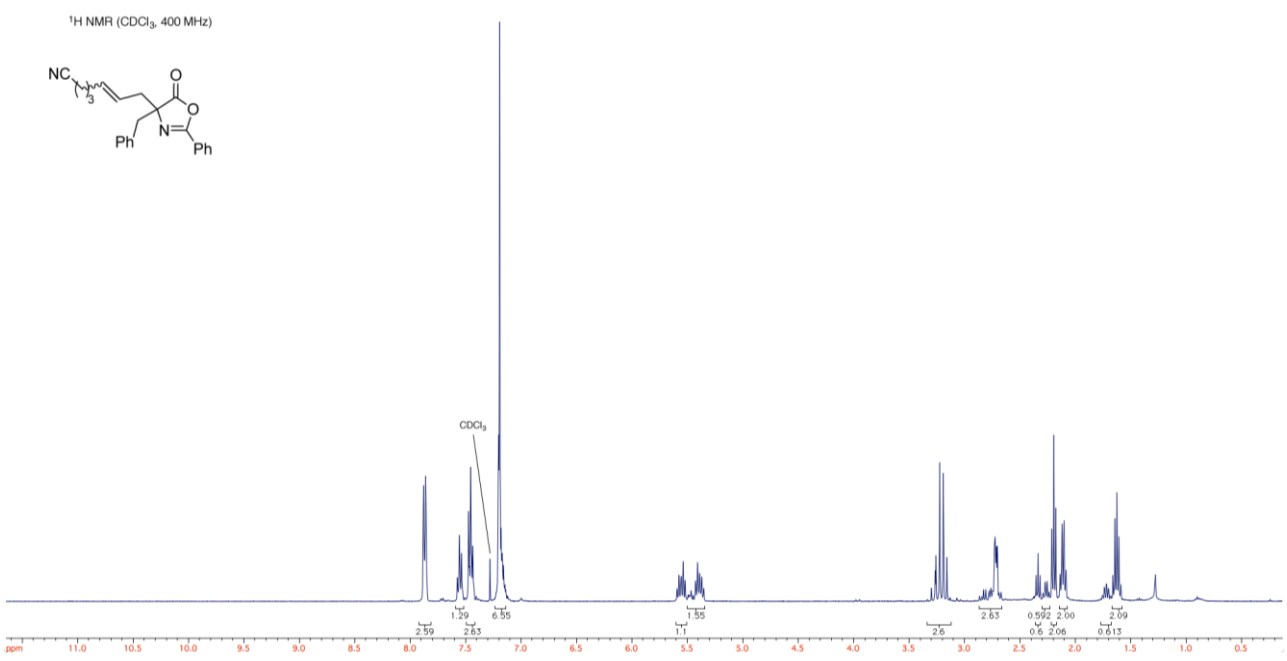

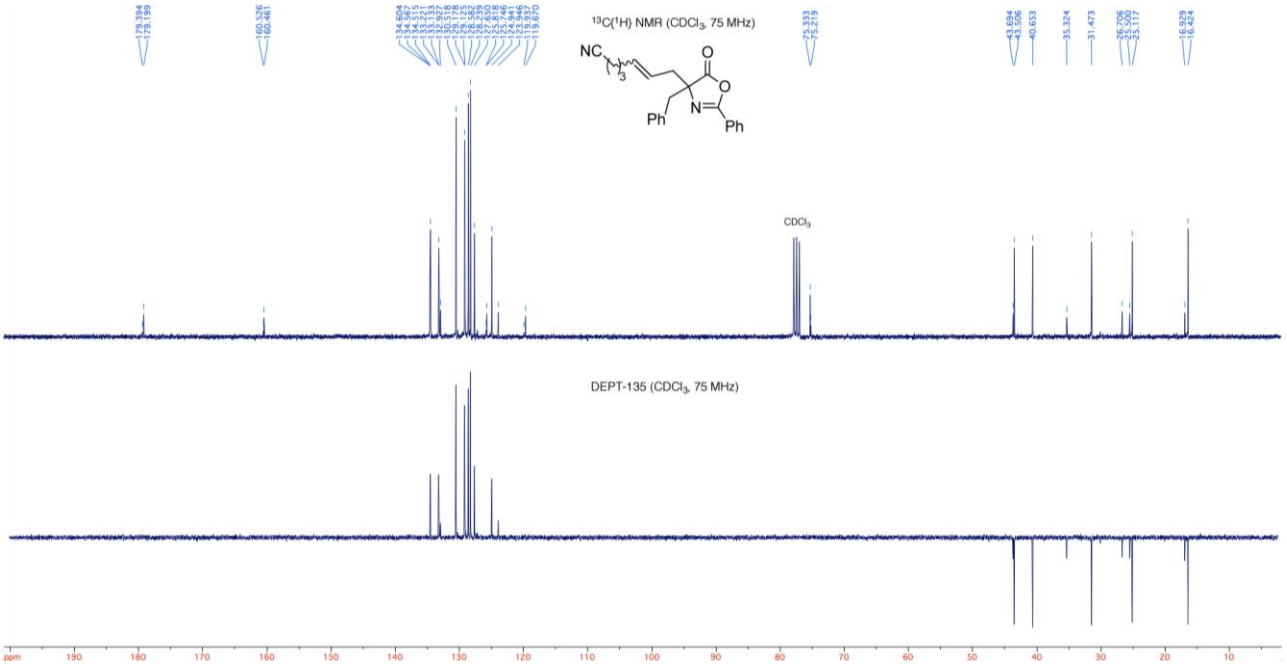

^{1}H NMR (400 MHz), ^{13}C NMR and DEPT 135 spectra of compound 113

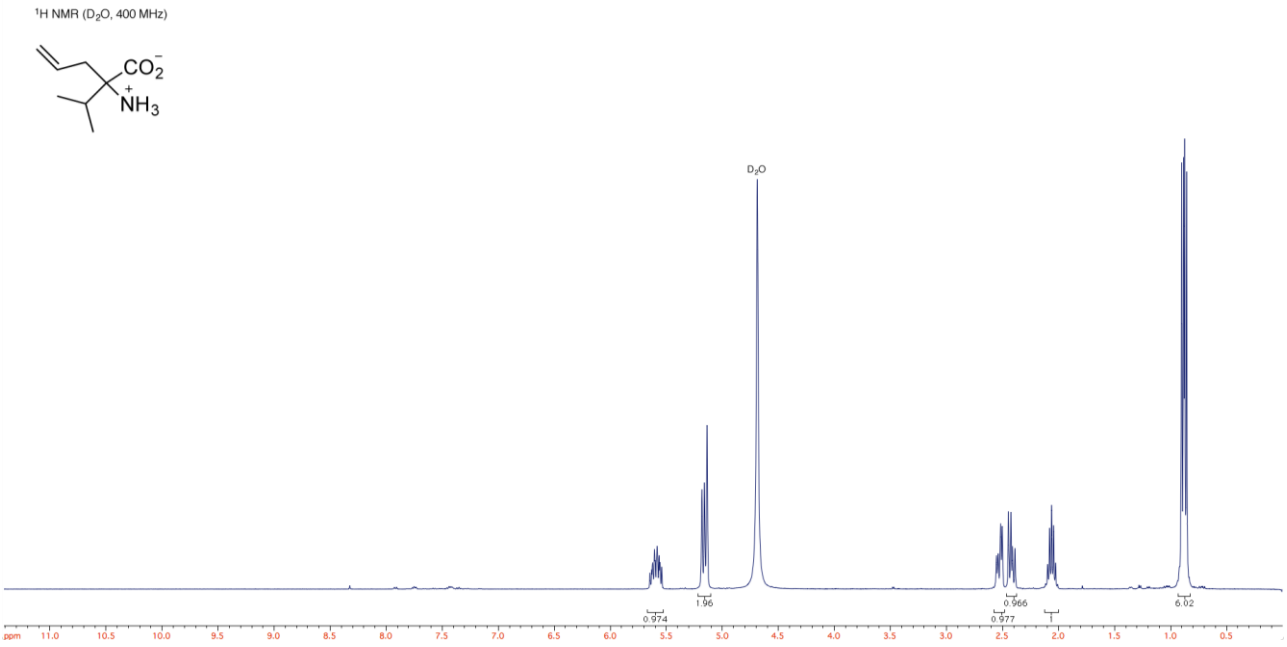

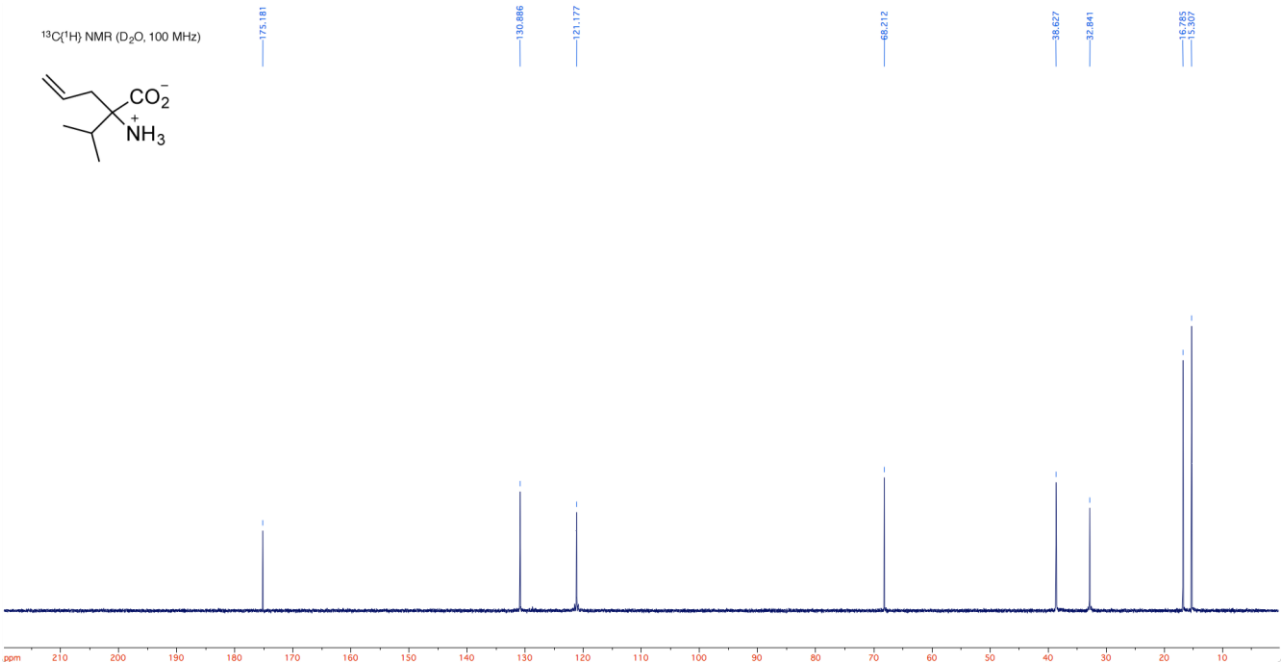

^{1}H NMR (400 MHz), ^{13}C NMR and DEPT 135 spectra of compound 114

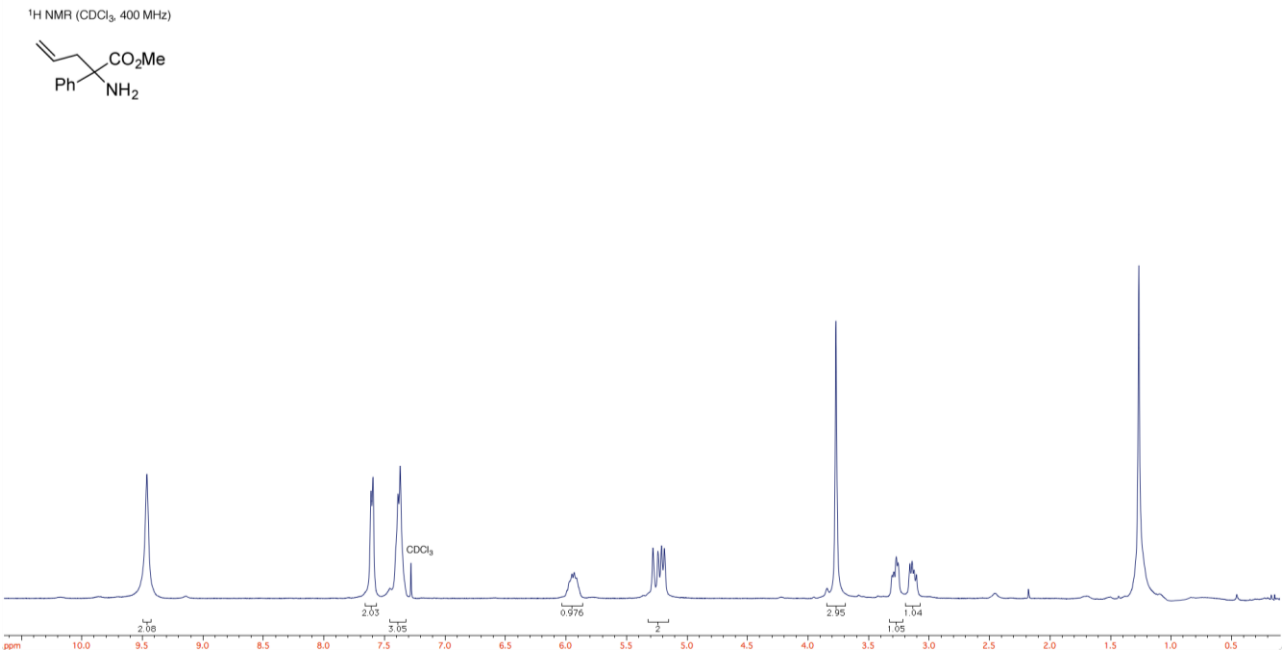

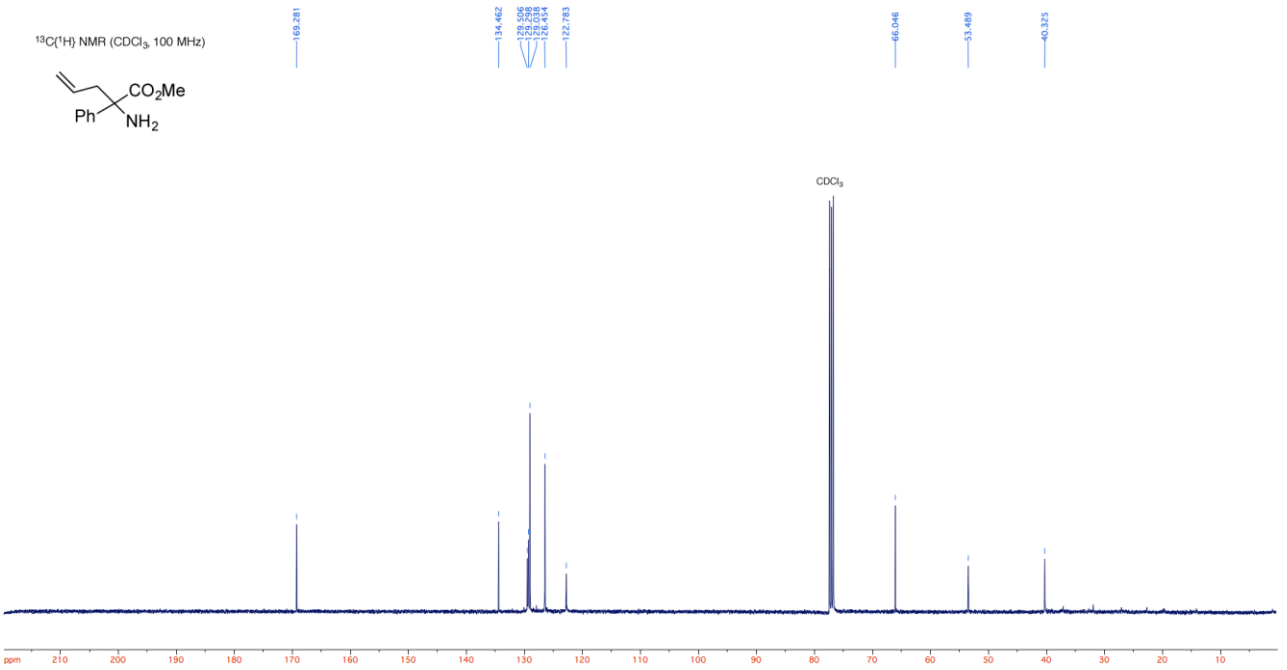

^{1}H NMR (400 MHz), ^{13}C NMR and DEPT 135 spectra of compound 115

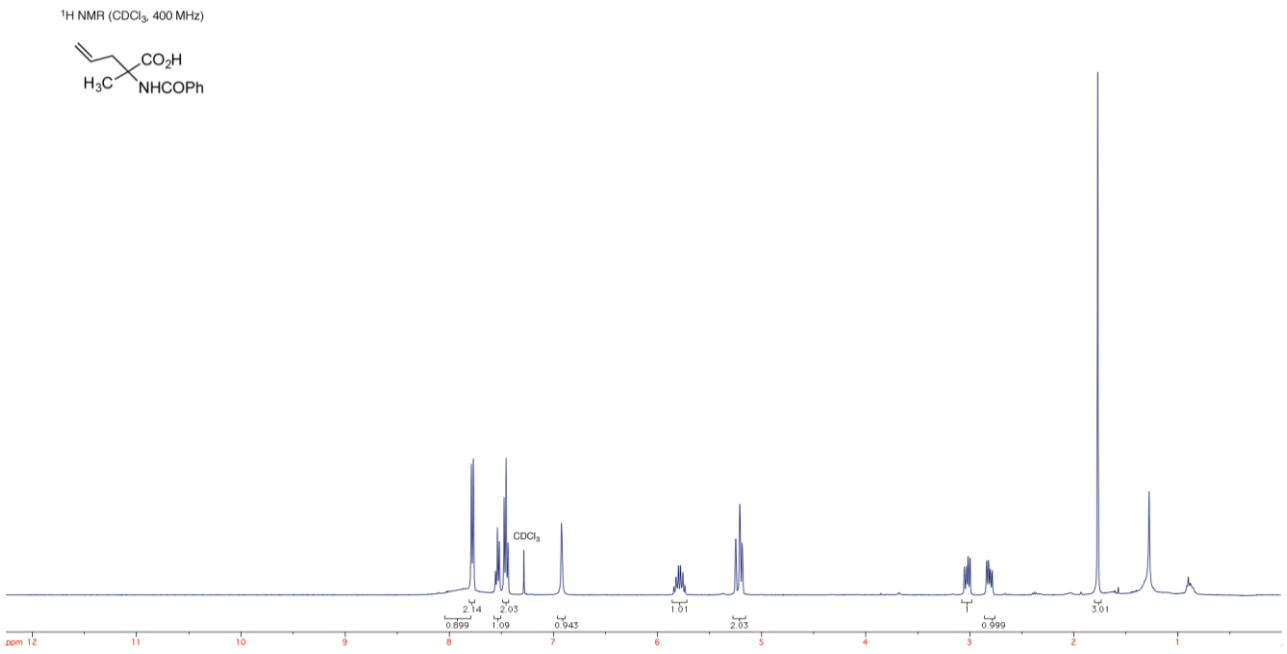

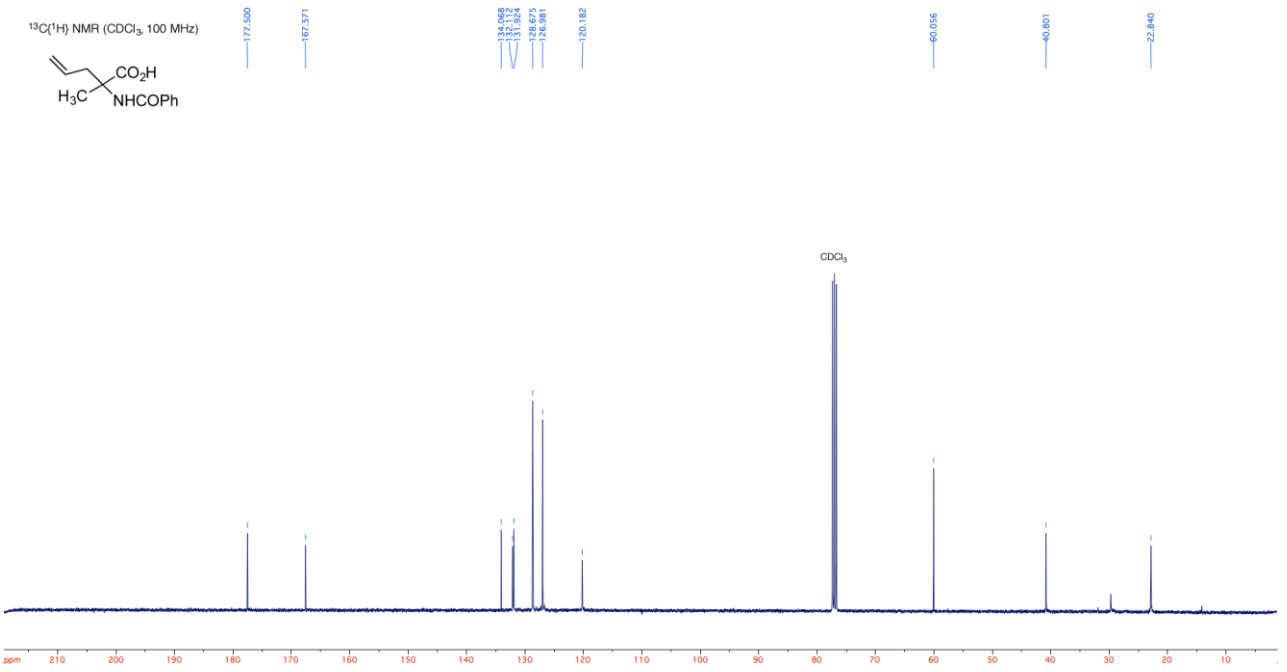

^{1}H NMR (400 MHz), ^{13}C NMR and DEPT 135 spectra of compound 116

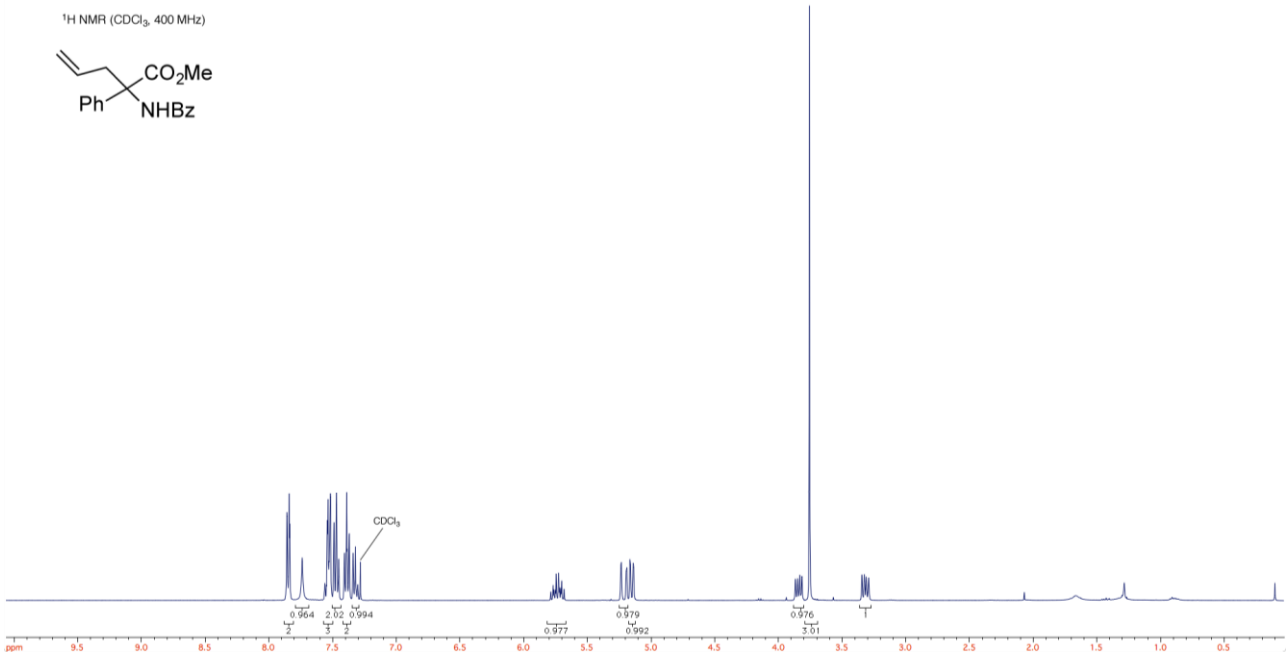

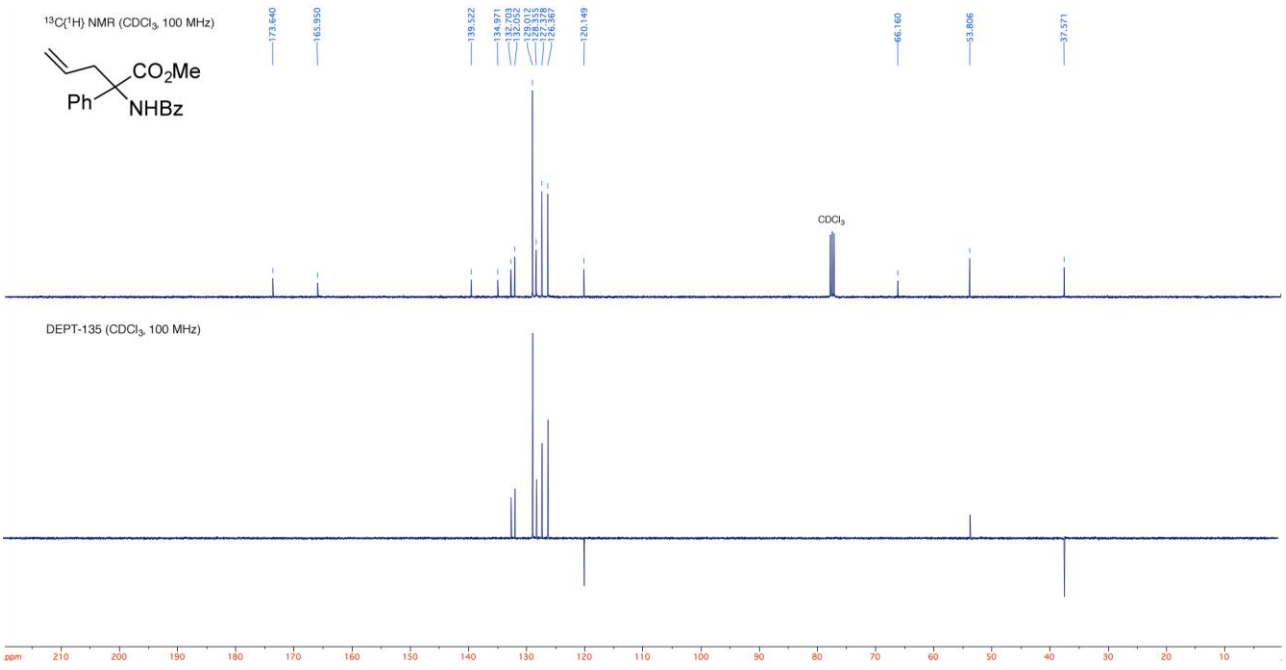

^{1}H NMR (400 MHz), ^{13}C NMR and DEPT 135 spectra of compound 117

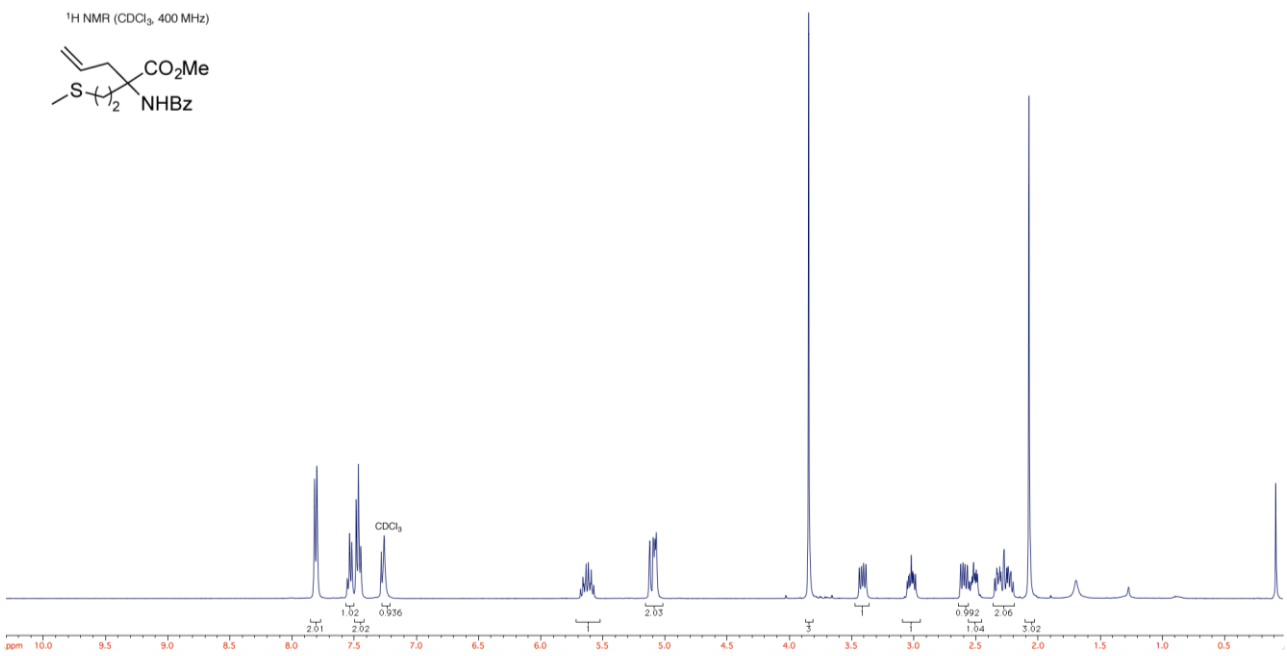

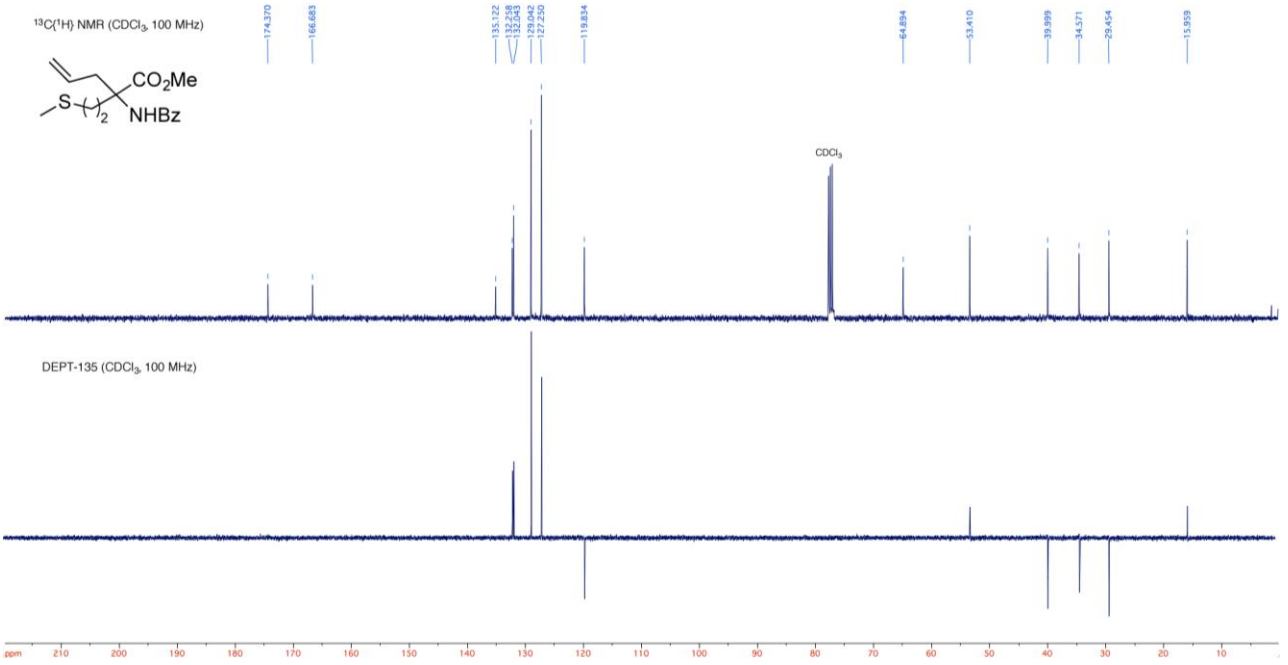

Chiral HPLC separation

The chiral HPLC separations were performed using a Merck-Hitachi bench-top apparatus including a quaternary pump model LaChrom L-7100, a Rheodyne manual injector model 77251 with a 5 µL loop, and a UV detector model LaChrom L-7400. The HPLC was operated under the control of a personal computer using the DataApex Clarity™ v.4.0.02.784 advanced chromatography software for Windows operating in Microsoft® Windows 7 environment.
All separations were carried out using a Phenomenex Lux 5µ Cellulose-1 New Column 250x4.6 mm.
The chiral HPLC methods were assessed with the corresponding racemic mixtures. The separations were carried out at room temperature under constant flow rate of 1 mL/min in isocratic mode applying mobile phases containing *n*-hexane and isopropyl alcohol (Sigma-Aldrich, HPLC-grade purity) on the column in proportions depending strongly on the type of analyte being studied. The concentrations of n-hexane in the mobile phases used ranged from 95% up to 99.85%. All samples were prepared dissolving the analytes in *n*-hexane at a concentration level of about 1 mg/mL. Analytes were detected at 254 nm.
At the end of each analytical session, the column was flushed with 20 volumes of a mixture of *n*-hexane and isopropyl alcohol (90:10%, v/v), and stored using this same mixture.
Under the conditions described, the analytes eluted as well-resolved and symmetric peaks at the retention times shown in the legends of reported chromatograms.
In the following tables “W05” refers to the peak width measured at 50% of the peak height as prescribed in Chapter <612> “Chromatography” of the USP guidelines.

Copies of chiral HPLC chromatograms for compound 24

Mobile phase: hexane/isopropanol 99.75:0.25

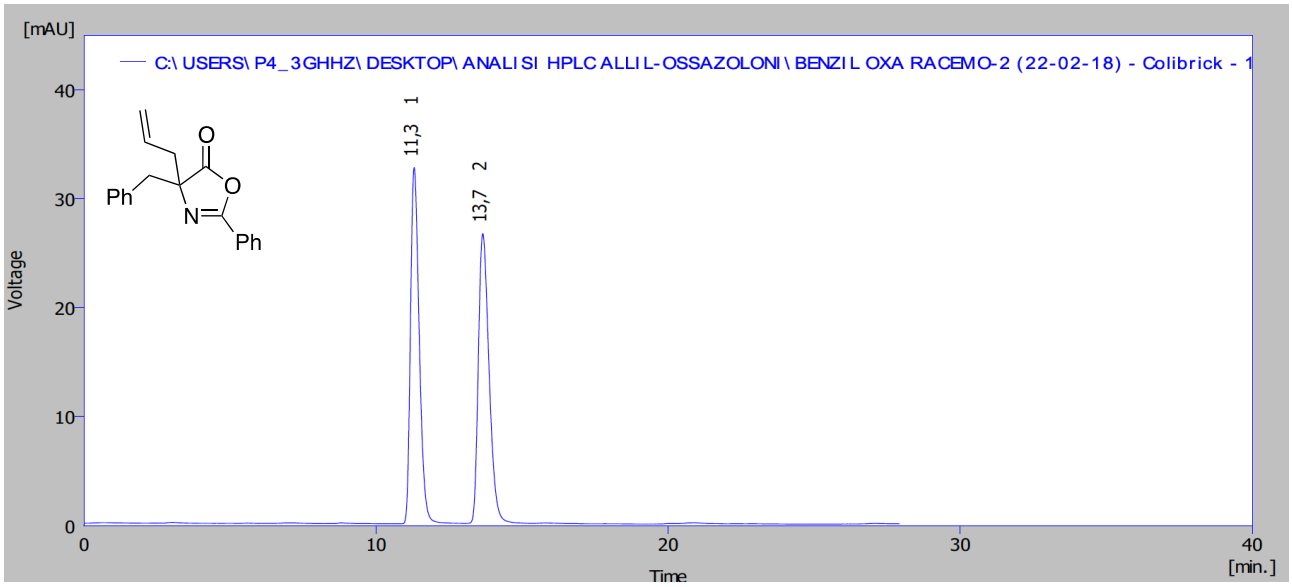

	Reten. Time [min]	Start Time [min]	End Time [min]	Start Value [mV]	End Value [mV]	Area [mV.s]	Height [mV]	Area [%]	Height [%]	W05 [min]
1	11,304	10,900	12,468	0,159	0,236	676,907	32,672	50,0	55,1	0,32
2	13,652	13,148	14,972	0,200	0,227	675,744	26,576	50,0	44,9	0,40
	Total					1352,651	59,248	100,0	100,0	

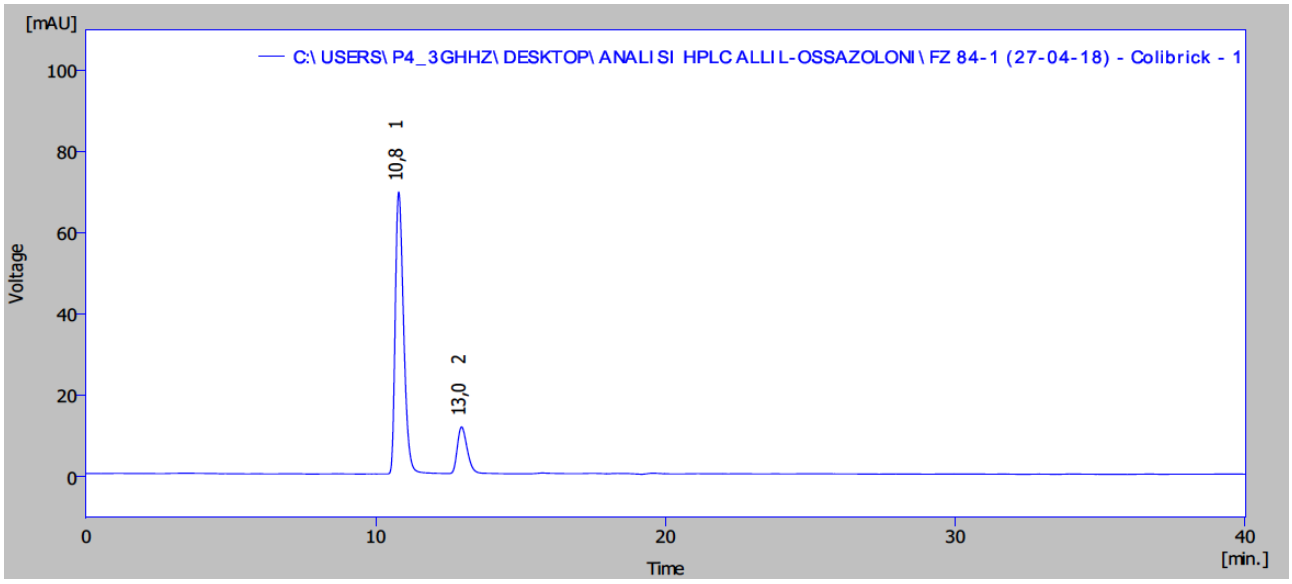

	Reten. Time [min]	Start Time [min]	End Time [min]	Start Value [mV]	End Value [mV]	Area [mV.s]	Height [mV]	Area [%]	Height [%]	W05 [min]
1	10,792	10,452	11,344	0,755	1,750	1348,863	68,914	84,9	86,2	0,31
2	12,960	12,620	13,400	0,954	1,593	240,504	11,001	15,1	13,8	0,36
	Total					1589,367	79,915	100,0	100,0	

Copies of chiral HPLC chromatograms for compound 102

Mobile phase: hexane/isopropanol 99.85:0.15

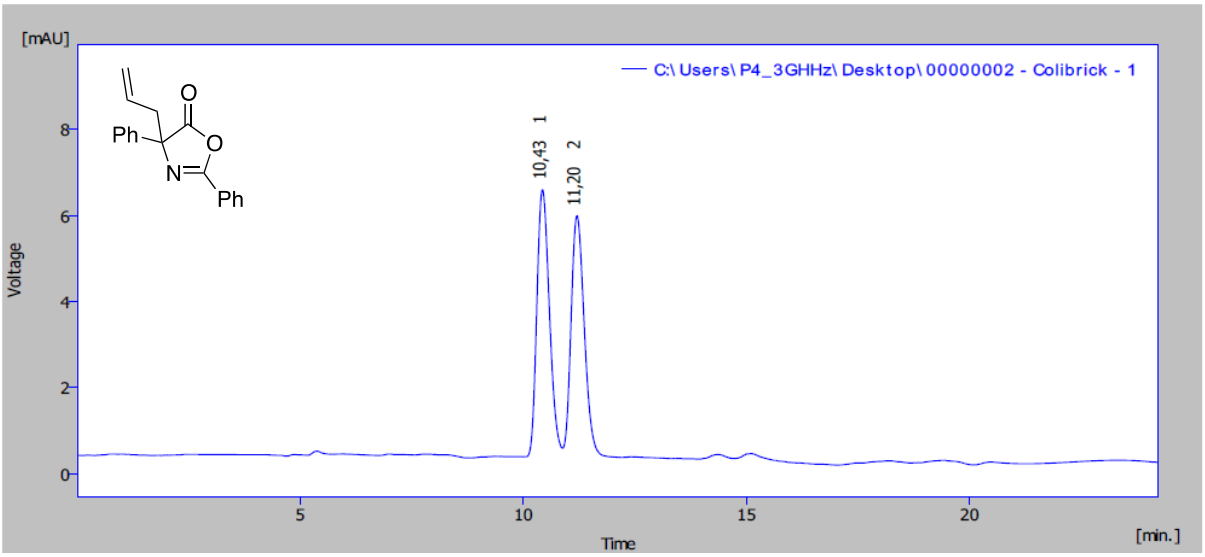

	Reten. Time [min]	Start Time [min]	End Time [min]	Start Value [mV]	End Value [mV]	Area [mV.s]	Height [mV]	Area [%]	Height [%]	W05 [min]
1	10,432	8,840	10,876	0,357	0,368	124,144	6,228	51,6	52,6	0,31
2	11,204	10,876	12,084	0,368	0,375	116,494	5,617	48,4	47,4	0,32
	Total					240,638	11,846	100,0	100,0	

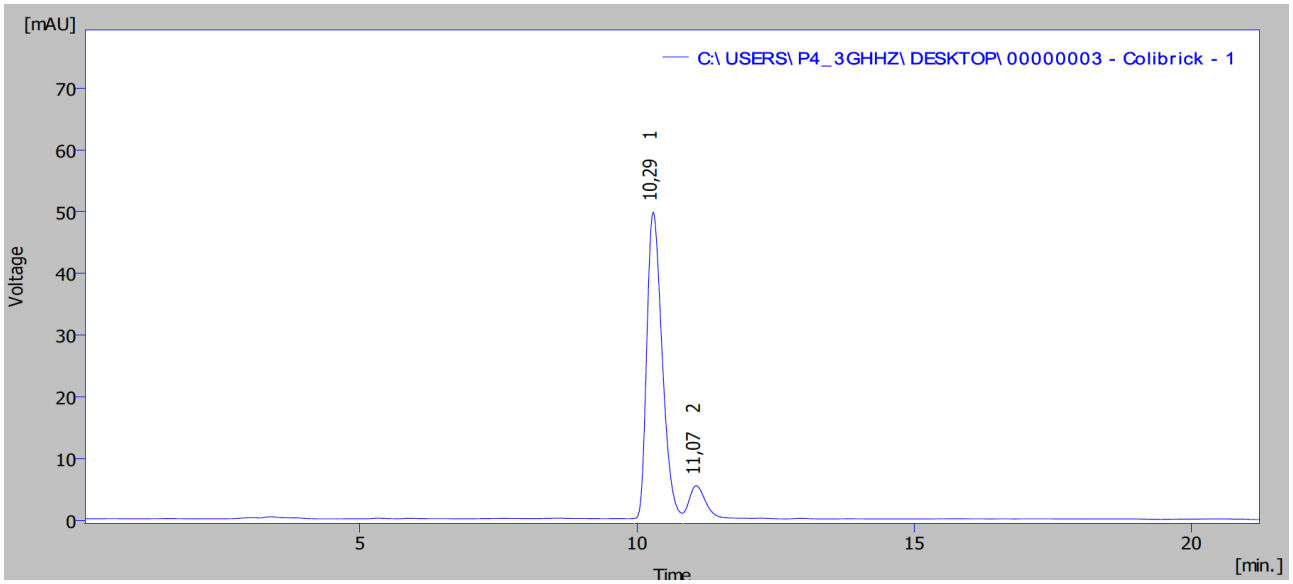

	Reten. Time [min]	Start Time [min]	End Time [min]	Start Value [mV]	End Value [mV]	Area [mV.s]	Height [mV]	Area [%]	Height [%]	W05 [min]
1	10,292	9,960	10,780	0,338	1,307	923,966	49,164	92,7	91,8	0,30
2	11,072	10,820	11,360	1,179	1,314	72,771	4,383	7,3	8,2	0,28
	Total					996,737	53,547	100,0	100,0	

Copies of chiral HPLC chromatograms for compound 103

Mobile phase: hexane/isopropanol 99.75:0.25

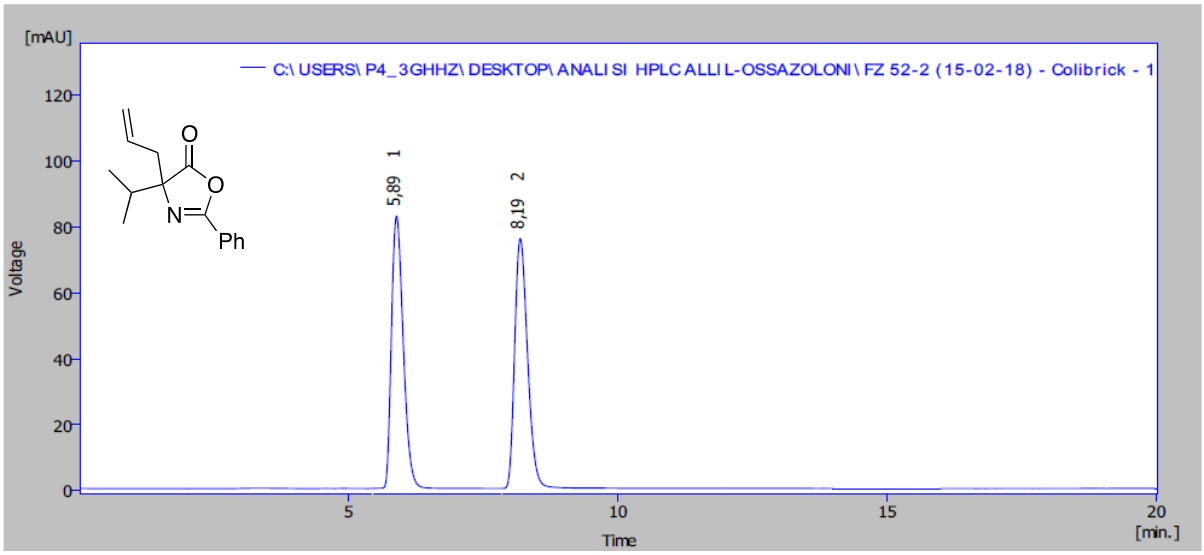

	Reten. Time [min]	Start Time [min]	End Time [min]	Start Value [mV]	End Value [mV]	Area [mV.s]	Height [mV]	Area [%]	Height [%]	W05 [min]
1	5,888	5,440	6,896	0,633	0,670	1254,969	82,653	49,9	52,2	0,24
2	8,188	7,832	9,444	0,621	0,741	1259,509	75,836	50,1	47,8	0,26
	Total					2514,478	158,489	100,0	100,0	

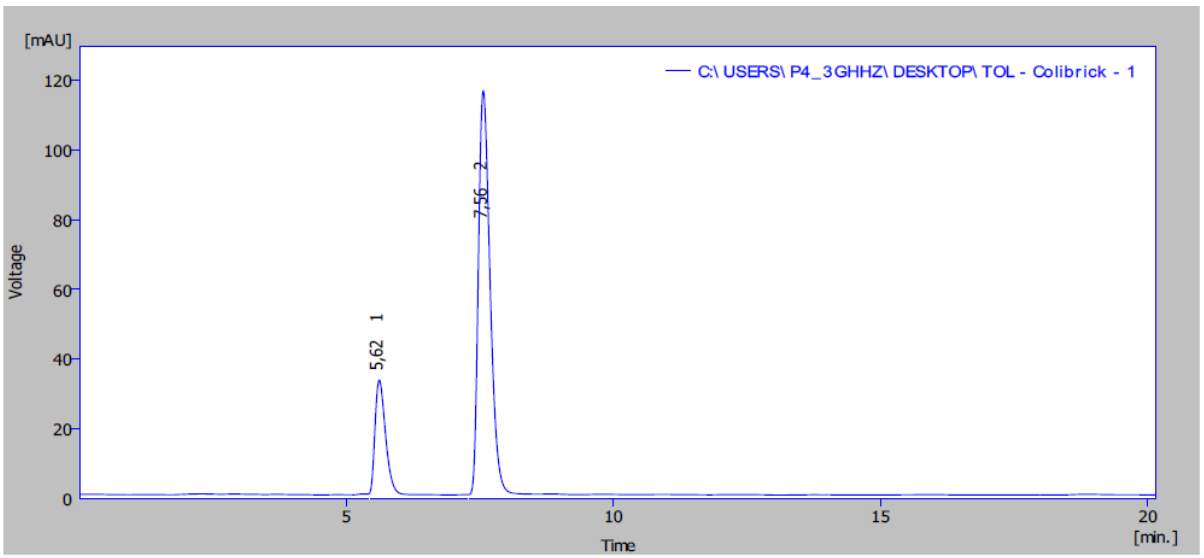

	Reten. Time [min]	Start Time [min]	End Time [min]	Start Value [mV]	End Value [mV]	Area [mV.s]	Height [mV]	Area [%]	Height [%]	W05 [min]
1	5,616	5,444	5,892	1,724	3,410	400,280	31,568	18,7	21,4	0,21
2	7,564	7,284	8,184	1,080	1,393	1745,583	115,754	81,3	78,6	0,24
	Total					2145,863	147,322	100,0	100,0	

Copies of chiral HPLC chromatograms for compound 104

Mobile phase: hexane/isopropanol 99.75:0.25

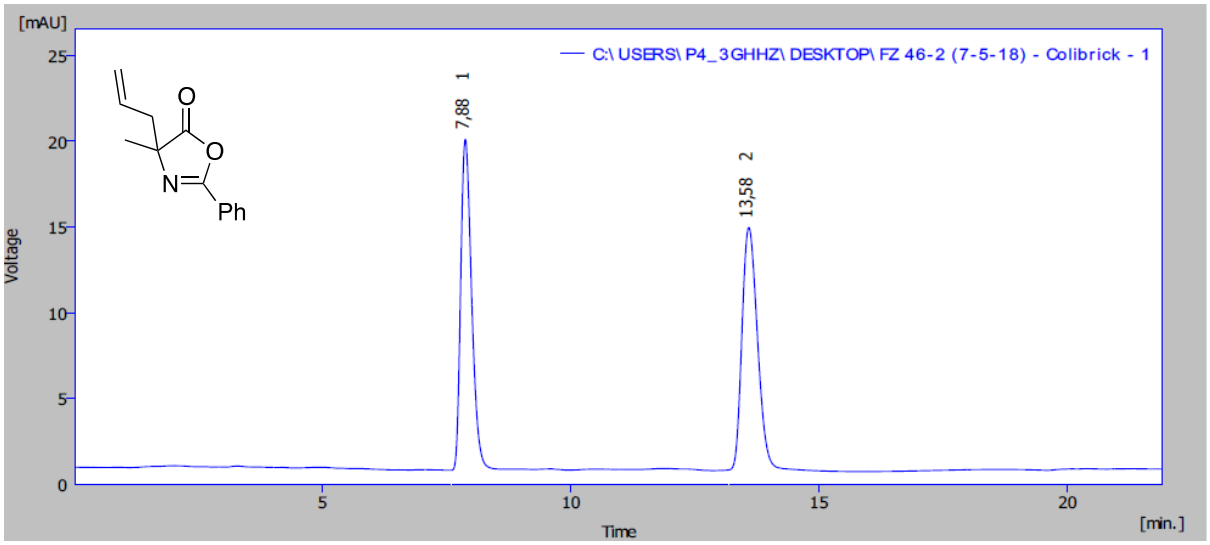

	Reten. Time [min]	Start Time [min]	End Time [min]	Start Value [mV]	End Value [mV]	Area [mV.s]	Height [mV]	Area [%]	Height [%]	W05 [min]
1	7,876	7,584	8,504	0,812	0,890	292,942	19,269	48,9	57,7	0,24
2	13,584	13,172	14,572	0,828	0,843	305,649	14,131	51,1	42,3	0,34
	Total					598,591	33,400	100,0	100,0	

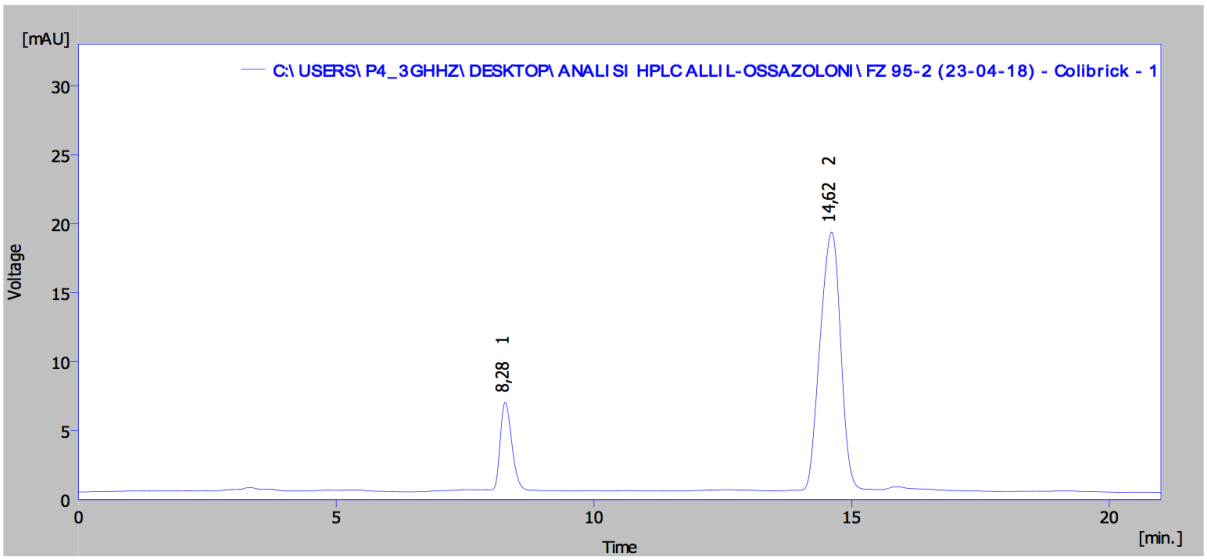

	Reten. Time [min]	Start Time [min]	End Time [min]	Start Value [mV]	End Value [mV]	Area [mV.s]	Height [mV]	Area [%]	Height [%]	W05 [min]
1	8,280	8,036	8,572	0,723	1,103	89,821	6,157	14,9	24,8	0,24
2	14,616	14,032	15,188	0,679	0,794	512,940	18,655	85,1	75,2	0,45
	Total					602,761	24,812	100,0	100,0	

Copies of chiral HPLC chromatograms for compound 106

Mobile phase: hexane/isopropanol 99.75:0.25

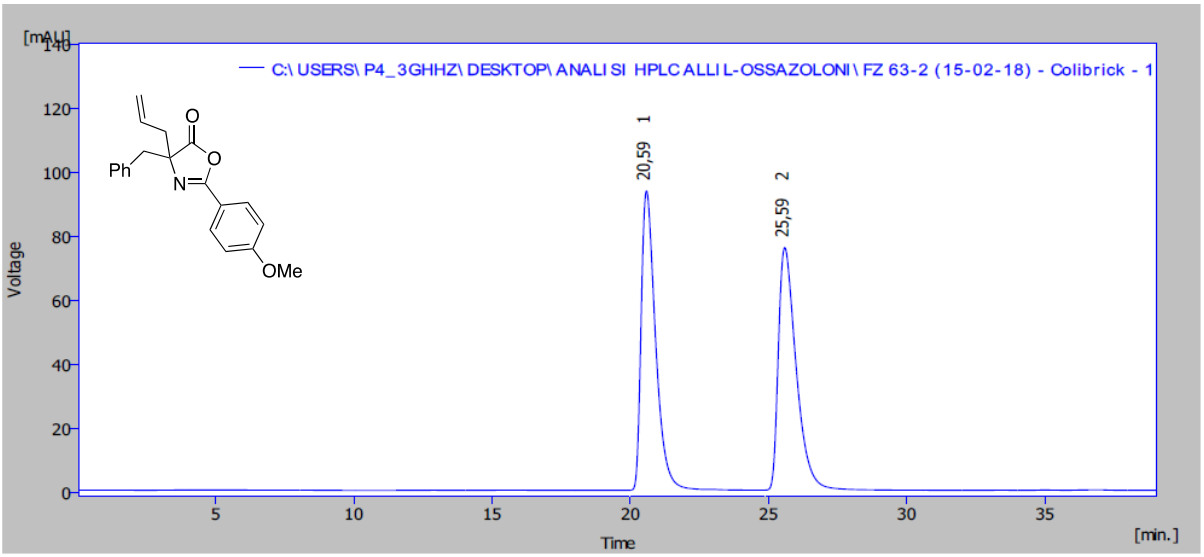

	Reten. Time [min]	Start Time [min]	End Time [min]	Start Value [mV]	End Value [mV]	Area [mV.s]	Height [mV]	Area [%]	Height [%]	W05 [min]
1	20,588	19,992	22,852	0,828	1,089	3360,543	93,388	50,0	55,2	0,54
2	25,592	24,888	28,208	0,875	1,042	3365,016	75,664	50,0	44,8	0,68
	Total					6725,558	169,052	100,0	100,0	

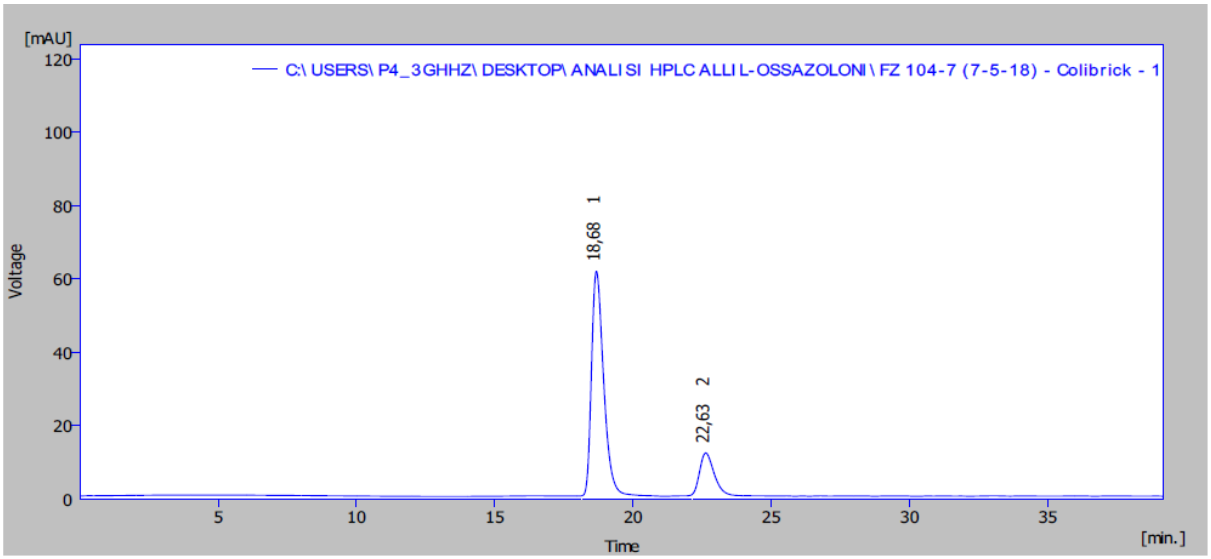

	Reten. Time [min]	Start Time [min]	End Time [min]	Start Value [mV]	End Value [mV]	Area [mV.s]	Height [mV]	Area [%]	Height [%]	W05 [min]
1	18,676	18,152	19,824	0,857	1,242	1836,461	61,063	83,7	84,8	0,46
2	22,632	22,136	23,272	1,208	2,094	356,929	10,907	16,3	15,2	0,54
	Total					2193,390	71,970	100,0	100,0	

Copies of chiral HPLC chromatograms for compound 107

Mobile phase: hexane/isopropanol 99.75:0.25

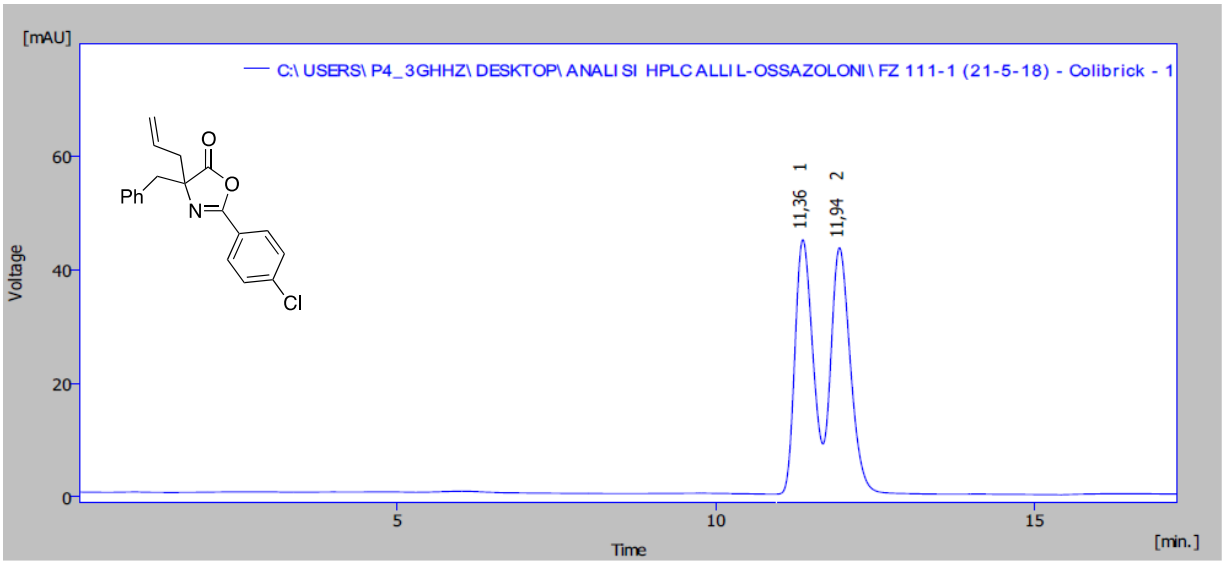

	Reten. Time [min]	Start Time [min]	End Time [min]	Start Value [mV]	End Value [mV]	Area [mV.s]	Height [mV]	Area [%]	Height [%]	W05 [min]
1	11,364	10,948	11,680	0,452	0,477	864,693	44,843	48,2	50,8	0,31
2	11,940	11,680	13,128	0,477	0,527	927,665	43,399	51,8	49,2	0,33
	Total					1792,358	88,242	100,0	100,0	

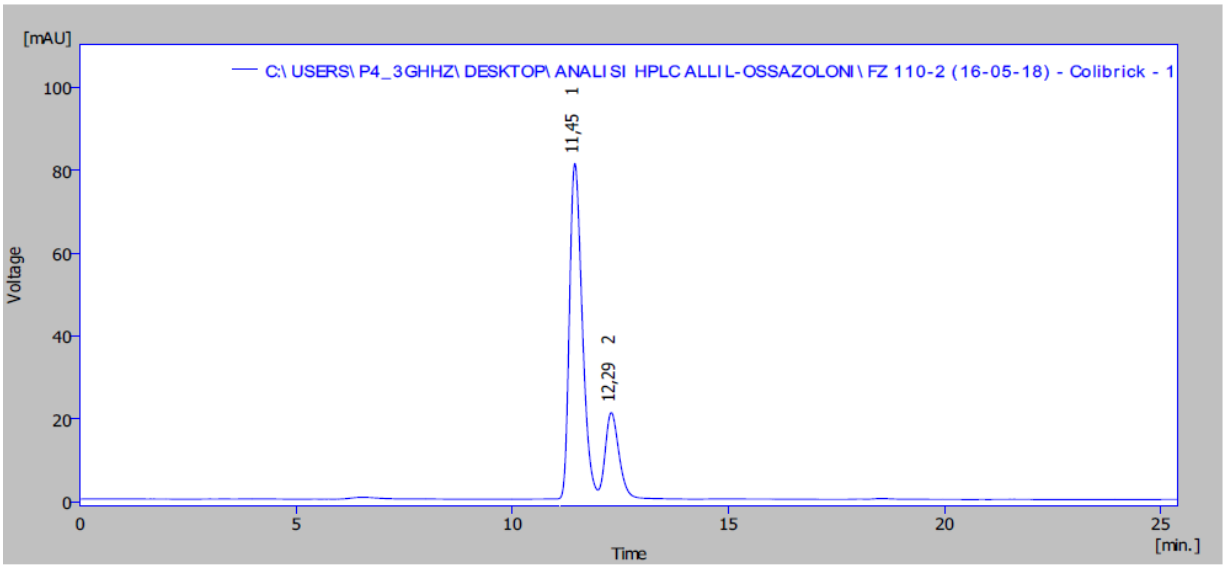

	Reten. Time [min]	Start Time [min]	End Time [min]	Start Value [mV]	End Value [mV]	Area [mV.s]	Height [mV]	Area [%]	Height [%]	W05 [min]
1	11,448	11,092	11,944	0,790	3,107	1591,248	79,953	80,9	80,9	0,32
2	12,292	12,016	12,748	3,180	1,662	375,998	18,912	19,1	19,1	0,32
	Total					1967,245	98,865	100,0	100,0	

Copies of chiral HPLC chromatograms for compound 108

Mobile phase: Hexane/isopropanol 99.75:0.25

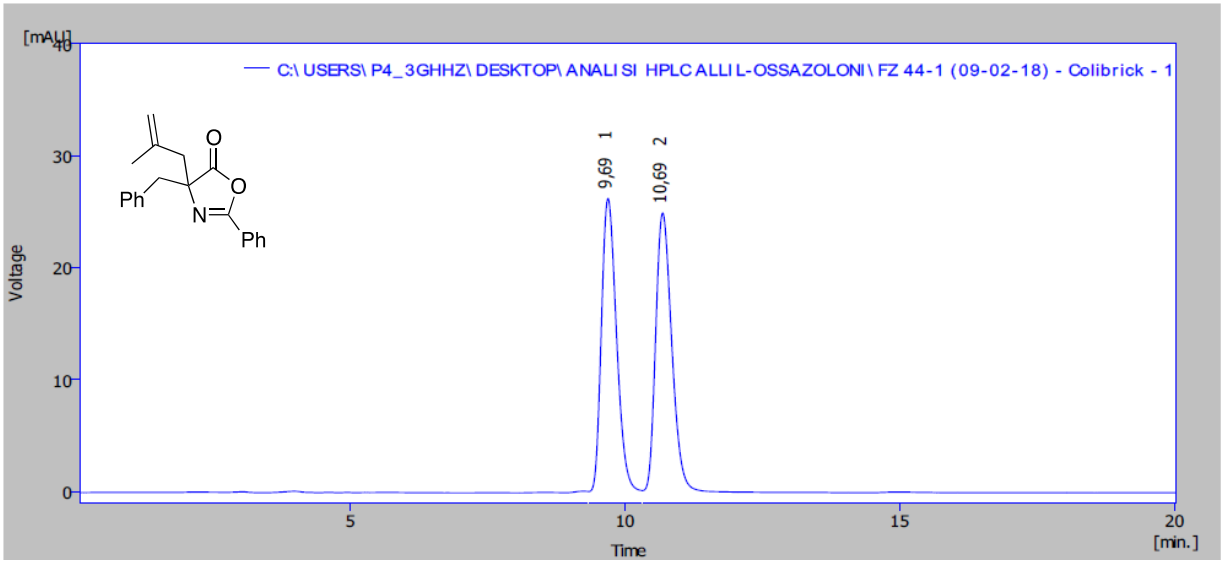

	Reten. Time [min]	Start Time [min]	End Time [min]	Start Value [mV]	End Value [mV]	Area [mV.s]	Height [mV]	Area [%]	Height [%]	W05 [min]
1	9,692	9,340	10,324	0,024	0,029	495,896	26,164	49,7	51,3	0,30
2	10,688	10,324	11,516	0,029	0,036	501,887	24,862	50,3	48,7	0,32
	Total					997,783	51,026	100,0	100,0	

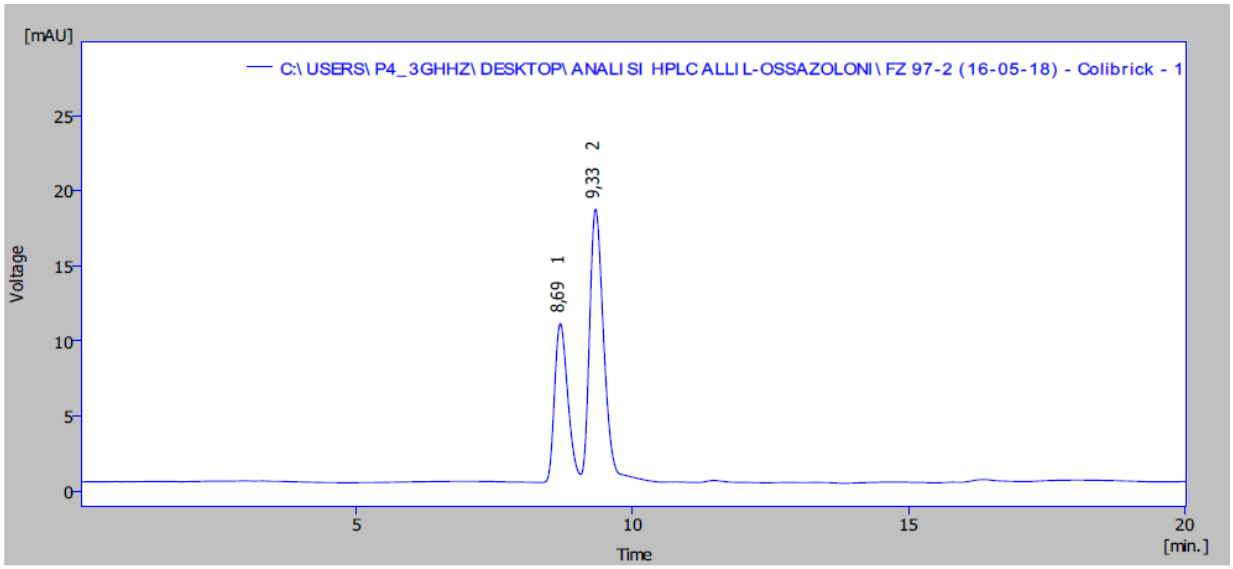

	Reten. Time [min]	Start Time [min]	End Time [min]	Start Value [mV]	End Value [mV]	Area [mV.s]	Height [mV]	Area [%]	Height [%]	W05 [min]
1	8,692	8,380	9,060	0,593	0,622	175,445	10,557	35,0	36,8	0,26
2	9,332	9,060	10,344	0,622	0,677	325,569	18,135	65,0	63,2	0,28
	Total					501,014	28,692	100,0	100,0	

Copies of chiral HPLC chromatograms for compound 116

Mobile phase: hexane/isopropanol 95:05

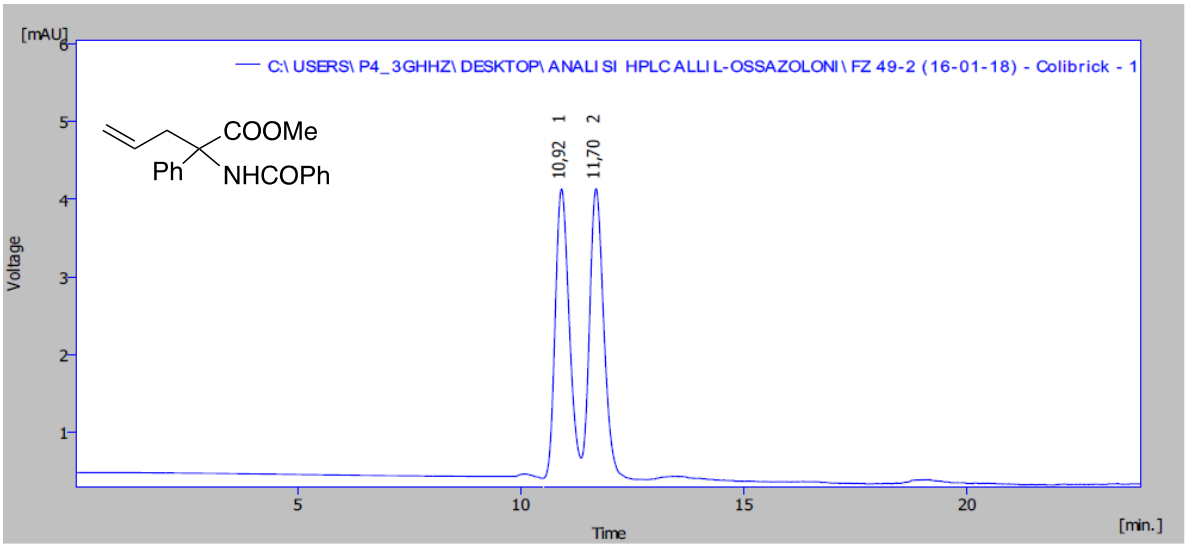

	Reten. Time [min]	Start Time [min]	End Time [min]	Start Value [mV]	End Value [mV]	Area [mV.s]	Height [mV]	Area [%]	Height [%]	W05 [min]
1	10,916	10,524	11,364	0,418	0,409	80,447	3,718	49,4	49,9	0,34
2	11,696	11,364	12,544	0,409	0,396	82,471	3,731	50,6	50,1	0,34
	Total					162,918	7,449	100,0	100,0	

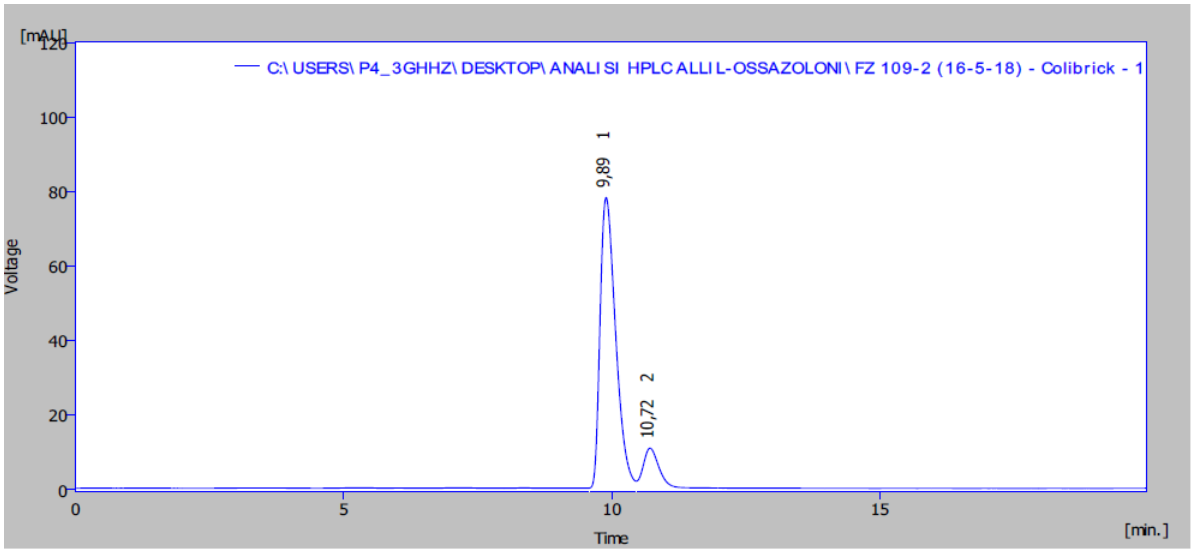

	Reten. Time [min]	Start Time [min]	End Time [min]	Start Value [mV]	End Value [mV]	Area [mV.s]	Height [mV]	Area [%]	Height [%]	W05 [min]
1	9,892	9,584	10,456	0,442	2,090	1528,358	77,399	91,8	90,0	0,31
2	10,716	10,456	10,972	2,090	3,065	136,725	8,579	8,2	10,0	0,27
	Total					1665,083	85,978	100,0	100,0	

Copies of chiral HPLC chromatograms for compound 117

Mobile phase: hexane/isopropanol 99:1

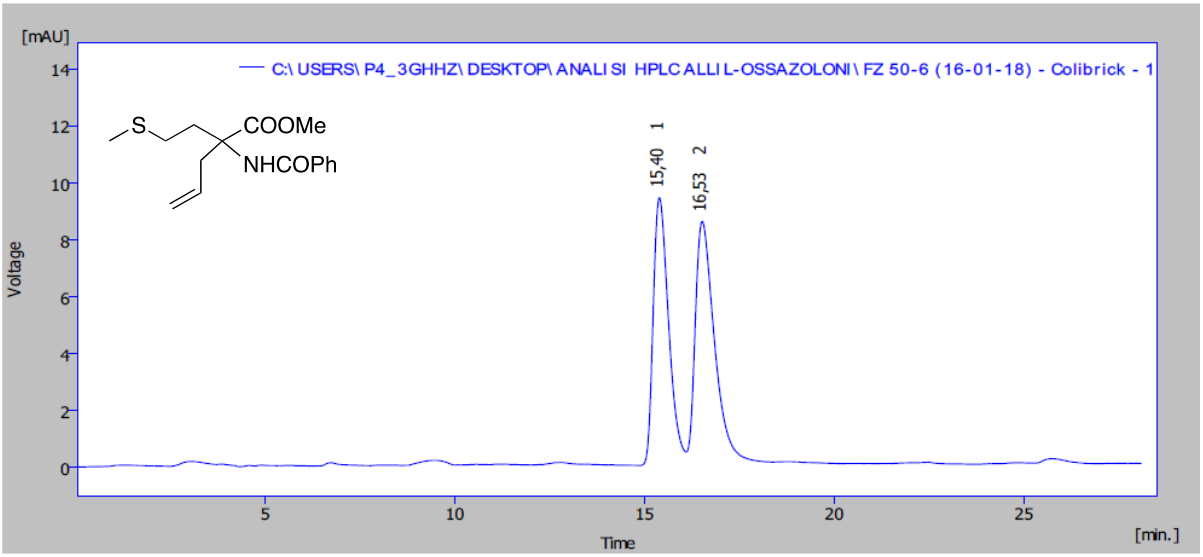

	Reten. Time [min]	Start Time [min]	End Time [min]	Start Value [mV]	End Value [mV]	Area [mV.s]	Height [mV]	Area [%]	Height [%]	W05 [min]
1	15,396	14,892	16,088	0,076	0,132	264,235	9,396	47,0	52,5	0,44
2	16,528	16,088	18,064	0,132	0,224	298,498	8,508	53,0	47,5	0,53
	Total					562,733	17,904	100,0	100,0	

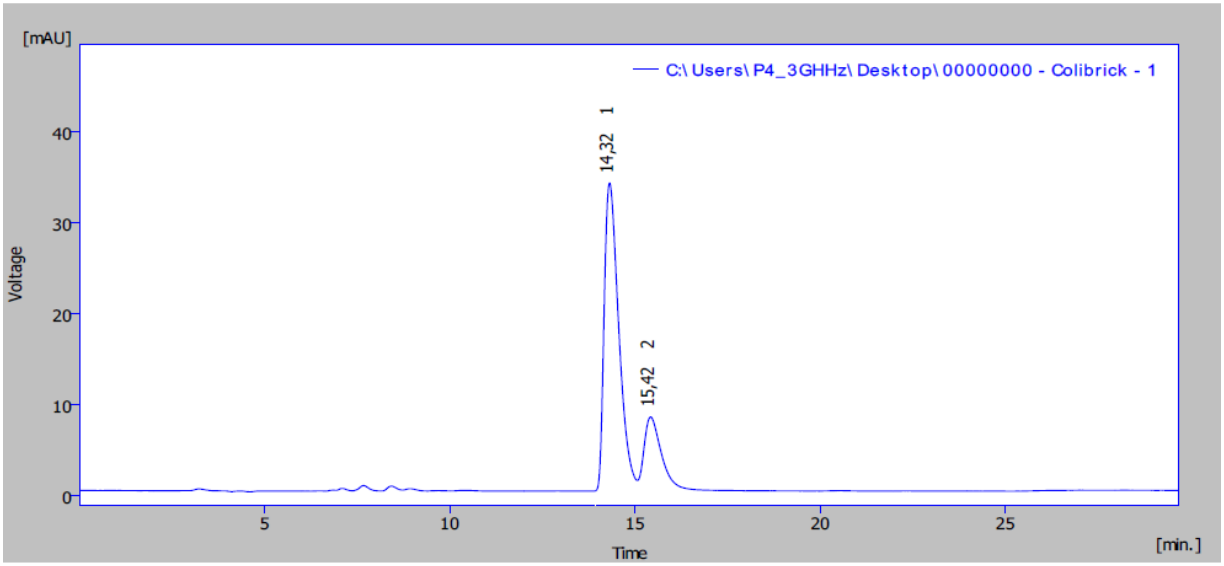

	Reten. Time [min]	Start Time [min]	End Time [min]	Start Value [mV]	End Value [mV]	Area [mV.s]	Height [mV]	Area [%]	Height [%]	W05 [min]
1	14,320	13,928	15,060	0,550	1,712	886,809	33,466	81,8	82,6	0,42
2	15,424	15,104	16,108	1,823	1,296	196,708	7,027	18,2	17,4	0,44
	Total					1083,518	40,493	100,0	100,0	

5. References

1. Hehlgans, S.; Haase, M.; Cordes, N. *Biochim Biophys Acta* **2007**, *1775*, 163–180.
2. Pan, L.; Zhao, Y.; Yuan, Z; Pan, G. Q. *SpringerPlus* **2016**, *5*, 1094.
3. Rathinam, R.; Alahari, S. K. *Cancer metastasis Rev* **2010**, *29*, 223-237.
4. a) Hood, J. D.; Bednarski, M.; Frausto, R.; Guccione, S.; Reisfeld, R. A.; Xiang, R.; Cheresh, D. A. *Science* **2002**, *296*, 2404–2407; b) Eliceiri, B. P.; Cheresh, D. A. *Current Opinion in Cell Biology* **2001**, *13*, 563–568. c) Aplin, A. E.; Howe, A.; Alahari, S. K.; Juliani, R. L. *Pharmacological Reviews* **1998**, *50*, 197–263. d) Gumbiner, B. M. *Cell* **1996**, *84*, 345–357.
5. Colombatti, A.; Bonaldo, P.; Doliana, R. *Matrix* **1993**, *13*, 297–306.
6. Jin, H.; Varner, J. *Br J Cancer.* **2004**, *90*, 561–565.
7. a) Reszka, A. A.; Hayashi, Y; Horwitz, A. F. *J Cell Biol* **1992**, *117*, 1321–1330. b) Otey, C. A.; Vasquez, G. B.; Burridge, K.; Erickson, B. W. *J Biol Chem* **1993**, *268*, 21193–21197. c) Lyman, S.; Gilmore, A.; Burridge, K.; Gidwitz, S.; White, G. C. *J Biol Chem* **1997**, *272*, 22538–22547. d) Geiger, B.; Bershadsky, A.; Pankov, R.; Yamada, K. M. *Nat Rev Mol Cell Biol* **2001**, *2*, 793–805.
8. Luo, B. H.; Springer, T. A. *Curr Opin Cell Biol* **2006**, *18*, 579–586.
9. Ginsberg, M. H.; Partridge, A.; Shattil, S. J. *Curr Opin Cell Biol* **2005**, *17*, 509–516.
10. Gottschalk, K. E.; Gunther, R.; Kessler, H. *ChemBioChem*, **2002**, *5, 470–473.*
11. Legate, K.; Wickström, S. A.; Fässler, R. *Genes Dev* **2009**, 23, 397–418.
12. Hynes, R. O. *Cell* **2002**; *110*, 673–687.
13. a) Assoian, R. K.; Klein, E. A. *Trends Cell Biol.* **2008**, *18*, 347–352. b) Kim, S. H.; Turnbull, J.; Guimond, S. *Journal of Endocronology* **2011**, *209*, 139–151.
14. a) Xiong, J.; Balcioglu, H. E.; Danen, E. H. J. *The International J. of Biochem. & Cell Biol.* **2013**, *45*, 1012–1015; b) Clemetson, K. J.; Clemetson, J. M.; *Cell. Mol. Life Sci.* **1998**, *54*, 502–513.
15. Danhier, F.; Le Breton, A.; Préat, V. *Mol. Pharmaceutics* **2012**, *9*, 2961–2973.
16. Qin, J.; Vinogradova, O.; Plow, E. F. *PLoS Biology* **2004**, *2*, 0726–0729.
17. Hamidi, H.; Pietila, M.; Ivaska, J. *British Journal of Cancer* **2016**, *115*, 1017–1023.
18. Alanko, J.; Mai, A.; Jacquemet, G.; Schauer, K.; Kaukonen, R.; Saari, M.; Goud, B.; Ivaska, J. *Nat Cell Biol* **2015**, *17*, 1412–1421.
19. Nader, G. P.; Ezratty, E. J.; Gundersen, G. G. *Nat Cell Biol* **2016**, *18*, 491–503.
20. Serrels, A.; Lund, T.; Serrels, B.; Byron, A.; McPherson, R. C.; von Kriegsheim, A.; Gomez-Cuadrado, L.; Canel, M.; Muir, M.; Ring, J. E.; Maniati, E.; Sims, A. H.; Pachter, J. A.; Brunton, V. G.; Gilbert, N.; Anderton, S. M.; Nibbs, R. J.; Frame, M. C. *Cell* **2015**, *163*, 160–173.
21. Fedele, C.; Singh, A.; Zerlanko, B. J.; Iozzo, R. V.; Languino, L. R. *J Biol Chem* **2015**, *290*, 4545–4551.
22. Hoshino, A.; Costa-Silva, B.; Shen, T. L.; Rodrigues, G.; Hashimoto, A.; Tesic Mark, M.; Molina, H.; Kohsaka, S.; Di Giannatale, A.; Ceder, S.; Singh, S.; Williams, C.; Soplop, N.; Uryu, K.; Pharmer, L.; King, T.; Bojmar, L.; Davies, A. E.; Ararso, Y.; Zhang, T.; Zhang, H.; Hernandez, J.; Weiss, J. M.; Dumont-Cole, V. D.; Kramer, K.; Wexler, L. H.; Narendran, A.; Schwartz, G. K.;

Healey, J. H.; Sandstrom, P.; Labori, K. J; Kure, E. H.; Grandgenett, P. M.; Hollingsworth, M. A.; de Sousa, M.; Kaur, S.; Jain, M.; Mallya, K.; Batra, S. K.; Jarnagin, W. R.; Brady, M. S.; Fodstad, O.; Muller, V.; Pantel, K.; Minn, A. J.; Bissell, M. J.; Garcia, B. A.; Kang, Y.; Rajasekhar, V. K; Ghajar, C. M.; Matei, I.; Peinado, H.; Bromberg, J.; Lyden, D. *Nature* **2015**, *527*, 329–335.

23. Chowdhury, R.; Webber, J. P.; Gurney, M.; Mason, M. D.; Tabi, Z.; Clayton, A *Oncotarget* **2015**, *6*, 715–731.
24. Ivaska, J.; Heino, J. *Annu Rev Cell Dev Biol* **2011**, *27*, 291–320.
25. Lee, S. T.; Jang, M.; Lee, G.; Lim, J. M. *Organogenesis* **2013**, *9*, 143–148.
26. Brafman, D. A.; Phung, C.; Kumar, N.; Willert, K. *Cell Death Differ* **2013**, *20*, 369–381.
27. Sakuma, T.; Sari, I.; Goodman, C. N.; Lindner, J. R.; Klibanov, A. L.; Kaul, S. *Cardiovasc Res.* **2005**, *66*, 552–561.
28. Coleman, P. J.; Brashear, K. M.; Askew, B. C.; Hutchinson, J. H.; McVean, C. A.; Duong, L. T.; Feuston, B. P.; Fernandez-Metzler, C.; Gentile, M. A.; Hartman, G. D.; Kimmel, D. B.; Leu, C.-T.; Lipfert, L.; Merkle, K.; Pennypacker, B.; Prueksaritanont, T.; Rodan, G. A.; Wesolowski, G. A.; Rodan, S. B.; Duggan, M. E. *J Med Chem* **2004**, *47*, 4829–4837.
29. Wang, Y.; Wang, X.; Zhang, Y.; Yang, S.; Wang, J.; Zhang, X.; Zhang, Q. *Journal of drug targeting* **2009**, *17*, 459–467.
30. Meyer, T.; Marshall, J. F.; Hart, I. R. *British Journal of Cancer* **1998**, *77*, 530–536.
31. Rolli, M.; Fransvea, E.; Pilch, J.; Saven, A.; Felding-Habermann, B. *Proceedings of the National Academy of Sciences, of the United States of America* **2003**, *100*, 9482–9487.
32. Nieswandt, B.; Hafner, M.; Echtenacher, B.; Mannel, D. N. *Cancer research* **1999**, *59*, 1295–1300.
33. Chung, A. S.; Ferrara, N.; *Annu Rev Cell Dev Biol* **2011**, *27*, 563–584.
34. Francavilla, C.; Maddaluno, L.; Cavallaro, U. *Semin. Cancer Biol.* **2009**, *19*, 298–309.
35. a) Inman, G. J. *Curr Opin Genet Dev* **2011**, *21*, 93–99. b) Papageorgis, P. *J. Oncol.* **2015**.
36. Khan, Z.; Marshall, J. F. *Cell Tissue Res* **2016,** *365*, 657–673.
37. Paolillo, M.; Serra, M.; Schinelli, S. *Pharmacological Research* **2016**, *113*, 55–61.
38. Stucci, S.; Tucci, M.; Passarelli, A.; Silvestris, F. *Critical Reviews in Oncology/Hematology* **2015**, *96*, 183–193.
39. Medema, J. P. *Nat Cell Biol* **2013**, *15*, 338–344.
40. Pierschbacher, M. D.; Ruoslahti, E. *Proc. Natl. Acad. Sci. USA* **1984**, *81*, 5985–5988.
41. Aumailley, M.; Gurrath, M.; Müller, G.; Calvete, J.; Timpl, R.; Kessler, H. *FEBS Lett.*, **1991**, *291*, 50–54.
42. Gurrath, M.; Müller, G.; Kessler, H. *Eur. J. Biochem.*, **1992**, *210*, 911–921.
43. a) Goodman, S. L.; Hçlzemann, G.; Sulyok, G. A. G.; Kessler, H. *J. Med. Chem.* **2002**, *45*, 1045–1051. b) Knappe, T. A. *Angew. Chem. Int. Ed.* **2011**, *50*, 8714–8717. c) Knappe, T. H.;

Manzenrieder, F.; Mas-Moruno, C.; Linne, U.; Sasse, F.; Kessler, H.; Xie, X.; Marahiel, M. A. *Angew. Chem.* **2011**, *123*, 8873–8876.

44. a) Stupp, R.; Hegi, M. E.; Gorlia, T.; Erridge, S. C.; Perry, J.; Hong, Y. K.; Aldape, K. D.; Lhermitte, B.; Pietsch, T.; Grujicic, D.; Steinbach, J. P.; Wick, W.; Tarnawski, R.; Nam, D. H.; Hau, P.; Weyerbrock, A.; Taphoorn, M. J.; Shen, C. C.; Rao, N.; Thurzo, L.; Herrlinger, U.; Gupta, T.; Kortmann, R. D.; Adamska, K.; McBain, C.; Brandes, A. A.; Tonn, J. C.; Schnell, O.; Wiegel, T.; Kim, C. Y.; Nabors, L. B.; Reardon, D. A.; van den Bent, M. J.; Hicking, C.; Markivskyy, A.; Picard, M.; Weller, M. *Lancet Oncol.* **2014**, *15*, 1100–1108. b) Ruffini, F.; Graziani, G.; Levati, L.; Tentori, L.; D'Atri, S.; Lacal, P. M. *Int J Cancer* **2015**, *136*, E545–558.
45. National Cancer Institute Clinical Trials, clinicaltrials.gov.
46. Reynolds, A. R.; Hart, I. R.; Watson, A. R.; Welti, J. C.; Silva, R. G.; Robinson, S. D.; Da Violante, G.; Gourlaouen, M.; Salih, M.; Jones, M. C.; Jones, D. T.; Saunders, G.; Kostourou, V.; Perron-Sierra, F.; Norman, J. C.; Tucker, G. C.; Hodivala-Dilke, K. M. *Nature Medicine* **2009***, 15*, 392;
47. a) Van Agthoven, J. F., Xlong J. P., Alonso J. L., Rul, X., Adalr, B. D., Goodman, S. L., Arnaout, M. A., *Nat. Struct. Mol. Biol.*, **2014**, *21*, 383-388; b) Russo, M.A.; Paolillo, M.; Sanchez-Hernandez, Y.; Curti, D.; Ciusani, E.; Serra, M.; Colombo, L.; Schinelli, S. *International Journal of Oncology* **2013**, *42*, 83–92; c) Paolillo, M.; Galiazzo, M.C.; Daga, A.; Ciusani, E.; Serra, M.; Colombo, L.; Schinelli, S. *International journal of oncology* **2018**, *53*, 2683–2694; d) Panzeri, S.; Zanella, S.; Arosio, D.; Vahdati, L.; Dal Corso, A.; Pignataro, L.; Paolillo, M.; Schinelli, S.; Belvisi, L.; Gennari, C.; Piarulli, U. *Chem. Eur. J.* **2015**, *21*, 1–8.
48. a) Sheldrake, H. M.; Patterson, L. H. *J. Med. Chem.* **2014**, *57*, 6301–6315. b) Cirkel, G.; Kerklaan, G. A.; Vanhoutte, B. M.; Van der Aa, A.; Lorenzon, G.; Namour, F.; Pujuguet, P.; Darquenne, S.; de Vos, F. Y. F.; Snijders, T. J.; Voest, E. E.; Schellens, J. H. M.; Lolkema, M. P. *Invest. New Drugs* **2016**, *34*, 184–192. c) NCT01580644, NCT00928343 and one in solid tumours: NCT01313598.
49. a) Hall, E. R.; Bibby, L. I.; Slack, R. J. *Biochem. Pharmacol.* **2016**, *117*, 88–96. b) Anderson, N. A.; Fallon, B. J.; Pritchard, J. M. WO 2014154725A1. healthy volunteers and IPF patients (NCT02612051 and NCT03069989, PET study)
50. a) CAS 1604799-48-5. Clinical trials in diabetic macular oedema, diabetic retinopathy and wet age-related macular degeneration (NCT01482871, NCT02348918, NCT02435862, NCT01749891). b) Hatley, R. J. D.; Macdonald, S. J. F.; Slack, R. J.; Le, J.; Ludbrook, S. B.; Lukey, P. T. *Angew. Chem. Int. Ed.* **2018**, *57*, 3298 – 3321
51. Xiong, J. P.; Stehle, T.; Diefenbach, B.; Zhang, R.; Dunker, R.; Scott, D. L.; Joachimiak, A.; Goodman, S. L.; Arnaout, M. A. *Science*, **2001**, *294*, 339.
52. a) Hutchinson, J. H.; Halczenko, W.; Brashear, K. M.; Breslin, M. J.; Coleman, P. J.; Duong, L. T.; Fernandez-Metzler, C.; Gentile, M. A.; Fisher, J. E.; Hartman, G. D.; Huff, J. R.; Kimmel, D. B.; Leu, C.-T.; Meissner, R. S.; Merkle, K.; Nagy, R.; Pennypacker, B.; Perkins, J. J.;

Prueksaritanont, T.; Rodan, G. A.; Varga, S. L.; Wesolowski, G. A.; Zartman, A. E.; Rodan, S. B.; Duggan M. E. *J. Med. Chem.* **2003,** *46,* 4790–4798. b) Pickarski, M.; Gleason, A.; Bednar, B.; Duong, L. T. *Oncol. Rep.* **2015**, *33*, 2737–2745.

53. Rosenthal, M. A.; Davidson, P.; Rolland, F.; Capone, M.; Xue, L.; Han, H. T.; Mehta, A.; Berd, Y.; He, W.; Lombardi, A. *Asia Pac J Clin Oncol.* **2010**, *6*, 42–48.
54. Raab-Westphal, S.; Marshall, J. F.; Goodman, S. L. *Cancers* **2017**, *9*, 110.
55. Michelson, A.D. *Nat. Rev. Drug Discov.* **2010**, 9, 154–169.
56. Hersey, P.; Sosman, J.; O'Day, S.; Richards, J.; Bedikian, A.; Gonzalez, R.; Sharfman, W.; Weber, R.; Logan, T.; Buzoianu, M.; Hammershaimb, L.; Kirkwood, J. M. *Cancer* **2010**, *116*, 1526–1534.
57. O'Day, S.; Pavlick, A.; Loquai, C.; Lawson, D.; Gutzmer, R.; Richards, J.; Schadendorf, D.; Thompson, J.A.; Gonzalez, R.; Trefzer, U.; Mohr, P.; Ottensmeier, C.; Chao, D.; Zhong, B.; de Boer, C. J.; Uhlar, C.; Marshall, D.; Gore, M. E.; Lang, Z.; Hait, W.; Ho, P. *Br. J. Cancer* **2011**, *105*, 346–352.
58. Heidenreich, A.; Rawal, S. K.; Szkarlat, K.; Bogdanova, N.; Dirix, L.; Stenzl, A.; Welslau, M.; Wang, G.; Dawkins, F.; de Boer, C. J.; Schrijvers, D. A. *Ann. Oncol.* **2013**, *24*, 329–336.
59. Thompson, D. S.; Patnaik, A.; Bendell, J. C.; Papadopoulos, K.; Infante, J. R.; Mastico, R. A.; Johnson, D.; Qin, A.; O'Leary, J. J.; Tolcher, A. W. *J. Clin. Oncol.* **2010**, *28*, 3058.
60. (NCT00721669)
61. (NCT01008475)
62. Sharom, F. J. *Pharmacogenomics* 2008, *9*, 105–127.
63. Desgrosellier, J. S.; Cheresh, D. A. *Nat Rev Cancer* **2010**, *10*, 9–22.
64. Ehrlich, P. Address in pathology, ON CHEMIOTHERAPY: delivered before the seventeenth International Congress of Medicine. *Br Med J* **1913**, *2*, 353–359.
65. Marelli, U. K.; Rechenmacher, F.; Sobahi, T. R. A.; Mas-Moruno, C.; Kessler, H. *Frontiers in Oncology* **2013**, *3*, 222.
66. Diamantis, N.; Banerji, U. *Br. J. Cancer* **2016**, *114*, 362–367.
67. Peters, C.; Brown, S. *Biosci. Rep.* **2015**, *35*, e00225.
68. a) Caswell, P.; Norman, J. *Trends Cell Biol.* **2008**, *18*, 257–263. b) Chen, K.; Chen, X.; *Theranostics* **2011**, *1*, 189–200.
69. Tsuchikama, K.; An, Z. *Protein Cell* **2018**, *9*, 33–46.
70. Sievers, E. L.; Larson, R. A.; Stadtmauer, E. A.; Estey, E.; Löwenberg, B.; Dombret, H.; Karanes, C.; Theobald, M.; Bennett, J. M.; Sherman, M. L.; Berger, M. S.; Eten, C. B.; Loken, M. R.; van Dongen, J. J.; Bernstein, I. D.; Appelbaum, F. R. *J Clin Oncol* **2001**, *19*, 3244–3254.
71. Younes, A.; Bartlett, N. L.; Leonard, J. P.; Kennedy, D. A.; Lynch, C. M.; Sievers, E. L.; Forero-Torres, A. *N Engl J Med* **2010**, *363*, 1812–1821.

72. a) Lo Russo, P. M.; Weiss, D.; Guardino, E.; Girish, S.; Sliwkowski, M. X. *Clin Cancer Res* **2011**, *17*, 6437–6447. b) Verma, S.; Miles, D.; Gianni, L.; Krop, I. E.; Welslau, M.; Baselga, J.; Pegram, M.; Oh, D.-Y.; Diéras, V.; Guardino, E.; Fang, L.; Lu, M. W.; Olsen, S.; Blackwell, K.; *N Engl J Med* **2012**, *367*, 1783–1791.
73. ten Cate, B.; Bremer, E.; de Bruyn, M.; Bijma, T.; Samplonius, D.; Schwemmlein, M.; Huls, G.; Fey, G.; Helfrich, W. *Leukemia* **2009**, *23*, 1389–1397.
74. Ornes, S. *Proc. Natl. Acad. Sci. USA* **2013**, *110*, 13695.
75. Drake, P.M.; Rabuka, D. *Curr. Opin. Chem. Biol.* **2015**, *28*, 174–180.
76. Nasiri, H.; Valedkarimi, Z.; Aghebati-Maleki, L.; Majidi, J. *Cell Physiol.* **2018**, *233*, 6441–6457.
77. a) Chari, R. *Accounts of Chemical Research* **2008**, *41*, 98. b) Laguzza, B. C.; Nichols, C. L.; Briggs, S. L.; Cullinan, G. J.; Johnson, D. A.; Starling, J. J.; Baker, A. L.; Bumol, T. F.; Corvalan, J. R. F. *Journal of Medicinal Chemistry* **1989**, *32*, 548–555. c) Pietersz, G.; Krauer, K. *Journal of Drug Targeting* **1994**, *2*, 183–215.
78. Lu, J.; Jiang, F.; Lu, A.; Zhang, G. *Int. J. Mol. Sci.* **2016**, *17*, 561.
79. Tabrizi, M.; Bornstein, G.G.; Suria, H. *AAPS J.* **2010**, *12*, 33–43.
80. a) Thurber, G. M.; Schmidt, M. M.; Wittrup, K. D. *Adv. Drug Deliv. Rev.* **2008**, *60*, 1421–34. b) Adams, G. P.; Schier, R.; McCall, A. M.; Simmons, H. H.; Horak, E. M.; Alpaugh, R. K.; Marks, J. D.; Weiner, L. M. *Cancer Res*. **2001**, *61*, 4750–4755.
81. Lee, C. M.; Tannock, I. F. *BMC Cancer* **2010**, *10*, 255.
82. a) Teicher, B. A.; Chari, R. V. J. *Clin Cancer Res* **2011**, *17*, 6389–6397. b) Sedlacek, H. H.; Seemann, G.; Hoffmann, D.; Czech, J. *Contrib Oncol* **1992**, *43*, 1–145.
83. Dal Corso, A.; Pignataro, L.; Belvisi, L.; Gennari, C. *Current Topics in Medicinal Chemistry* **2016***, 16,* 314–329.
84. Wang, X.; Ma, D.; Olson, W. C.; Heston, W. D. W. *Mol. Cancer Ther.* **2011**, *10*, 1728–1739.
85. Warburg, O. *Science* **1956**, *124*, 269–270.
86. Ducry, L.; Stump, B. *Bioconjugate Chem.* **2010**, *21*, 5–13.
87. Böhme, D.; Beck-Sickinger A. G. *J. Pept. Sci.* **2015**, *21*, 186–200.
88. Burkhart, D. J.; Kalet, B. T.; Coleman, M. P.; Post, G. C.; Koch, T.H. *Mol. Cancer Ther.* **2004**, *3*, 1593–1604.
89. a) Meister, A.; Anderson, M. E. *Annu. Rev. Biochem.* **1983**, *52*, 711–760. b) Saito, G.; Swanson, J. A.; Lee, K. D. *Adv. Drug Deliv. Rev.* **2003**, *55*, 199–215.
90. Lee, M. H.; Kim, J. Y.; Han, J. H.; Bhuniya, S.; Sessler, J. L.; Kang, C.; Kim, J. S. *J. Am. Chem.Soc.* **2012**, *134*, 12668–12674.
91. Ciechanover, A. *Angew. Chem. Int. Ed. Engl.* **2005**, *44*, 5944–5967.
92. Dubowchik, G. M.; Firestone, R. A. *Bioorg. Med. Chem. Lett.* **1998**, *8*, 3341–3346.
93. Vartak, D. G.; Lee, B.-S.; Gemeinhart, R. A. *Mol. Pharm.* **2009**, *6*, 1856–1867.
94. Dal Corso, A.; Caruso, M.; Belvisi, L.; Arosio, D.; Piarulli, U.; Albanese, C.; Gasparri, F.;

Marsiglio, A.; Sola, F.; Troiani, S.; Valsasina, B.; Pignataro, L.; Donati, D.; Gennari, C. *Chem. Eur. J.* **2015**, *21*, 6921–6929.

95. a) Hartley, J. A. *Expert Opin Investig Drugs* **2011**, *20*, 733–744. b) Dubowchik, G. M.; Firestone, R. A.; Padilla, L.; Willner, D.; Hofstead, S. J.; Mosure, K.; Knipe, J. O.; Lasch, S. J.; Trail, P. A. *Bioconjugate Chem* **2002**, *13*, 855–869.
96. Jain, N.; Smith, S. W.; Ghone, S.; Tomczuk, B. *Pharm. Res.* **2015**, *32*, 3526–3540.
97. Ducry, L. Antibody Drug Conjugates; *Humana Press*: New York, NY, USA, **2013**.
98. Zhou, Y.; Chakraborty, S.; Liu, S. *Theranostics* **2011**, *1*, 58-82.
99. Nielsen, C. H.; Kimura, R. H.; Withofs, N.; Tran, P. T.; Miao, Z.; Cochran, J. R.; Cheng, Z.; Felsher, D.; Kjær, A.; Willmann, J. K.; Gambhir, S. S. *Cancer Res.* **2010**, *70*, 9022–9030.
100. a) Maeda, H.; Matsumura, Y. *Cancer Res.* **1986**, *46*, 6387–6392. b) Maeda, H.; Wu, J.; Sawa, T.; Matsumura, Y.; Hori, K.; *J. Control. Release* **2000**, *65*, 271–284.
101. Arosio, D.; Casagrande, C. *Advanced Drug Delivery Reviews* **2016**, *97*, 111–143.
102. Duro-Castano, A.; Gallon, E.; Decker, C.; Vicent, M. J. *Advanced Drug Delivery Reviews* **2017**, *119*, 101–119.
103. Ji, S.; Xu, J.; Zhang, B.; Yao, W.; Xu, W.; Wu, W.; Xu, Y.; Wang, H.; Ni, Q.; Hou, H.; Yu, X.*Cancer Biol Ther* **2012**, *13*, 206–215.
104. Gormley, A. J.; Malugin, A.; Ray, A.; Robinson, R.; Ghandehari, H. *J Drug Target* **2011**, *19*, 915–924.
105. Robinson, J. T.; Tabakman, S. M.; Liang, Y.; Wang, H.; Casalongue, H. S.; Vinh, D.; Dai, H. *J. Am. Chem. Soc.* **2011**, *133*, 6825–6831.
106. a) Jain, R. K.; Stylianopoulos, T.; *Nat. Rev. Clin. Oncol.* **2010**, *7*, 653–664. b) Bae, Y. H.; Park, K. *J. Control. Release* **2011**, *153*, 198–205.
107. Lammers, T.; Kiessling, F.; Hennink, W. E.; Storm G. *Journal of Controlled Release* **2012**, *161*, 175–118.
108. Popovic, Z.; Liu, W.; Chauhan, V. P.; Lee, J.; Wong, C.; Greytak, A. B.; Insin, N.; Nocera, D. G.; Fukumura, D.; Jain, R. K.; Bawendi, M. G. *Angew. Chem. Int. Ed Engl.* **2010**, *49*, 8649–8652.
109. Juweid, M.; Neumann, R.; Paik, C.; Perez-Bacete, M. J.; Sato, J.; van Osdol, W.; Weinstein, J. *N. Cancer Res.* **1992**, *52*, 5144–5153.
110. a) Rihova, B.; Kovar, M. *Adv. Drug Deliv. Rev.* **2010**, *62*, 184–191. b) Rihova, B.;Strohalm, J.; Prausova, J.; Kubackova, K.; Jelinkova, M.; Rozprimova, L.; Sirova, M.; Plocova, D.; Etrych, T.; Subr, V.; Mrkvan, T.; Kovar, M.; Ulbrich, K. *J. Control. Release* **2003**, *91*, 1–16.
111. Halab, L.; Gosselin, F.; Lubell, W. D. *Biopolymers (Peptide Science)* **2000**, *55*, 101–122.
112. Arosio, D.; Belvisi, L.; Colombo, L.; Colombo, M.; Invernizzi, D.; Manzoni, L.; Potenza, D.; Serra, M.; Castorina, M.; Pisano, C.; Scolastico, C. *ChemMedChem* **2008**, *3*, 1589–1603.
113. Seneci, P.; Bianchi, A.; Battaglia, C.; Belvisi, L.; Bolognesi, M.; Caprini, A.; Cossu, F.; de Franco, E.; de Matteo, M.; Delia, D.; Drago, C.; Khaled, A.; Lecis, D.; Manzoni, L.; Marizzoni, M.;

Mastrangelo, E.; Milani, M.; Motto, I.; Moroni, E.; Potenza, D.; Rizzo, V.; Servida, F.; Turlizzi, E.; Varrone, M.; Vasile, F.; Scolastico, C. *Bioorganic & Medicinal Chemistry* **2009**, *17*, 5834–5856.

114. Alcaro, M.; Vinci, V.; D'Ursi, A. M.; Scrima, M.; Chelli, M.; Giuliani, S.; Meini, S.; Di Giacomo, M.; Colombo, L.; Papini, A. M. *Bioorg. Med. Chem. Lett.* **2006**, *16*, 2387–2390.
115. a) Hanessian, S.; Therrien, E.; Granberg K.; Nilsson, I. *Bioorganic & Medicinal Chemistry Letters* **2002**, *12*, 2907–2911. b) Hanessian, S.; Balaux, E.; Musil, D.; Olsson, L.-L.; Nilsson, I. *Bioorganic & Medicinal Chemistry Letters* **2000**, *10*, 243–247.
116. a) Li, T.-J.; Liu, Z.-Q.; Yin, H.-M.; Yao, C.-S.; Jiang, B.; Wang, X.-S.; Tu, S.-J.; Li, X.-L.; Li, G. *J. Org. Chem.* **2013**, *78*, 11414–11420. b) Boukanoun, M. K.; Hou, X.; Nikolajev, L.; Ratni, S.; Olson, D.; Claing, A.; Laporte, S. A.; Chemtobb, S.; Lubell, W. D. *Org. Biomol. Chem.* **2015**, *13*, 7750–7761. c) Hanessian, S.; McNaughton-Smith, G. *Bioorganic & Medicinal Chemistry Letters* **1996**, *6*, 1567–1572.
117. Serra, M.; Tambini, S. M.; Di Giacomo, M.; Peviani, E. G.; Belvisi, L.; Colombo, L. *Eur. J. Org. Chem.* **2015**, *34*, 7557–7570.
118. Serra, M.; Peviani, E. G.; Bernardi, E.; Colombo, L. *J. Org. Chem.* **2017**, *82*, 11091–11101.
119. a) Fu, Y.; Etienne, M. A.; Hammer, R. P. *J. Org. Chem.* **2003**, *68*, 9854–9857. b)Kricheldorf, H. R. *Ann. Chem.* **1972**, *763***,** 17–38.
120. Godina, T. A.; Lubell, W. D. *J. Org. Chem.* **2011**, *76*, 5846–5849.
121. Nicolaou, K. C.; Estrada, A. A.; Zak, M.; Lee, S. H.; Safina, B. S. *Angew. Chem. Int. Ed.* **2005**, *44*, 1378–1382.
122. Zask, A.; Helquist, P. *J. Org. Chem.* **1978**, *43*, 1619–1620.
123. Ikawa, T.; Sajinki, H.; Hirota, K. *Tetrahedron* **2005**, *61*, 2217–2231.
124. a) Perteghella, S.; Crivelli, B.; Catenacci, L.; Sorrenti, M.; Bruni, G.; Necchi, V.; Vigania, B.; Sorlinie, M.; Torre, M. L.; Chlapanidas, T. *International Journal of Pharmaceutics* **2017**, *520* 86–97. b) Kundu, B.; Rajkhowa, R.; Kundu, S.C.; Wang, X. *Adv. Drug Deliv. Rev.* **2013**, *65*, 457–470. c) Wang, H.-Y.; Zhang, Q. *Biotechnol. Progr.* **2015**, *31*, 630–640.
125. Aggarwal, B. B.; Harikumar, K. B. *Int. J. Biochem. Cell Biol.* **2009**, *41*, 40–59.
126. Rodriguez-Nogales, A.; Algieri, F.; De Matteis, L.; Lozano-Perez, A. A.; Garrido-Mesa, Jose.; Vezza, T.; de la Fuente, J. M.; Cenis, J. L.; Gálvez, J.; Rodriguez-Cabezas, M. E. *International Journal of Nanomedicine* **2016**, *11*, 5945–5958.
127. Jezowska, M.; Honcharenko, D.; Ghidini, A.; Stromberg, R.; Honcharenko, M. *Bioconjugate Chem.* **2016**, *27*, 2620–2628.
128. Kwiatkowski, S.; Knap, B.; Przystupski, D.; Saczko, J.; Kędzierska, E.; Knap-Czop, K.; Kotlińska, J.; Michel, O.; Kotowski, K.; Kulbacka, J. *Biomedicine & Pharmacotherapy* **2018**, *106*, 1098–1107.
129. a) Norum, O.-J.; Selbo, P. K.; Weyergang, A.; Giercksky, K.-E.; Berg, K. *Journal of Photochemistry and Photobiology B: Biology* **2009**, *96*, 83–92. b) Obaid, G.; Broekgaarden, M.; Bulin, A.-L.; Huang, H.-C.; Kuriakose, J.; Liu, J.; Hasan, T. *Nanoscale* **2016**, *8*, 12471–12503.

c) Weyergang, A.; Berstad, M. E. B.; Bull-Hansen, B.; Olsen, C. E.; Selboa, P. K.; Berga, K. *Photochem. Photobiol. Sci.* **2015**, *14*, 1465–1475.

130. Crespi, S.; Protti, S.; Fagnoni, M. *J. Org. Chem.*, **2016**, *81*, 9612–9619.
131. a) Rasmussen, L. K.; Boren, B. C.; Fokin, V. V. *Org. Lett.* **2007**, *9*, 5337–5339. b) Shao, C.; Wang, X.; Zhang, Q.; Luo, S.; Zhao, J.; Hu, Y. *J. Org. Chem.* **2011**, *76*, 6832–6836.
132. Serra, M.; Bernardi, E.; Marrubini, G.; Colombo, L. *Eur. J. Org. Chem.* **2017**, *20*, 2964–2970.
133. Mori, M.; Sakakibara, N.; Kinoshita, A *J. Org. Chem.*, **1998**, *63*, 6082–6083.
134. Search conducted on "SciFinder a CAS solution", 19-09-2018.
135. Venkatraman, J.; Shankaramma, S. C.; Balaram, P. *Chem. Rev.* **2001**, *101*, 3131–3152.
136. a) Vogt, H.; Bräse, S. *Org. Biomol. Chem.* **2007**, *5*, 406–430. b) Cativiela, C.; Díaz-de-Villegas, M. D. *Tetrahedron: Asymmetry* **1998**, *9*, 3517–3599. c) Cativiela, C.; Díaz-de-Villegas, M. D. *Tetrahedron: Asymmetry* **2000**, *11*, 645– 732. d) Toniolo, C.; Formaggio, F.; Kaptein, B.; Broxterman, Q. B. *Synlett* **2006**, *9*, 1295–1310.
137. Bock, J. E.; Gavenonis, J.; Kritzer, J. A. *ACS Chem Biol.* 2**013**, *8*, 488–499.
138. a) Roxin, A.; Zheng, G. *Future Med. Chem.* **2012**, *4*, 1601–1618. b) White, C. J.; Yudin, A. K. *Nature Chemistry* **2011**, *3*, 509–524. (c) Cardote, T. A. F.; Ciulli, A. *ChemMedChem* **2016**, *11*, 787–794. d) For ring-closing metathesis reactions applied to the synthesis of cyclic peptides see: Gleeson, E. C.; Jackson, W. R.; Robinson, A. J. Tetrahedron Letters 2016, 57, 4325–4333.
139. a) Walensky, L.D.; Bird, G. H. J. *Med. Chem.* **2014**, *57*, 6275–6288. b) Lau, Y. H.; de Andrade, P.; Wu, Y.; Spring, D. R. *Chem. Soc. Rev.* **2015**, *44*, 91–102.
140. a) Chalker, J. M.; Bernardes, G. J. L.; Davis, B. G. *Acc Chem Res.* **2011**, *44*, 730–741. b) Antos, J. M.; Francis, M. B. *Curr Opin Chem Biol.* **2006**, *10*, 253–262.
141. a) Fosgerau, K.; Hoffmann T. *Drug Discovery Today* **2015**, *20*, 122–128. (b) Dehn, S.; Chapman, R.; Jolliffe, K. A.; Perrier, S. *Polym Rev.* **2011**, *51*, 214–234. c) Hamley, I. W. *Biomacromolecules* **2014**, *15*, 1543–1559.
142. Keith, J. A.; Behenna, D. C.; Mohr, J. T.; Ma, S.; Marinescu, S. C.; Oxgaard, J.; Stoltz, B. M.; Goddard, III, W. A. *J. Am. Chem. Soc.* **2007**, *129*, 11876–11877.
143. Racys, D.T; Eastoe, J.; Norrby, P.O; Grillo, I; Rogers, S.E; Lloyd-Jones, G.C. *Chem. Sci.,* **2015**, 6, 5793–5801.
144. Ghosh, S.; Chaudhuri, S.; Bisai, A. *Chem. Eur. J.* **2015**, *21*, 17478–17484.
145. a) Uraguchi, D.; Asai, Y.; Seto, Y.; Ooi, T. *Synlett*, **2009**, *4*, 658–660. b) Vedejs, E.; Fields, S. C.; Hayashi, R.; Hitchcock, S. R.; Powell, D. R.; Schrimpf, M. R. *J. Am. Chem. Soc.*, **1999,** *121,* 2460–2470. c) Reyes-Rangel, G.; Bandala, Y.; García-Flores, F.; Juaristi, E. *Chirality*, **2013**, *25*, 529–540. d) Trost, B. M.; Ariza, X. J. *Am. Chem. Soc.*, **1999**, *121,* 10727–10737.
146. a) Krautwald, S.; Carreira, E. J. Am. Chem. Soc., **2017**, 1*39*, 5627–5639. b) Jiang, X.; Beiger, J. J.; Hartwig, J. F. *J. Am. Chem. Soc.* **2017**, *139*, 87–90.
147. 147 Armarego, W. L. F.; Chai, C. L. L In *Purification of Laboratory Chemicals*, 7th ed.; Butterworth-Heinemann: Oxford, UK, 2013.

148. 148 Movahhed, S.; Westphal, J.; Dindaroğlu, M.; Falk, A.; Schmalz, H.-G.; *Chem. Eur. J.* **2016**, *22*, 7381–7384.
149. Tokunaga, M.; Kiyosu, J.; Obora, Y.; Tsuji, Y. *J. Am. Chem. Soc.* **2006**, *128*, 4481–4486.
150. Jenny, C.; Heimgartner, H. *Helv. Chim. Acta* **1989***, 72*, 1639–1646.
151. Tarí, S.; Avila, A.; Chinchilla, R.; Nájera, C.; *Tetrahedron: Asymmetry* **2012**, *23*, 176–180.

5.1. Images references

Figure 1. Schnittert, J.;Bansal, R.; Storm, G.; Prakash, J. *Advanced Drug Delivery Reviews* **2018**, *129*, 37–53.

Figura 2. Gottschalk, K. E.; Kessler, H. *Angew. Chem. Int. Ed.* **2002**, *41*, 3767–3774.

Figure 3. Hamidi, H.; Pietila, M.; Ivaska, J. *British Journal of Cancer* **2016**, *115*, 1017–1023.

Figure 4. Hamidi, H.; Pietila, M.; Ivaska, J. *British Journal of Cancer* **2016**, *115*, 1017–1023.

Figure 5. Hamidi, H.; Pietila, M.; Ivaska, J. *British Journal of Cancer* **2016**, *115*, 1017–1023.

Figure 6. Goodman, S.L.; Picard, M. *Trends in Pharmacological Sciences* **2012**, *33*, 405–412.

Figure 7. Khan, Z.; Marshall, J. F. *Cell Tissue Res* **2016**, *365*, 657–673.

Figure 10. Srinivasarao, M.; Galliford, C. V.; Low, P. S. *Nature Reviews Drug Discovery* **2015**, *14*, 203–219.

Figure 11. Tsuchikama, K.; An, Z. *Protein Cell* **2018**, *9*, 33–46.

Figure 20. Serra, M.; Peviani, E. G.; Bernardi, E.; Colombo, L. *J. Org. Chem.* **2017**, *82*, 11091–11101.

Figure 21. Serra, M.; Peviani, E. G.; Bernardi, E.; Colombo, L. *J. Org. Chem.* **2017**, *82*, 11091–11101.

Figure 22. Serra, M.; Peviani, E. G.; Bernardi, E.; Colombo, L. *J. Org. Chem.* **2017**, *82*, 11091–11101.

Figure 24. Serra, M.; Peviani, E. G.; Bernardi, E.; Colombo, L. *J. Org. Chem.* **2017**, *82*, 11091–11101.